Chemical modulation of guanine nucleotide exchange factor activity

A small molecule inhibitor for the
Rabex-5 mediated Rab5 activation

Dissertation

zur

Erlangung des Doktorgrades (Dr. rer. nat.)

der

Mathematisch-Naturwissenschaftlichen Fakultät

der

Rheinischen Friedrich-Wilhelms-Universität Bonn

vorgelegt von

Christine Irene Wosnitza

aus

Bonn

Bonn 2013

Angefertigt mit Genehmigung der Mathematisch-Naturwissenschaftlichen
Fakultät der Rheinischen Friedrich-Wilhelms-Universität Bonn

CONTENTS

LIST OF ABBREVIATIONS

k	kilo-
c	centi-
m	milli-
μ	mirco-
n	nano-
°C	degree Celsius
%	per cent
Δ	delta; difference
μ	(arithmetic) mean
σ	standard deviation (SD)
2xYT	2x tryptone broth; culture medium for bacteria
A	absorption
aa	amino acid
AP2	protein complex, adaptor in clathrin-mediated endocytosis
API-ESI	atmospheric pressure interface-electrospray ionisation
ACN	acetonitrile
ADLOC	aptamer-displacement assay based on luminescent oxygen channelling
AHT	anhydrotetracycline
amp	ampicillin
APPL	adaptor protein containing PH domain, PTB domain and Leucine zipper motif
APS	ammonium persulfate
Arf	ADP ribosylation factor
Cytohesin-2	ArfGEF, also known as ARF nucleotide-binding site opener (ARNO)
Sec7	Sec7 domain, GEF domain of ArfGEFs
ATP	adenosine-5'-triphosphate
BamHI	restriction site of BamHI enzyme
bp	base pair
BFA	BrefeldinA
Bla	β-lactamase gene, ampicillin resistance gene
β-ME	β-mercaptoethanol
BSA	bovine serum albumin
CC	coiled coil; protein domain for protein-protein interaction
C. elegans	*Caenorhabditis elegans*, nematode used as model organism
CIAP	calf intestine alkaline phosphatase
CO_2	carbon dioxide
cpd	compound
Cys	cysteine
Da	Dalton
DACM	N-(7-dimethylamino-4-methylcoumarin-3-yl))maleimide
DCAI	4,6-dichloro-2-methyl-3-aminoethyl-indole; Ras inhibitor
DH	DBL homology domain; GEF domain of RhoGEFs
DMEM	Dulbecco's Modified Eagle's Medium, cell culture medium for mammalian cells
DMSO	dimethyl sulfoxide
DNA	deoxyribonucleic acid
dNTP	deoxyribonucleoside triphosphate
DTT	dithiothreitol
ECL	enhanced chemiluminescence
E.coli	*Escherichia coli,* gram negative bacterium

EDC	1-ethyl-3-(3-dimethylaminopropyl) carbodiimide
EDTA	ethylenediaminetetraacetic acid
EEA1	early endosomal antigen 1
EET	early endosome targeting domain; protein domain of Rabex-5
e.g.	*exempli gratia* (for example)
EGF	epidermal growth factor
EGFR	EGF-receptor
EGTA	ethylene glycol tetraacetic acid
ER	endoplasmatic reticulum
ESI	electro spray ionisation
FA	formic acid
FBLD	fragment based lead discovery
f.c.	final concentration
FCS	fetal calf serum
FITC	fluorescein isothiocyanate
FL	full length
FPLC	fast protein liquid chromatography
g	gram
g	gravitational acceleration, $9.8 \ m/s^2$
GAP	GTPase activating protein
GDP	guanosine-5'-diphosphate
GEF	guanine nucleotide exchange factor
GST	gluthathione-S-transferase
GTP	guanosine-5'-triphosphate
GppNHp	guanosine-5'-(($\beta\gamma$)-imino)-triphosphate; non-hydrolysable GTP
GTPγS	guanosine 5'-(γ-thio)-triphosphate; non-hydrolysable GTP
GTPγ^{35}S	GTPγS radioactively labelled with ^{35}S
h	human
HA	human influenza hemagglutinin, aa98-106, used as tag
HB	helical bundle, protein domain of Rabex-5
HCCA	α-cyano-4-hydroxycinnamic acid
HCl	hydrochloric acid
HeLa cells	cervical cancer cell line (derived from patient Henrietta Lacks)
Hek cells	Human embryonic kidney 293 cells
Hepes	2-(4-(2-hydroxyethyl)-piperazin-1-yl)-ethanesulfonic acid
His	histidine
HPLC	high-performance liquid chromatography
HRP	horseradish peroxidase
hr(s)	hour(s)
HTS	high-throughput-screening
hyg	hygromycin
IC$_{50}$	half maximal inhibitory concentration
i.e.	*id est* (that is)
IPTG	isopropyl β-D-1-thiogalactopyranoside
ITC	isothermal titration calorimetry
JIP4	JNK (=c-Jun N-terminal kinase)-interacting protein 4
kana	kanamycin
k$_{cat}$	catalytic constant
K_d	dissociation constant
k$_{intr}$	intrinsic catalytic constant
K_m	Michaelis constant
k$_{obs}$	observed rate constant
L	litre

lac	lac operon; operon for transport and metabolism of lactose
LB	growth medium for the cultivation bacteria
logP	measure of lipophilicity: log(solute in water/solute in octanol)
M	molar
m	meter
mA	milli-Ampere
MALDI-TOF	Matrix-assisted laser desorption/ionization – time of flight
mantGDP	N-methylanthraniloyl-GDP
MBM	membrane binding motif, protein structure of Rabex-5
$MgCl_2$	magnesium chloride
min	minute
MIU	motif interacting with ubiquitin, protein domain of Rabex-5
mRNA	messengerRNA
MS	mass spectrometry
MST	microscale thermophoresis
MW	molecular weight
m/z	mass to charge ratio
NH_4HCO_3	ammonium bicarbonate
NaCl	sodium chloride
NaOH	sodium hydroxide
neo	neomycin
NGF	nerve growth factor
NHS	N-hydroxysuccinimide
Ni	nickel
NMR	nuclear magnetic resonance
nt	nucleotide
NTA	nitrilotriacetic acid
NTP	nucleoside triphosphate
OH	hydroxyl group
o/n	over night
PAA	polyacrylamide
PAGE	polyacrylamide gel electrophoresis
PBS	phosphate buffered saline
PCR	polymerase chain reaction
pH	negative decade logarithm of the hydrogen ion activity
PH	pleckstrin homology domain
pI	isoelectric point
PI	phosphoinositides
PI3K	PI3 kinase
pKa	acid dissociation constant at logarithmic scale
psi	pound-force per square inch, a unit of pressure (6895 Pa)
PSL	photostimulated luminescence
R5BD	Rab5 binding domain of Rabaptin-5
Rabankyrin-5	Rab5 binding and ankyrin repeats containing protein
Rab5	Ras-related in brain-5, GTPase
Rabex-5	Rabaptin-5-associated exchange factor for Rab5 (alternative name: RabGEF1)
RabGGT	Rab geranylgeranyl transferase
Rac	Ras-related C3 botulinum toxin substrate, Rho GTPase
Ras	Rat sarcoma, GTPase
RBD	Ras binding domain
RME-6	Receptor-mediated endocytosis protein 6
RFU	relative fluorescence units

Rho	Ras-like GTPase
RTK	Receptor tyrosine kinase
RNA	ribonucleic acid
RNAi	RNA interference
RPMI	RPMI-1640, cell culture medium for mammalian cells; developed at the Roswell Park Memorial Institute (RPMI)
rpm	revolutions per minute
RT	room temperature
RUZ	Rabex-5 ubiquitin binding zinc finger, protein domain of Rabex-5
s	second
SalI	restriction site of SalI enzyme
SAR	structure activity relationship
SD	standard deviation
SDS	sodium dodecyl sulphate
SEC	size exclusion chromatography
Secin	Sec7-inhibitor; small molecule inhibitors targeting Cytohesin GEFs
SEM	standard error of the mean
SH	thiol group
siRNA	small interfering RNA
SNARE	Soluble N-ethylmaleimide sensitive factor attachment protein receptor
SOC	SOB (super optimal broth) medium supplemented with 20 mM Glucose
SPR	surface plasmon resonance
Strep	Steptavidin
t	time
T7 promotor	promotor for T7 polymerase (derived from phage T7)
TBE	Tris borate EDTA buffer
TCA	trichloroacetic acid
TE	Tris EDTA buffer
TEMED	N,N,N',N'-tetramethyl-ethane-1,2-diamine
tet	tetracycline
TFA	trifluoroacetic acid
Tiam-1	T-cell lymphoma invasion and metastasis-1 protein
Tris	Tris-(hydroxymethyl)-aminomethan
tRNA	transfer RNA
Trp	tryptophan
u	unit
U87 cells	human glioblastoma cell line, also known as U87-MG
UIM	Ubiquitin-interacting motif, protein domain of Rabex-5
UV	ultraviolet
V	volt
Vav-1	Proto-oncogene vav, RhoGEF
vs.	versus
v/v	volume percent (volume per volume)
w.c.	working concentration
wrt	with respect to
wt	wildtype
w/	with
w/o	without
w/v	weight per volume
w/w	weight per weight
Z'	Z-factor, screening window coefficient in absence of compounds

LIST OF FIGURES

LIST OF TABLES

XIII

ZUSAMMENFASSUNG

Die GTPase Rab5 reguliert zentrale Funktionen des frühen endosomalen Transportweges. Die Aktivität von Rab5 wird durch vielzählige GTP-Austauschfaktoren, die den Austausch von GDP zu GTP katalysieren, kontrolliert. Allerdings ist die genaue Rolle einzelner GTP-Austauschfaktoren, wie Rabex-5, an der Steuerung der verschiedenen Rab5 Effekte bislang ungeklärt. Kleine organische Moleküle, die als Inhibitoren der Rab-GTP-Austauschfaktoren fungieren, könnten eingesetzt werden, um die komplexen Funktionen von Rab5 aufzuklären. Jedoch sind bislang keine Substanzen bekannt, die Rab-GTP-Austauschfaktoren spezifisch hemmen. Daher ist unklar, ob diese Proteinklasse überhaupt mit niedermolekularen Inhibitoren moduliert werden kann.

Diese Arbeit stellt die Identifizierung und Charakterisierung des ersten Inhibitors für Rabex-5 vor. Eine Bibliothek mit 13000 Substanzen wurde in einem Screening getestet. In dem Screening wurde der Rabex-5 katalysierten Nukleotid Austausch an Rab5 in einem fluoreszenzbasierten Assay detektiert. Dabei wurde die Substanz JH5 sowie weitere Primärhits identifiziert. Die Aktivität der vielversprechendsten Hits wurde in einem unabhängigen radioaktiven Nukleotid-Austausch-Assay verifiziert. In der anschließenden *in vitro* Charakterisierung von JH5 konnte gezeigt werden, dass JH5 mit einer K_d von 2.6 µM an Rabex-5 bindet und dadurch die Aktivierung von Rab5 inhibiert. Im Vergleich zu den bekannten niedermolekularen Inhibitoren anderer GTP-Austauschfaktoren, welche Affinitäten im mittelern mikromolaren Bereich besitzen, ist JH5 einer der affinsten Inhibitoren. Obwohl die katalytischen Domänen der verschiedenen GTP-Austauschfaktoren strukturelle Ähnlichkeiten aufweisen, ist es gelungen, einen Inhibitor zu identifizieren, der den Rabex-5 vermittelten Nukleotid-Austausch selektiv unterbindet. Der Rho-GTP-Austauschfaktor Vav-1, der Rab-GTP-Austauschfaktor DrrA und der Arf-GTP-Austauschfaktor Cytohesin-2 werden nicht von JH5 inhibiert. Unter diesen Proteinen stellen Cytohesin-2 und DrrA die stringenteren Kontrollen dar, da ihr katalytischer Mechanismus dem von Rabex-5 ähnelt.

Untersuchungen der Struktur-Aktivitäts-Beziehungen von JH5 legten nahe, dass die Thiol-Gruppe an Position 3 des zentralen 1,2,4-Triazol-Zentrums von entscheidender Bedeutung ist. Da die Zugabe des Reduktionsmittels Dithiothreitol JH5 inaktiviert, wurde ein kovalenter Wirkmechanismus vermutet. Massen-Spektrometrie-Analysen und Rabex-5 Cystein-zu-Serin-Mutanten deuteten auf eine Interaktion von JH5 mit einem der C-terminal positionierten Cystein-Reste in der katalytischen Domäne von Rabex-5 hin. Obwohl die zelluläre Anwendbarkeit von JH5 noch nicht bewiesen ist, zeigt die Entdeckung dieses Moleküls, dass Rab-GTP-Austauschfaktoren geeignete Zielstrukturen für die Entwicklung von kleinen organischen Molekülen als Inhibitoren sind. Die hohe Affinität von JH5 bei exzellenter Spezifität gegenüber anderen GTP-Austauschfaktoren machen JH5 zu einem vielversprechenden Werkzeug für die Analyse der biologischen Funktionen von Rabex-5 und Rab5. Des Weiteren stellt JH5 eine Leitstruktur für Optimierungen sowie einen Ausgangspunkt für virtuelle Screenings dar, aus denen noch potentere Substanzen hervorgehen sollten. Diese werden der Aufklärung der komplexen Funktionen von Rabex-5 und Rab5 in (patho-)physiologischen Systemen dienen.

ABSTRACT

The small GTPase Rab5 is a key regulator in the early endocytic pathway. The activity of Rab5 is controlled by numerous guanine nucleotide exchange factors (GEFs), which catalyse the exchange of GDP for GTP. However, the precise role of specific GEFs, e.g. Rabex-5, for the regulation of certain Rab5 functions remains to be solved. Small molecule inhibitors that target Rab5GEFs could be used to unravel the complex regulation of Rab5. For none of the RabGEFs a specific small molecule inhibitor is available, despite their interesting biological role. Hence, it is questionable whether these proteins represent a class of druggable targets.

In this thesis, the identification and characterization of the first small molecule inhibitor of Rabex-5 is reported. The inhibitor was identified in a screening approach that monitored the Rabex-5-catalysed nucleotide exchange on Rab5 in a fluorescence-based assay. Screening of a library containing 13,000 compounds yielded the small molecule JH5 among several other primary hits. The activity of the most promising hits was confirmed in an independent radioactive nucleotide exchange assay. The *in vitro* characterization of JH5 revealed that this compound inhibits the Rab5 activation by binding to Rabex-5 with a K_d of 2.6 µM. This affinity is among the strongest compared to the already reported ArfGEF and RhoGEF inhibitors with activities in the mid-micromolar range. Although various GEF domains show structural similarities, it was possible to identify a small molecule that can selectively inhibit the Rabex-5 nucleotide exchange. The nucleotide exchange of the RhoGEF Vav-1, the RabGEF DrrA and the Arf1GEF Cytohesin-2 was not disturbed by JH5. Among these, Cytohesin-2 and DrrA represent the most stringent controls because they act by a catalytic mechanism which is similar to that of Rabex-5.

Investigation of the structure activity relationship of JH5 revealed the importance of the thiol group at position 3 of the central 1,2,4-triazole core. Since addition of the reducing agent dithiothreitol abolished the activity of JH5, a covalent binding mechanism was suspected. Mass spectrometry analysis and Rabex-5 cysteine-to-serine-mutants revealed that JH5 might indeed interact with one of the C-terminal positioned cysteines of the Rabex-5 GEF domain. Although the proof for the intracellular applicability of JH5 is pending, its identification and characterization supports the hypothesis that RabGEFs are suitable targets for the development of specific small molecule inhibitors. Due to the combination of high affinity with excellent specificity over other GEFs, JH5 is a promising lead compound for the investigation of Rabex-5 and Rab5 biology. Moreover, JH5 provides a starting point for lead optimization or virtual screening approaches, which are likely to yield even more potent compounds. These can assist in unravelling the complex role of Rabex-5 and Rab5 in health and disease.

1 INTRODUCTION

1.1 Cellular homeostasis and communication in living organisms

All the diverse living organisms on our planet share a common building block: they consist of cells. There are unicellular organisms like archaea or most bacteria and multicellular organisms like plants and animals. These organisms have in common that their cells are surrounded by a plasma membrane which is the boundary towards the extracellular environment. This enables the maintenance of intracellular homeostasis but this border has to be flexible enough to allow integration of signals from the environment and transport of all kinds of molecules over the membrane, e.g. nutrients or ions.

Eukaryotic cells are further compartmentalized into membrane-enclosed organelles that differ in morphology, content, and function. Between these compartments extensive transport processes are taking place which have to be conducted specifically and with high fidelity. The transport is achieved by the use of spherical or tubular membrane enclosed transport containers called vesicles. Besides the transport of vesicle content (cargo), parts of the membrane that build the vesicle are removed from the donor compartment and added at the acceptor compartment. Thereby the composition of proteins and lipids at both membranes is changed.

To maintain the cellular homeostasis constantly and under all environmental conditions, cells have to adapt to the environment. Cells express a variety of membrane receptors to sense extracellular signals, e.g. the presence of growth factors, and adapt accordingly. Upon receptor activation by ligand binding, the intracellular signal transduction machinery triggers changes in gene regulation, protein expression or protein activation states. The receptors are often internalized in vesicles after activation, either to terminate the signalling or to change the quality of the signal.[1, 2] Several signalling pathways and complex networks contribute to the precise regulation of basic cellular functions at all times which is important since defective regulation may lead to pathological conditions.

In this context small GTPases of the Ras superfamily are noteworthy: these proteins can regulate signalling pathways and integrate the signals of the receptors. Furthermore, small GTPases are controlling vesicular transport and define intracellular compartments. Since defective regulation of small GTPases leads to pathological conditions, they are attractive targets for the development of small molecule modulators, i.e. inhibitors or activators. These modulators could not only be used as therapeutics but also as tools to elucidate the complex protein networks in which GTPases are involved in.

This work aims for the identification of an inhibitor for the Rabex-5 mediated Rab5 activation. Thus, after a brief introduction of GTPases and GEFs in general (Section 1.1.1 and 1.1.2), Section 1.2 focusses on Rab GTPases - the family Rab5 belongs to. Detailed information on Rab5 and Rabex-5 is presented in Section 1.3 and 1.4. The introduction closes with a description of the currently available inhibitors and a discussion about the use of inhibitors for the investigation of GTPase and GEF biology (Section 1.5).

1.1.1 Small GTPases regulate signalling and vesicular transport

Proteins of the Ras superfamily of small GTPases are often referred to as molecular switches.[3] They are proteins that are able to bind and hydrolyse GTP thereby cycling between an active, GTP (guanosine triphosphate) loaded, and an inactive, GDP (guanosine diphosphate) loaded state (Figure 1A).[4] In their active form they can bind effector proteins which triggers signalling cascades or other cellular effects (Figure 1B).[5] The switching process is tightly regulated by GEFs (guanine nucleotide exchange factors) and GAPs (GTPase activating proteins).[6] GEFs catalyse the exchange of GDP for GTP and consequently facilitate the switch of the GTPase to an active state.[7] GAPs stimulate the hydrolysis activity of the GTPase resulting in a GDP-loaded, quiescent GTPase.[8]

The Ras protein was the founding member of the family of small GTPases, discovered about 30 years ago.[9] Ever since it was revealed that Ras mutations are strongly involved in cancer this protein and its relatives have been studied extensively.[10, 11] The superfamily of small GTPases is grouped into five families: the Ras, Rho, Rab, Arf and Ran family.[12] Ras GTPases control cytoplasmic signalling networks transporting extracellular stimuli which trigger changes in gene expression for regulation of cell proliferation, differentiation and survival.[12] Signal transduction by Rho GTPases influences the cytoskeleton, membrane transport pathways and transcription.[13] Intracellular trafficking of proteins, vesicular transport and regulation of endocytic pathways are managed by Rab and Arf proteins.[14, 15] The smallest family is the Ran GTPase with a single member[12] that controls transport through the nuclear pore and organization of the mitotic spindle.[16]

1.1.2 Activation of small GTPases enables effector binding

To be activated by GEFs, the GTPase has to be recruited to its target membrane.[17-20] Subsequently, it is activated by the GEF and can bind effector proteins (Figure 1B).

In particular, GEFs assist the GTPase in the release of the bound nucleotide and hence the exchange is not specific for GDP or GTP.[21] However, GTP is about ten times more abundant in the cell than GDP and the re-association with GDP is prevented by high GTP concentrations.[21, 22] The mechanisms of several GEFs, though they are distinct in structure, are thought to have common actions. The nucleotide binding involves the switch regions (switch I, switch II) and the phosphate binding loop (P-loop) of the GTPase (Figure 2).[3] To release the nucleotide from the GTPase, an intermediate ternary complex is formed between GTPase, nucleotide and GEF.[3] In this complex, the affinity of the GTPase towards both interaction partners is weaker than in a binary complex with either one of the ligands (nucleotide or GEF) resulting in accelerated nucleotide release from the GTPase.[22, 23] The breakdown of the ternary complex is achieved by GEF-triggered structural rearrangements of the nucleotide binding site and displacement of the Mg^{2+} ion resulting in the dissociation of the nucleotide.[3, 23]
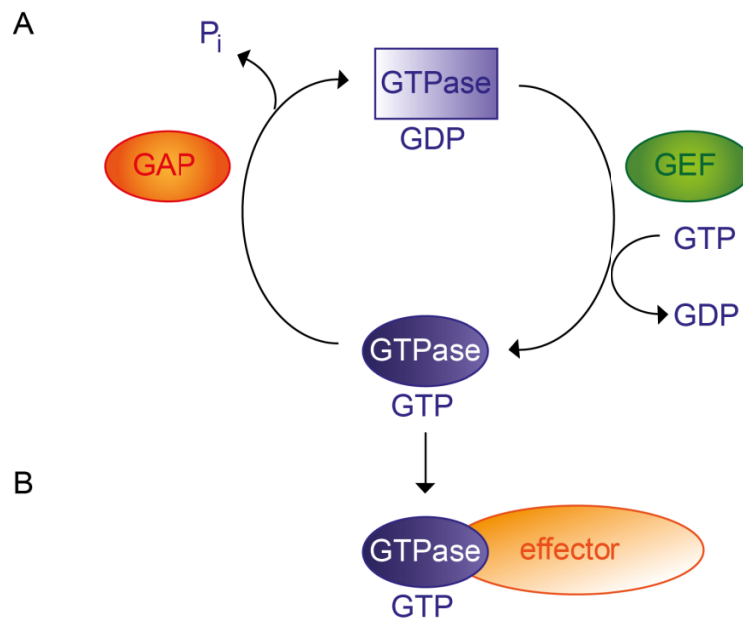
Figure 1   Small GTPases act as molecular switches.
A) The small GTPase is active when it is GTP bound in its nucleotide binding pocket, and inactive with GDP bound. These two states are highly regulated by GEFs and GAPs. The GAPs stimulate the hydrolysis of the GTP nucleotide and the GEFs catalyse the exchange of GDP for GTP. **B)** In the active state, the small GTPase can bind effector proteins which are important for the cellular functions of the small GTPase.
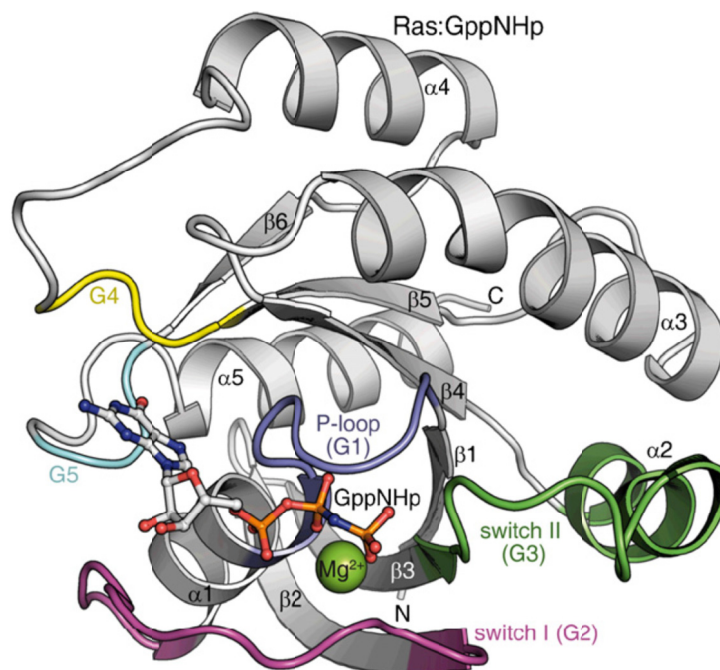
Figure 2   Overview of the 3D structure of H-Ras in complex with the non-cleavable GTP analogue GppNHp.
Rab, Arf and Rho GTPases have the same basic secondary structure elements and G1–G5 regions. […] Reprinted from Seminars in Cell & Developmental Biology, Volume 22, Issue 1, Aymelt Itzen, Roger S. Goody, GTPases involved in vesicular trafficking: Structures and mechanisms, Pages 48–56, Copyright (2011), with permission from Elsevier.
The Mg^{2+}-ion is depicted as a green ball and the nucleotide is shown in ball-and-stick presentation. The protein is illustrated as ribbon drawing. Conserved regions for the coordination of nucleotide and Mg^{2+}-ion are highlighted in blue (P-loop), purple (switch I), green (switch II) and light blue and yellow. The switch regions and the P-loop coordinated the nucleotide and the Mg^{2+}-ion.[3]

By interaction with its effector proteins the GTPase promotes its biological functions like transmission of signals to downstream targets. Effector proteins bind to the areas of the GTPase that depend most on the nucleotide state, which are the switch I, the switch II and the interswitch regions.[23] In general, it seems that these structures are more defined in the presence of GTP and then effector binding is favoured.[23] Another observed mechanism is the exposure of a hydrophobic patch upon GTP binding.[23] Ras proteins mainly use the switch regions for effector interaction while Rab GTPases have additional areas for interaction with the effector.[24, 25] These complementarity determining regions differ between distinct Rabs but remain unaltered upon GTP uptake.[26] Thus, Rab effectors recognize a combination of nucleotide-dependent and Rab-dependent areas which ensure that the correct and active Rab is bound.[26]

A sophisticated network of regulators and effectors together with the accurate localization of the GTPase enables these proteins to function as modulators of an extensive number of diverse cellular processes. They allow the cells to transport signals and molecules in an appropriate manner and thereby adapt to extracellular environmental challenges.

1.2   Rab GTPases control membrane traffic

With over 60 members in mammals, the family of Rab (<u>Ra</u>s like proteins in <u>b</u>rain) GTPases is the biggest subdivision of the Ras superfamily.[12, 24] The Rab GTPases control consecutive stages of vesicular trafficking along all cellular compartments like endosomes, Golgi, endoplasmatic reticulum (ER) and lysosomes.[27] The individual Rabs are associated with particular compartments and ensure specificity in the transport processes.[27] Although the general mechanisms of Rab biology are fairly understood, the complex cooperation of these GTPases with their GEFs, GAPs, and effectors remains ambiguous. Small molecule inhibitors can be used as excellent tools to study protein biology, but neither for Rab GTPases nor for RabGEFs a sufficient amount of small molecule tools is available.[28] This emphasises the need for novel tools to study Rab GTPase and GEF biology. To understand the biology of Rab GTPases it is inevitable to establish small molecule inhibitors. In the following sections the several aspects of general Rab function in membrane traffic, which are important to understand the context of Rab5 and Rabex-5 biology, are presented. This comprises the endocytic pathway (Section 1.2.1) and the formation of Rab microdomains on the membrane of organelles (Section 1.2.2). In order to operate precisely, Rab proteins have to be correctly localized (Section 1.2.3) and cycle between distinct activation states (Section 1.2.4).

1.2.1   The endocytic pathway

Endosomes are membrane-bound compartments of eukaryotic cells that can be grouped into early endosomes, late endosomes and recycling endosomes.[29, 30] These organelles are involved in the endocytic pathway performing the internalization of molecules for recycling and degradation. Thereby the composition of the plasma membrane,[31] the

intracellular homeostasis and signalling are controlled.[30] In mammalian cells extensive parts of the cellular surface are endocytosed and recycled, e.g. fibroblasts internalize the equivalent of 50 % of their plasma membrane during one hour.[32]

Endocytosis is the general term for internalization of extracellular molecules and plasma membrane components by formation of vesicles.[33, 34] There are several forms of endocytosis based on diverse mechanism and vesicle types.[35] In this work, the term endocytosis refers to the clathrin mediated endocytosis if not stated otherwise. Clathrin is a triskelion-shaped protein complex that assembles with adapter proteins to form the coat of vesicles.[36] After the fission of the endocytic vesicles from the plasma membrane the coat disassembles and the vesicles are transported to the early endosomes for fusion.[37] Proteins can be transported along the endocytic pathway from the plasma membrane via the early endosomes to the late endosomes (Figure 3).[30] The transport from the late endosomes is directed towards the lysosomes,[34] the organelles that degrade proteins and organelle-debris.[27] The early endosomes are also known as sorting endosomes.[38] From here, cargo can take distinct routes. Instead of being transported via the late endocytic pathway towards degradation, molecules can be recycled back to the plasma membrane in recycling endosomes.[39] Further transport processes take place between the endosomes and the Golgi or ER.[40]

All these transport processes are performed by the use of vesicles (Figure 3, Insert). The budding and delivery of vesicles requires coat proteins, sorting adaptors, motor proteins, kinases, phosphatases, tethering factors and SNAREs (Soluble N-ethylmaleimidesensitive factor attachment protein receptors) which are all coordinated by Rab GTPases.[41] Tethering factors enable the catching of vesicles when these arrive at the acceptor membrane and this process depends on Rab effectors.[14, 27] Vesicle fusion is mediated by the SNARE complex.[42] Located on the vesicle and the destination membrane, the SNAREs build intertwined complexes bringing the membranes in close proximity to mediate fusion.[43]

1.2.2 Rab microdomains define organelles

Every cellular compartment in the endocytic pathways is associated with a specific set of Rab GTPases, e.g. the early endosomes are characterized by high Rab4, Rab5 and Rab11 expression.[15, 44, 45] Therefore, Rab proteins are considered to be markers for the individual compartments (Figure 3). In fact, they facilitate the assembly of other proteins that altogether define the identity of compartments.[26] The correct identity of different organelles ensures that transport processes are regulated in an accurate manner and vice versa.

The organelles are even further subdivided into functional microdomains by local protein-protein assemblies.[26] In case of the early endosomes, the three GTPases are located in separate Rab-specific domains.[15, 45] The detailed description of the Rab5 microdomain will be revisited in Section 1.3.2. It was suggested that effector proteins contribute to the stabilization of the Rab-domains by amplifying the local Rab activation.[41] For example, the effectors Rabpatin-5 and Rabenosyn-5 interact with Rab5

and Rab4 and this dual interaction is referred to as effector coupling.[46, 47] Effector coupling is thought to integrate and fine tune Rab action and localization of different Rab proteins that work on the same membrane compartment.[41] Since Rab4 is essential for the recycling of receptors to the plasma membrane, dual Rab4-Rab5 effectors potentially regulate the fine tuning of recycling endosome formation.[37, 48] Thereby, the sequential regulation of transport through the endocytic pathway is ensured.[40]
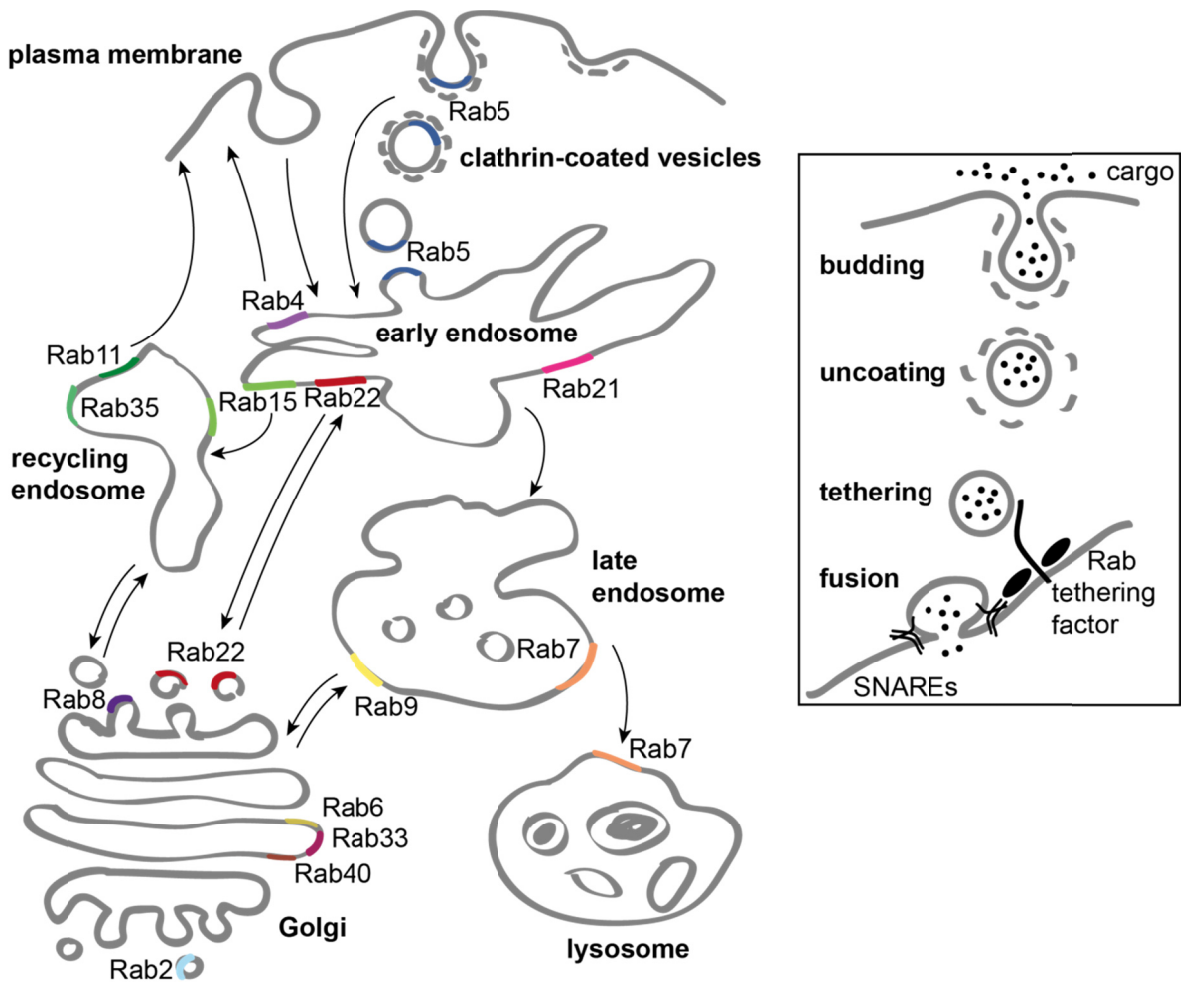
Figure 3   The endocytic pathway.
The endocytic pathway mediates the internalization of molecules for recycling or degradation. It is part of the intracellular membrane traffic system connecting all organelles. Via endocytosis, e.g. in clathrin-coated vesicles, molecules are taken up and transported to the early endosomes. From here, they are distributed to the recycling endosome, to the Golgi or to the lysosome via the late endosome. The pathway along the recycling endosome transports molecules back to the plasma membrane. The arrows indicate transport routes. Specific Rabs are localized to individual compartments (Rabs are indicated in colours). Rab5 (blue) is localized to early endosomes, clathrin-coated vesicles and the plasma membrane. The early endosome also contains Rab21 (pink), Rab22 (red), Rab4 (purple), and Rab15 (light green). Rab22 mediates transport to and from the Golgi, and Rab4 the recycling to the plasma membrane. Rab15 contributes to trafficking to the recycling endosome on which Rab11 (green) and Rab35 (dark green) regulate the slow endocytic recycling. The Golgi-localized Rabs are Rab2, Rab6, Rab8, Rab33 and Rab40. Rab7 (orange) and Rab9 (yellow) reside on late endosomes and control the route to the lysosome and the Golgi, respectively. **Insert:** Zoom to the process of vesicle budding and fission from the donor compartment with subsequent uncoating, docking and fusion at the acceptor compartment. Indicated proteins are cargo (black dots), coat/adaptor proteins (grey dotted lines), Rab GTPase (black oval), tethering factors (black line) and SNAREs (black bundle). The Figure is partially (Rab localization) adapted from [41].

1.2.3 Membrane localization is essential for Rab function

As indicated in the previous sections, the correct localisation of Rabs to their individual compartments ensures the fidelity of transport processes.[18] Membrane localization requires definition of the correct destination (specific membrane localization) and anchorage of Rab at the membrane (membrane binding).

For membrane anchorage, many small GTPases carry a prenylation at the C-terminus.[12, 49] In case of the Rab proteins, the association with the membrane is facilitated by two geranylgeranyl groups that the Rab GGTase (geranylgeranyltransferase, also called GGTase II) attaches.[23, 50] The prenylation attachment by the Rab GGTase is supported by the Rab escort protein. The Rab escort protein binds the unprenylated Rab, assists the Rab GGTase and subsequently accompanies the prenylated, mainly GDP-loaded Rab protein to the membrane.[51, 52]

The C-terminal hypervariable domain of Rabs was the first domain of these proteins implicated in membrane binding and specific localization.[53-55] However, the importance of the hypervariable domain for determination of the specific Rab destination was challenged recently.[56] Ultimately, multiple domains of the Rab proteins might be involved in defining the membrane destination in addition to the hypervariable domain.[18, 56]

Further regulation of the specific Rab membrane localization is achieved by interaction with other proteins. The GDI (GDP dissociation inhibitor) proteins can prevent interaction of GTPases with the plasma membrane by masking the prenyl modification (Figure 4).[12, 57] The Rab GDI prefers Rab-GDP, stabilizes the GDP-form, and shuttles the GTPase back to its compartment of origin after vesicle fusion.[26, 41] During the interaction of the Rab and its GDI, no nucleotide exchange can take place.[58] The GDI is surely important for solubilizing and storing the cytosolic pool of Rabs,[59] but regarding the targeting of Rabs to their destination the influence of the GDI is less plain. Since only two GDI isoforms are known to date, the question has to be raised how the diverse Rabs are specifically shuttled to the correct compartment.[41, 60] For endosomal Rab proteins (Rab5, Rab7, Rab9) a GDI displacement factor (GDF) was described that can release the GTPase from its GDI.[58, 61] However, no further GDFs have been discovered, yet. Thus, the idea of GDI and GDF as mediators of correct membrane targeting cannot be assumed to be a general mechanism. Recently, GEFs and effector proteins were suggested to be involved in membrane targeting and localization of Rabs.[62, 63] They provide another level of regulation of Rab-membrane-association.

Although several mechanisms of membrane targeting have been described, for many Rabs the exact mechanisms remain to be fully understood and a general mechanistic understanding awaits discovery.[64] Possibly, diverse mechanisms control the correct membrane localization of the different Rab proteins.[18] Especially the recent implications of GEFs in Rab membrane localization [62, 63] emphasise the urge for in depth understanding of GEF biology.
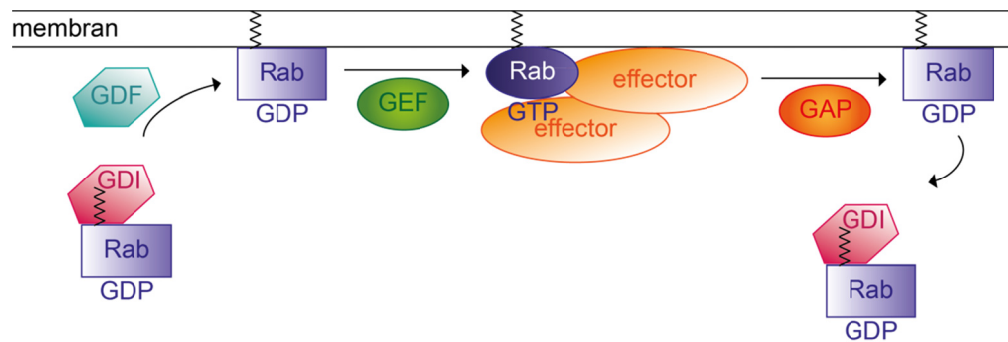
Figure 4   Rab GTPases cycle between membrane and cytosol.
Rab GTPases (blue) cycle not only between active (GTP bound) and inactive (GDP bound) states as depicted in Figure 1 but also between membrane bound and cytosolic states. The inactive Rab GTPase present in the cytosol is in complex with GDI (dark red) that masks the prenylation and keeps Rab soluble in cytosol. The membrane attachment of Rab is supposed to be enabled by a GDF (aquamarine) which facilitates the dissociation of Rab and the GDI. At the membrane, a GEF (green) can catalyze the nucleotide exchange of GDP for GTP and the active Rab subsequently binds its effector proteins (orange). Specific GAPs (light red) accelerate the hydrolysis of GTP to GDP and the inactive Rab can be extracted from the membrane by GDI. This Figure is adapted from [5].

1.2.4   Rabs cycle between membrane bound and cytosolic states

After being shuttled to the target membrane the activity of the GTPase is regulated by GEFs and GAPs (Figure 4).[5, 27, 65] The GTP-GDP cycle works as a timer and is important for the temporal regulation of fusion and transport events.[14, 26, 66] This observation highlights the role of GEFs in the regulation of transport processes.

Certainly, the number of known RabGEFs is surprisingly small with respect to the size of the Rab family.[23] *In silico* prediction of new RabGEFs is complicated by the fact that the few RabGEFs identified so far differ more in their structure among each other than e.g. the RhoGEFs.[23] Nevertheless, it is likely that more RabGEFs will be discovered in the future. However, the known RabGEFs are highly conserved among different species: for example the known Rab5GEFs all contain a Vps9 domain.[24]

With the help of GAPs, the Rabs are turned back into the inactive state and can be retrieved from the membrane by RabGDI proteins to be available for the next cycle.[18, 65] It was speculated that Rabs in heterotypic fusion events have to be retrieved from the target membrane which is not their original location.[26] On the contrary, in homotypic fusion events the GTPase might undergo several GTP-GDP cycles before being released from the membrane.[26]

In summary, the Rab proteins cycle not only between active and inactive state as described earlier (Section 1.1.1) but also between cytosolic and membrane bound state.

1.3   Rab5 is a master regulator of early endosomes

As described in Section 1.2.1, the early endosomes pose a key position within the protein trafficking pathways.[67] At the early endosomes, vesicles from the plasma membrane arrive and the cargo is sorted.[40] The cargo can be directed back to the plasma membrane

for recycling, transported to the trans-Golgi-network for retrieval, or to the lysosomes for degradation.[67, 68] Rab5 controls the early steps in the endocytic pathway and the fusion of vesicles at the early endosomes is dependent on Rab5 activity.[69-71]

The Rab5 subfamily consists of Rab5a, Rab5b, Rab5c, Rab17, Rab21, Rab22a and Rab22b (=Rab31).[6] The three Rab5 isoforms (Rab5a-c), which are highly conserved in sequence, localization, and function, are ubiquitously expressed in adult mouse tissue.[71] Rab21 and Rab22 are most closely related to Rab5 [24] and are also localized at the early steps of the endosomal pathway with additional functions in Golgi traffic.[72-75]

Absence of Rab5 has a dramatic effect: in *C. elegans* a knockdown was found to be embryonic lethal [76] and no Rab5 knockout mouse has been described to date.[72] These observations underline the importance of Rab5. The variety of distinct Rab5 functions known to date will be presented in the following sections. Rab5 activity is tightly connected with several GEFs and effector proteins (Section 1.3.1) that interact in a sophisticated manner to form distinct Rab5 microdomains (Section 1.3.2). Rab5 is essential in the transport process of vesicles (Section 1.3.3) but has additional functions in cytoskeleton dynamics, mitosis and signalling (Section 1.3.4).

1.3.1　　GEFs activate Rab5 to interact with effector proteins

The intrinsic exchange rate of Rab5 is slow [77] and Rab5 activity is fine-tuned by numerous GEFs. Yet the precise contribution of specific GEFs to the regulation of diverse Rab5 functions is not completely understood. The family of Vps9-domain proteins comprises GEFs for the Rab5 subfamily and has a growing number of members. In the SMART database [78] nine Vps9 domain proteins were reported in 2006.[79] In November 2012 there were 39 potential human proteins containing Vps9 domains listed (see Appendix, page 156). The GEF activity for GTPases of the Rab5 subfamily is confirmed for ten proteins: Rabex-5 [80], RIN1-3 (Ras and Rab interactor 1-3) [81-83], RIN-like [84], ALS2 (Amyotrophic lateral sclerosis 2) [85], ALS2CL (ALS2 C-terminal like) [86], hRME-6 (human homologue of *C. elegans* receptor-mediated endocytosis protein-6, also known as Gapex5) [87, 88], VARP (Vps9 domain-ankyrin-repeat protein) [89] and RAP6 (Rab5-activating protein 6) [90] and it is likely that more will follow.

In addition, over 20 Rab5 effector proteins have been identified.[91] Several Rab5 effectors will be introduced in the following sections. Some general information will be given here briefly to facilitate the reader's comprehension. The Early Endosome Antigen 1 (EEA1) and Rabenosyn-5 are tethering factors implicated in the docking of the vesicle at the acceptor membrane.[71, 92-94] In addition, Rabaptin-5 interacts with the GEF Rabex-5.[80, 95] hVps34 is a phosphatidyl-inositol-3-kinase (PI3K) that generates phosphatidyl-inositol-3-phosphate (PI3P).[96, 97] The complex interplay and the biological relevance of Rab5 and its effectors will be discussed in the subsequent sections. The GEF that is relevant in this study is Rabex-5. All Rabex-5 related Rab5 information will be given in Section 1.4. An exception is the Rabex-5 contribution to the formation of Rab5 microdomains which is discussed in the following section.

1.3.2   Rab5 effectors form a network of complex interaction

1.3.2.1   A positive feedback loop to establish local Rab5 microdomains

Evidence that active Rab5 microdomains are present on the early endosome comes from the observation that Rab5 is 15 to 20 fold more abundant than Rabex-5 or Rabaptin-5.[95] The Rab5 microdomains are likely established by the cooperativity of Rabex-5 and Rabaptin-5 working in an effector loop.[77, 95] Positive feedback loops produce locally high amounts of activated Rab (Figure 5).

Rabaptin-5 is found on early endosomes and clathrin-coated vesicles; on the early endosomes its presence seems to intensify recruitment of EEA1.[98] Rabaptin-5 is recruited to the early endosomes by interaction with Rabex-5 and Rab5.[95] Rabex-5 has a dual role in Rab5 activation and Rabaptin-5 interaction.[80, 95] Thereby, the Rabaptin-5 interaction with Rab5-GTP is intensified and results in a positive feedback loop. Thus, efficient effector binding and GEF activity in a concentrated spot increase the number of Rab5-GTP proteins and effectors with every GTP-GDP cycle. Finally, a functional Rab5 microdomain is created.[5]
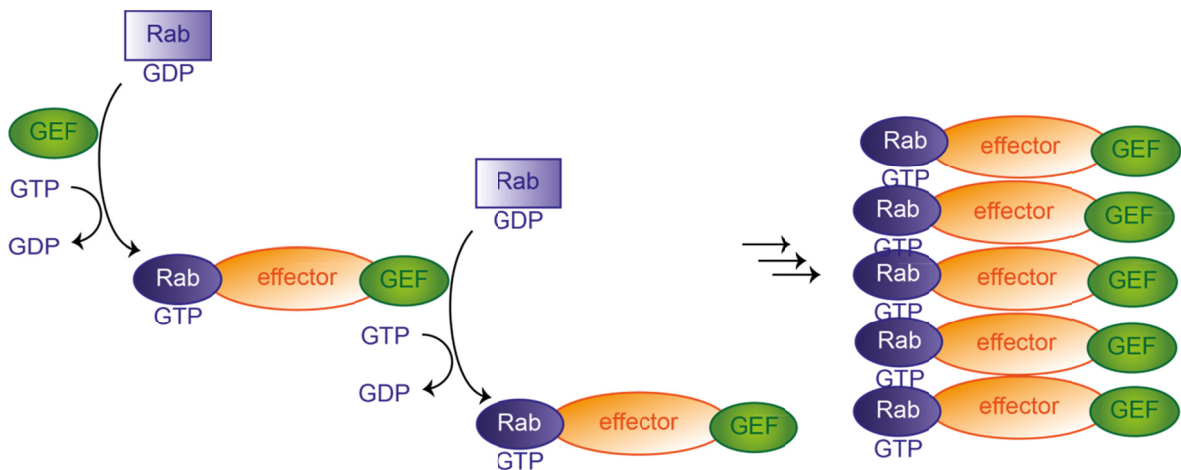
Figure 5   GEF-effector loop produces locally high amounts of active Rab.
The GEF-effector loop (or positive feedback loop) ensures the maintenance of the local activity of a certain Rab.[5] The GEF-effector loop is characterized by the interaction of a GEF (green) and an effector (orange) that both interact with the same GTPase (blue) and thus are in close proximity.[15, 41] The active Rab binds the effector and stabilizes the Rab in the GTP-bound form.[66] Since the effector also interacts with the GEF that activates additional Rabs, which in turn binds the effector, the activated GTPase state induced by the GEF is preserved and stabilized. This loop represents a positive feedback which clusters GEF activity and effector binding and results in a membrane microdomain of highly active Rab.[80, 95] This Figure is modified from [41].

A further level of stabilisation of the Rab5 microdomain is obtained by interaction with Rab5 effectors. These can form oligomers with Rabex-5 on the early endosome membrane thereby facilitating the Rabex-5-Rabpatin-5 feedback loop and stabilizing the Rab5 microdomain (Figure 6A).[99] The effector-clustering strengthens and maintains the microdomain that contributes to specificity and dynamics of the early endosome Rab5 functions.[14] In addition, the kinase hVPS34 produces PI3P which serves as docking site for Rab5 effectors containing PI3P binding FYVE domains, e.g. EEA1 and Rabenosyn-5.[14, 92] Without the hVps34 activity generating PI3P, Rab5 is not able to recruit FYVE-effectors.[96] For example, EEA1 is not present on clathrin-coated vesicles which lack PI3P.[98, 100] These observations suggest that Rab5 microdomains with locally diverse effector content are formed.[101]

1.3.2.2 *Local effector assemblies ensure specificity of Rab5 activities*

The variety of diverse Rab5 functions raises the question how these individual tasks are spatially and temporally regulated. It was suggested that the local clustering of particular effectors to Rab5 microdomains ensures accurate control of the distinct Rab5 functions by their specific composition.[14, 40] These collections of effector proteins act synergistically to mediate Rab5 functions.[102] Some examples of distinct Rab5 effector assemblies are presented briefly (Figure 6B).

The Rab5 effector proteins APPL1/2 (Adaptor protein containing PH domain, PTB domain and Leucine zipper motif) link Rab5 dependent endocytosis with signal transduction to the nucleus.[103] It is speculated that APPL patches on the early endosome represent a special form of Rab5 microdomains (APPL endosomes) which are involved in fine-tuning of signalling.[103, 104] APPL endosomes seem to be converted to classical PI3P-EEA1 positive early endosomes in the course of the endocytic pathway.[105]

EEA1 is a multi-functional effector and connects several different proteins and distinct effects. EEA1, which is only present on the membrane of the early endosomes, represents a tethering factor that provides directionality of the fusion process.[98, 101] Active Rab5 is required on both membranes engaged in fusion, e.g. clathrin-coated vesicles and early endosomes.[70, 106] The absence of PI3P from clathrin-coated vesicles explains why EEA1 is also not present.[92, 96] Thus, divergence between donor and acceptor membrane is created. EEA1 does not only interact with Rab5 but is also an effector for Rab22a [73] which represents another example of effector coupling.

Furthermore, EEA1 colocalizes with Rabankyrin-5. In absence of EEA1, Rabankyrin-5 is involved in marcopinocytosis, and places Rab5 in context of clathrin-independent internalization.[107]

In summary, Rab5 dependent events in the early endosomal pathway are highly dependent on the cooperativity of the Rab5 effectors.[40, 108] The asymmetric localisation of Rab5 effectors has additional impact on the diverse Rab5 functions. However, we are still at the beginning of understanding the exact spatio-temporal regulation and the interplay of Rab5, GEFs and effectors.
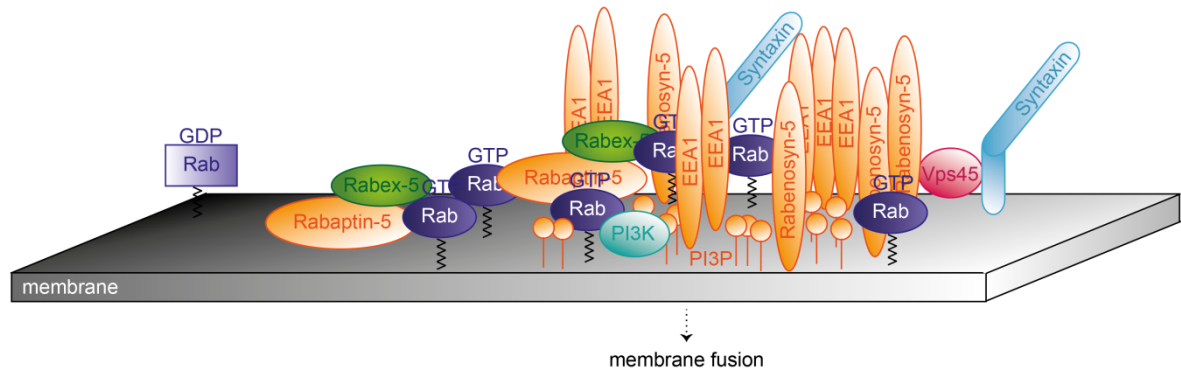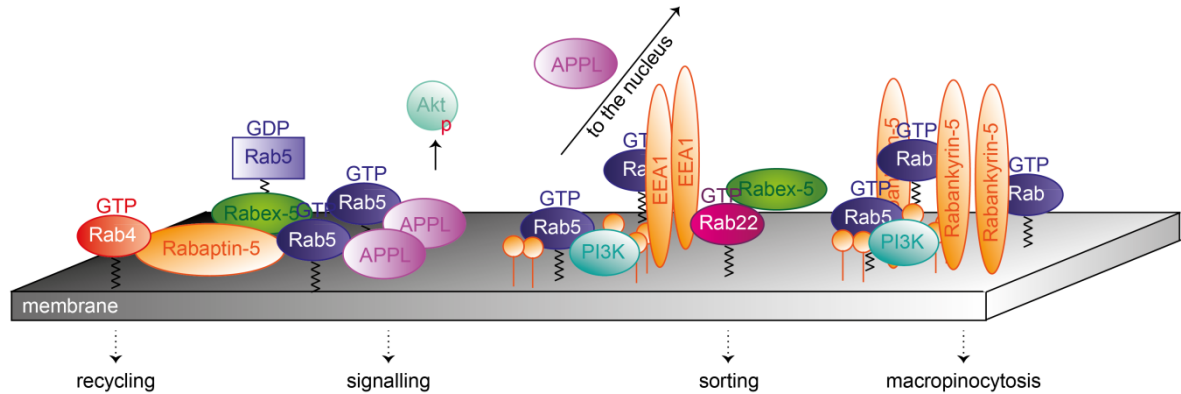
Figure 6   **Rab5 microdomain formation.**
A) Rab5 microdomains are formed by clustering of effector proteins. This process is initiated by the GEF-effector loop of Rabex-5 and Rabaptin-5 that produces high amounts of active Rab5. The Rab effector hVps34 produces PI3P that accumulates locally.[96, 97] The effector EEA1 is recruited by a combination of direct binding with Rab5 and interaction with PI3P.[92, 109] This dual role of effector recruiting (direct binding and PI3P level regulation) ensures the specificity of effector assembly.[40, 41, 110] Rabaptin-5, EEA1 and Rabex-5 form oligomeric complexes with components of the SNARE machinery (e.g. Syntaxin13) in the Rab5 microdomains, thereby creating platforms that include all proteins necessary for membrane fusion.[99] This part of the figure was adapted from [14]. **B)** Examples of distinct Rab5 microdomains with individual effects are depicted. On the left, the effector coupling provided by Rabaptin-5 is indicated. Rab4 is necessary for the recycling of receptors to the plasma membrane, and hence, Rabaptin-5 might be involved in the fine-tuning of recycling endosome formation.[37, 48] The next example depicts the Rab5 microdomain on APPL endosomes. The endosomal localization of APPL is needed for the recruitment of several downstream signalling molecules like Akt and thereby fine-tunes the affected signalling pathways.[104] In the course of the early endosomal pathway, APPL endosomes arise after vesicle fission and precede the formation of classical PI3P-EEA1 positive early endosomes.[105] Potentially, the competition between APPL and EEA1 defines different Rab5 microdomains: in presence of PI3P APPL is displaced by Rab5 effectors like EEA1, which interact with Rab5 and PI3P, while APPL is transported to the nucleus.[105, 111] EEA1 has several possible interaction partners as depicted on the right side. Via effector coupling it provides a link to Rab22a which regulates the transport from the endosomes to the Golgi and to recycling endosomes.[112, 113] It was suggested to be the Rab on the early endosomes that controls the exit of molecules.[112] The connection with macropinocytosis is created by Rabankyrin-5 that co-localises with EEA1 on early endosomes but is additionally found on pinocytic vesicles that lack EEA1.[107] How Rab5 and EEA1 are involved in vesicle fusion is illustrated in part A of this figure.

1.3.3   Rab5 controls the vesicle transport process

Rab proteins regulate essentially all steps in vesicle transport (Figure 7).[29, 41] The first stage of this process is the formation of the vesicle which requires sorting of cargo, coat assembly, invagination and finally fission of the endocytic vesicle (Figure 7A). During the transport of the vesicle, the coat is disassembled since it would interfere with the fusion at

the target membrane (Figure 7B). The transport occurs along the cytoskeleton by interaction with motor proteins and can be controlled by several Rabs (Figure 7C).[114, 115] The vesicle is docked at its destination by tethering factors (Figure 7D). Finally, the vesicle fuses with the target membrane and releases of its content (Figure 7E). After completion of the vesicle fusion the Rab GTPase is transported back to the donor compartment by GDI proteins as described above (Section 1.2.3 - 1.2.4). In the following paragraphs the impact of Rab5 on the vesicle transport to the early endosomes is described.

Rab5 was shown to be important for the invagination of clathrin-coated pits, sequestration of the ligand and endocytosis of the transferrin receptor.[116] Moreover, the effector Rabptin-5 interacts with γ-adaptin, a constituent of the clathrin coat.[36, 117] Hence, Rab5 is essential for the sorting of cargo and the invagination of the membrane to form clathrin-coated vesicles.

Rab5 is also involved in the disassembly of clathrin from these endocytic vesicles. For the coat assembly, the AP2 cargo adaptor is stabilized by interaction with phosphatidyl-inositol-4,5-bisphosphate and the phosphorylation of its µ2 subunit by the AP2-associated-kinase-1.[33, 41, 118] The Rab5 GEF hRME-6 counteracts the stabilizing effects of µ2 phosphorylation and thereby facilitates the uncoating of the vesicle.[119] In addition, the level of phosphatidyl-inositol-4,5-bisphosphate is regulated by the Rab5 effectors PI3K and PI phosphatase.[96, 120]

Motility of early endosomes is dependent on an indirect interaction of motor proteins with PI3P.[121, 122] Rab5 contributes to the regulation of transport along actin filaments and microtubules by control of PI3P.[96, 121]

Among the Rab5 effectors are tethering factors like the Early Endosome Antigen 1 (EEA1) and Rabenosyn-5 that mediate the vesicle docking.[71, 92-94] On the early endosomes, Rabaptin-5 is required for Rab5 dependent membrane docking of vesicles.[123]

Evidence for the importance of Rab5 for fusion events is based on the observation that that Rab5 overexpression results in enlarged endosomes.[69] This implicates that Rab5 is not only relevant for the homotypic fusion of endosomes but also for fusion of vesicles from the plasma membrane with early endosomes.[54, 69, 70, 98] Besides the cognate SNAREs, which are mandatory for vesicle fusion, the Rabaptin-5-Rabex-5 complex, hVps34, EEA1, Rabenosyn-5, and hVps45 are required *in vitro*.[108] These proteins are all associated with Rab5 in microdomains (Figure 6). EEA1 interacts with SNAREs like Syntaxin13 which are required for endosome fusion.[91, 99] Additional connection of Rab5 to the SNARE complex is provided by Rabenosyn-5. Rabenosyn-5 binds the protein hVps45 that interacts with the SNAREs Syntaxin4, Syntaxin6, and Syntaxin13.[93, 124]

The Rab5 effectors assemble to microdomains as illustrated in Figure 6A thereby creating platforms that include all proteins required for membrane fusion.[99] The cognate SNAREs were found to stabilize the Rab5 effectors and might contribute to their recruitment.[108] This indicates a mutual stabilization of Rab5 effectors and SNAREs. In conclusion, the coordinated assembly of Rab5 microdomains and their cooperative interaction with the SNARE complex enables fusion of membranes. These examples illustrate how Rab5 contributes tremendously to all stages of vesicle transport in the early endosome compartment.
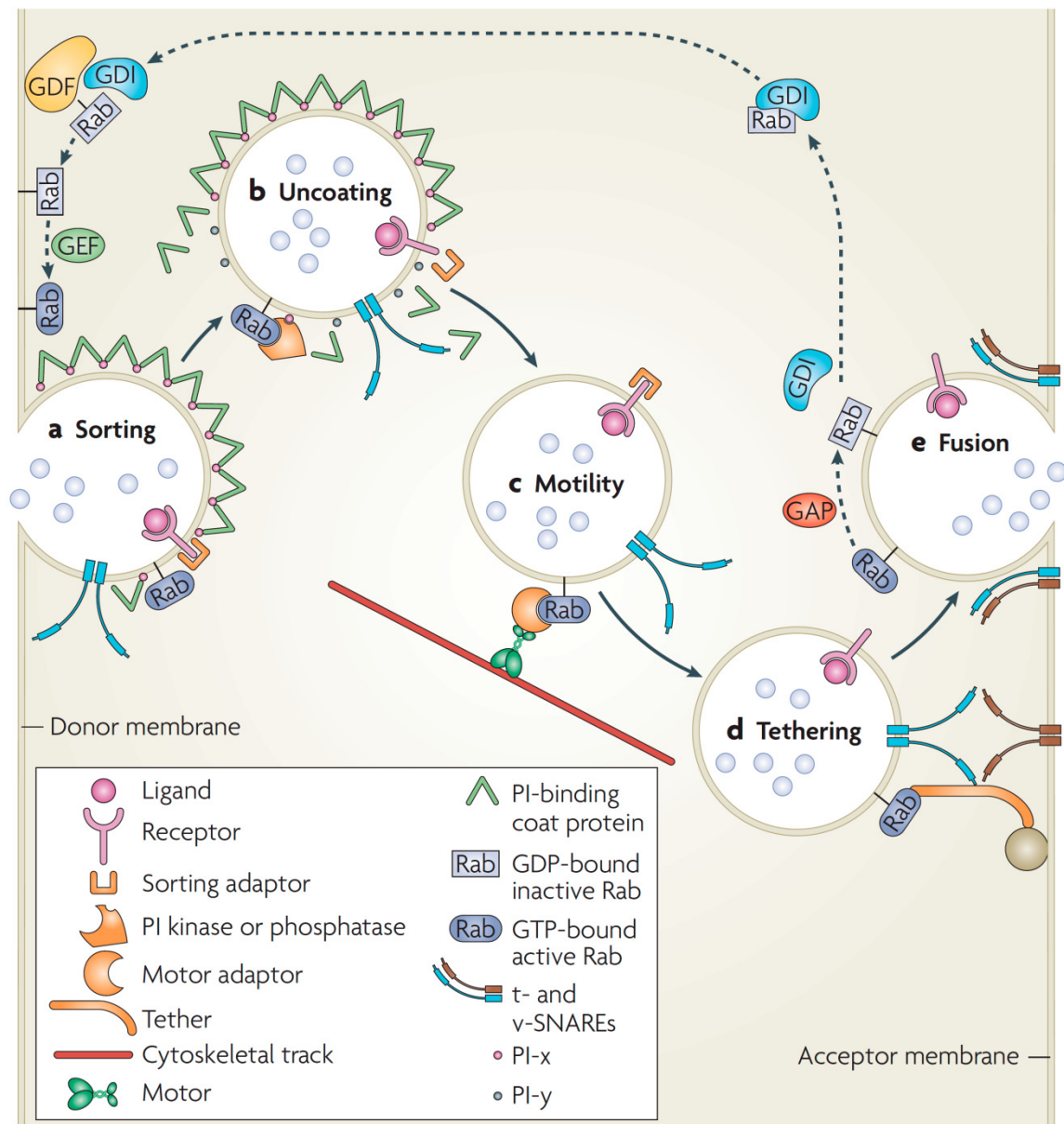
Figure 7   Rab GTPase functions in vesicle trafficking.
Distinct membrane trafficking steps that can be controlled by a Rab GTPase and its effectors (indicated in orange). **a)** An active GTP-bound Rab can activate a sorting adaptor to sort a receptor into a budding vesicle. **b)** Through recruitment of phosphoinositide (PI) kinases or phosphatases, the PI composition of a transport vesicle might be altered (the conversion of PI-x into PI-y) and thereby cause uncoating through the dissociation of PI-binding coat proteins. **c)** Rab GTPases can mediate vesicle transport along actin filaments or microtubules (collectively referred to as cytoskeletal tracts) by recruiting motor adaptors or by binding directly to motors (not shown). **d)** Rab GTPases can mediate vesicle tethering by recruiting rod-shaped tethering factors that interact with molecules in the acceptor membrane. Such factors might interact with SNAREs and their regulators to activate SNARE complex formation, which results in membrane fusion. **e)** Following membrane fusion and exocytosis, the Rab GTPase is converted to its inactive GDP-bound form through hydrolysis of GTP, which is stimulated by a GTPase-activating protein (GAP). Targeting of the Rab-GDP dissociation inhibitor (GDI) complex back to the donor membrane is mediated by interaction with a membrane-bound GDI displacement factor (GDF). Conversion of the GDP-bound Rab into the GTP-bound form is catalysed by a guanine nucleotide exchange factor (GEF). Reprinted by permission from Macmillan Publishers Ltd: Nature Reviews Molecular Cell Biology, Volume 10, Harald Stenmark, Rab GTPases as coordinators of vesicle traffic, Pages 513–525, copyright (2009).

1.3.4   Rab5 impact on actin dynamics, mitosis and signalling

The original conception of Rab5 being exclusively a master regulator of early endocytosis was challenged several years ago. Rab5 was found to be additionally involved in dynamics of the cytoskeleton, mitosis and signalling.

The dynamics of the actin cytoskeleton e.g. the formation of circular ruffling [125] or lamellipodia [126] partly depend on Rab5. Active Rab5 stimulates lamellipodia formation and cell migration independent of PI3-K or Ras.[126] Circular ruffles (also known as dorsal surface ruffles) are induced by receptor tyrosine kinase signalling [127] and are promoted by simultaneous activity of the PI3-K, Rac and Rab5.[125] Circular ruffling and macropinocytosis are regarded as means of endocytosis independent of clathrin.[35, 128] Rab5 indirectly activates Actinin4 [125] which is an Actin binding protein involved in circular ruffling and macropinocytosis.[129] Activation of Rab5 by its GEFs Rabex-5 and RIN1 stabilizes macropinosomes [130] and Rabankyrin-5 increases the amount of macropinosomes.[107] These observations indicate that the Rab5 involvement in actin dynamics is relevant for these special types of endocytosis. Moreover, endocytosis as a process per se controls actin dynamics.[131] The clathrin- and Rab5-dependent endocytosis is required for specific localization of the RhoGTPase Rac and cell migration.[131] Circular ruffling affects the cell motility, and through this interconnection Rab5 is not only relevant in endocytosis but also in cellular motility.[127, 131] Thus, the observations of Rab5 involvement in cytoskeleton dynamics point back towards regulation of endocytosis.

Furthermore, Rab5 is involved in mitosis. The formation of tubular ER structures in *C. elegans* is dependent on Rab5 activity.[132, 133] Related to this is the regulation of nuclear membrane disassembly which is also Rab5 dependent.[132, 133] Rabex-5 and RME-6 are the GEFs implicated in these Rab5 activities while the Rab5 effectors EEA-1, Rabenosyn-5, Rabaptin-5, and hVps34 are not engaged.[133] Rab5 is also involved in chromosome alignment during the metaphase which is important for chromosome segregation and proper mitosis.[132, 134] This function seems to be independent of endocytosis in general; it is more likely that Rab5 contributes to the stability of kinetochore-fibres.[132]

Finally, several studies have connected Rab5 activity with signalling pathways. The endosomes in general have been considered to be signalling compartments providing the benefit of additional spatial and temporal control of signalling events.[2] For instance, impaired EGFR endocytosis results in decreased activation of downstream signalling targets.[135] Further details on Rab5 participation in signalling in context of its GEF Rabex-5 will be given in Section 1.4.3.

To sum up, Rab5 has even more relevant functions in the cellular homeostasis than initially thought. It is a key regulator of the early endosome pathway with additional functions in mitosis, the dynamics of the cytoskeleton and signalling.

1.4 The GEF Rabex-5 controls Rab5 activity

The mammalian protein Rabex-5 (Rabaptin-5 associated exchange factor for Rab5 also known as RabGEF1) belongs to the family of Vps9-domain proteins which are GEFs for the Rab5 subfamily.[80] Rabex-5 has GEF activity for Rab5, Rab17, Rab21 and Rab22.[136-138] However, for Rab22 the catalytic activity is about 100fold lower than for Rab5 and Rab21.[136] Since Rab22 is thought to be more closely related to Rab5 [24] this finding was rather unexpected.[79]

Loss of Rabex-5 leads to lethality in larval or pupal stage in *Drosophila melanogaster* [139] and Rabex-5 knockout mice do not survive to reach adulthood.[140] These strong phenotypes indicate that Rabex-5 has essential functions.

1.4.1 Activity of the multi-domain protein Rabex-5 requires early endosomal localization

Rabex-5 is a multi-domain protein harbouring several domains with distinct functions.[22] Rabex-5 comprises two ubiquitin-associated domains (RUZ & MIU), an early endosomal targeting domain (EET domain), the GEF domain, and a coiled-coil-domain (CC-domain) at the C-terminus (Figure 8).[77, 141-143] The central catalytic core holds the GEF function and consists of the Vps9 domain stabilized by a helical bundle (HB).[136] In the following sections the domains and their functions in Rabex-5 biology are introduced.
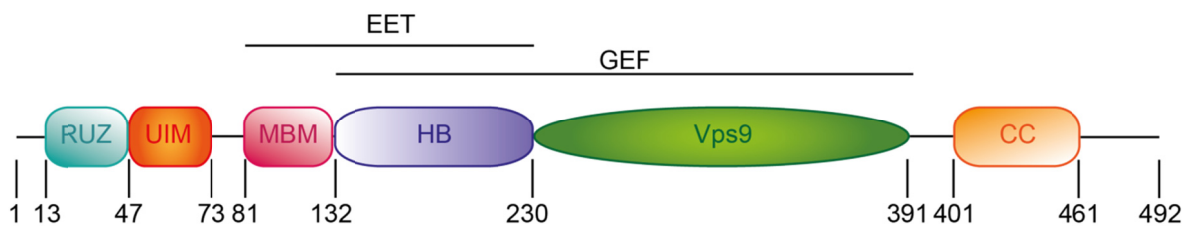
Figure 8   Domain structure of Rabex-5.
The amino acid borders of the domains vary in literature - probably due to the use of varying protein constructs and smooth transitions between some domains. The designations in this figure correspond to human Rabex-5 isoform 2 which was used in this study (http://www.uniprot.org/uniprot/Q9UJ41). The definition of Rabex-5 ubiquitin binding zinc finger (RUZ) corresponds to reports of [142, 144] and ubiquitin interacting motif (UIM) border definition corresponds to [144]. The membrane binding motif (MBM) starts at aa81 [77] and forms together with the helical bundle (HB) the early endosome targeting (EET) domain [77]. The HB-Vps9 tandem (GEF domain) is depicted according to [136] (in [77] the HB is defined from aa135-230 while the Vps9 is considered to span up to aa399), and the definition of the coiled-coil (CC) domain corresponds to [142].

1.4.1.1   *Ubiquitin interacting domains mediate cargo binding*

The RUZ (Rabex-5 ubiquitin binding zinc finger) domain is an A20 type zinc finger [145] with the ability to bind ubiquitin.[141, 142] Adjacent to the RUZ domain another ubiquitin binding domain resides.[142] The sequence of this domain is reversed compared to the established UIM (ubiquitin interacting motif) domain and hence was named MIU (motif interacting with ubiquitin, also known as inverted UIM).[141, 144] Both ubiquitin-interacting domains can individually interact with ubiquitinated EGFR.[141] This interaction enables

Rabex-5 recruitment to the plasma membrane or the early endosomes and is relevant for the fate of the EGFR in the endocytic pathway.[141]

1.4.1.2   *The GEF mechanism of Rabex-5 resembles that of the Sec7 GEFs*

The mechanism of the nucleotide exchange was illuminated by crystal structures of the Rabex-5 HB-Vps9 tandem, alone and in complex with Rab21.[136, 146]
The "V-shaped" arrangement of the αV4 and αV6 helices of the Vps9 domain builds a hydrophobic groove (Figure 9).[136] This groove is the centre of interaction with P-loop, switch and interswitch regions of the Rab protein.[146] These areas of the Rab are important for the interaction with the nucleotide (Section 1.1.2). Nucleotide exchange on Rab is performed by interaction of the Vps9 domain with the switch-interswitch regions of Rab and the insertion of an aspartate finger (Asp313) which disturbs the Mg^{2+}-phosphate binding and subsequently interacts with the P-loop.[6, 136, 146] The switch I is brought to an open conformation allowing the nucleotide exchange while the aspartate finger stabilizes the P-loop by mimicking interaction of the γ-phosphate of GTP.[146] This mechanism resembles very much the glutamate finger of the Sec7 domain ArfGEFs, although the general fold of these GEFs is not related.[7, 136, 146] Specificity of Rabex-5 for GTPases of the Rab5 subfamily is achieved by interaction with conserved amino acids specific for the Rab5 subfamily in the switch-interswitch regions.[136, 146]

In short, the mechanism of nucleotide exchange performed by the Vps9 domain of Rabex-5 resembles the prior reported mechanism of Sec7 domain proteins. The knowledge regarding the nucleotide exchange mechanism was mainly obtained by structural analysis.

1.4.1.3   *Rabex-5 localization and activity in vivo*

For the Rabex-5 activity *in vivo* it is relevant that the protein is located correctly and several domains contribute to the targeting of Rabex-5.
Rabaptin-5 can recruit Rabex-5: the CC domain of Rabex-5 interacts with the four-helical bundle region of Rabaptin-5 (aa572-641).[77] *In vitro*, Rabaptin-5 was found to increase the low GEF activity of Rabex-5 full-length protein.[95, 147] The Rabaptin-5 dependence can be bypassed by the use of a shorter construct (aa132-391, GEF domain, Figure 8).[136] Also, the activity of Rabex-5 full-length can be increased by addition of the Rabaptin-5aa551-862 construct which indicates that the amphipathic helix on the C-terminal side of the Vps9 domain represents an auto-inhibitory mechanism.[146] Therefore, Rabex-5 was thought to be dependent on Rabaptin-5 but surprisingly the Rabex-5 GEF function *in vivo* is not absolutely dependent on Rabaptin-5.[77] *In vivo*, Rabex-5 full-length is mostly membrane associated and has stronger GEF activity than the single Rabex-5 GEF domain (aa135-399).[77] This was observed by the use of mutant Rabex-5 proteins overexpressed in baby hamster kidney cells.[77]

Moreover, Rabex-5 can be recruited to early endosomes in a Rab5 independent manner.[95] Via its EET-domain, comprised of the MBM and the HB (Figure 8), Rabex-5 can be targeted to early endosomes by interaction with Rab22-GTP.[143] Subsequently, Rabex-5 activates Rab5. This interaction is a Rab cascade (explained in Figure 10A) in which

Rabex-5 has a dual role as Rab22 effector and Rab5GEF. The two GTPases are both found on the early endosomes but differ in their temporal impact.[143] Rab22 interacts with EEA1 but was also implicated in Golgi function.[73] The endosome fusion mediated by Rab5 or Rab22 is temporally and functionally distinct and Rab22 provides a link to Golgi-endosome transport and receptor recycling.[73, 112] Potentially Rabex-5 can fine tune Rab5 and Rab22 activity on the early endosomes.[143]   Hence, the second way of Rabex-5 localization to the early endosomes is conducted by the EET domain.

Finally, Rabex-5 can interact with ubiquitinated cargo by its ubiquitin interacting domains (Section 1.4.1.1).

Altogether, Rabex-5 localization can either be achieved by the presence of the Rabex-5 EET-domain, binding to Rabaptin-5, or interaction with ubiquitinated cargo like the EGFR.[67, 77, 148, 149] The interaction with cargo molecules and Rab5 effectors like Rabaptin-5, Rabaptin-5β, Rabenosyn-5 keep Rabex-5 activity focused on early endosomes.[6, 67, 150]
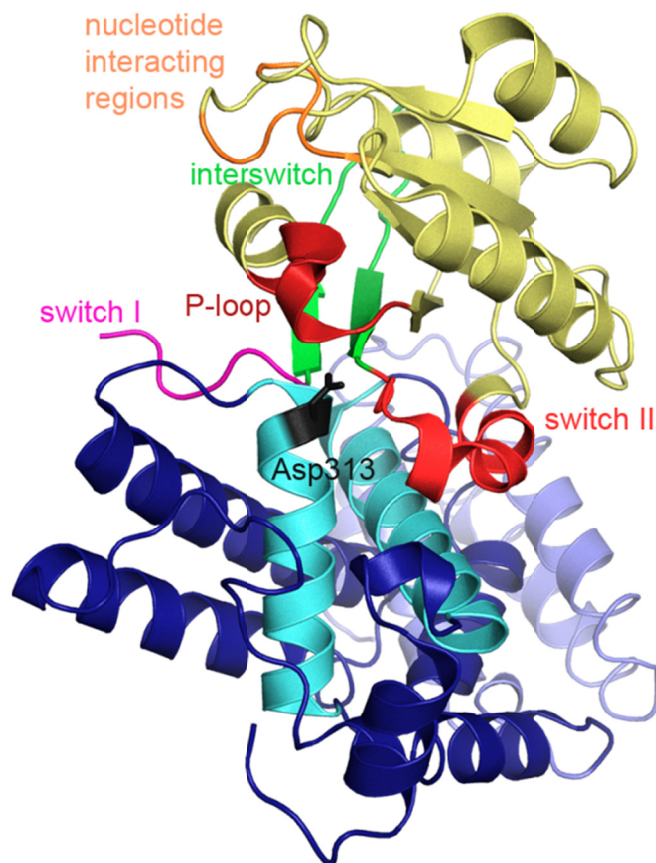
Figure 9   GEF-domain of Rabex-5 in complex with Rab21.
The proteins are shown as cartoon representation; the data is taken from the PDB file 2ot3 and was rendered by the use of PyMol software. The catalytic core of Rabex-5 consists of the helical bundle (light blue; αHB1–αHB4), the VPS9 domain (blue and aquamarine; αV1–αV6) and a C-terminal helix (dark blue; αC). The hydrophobic groove of αV4 and αV6 is depicted in aquamarine and the aspartate finger (Asp313) is illustrated in black. Rab21 (α1–α5 and β1–β6) is depicted in yellow with the P-loop (dark red), switch (light red and pink) and interswitch (green) regions. Further nucleotide interacting regions (orange) are given as defined in UniProtKB (http://www.uniprot.org/).

1.4.2 Rabex-5 influences the transition of early to late endosomes

Recently, Rabex-5 has been implicated in transition of early to late endosomes. Early endosomes are marked by high Rab5 levels while late endosomes possess high amounts of Rab7 (Figure 3).[44] Two different models have been proposed how these two compartments are formed. The vesicle shuttle model suggests transport between to pre-existing compartments.[151, 152] The maturation model implies that early endosomes are transformed to late endosomes by transition of Rab5 to Rab7.[153] The transition is probably achieved by the mechanism of Rab conversion (explained in Figure 10B).[153] At the same time, the maturation requires a disruption of the Rabex-5 dependent positive feedback loop (Section 1.3.2.1) to decrease the local levels of Rab5.[154]

Interaction with Rabex-5 and PI3P recruits the protein Mon-1 to the early endosomes.[15] Here, Mon-1 forms a complex with the protein Ccz1 as observed in *C. elegans*.[154] In addition, it displaces Rabex-5 resulting in decreased Rab5 activation.[154] Subsequently, the interaction of the Mon1-Ccz1 complex with the HOPS complex (protein complex interacting with Rab7 and also involved in Rab5-to-Rab7 transition) [153] facilitates recruitment and activation of Rab7.[155] These sequential events enable Rab5-to-Rab7 transition.[15, 154, 155]

Nevertheless, it remains unclear how Rab5 is removed from the early endosomes and if other proteins are involved in this regulation. It was suggested that Mon1-Ccz1 not only displaces Rabex-5 but also recruits a Rab5-GAP.[68] But then it might be enough to remove Rabex-5 and to disrupt the positive feedback-loop clustering Rab5.

In summary, the participation of Rabex-5 in the transition of Rab5 to Rab7 supports on the one hand, the maturation model. On the other hand it underlines the multifunctional impact of Rabex-5 on Rab5 that requires further elucidation.
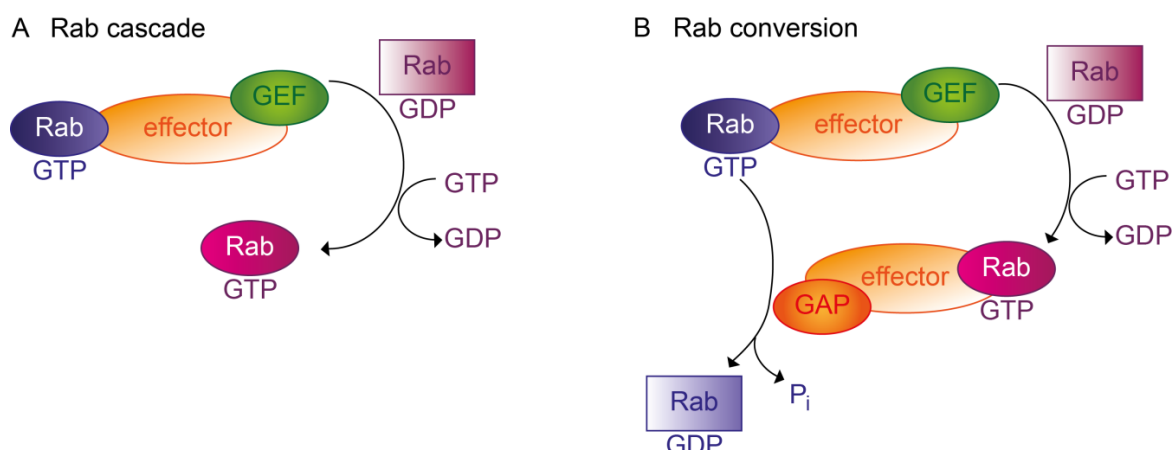
Figure 10   Coordination of the localisation of active Rab by conserved mechanisms.
A) The Rab cascade causes the activation of a second Rab protein in a consecutive fashion. The interaction of the first Rab (blue) with the effector protein (orange) leads to activation of a GEF (green).[156] Subsequently, this GEF activates the second, downstream Rab GTPase (purple).[156] **B)** The Rab conversion is an expansion of the Rab cascade. In addition to the activation of the downstream Rab (purple), the upstream Rab (blue) is silenced. Therefore, the effector of the second, activated Rab might be or activate a GAP (red) targeting the first Rab so that the activation of the upstream Rab is terminated.[41, 157] These two conserved regulatory mechanisms allow the subsequent activation of different Rabs which is important in the maturation process of vesicular organelles e.g. the transition of early endosomes to late endosomes.[15] The Figure is adapted from [41].

1.4.3 Rabex-5 regulates signalling pathways

Rabex-5 is involved in several signalling pathways. Often, the Rabex-5 effect on signalling is coupled with the internalization of membrane receptors. Although the picture just starts to emerge, the current understanding of the role of Rabex-5 in the EGFR and Ras signalling as well as mast-cell related signalling will be introduced in the following subsections.

1.4.3.1 The Rab5 GEFs Rabex-5 and RIN1 control EGFR signalling

Upon EGF stimulation Rab5 is activated and the GTP-bound form is found both at the plasma membrane and on early endosomes (Figure 11).[158] Subsequently, active Rab5 is responsible for endocytosis of the EGFR after stimulation.[158] Stimulation with low EGF concentrations favours internalization of the EGFR by clathrin-mediated endocytosis and results in prolonged signalling and receptor recycling.[111, 159] At high EGF concentrations both clathrin-mediated endocytosis and clathrin-independent endocytosis are equally involved in EGFR internalization and increased receptor degradation is observed.[111, 159] EGFR degradation after endocytosis into early endosomes is dependent on the endosome motility regulatory protein KIF16B, a kinesin regulated by Rab5-dependent PI3P levels.[122] Moreover, the Rab5 GAP RN-tre can attenuate the endocytosis of receptor tyrosine kinases like the EGFR.[160] Thus, Rab5 activity favours EGFR endocytosis and degradation. Rabex-5 binds the ubiquitinated EGFR and co-localises with the EGFR at the plasma membrane after EGF stimulation.[141] This eventually represents cargo-dependent Rab5 activation.[161] Interesting in this context is the observation that EGFR endocytosis in the clathrin-independent pathway requires receptor ubiquitination.[162] Hence, Rabex-5 might be involved in the EGFR degradation rather than in recycling. *Balaji et al.* observed that the EGFR degradation at high EGF concentrations was impaired in absence of Rabex-5.[163] In addition, it was reported that the fate of the EGFR upon stimulation depends on the Rin1 signalling. Rin1-Rab5 signalling preferentially leads to EGFR endocytosis and EGFR degradation, thus down-regulation of the EGF signalling.[81, 163] This implies a redundant function of Rabex-5 and Rin1. The picture is complicated by the observations that EGF stimulation has an inhibitory effect on the early-to-late-endosomal transport.[153] In addition, Rab21 and Rab22a are also involved in EGFR degradation and seem to slow down receptor degradation after EGF stimulation.[73, 74]

1.4.3.2 Rabex-5 participates in the termination of Ras activation

Ras is known to have a positive impact on Rab5 activity and endocytosis.[164] A prominent trigger for Ras activation is EGFR signalling (Figure 11).[165] Rabex-5 seems to be part of a negative feedback loop that terminates the Ras activation together with Rin1 and Rab5. Ras signalling activates Rin1 and subsequently Rab5.[81] The active Rab5 facilitates the binding of the Rabex-5-Rabaptin-5 complex to the early endosomes.[95] Rabex-5 can interact with Ras [140] and has an E3 ubiquitin ligase function which provides ubiquitination of Ras.[142] Thus, the Ras signalling via the Raf-Mek-Erk kinase cascade is terminated.[166] Altogether, the Ras signalling is down regulated while the Rab5 activity is kept at an elevated level. [139, 167] The effect of Rabex-5 on the Ras signalling is independent

of its GEF activity.[139, 167] These findings are supported by the previous report that Ras-Erk signalling is increased in Rabex-5 knock-out mice.[140] In summary, Ras can regulate its own ubiquitination state by controlling Rin1.[168] Since mono- and diubiquitination of Ras results in preferential localisation at endosomes [169] this regulation influences the subcellular localization of Ras. However, Rabex-5 acts downstream of Rin1 and the Rabex-5 activity alone is sufficient for the Ras blocking effect arguing for a strong impact of Rabex-5 on the Ras ubiquitination.[167]
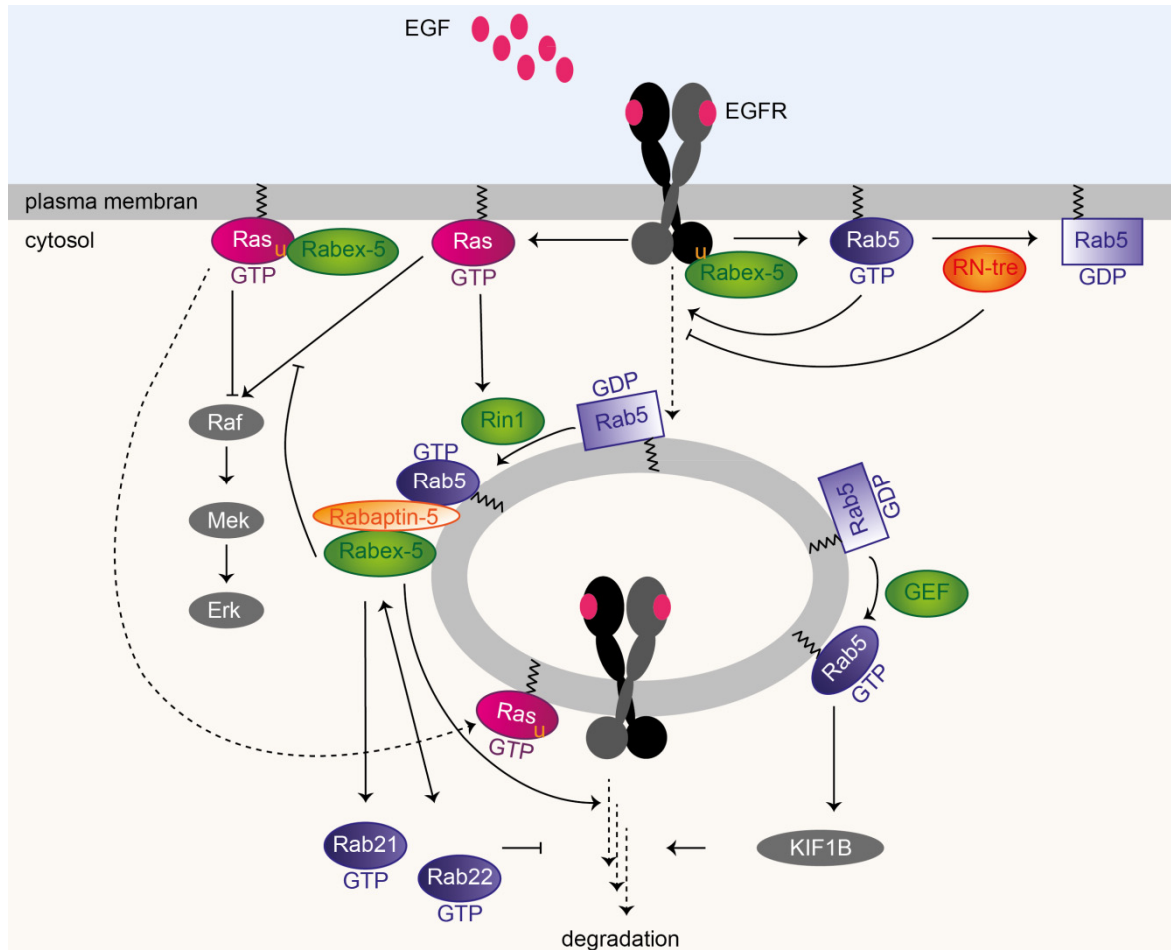
Figure 11   Rabex-5 implications in EGFR and Ras signalling.
EGF ligand binding to the EGFR stimulates the receptor. Subsequently, the EGFR is ubiquitinated (orange *u*) and provides a docking surface for Rabex-5. Also, EGF stimulation triggers Ras activation and the signal is transmitted by the Raf-Mek-Erk kinase cascade. Furthermore, active Ras is bound by Rin1 and in turn Rab5 is activated. Upon activation, a Rab5 microdomain containing Rab5 effectors like Rabaptin-5 is formed and promotes the internalization of the EGFR. The internalization is counteracted by the Rab5 GAP RN-tre. In addition, the presence of Rabex-5 at the Rab5 microdomain favours negative regulation of the Ras signal while the Rab5 activity is kept at an elevated level. This negative feedback regulation of Ras is enforced by ubiquitination of Ras through Rabex-5 which abrogates the Raf-Mek-Erk-kinase cascade and translocation of Ras to the early endosomes. The internalized EGFR is transported along the endocytic pathway to be degraded. This motion is promoted by Rabex-5, Rab5, KIF1B while Rab21 and Rab22 slow down the route to degradation. Rab21 in turn can be activated by Rabex-5, while Rabex-5 acts as effector for Rab22. Dotted arrows indicate transport processes, arrows illustrate activation and blunt end arrows show inhibition.

1.4.3.3 Rabex-5 is a negative regulator of mast cell activity

Rabex-5 diminishes Ras-mediated signalling in mast cells and is a negative regulator of the FcεRI (IgE receptor)-dependent mast cell activation.[140] In absence of Rabex-5, the endocytosis of FcεRI is delayed and the activation of Ras and Erk is increased.[140, 170] Moreover, the receptor endocytosis of c-Kit (receptor for the stem cell factor also known as mast cell growth factor), is regulated by Rabex-5.[171] Delayed c-kit endocytosis in Rabex-5 knockout mast cells affects several downstream targets, e.g. Ras, Erk, Akt, c-Jun N-terminal kinase and results in increased IL-6 production.[171] The GEF activity of Rabex-5 seem to be relevant for the regulation of mast cell receptors.[170] Rabex-5 also mediates the internalization of the immunoglobulin superfamily cell adhesion molecule L1.[149] In addition, the Rabex-5 binding partner Rabaptin-5 controls surface expression of membrane receptors like integrinβ1, FcεRIα, and IL-4R.[172] These receptors contribute to the regulation of mast cells activity and their attachment to extracellular matrices.[173] Their regulation by Rabaptin-5 is likely to contribute to the Rabex-5 knock-out phenotype in mice.

The observation that Rabex-5 regulates the receptor expression and signalling in mast cells underlines the previously indicated (Section 1.4.3.1 and 1.4.3.2) connection between the regulation of endocytic trafficking and signalling.[170] The multifunctional role of endosomal pathway regulators in signalling and the emerging picture of receptors that contribute to the regulation of their intracellular fate necessitate further investigations of these multi-layered signalling networks.[1]

1.5   Small molecule inhibitors as tools to study GEFs

1.5.1   Small molecules in chemical biology and therapeutics

Since the isolation of morphine from opium extract by *Friedrich Sertürner* in 1815, the postulation of chemoreceptors by *Paul Ehrlich* in the 1870s, and discovery of penicillin by *Alexander Fleming* in 1929 the efforts in drug research have noticeable increased.[174] To address the search for drugs systematically, combinatorial libraries are applied in high throughput screening (HTS) approaches.[175, 176] In the beginning of the 1990s it was already possible to screen about 200,000 compounds by the use of HTS.[174] Nevertheless, todays amount of validated drug targets are still low compared to the number of genes and proteins.[177] Small molecules are excellent tools not only for therapeutic purposes but also for scientific investigation of cell signalling cascades and cellular functions of proteins.[178, 179] The use of small molecules as tools to study biological systems is often referred to as chemical genetics.[175]

Small molecules have the advantage of targeting the protein level directly compared to knockout and knockdown methods that operate on DNA or RNA level (Figure 12).[180] In general, knockout/-down methods and small molecules are expected to result in the same effects when addressing the same target. However, domain specific inhibition of multidomain proteins is possible by small molecules if they are selected to target a

specific domain or function.[181, 182] In these cases, small molecules can block a specific function of their target while keeping the general level of protein expression constant and thus allowing the undisturbed exertion of other, e.g. scaffold functions of the target protein.[180, 181] Thus, the inhibitory effects of the small molecules are in some cases more accurate and might have different effects than RNAi.[180] A prominent example is rapamycin which distinguishes between the mTOR complex1 and mTOR complex2.[183, 184] Moreover, knockouts with lethal phenotypes as for example described for Rab5 and Rabex-5 (Section 1.3 and 1.4) complicate the analysis of the mutant organisms.[179] Chemical genetic approaches can complement genetic strategies by providing tools to inactivate proteins.[179]

Furthermore, small molecules are easy applicable, relatively stable, often cell permeable, and have rapid effects compared to RNAi (Figure 12).[175, 180, 185] Also, they can be applied in a conditional fashion at any point in development that is supposed to be studied.[179] Effects of small molecules are reversible because the effect will wear off if the compound is for example metabolized.[179, 185] Multiple small molecules can be used in combination and in a dose-dependent fashion for the induction of fine-tuned effects.[185] The application of medicinal chemistry (e.g. by combinatorial synthesis) allows to obtain a high variety of molecules and lead compound optimization can be performed by analysing structure activity relationships.[176, 186] Depending on the target protein, small molecules can be used as potential drug candidates although this happens rather infrequently.[181]

Instead, small molecules have been used in the past to verify suspected involvement of proteins in cellular functions and to uncover new functions. For example, small molecule inhibitors of the AuroraB kinase discovered an unknown function of the kinase in localization of spindle checkpoint components and chromosome alignment.[180, 187, 188] Another example is the small molecule SecinH3 (Section 1.5.2.2) targeting the Cytohesin-family.[189] SecinH3 revealed the influence of Cytohesins in the insulin signalling and confirmed an initial hypothesis derived from the *Drosophila melanogaster* homologue knock-out phenotype.[189] Sometimes small molecules can be of use if approaches interfering with the correct protein expression, e.g. ectopic expression of (mutant) proteins or knockout phenotypes, resulted in conflicting evidence.[187] The current limitations of chemical genetics compared to genetics is the amount of compounds available – to enable the genome wide use of small molecules (referred to as chemical genomics) many more molecules have to be discovered.[185]

Because small molecules and RNAi not always result in congruent results, it is even more important to apply a variety of methods to investigate the functions of a protein of interest since the combination of results deepens the understanding of its biological role.[180, 181] Therefore, it is important to have small molecule inhibitors available for the proteins of interest.
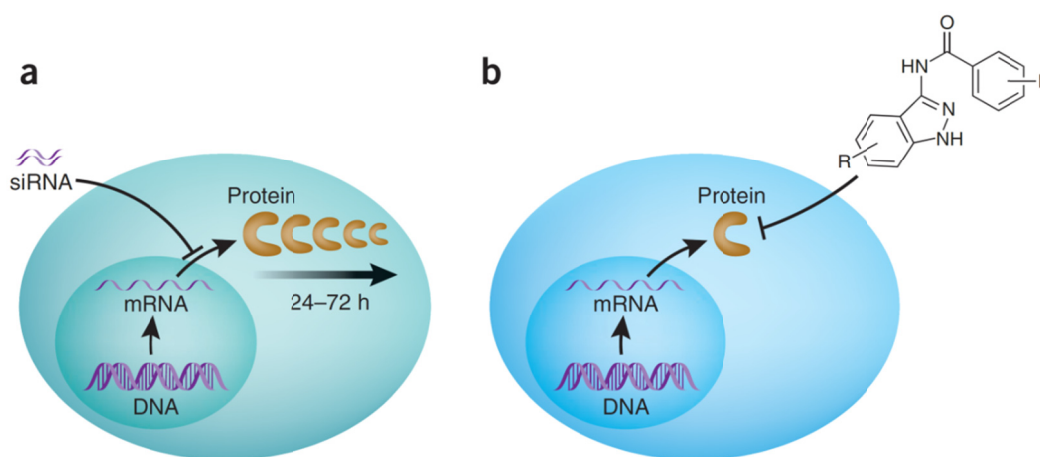
Figure 12   Modes of action for inhibition of protein activity.
a) Inhibition of protein expression by siRNA. **b)** Inhibition of protein activity by small molecules. Reprinted by permission from Macmillan Publishers Ltd: Nature Chemical Biology, Volume 3, Issue 12, William A Weiss, Stephen S Taylor and Kevan M Shokat, Recognizing and exploiting differences between RNAi and small molecule inhibitors, Pages 739–744, copyright (2007).
Inhibition of protein expression by siRNA prevents the protein biosynthesis. The loss of protein occurs over time (24 – 72 hours) and is dependent on the stability and turnover of the individual proteins. The Inhibition of protein activity by small molecules is achieved by targeting the protein directly.

1.5.2   Available inhibitors of GEFs and GTPases

Although GTPases and GEFs do not belong to the established targets in the development of drugs, several recent reports of inhibitors encourage the view that these protein classes might be druggable.[190] The presented inhibitors are summarized in Table 1.

1.5.2.1   Inhibitors of small GTPases

A very attractive target among the small GTPases is Ras due to its implication in cancer.[11] None of the molecules targeting Ras has been applicable as therapeutics, yet, although several Ras inhibitors have been described. The most recent structure reported is derived from an *in silico* screening approach targeting a pocket on Ras-GTP discovered in the crystal structure.[191] The identified molecule Kobe0065 inhibited interaction of Ras with effector proteins *in vitro* with activities in the mid-micromolar concentration range and showed anti-proliferative activity on cells with activating Ras oncogenes.[191] Previously, KRas binding small molecules that have been discovered in NMR-based fragment screens performed by two research groups. Interestingly, both studies report a binding side close to switch I / II and interference of the Ras-binders with the Ras-SOS interaction.[192, 193] This binding site partially overlaps with the binding pocket of Kobe0065.[191]

Among earlier reports are several small molecules carrying sugar-moieties or derivatives with bicyclic core derived from the natural sugar arabinose. Although capable of disrupting the GEF catalysed nucleotide exchange on Ras, they are needed in high micromolar concentrations and have limited solubility.[194-197]

Zn^{2+}-cyclen was identified as Ras binding molecule that stabilizes the Ras-GTP-GEF state and thereby interferes with Ras-effector binding.[198, 199] However, the affinity is in the millimolar range and no intracellular application has been reported, yet.[198]

The aryl amide MCP110 was discovered in a modified yeast-two-hybrid screening and can inhibit Ras-mediated Raf activation and reverse Ras-transformed phenotypes.[200, 201] The target of the compounds is assumed to be the Ras-Raf interface; however biochemical data to confirm this hypothesis has not been presented.[200] Ras inhibitors targeting the Ras-Raf signalling have been identified in a phenotype based screening of a library with derivatives of the non-steroidal anti-inflammatory drug Sulindac.[202, 203] Several inhibitors of Ras effectors like Raf have been described, indicating that the effectors might be easier to target than the highly conserved GTPases.[204]

Two small molecules inhibiting the GTPase Rac are known. The first, NSC23766, was identified in a structure-based *in silico* screening and binds to an area of Rac1 that is known to be critical for GEF interaction.[205] It blunts the nucleotide exchange of the RhoGEFs Tiam1 and Trio with an IC_{50} of about 50 μM.[205] The second compound, EHT1864, interacts with all Rac isoforms and displaces the nucleotide from the binding pocket.[206] Its association with Rac1 was determined to be about 40 nM.[206]

The combination of the high affinity of the nucleotide-GTPase interaction and the high intracellular GTP concentrations renders the development of competitive inhibitors challenging.[3, 190] Nevertheless, there was recent report of a competitive Rab7 inhibitor.[207] Yet, this inhibitor was also described to interact with Rab2 and thus has limited specificity.[207]

Because Ras and Rho GTPases are important in cancer development and progression, as well as tumour metastasis and invasion, the past efforts to targeting small GTPases with inhibitors concentrated on these two families.[208] Nevertheless, since inhibitors are valuable tools for research besides being used as therapeutics, future efforts will cover other small GTPases as well.

1.5.2.2   *Inhibitors of GEFs*

The first described inhibitor of a GEF is the macrocyclic lactone BrefeldinA (BFA) that interacts with the Arf1-GDP-Sec7 complex and blocks the GEF activity of Gea1.[209, 210] This natural substance is produced by several fungi and was initially recognized for inducing the breakdown of the Golgi and severely affecting vesicle transport processes.[211]

There are two classes of inhibitors targeting the BFA‑insensitive ArfGEFs called Cytohesins.[212] First, an RNA-aptamer, M69, has been reported to target the family of Cytohesins.[213] Later, small molecule inhibitors were described, among them the small molecule SecinH3 derived from M69 in an aptamer-displacement screening.[189] Another small molecule inhibitor was obtained in an *in silico* screening and acts by producing a non-functional Arf-GDP-Cytohesin2 complex.[214]

The compound GolgicideA targets the ArfGEF Golgi BFA resistance factor 1 (GBF1) and can block the transport from endosomes to the TGN.[215] GolgicideA was a relevant tool for the identification of GBF1 as important factor in maintaining Golgi structure.[215]

Table 1   GEF and GTPase inhibitors in comparison.

Inhibitor name / screening type	Inhibitor type	Target	IC$_{50}$	K_d	Reference
Kobe0065 / *in silico* screen	small molecule	Ras (effector interaction)	K_i : 46 ± 13 μM[a]		[191]
DCAI / fragment based screen	small molecule	K-Ras (SOS interaction)	~ 16 μM[b]	1 mM	[192]
fragment based screen	small molecules	K-Ras (SOS interaction)		0.2-2 mM	[193]
Arabinose derivatives / NMR-based binding	small molecule	H-Ras	~ 35 - 100 μM [c]	37 μM	[194, 197]
Zn^{2+}-cyclen	small molecule	H-Ras (Raf interaction)	millimolar range [d]		[198, 199]
MCP110 / yeast-two-hybrid screening	small molecule	Ras (Raf interaction)	2 – 25 μM [e]		[200, 201]
Sulindac-derivatives / phenotype based screen	small molecule	Ras (Raf interaction)	30 - 450 μM [f]		[202, 203]
NSC23766 / structure-based *in silico* screen	small molecule	Rac1	~ 50 μM [g]		[205]
EHT1864	small molecule	Rac1, Rab1b, Rac2, Rac3	Low micromolar range [h]	40 nM	[206]
CID 1067700 / bead-based flow cytometry HTS	small molecule	Rab7, Rab2	nanomolar range [i]		[207]
BFA	small molecule	Arf1-GDP-GEF complex	Micromolar range [j]		[216]
M69 / SELEX [l]	RNA aptamer	Cytohesin	Low micromolar range [k]	16 nM	[213]
SecinH3 / aptamer displacement screen	small molecule	Cytohesin	~ 5 μM [k] [m]		[189]
LM11 / *in silico* screen	small molecule	Cytohesin2	[n]	150 - 200 μM	[214]
GolgicideA / phenotype based HTS	small molecule	GBF1	3.3 μM [o]		[215, 217]
ITX3 / yeast exchange assay screening	small molecule	Trio	76 μM [p]		[218, 219]
TRIAPalpha / genetic screen in yeast	peptide aptamer	TrioGEFD2	~ 4 μM [q]		[220]

[a] Determined in an *in vitro* effector-pull-down assay. The compound was found to be active in cellular assays as well including antiproliferative activity in cells carrying activated ras oncogenes. [b] Cellular assay; in the *in vitro* nucleotide exchange assay the IC$_{50}$ was dependent on the concentration of the GEF SOS. [c] *In vitro* nucleotide exchange assay with Ras GEF CDC25. [d] Effect of the compound in isothermal titration calorimetry measurement with Ras and Raf. [e] IC$_{50}$ was dependent on the assay type – cellular assays were used. [f] I*n vitro* determination of Ras-Raf interaction; acts at 100 μM on the phosphorylation of the MAPKinase in Madin Darby canine kidney cells. [g] *In vitro* and intracellularly observed nucleotide exchange of Trio and Tiam1. [h] Several intracellular assays were used and concentrations of 5 to 50 μM result in complete inhibition of e.g. effector binding. [i] I*n vitro* nucleotide binding. [j] *In vitro* interaction with Arf1 and Sec7 domain. [k] *In vitro* nucleotide exchange of Arf1 and Cytohesin1. [l] Systematic evolution of ligands by exponential enrichment: strategy for generation of aptamers. [m] SecinH3 was also applied in intracellular assays with inhibitory activity in the low micromolar range. [n] Intracellular effects were observed at 100 μM compound. [o] Inhibitory effect on shiga toxin in Vero cells. [p] *In vitro* nucleotide exchange assay with TrioN and RhoG, cellular effects were observed with ~50 μM compound. [q] *In vitro* nucleotide exchange assay; intracellular effect was observed.

Moreover, the small molecule inhibitor ITX3 for the N-terminal DH domain of the RhoGEF Trio [218, 219] and a peptide aptamer targeting the TrioGEFD2 domain have been reported to date.[220] A variant of the peptide aptamer was further developed to specifically target the oncogenic isoform of the RhoGEF Trio (Tgat).[221]

These examples confirm that GEFs for Arf and Rho GTPases have been successfully targeted by inhibitory molecules.

1.5.3   Rab GTPases and GEFs as targets for small molecules

Rab GTPases and their GEFs are in many respects therapeutically interesting. Rabs can be hijacked by intracellular pathogens to avoid degradation, are involved in cancer, neurological, metabolic and immunological diseases.[41, 131] Besides therapeutic purposes, specific inhibitors targeting the diverse players in the interconnected and complicated networks of the early endosome biology would be important tools. Despite their interesting functions, no inhibitor for any RabGEF and only one Rab7 inhibitor have been reported, yet.[207] Further small molecules targeting RabGTPases and GEFs in the yet incompletely understood networks of membrane trafficking and signalling pathways would be valuable tools. They could be applied to study detailed protein activity of single components of this network, maybe even the function of single domains of proteins. Moreover, their use could dissect protein interactions and identify key players that can be targeted for treatment of various pathogenic scenarios.

As many Rab GTPases are able to hydrolyse GTP within an adequate time, the impact of regulation by GEFs seems to be stronger than the one by GAPs.[6] Thus, it is plausible to manipulate the GEF rather than the GAP to obtain a different activity state of the GTPase. An earlier approach was the inhibition of the RabGGTase to affect Rab membrane association and thereby activity (Section 1.2.3). But even if a RabGGTase inhibitor is specific for the RabGGTase and does not affect the other protein prenyltransferases it prevents prenylation of several Rabs at the same time.[222, 223] Thus, in contrast to potential RabGEF inhibitors, these RabGGTase inhibitors are less likely to be suitable to investigate a specific Rab.

Neither Rab GTPases nor RabGEFs belonged to the group of established target classes when this work was started [28] and even to date no sufficient coverage of inhibitors for these protein families is available. This not only indicates that these proteins may represent difficult targets but also underlines the need for identifying novel inhibitory molecules to add to the tools available for studying GEF and Rab GTPase biology.

2   AIM OF THE PROJECT

The Rab5 activity is controlled by numerous GEFs, yet the precise contribution of specific GEFs to the regulation of the diverse Rab5 functions is not completely understood. Moreover, GEFs often contain several other domains beside their catalytic GEF domain and have been associated with a diverse variety of effects. Of particular interest is Rabex-5, a GEF for Rab5, which was found to be essential for embryonic and pre-adult survival. In addition, it presumably controls the establishment of asymmetric assembled Rab5 microdomains, which serve as platforms of local Rab5 activity. Furthermore, it interacts with Rab5 effectors, potentially influences the Rab5 localization, and possibly plays a role in transition of early endosomes to late endosomes. Finally, the processing of membrane receptors after stimulation with their ligands is affected by Rabex-5. Importantly, for many of the effects it remains unclear whether the function of Rabex-5 as exchange factor is involved in these phenotypes: the exact role of each protein domain is still under investigation. Previous studies mainly used knockout, knockdown, and overexpression methods, which do not provide information regarding the specific function of the individual subdomains.

To dissect the complex network of protein interactions which control cellular processes, such as the regulation of the early endosome, small molecule inhibitors are invaluable tools. In particular, a domain specific inhibitor, targeting only the catalytic GEF domain of Rabex-5 would aid in elucidating the complex biological roles of Rabex-5 and subsequently Rab5.

At present, no small molecule inhibitors for Rab5 or any corresponding GEF are available. Therefore, the aim of this thesis was to identify a small molecule inhibitor targeting the Rabex-5 mediated Rab5c nucleotide exchange and to characterize this molecule *in vitro*. To obtain such an inhibitor, first, a screening assay to identify potential small molecule inhibitors from a compound library was established and applied. Subsequently, potential hits identified in this screening were tested for their inhibitory properties and specificity. An inhibitor with micromolar affinity for Rabex-5 and specificity for Rabex-5-Rab5 over multiple other GEF-GTPase pairs was identified in this study.

3 RESULTS

The identification and characterization of a small molecule inhibiting the Rabex-5 mediated Rab5 nucleotide exchange are presented in this chapter. This aim was approached by the use of an *in vitro* high-throughput-screening (HTS) assay monitoring this particular protein activity. The establishment of such an assay is outlined in the first section, followed by its application to screen a small molecule library (Section 3.1 and 3.2). Subsequently, the characterization of two chosen lead compounds is described, culminating in the choice of the molecule JH5 as sole lead compound for detailed *in vitro* characterization (Section 3.3). Section 3.4 presents the structure activity relationships of JH5 and its derivatives together with experiments to elucidate the mode of action of JH5. The chapter concludes with preliminary data on intracellular application of JH5 (Section 3.5) and a detailed, retrospective description of the validation of the screening hits and the selection of the most promising compounds (Section 3.6).

3.1 Production of Rabex-5GEF and Rab5c proteins

A small molecule inhibitor was sought by monitoring the disturbance of the Rabex-5 mediated nucleotide exchange on Rab5c in an *in vitro* assay. The measurement of this reaction required active, *in vitro* purified Rab5c and Rabex-5 proteins. Their production (Section 3.1.1 and 3.1.2) and evaluation (Section 3.1.3) is described in the following.

3.1.1 Expression constructs for Rab5c and Rabex-5GEF

The HB domain and the Vps9 domain comprising the amino acids (aa) 132-391 of the human Rabex-5 hold the GEF function of Rabex-5 (Figure 13A).[136] These domains are not only sufficient for protein activity *in vitro* but beyond that they form the only known construct applicable in an *in vitro* system. The full-length Rabex-5 requires the additional presence of the Rab5 effector Rabaptin-5 for full activity *in vitro*.[95] This construct will be referred to as Rabex-5GEF. In addition, by using only the GEF domain in the assay the likelihood of addressing this desired domain is increased and a GEF specific inhibitor should be identified.

The murine Rab5c was expressed as aa18-185 construct, missing the regions at both protein termini (Figure 13B). The hypervariable C-terminal domain and the cysteine residues, which are modified by the Rab geranylgeranyl transferase (RabGGT) for membrane anchorage, are important for the localization of the Rab protein (Section 1.2.3).[26, 53] The N-termini of Rab GTPases are very diverse in structure and function. In the case of Rab5 this N-terminal element is involved in endocytosis, fusion events, and additionally supports the prenylation process of the GTPase.[55, 224, 225] These parts were not needed for nucleotide and GEF binding and since the shortened construct was described to be active and suitable for *in vitro* assays [226] it was used here. This murine Rab5c construct is identical to the human isoform of the Rab5c protein because the

only three amino acids that differ between these homologues are located at the C-terminus (Section 8.2.3).

The Rabex-5GEF and Rab5c plasmids for protein expression are modified pET15b vectors containing a T7 promoter, a lac operon and an ampicillin resistance as well as a sequence coding for an N-terminal His-tag for affinity chromatography purification. The Rab5c and Rabex-5GEF DNA sequences corresponding to the above described amino acids had been cloned into the 5650 bp sized vector via the restriction sites BamHI and SalI. These plasmids were kindly provided by *Dr. Anna Delprato* (Laboratoire de Enzymologie et Biochimie Structurales, CNRS Gif-sur-Yvette, France; currently BioScience Project, Wakefield, MA, USA).[136] The vector maps and the insert sequences can be found in the appendix (Section 8.1). The correct open reading frame of both plasmids was verified by sequencing prior to use (Section 8.1.1). If not stated otherwise, the names Rab5c and Rabex-5GEF throughout this thesis will refer to these shortened constructs.
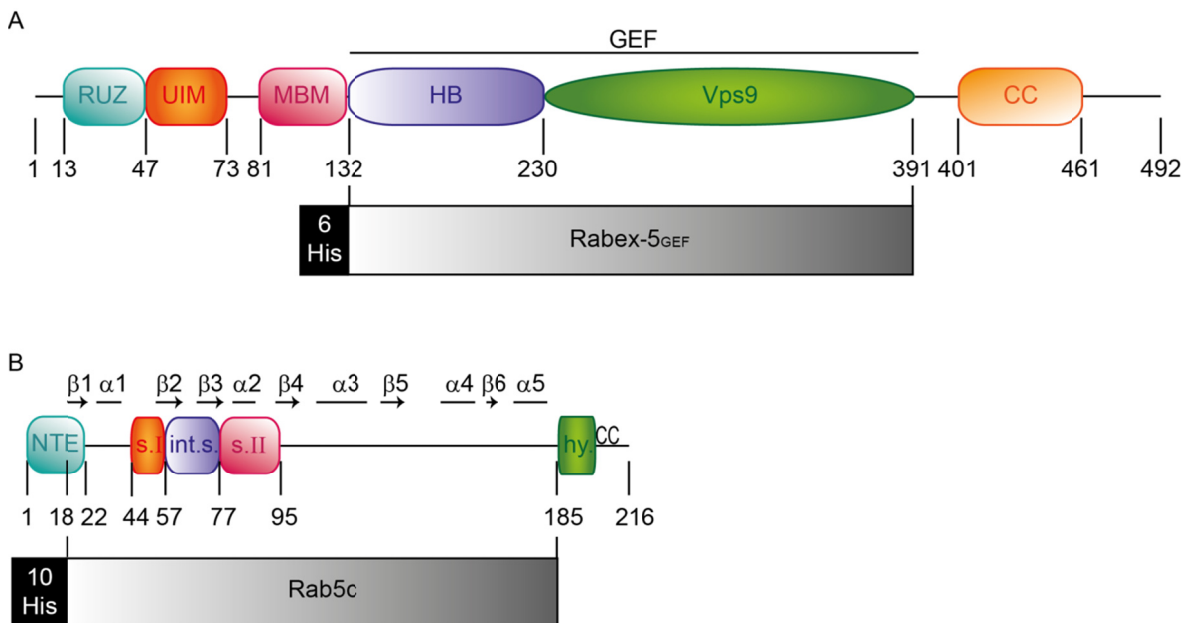
Figure 13   Schematic illustration of the expression constructs of Rabex-5GEF and Rab5c.
A) The human Rabex-5GEF construct (grey) comprises the helical bundle domain (HB) and the Vps9 domain (aa132-391) with an N-terminal 6-His tag. The full-length protein consists additionally of the Rabex-5 ubiquitin binding zinc finger domain RUZ, the ubiquitin interacting motif (UIM), the membrane binding motif (MBM), and the coiled coil (CC) domain. **B)** The Rab5c construct (grey) spans the amino acids 18 to 185 and is fused to an N-terminal 10-His tag. The definition of switch I (s.I), interswitch (int.s.), switch II (s.II), alpha-helices (αx) and beta-strands (βx) was taken from [227]. The N-terminal element (NTE) was described by [225].The definition of the C-terminal hypervariable domain (hy.) is according to [56]. "CC" indicates the C-terminal cysteines carrying the prenylation.

3.1.2 Purification of Rab5c and Rabex-5GEF

Rabex-5GEF and Rab5c were heterologously expressed in *E.coli* BL21-CodonPlus® (DE3)-RIL cells. These derivatives of BL21 cells supply additional copies of specific tRNA genes that are rare in E. coli (arginine, isoleucine, and leucine). Since Rabex-5GEF comprises 20.5 % of these amino acids, and Rab5c contains 16.5 % arginine, isoleucine and leucine (Section 8.2.2 and 8.2.3) the use of these cells was likely to increase the protein yield.

The induction of the gene expression by Isopropyl β-D-1-thiogalactopyranoside (IPTG) was monitored via SDS-PAGE as depicted in Figure 14A for Rab5c and Figure 14B for Rabex-5GEF. Increased abundance of a band with the expected size - 21 kDa for Rab5c and 31 kDa for Rabex-5GEF - was observed in both cases and indicated successful induction of gene expression. The lysates from *E.coli* cells were subjected to nickel-affinity chromatography and gel-filtration. Samples of all steps were collected and visualized by SDS-PAGE (Figure 14). Rabex-5GEF mainly eluted in the fractions 4 to 5 (60 - 100 mM imidazole) while the majority of Rab5c eluted in the fractions 5 to 6 (150 - 200 mM imidazole). This reflects the length of the His-tag of both protein constructs: the 10-His-tag of the Rab5c construct had higher affinity to the nickel-NTA column material than the 6-His tag of Rabex-5GEF. The longer tag allowed stronger washing without loss of Rab5c. The fractions which contained the highest quantity of pure protein after nickel affinity chromatography (Figure 14, lane 9 - 11 for both proteins) were pooled and concentrated prior to loading onto a Superdex200 column to perform gel-filtration (Figure 14A, lane 14; Figure 14B, lanes 13 - 14). A small amount of protein of a size of 18 kDa visible in the Rab5c sample could not be removed by the gel-filtration chromatography because this size difference was too small. After the gel filtration, the protein containing fractions were pooled, concentrated and frozen in liquid nitrogen prior to storage at -80 °C. Although minor impurities remained in the protein samples they were used for the screening assay. The integration of the bands on the Coomassie stained SDS-polyacrylamide gel revealed a purity of > 90 % for the Rabex-5GEF of > 95 % for Rab5c and protein. The yield was 50 mg for Rabex-5GEF at a concentration of 96 μM and 65 mg for Rab5c at a concentration of 260 μM from a two litre *E.coli* culture each.

The original protocol for purification included also an anion exchange chromatography step besides the nickel-affinity chromatography and the gel-filtration.[136] This protocol however had been designed to obtain protein for crystallography which demands very pure samples. For the aim of this work, the degree of purification obtained with nickel-affinity chromatography and gel-filtration chromatography alone was not only sufficient but even more appropriate. This is due to the fact that for a screening approach, a large amount of active protein was needed. Every purification step will decrease the yield but nevertheless, a screening would ideally be performed with the same protein batch to ensure reproducibility.[228] As the protein was already at least 90 % pure after the affinity chromatography, the anion-exchange chromatography was omitted. Gel-filtration chromatography was performed because dialysis or buffer exchange to remove the imidazole was necessary. The gel-filtration chromatography was performed for removal of the imidazole and provided an additional purification step.
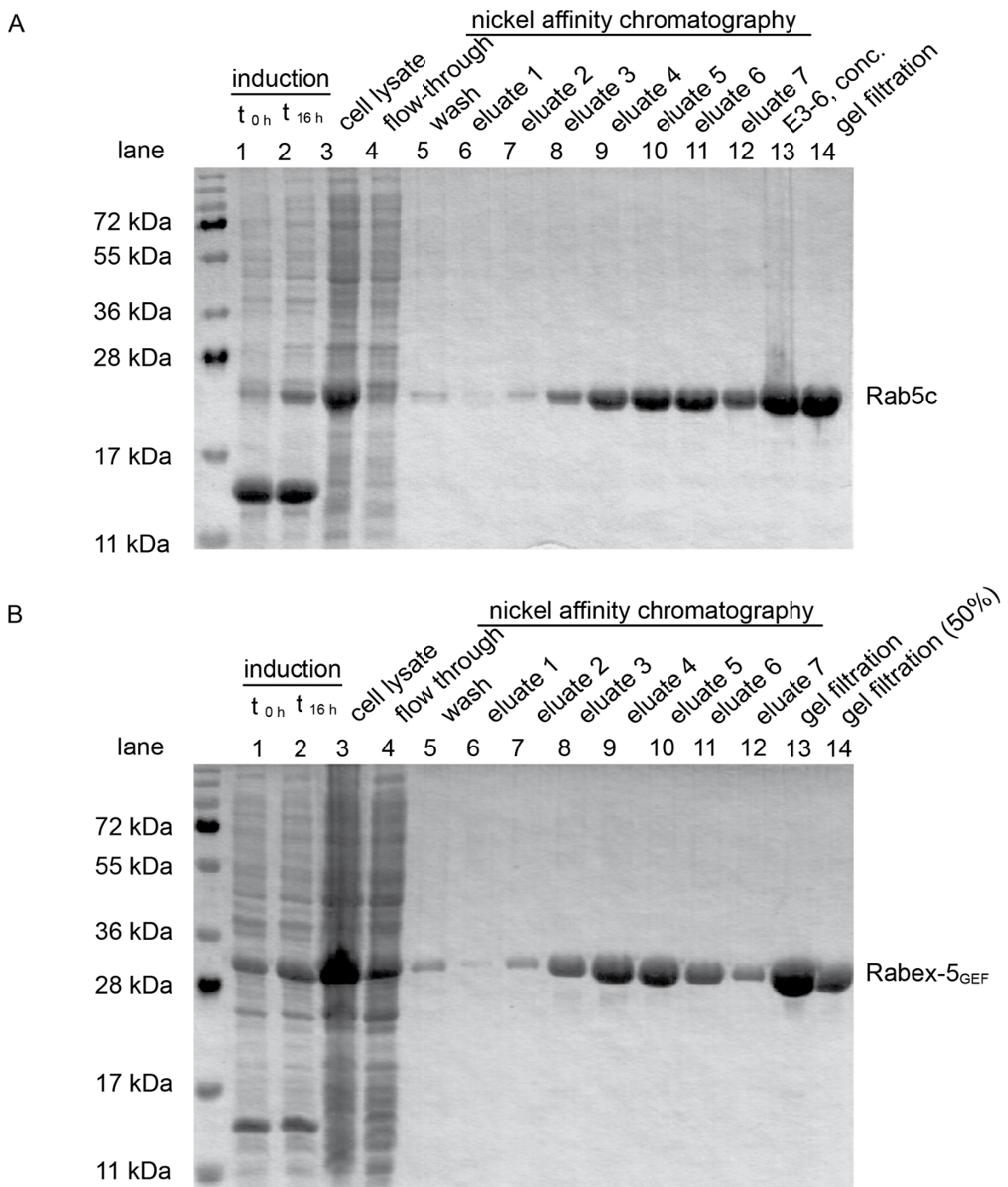
Figure 14 Expression and purification of Rab5c and Rabex-5GEF proteins.
15 % SDS polyacrylamide gels stained with Coomassie Brilliant Blue. The induction was observed by comparing cell lysate before (lane 1) and after induction with IPTG (lane 2). An increase of the proteins, with the expected size as indicate on the right side of the gels, was detected. The additional band appearing at 14 kDa is lysozyme (14.3 kDa theoretical mass) that had been used for cell lysis in these samples. Lane 3 shows the cell lysate after lysis with French Press without addition of lysozyme. In lane 4 to 12 fractions from the nickel affinity chromatography including the flow-through, the wash fraction and the elution fractions are depicted. The elution was performed with increasing concentrations of imidazole from 10 mM (lane 6, fraction 1) to 300 mM (lane 12, fraction 7). **A)** Rab5c. Lane 13 shows the pooled and concentrated protein sample that was loaded onto the gel filtration column, lane 14 contains the protein sample after gel filtration and concentration with Amicon filters. Small amounts of undesired proteins at a size of roughly 70 kDa can be seen in lane 7-11. **B)** Rabex-5GEF. Lane 13 - 14 show the protein sample after gel filtration; in lane 14 only half of the volume was loaded because the samples contained a highly concentrated protein solution. Small amounts of undesired proteins at a size of roughly 55 - 70 kDa are visible in lane 7 - 11.

3.1.3 Activity of the purified proteins

The *in vitro* expressed and purified proteins were tested for enzymatic activity in a nucleotide exchange assay. It was expected that active Rabex-5GEF should catalyse the exchange reaction in a dose-dependent manner.[136] As readout for the nucleotide exchange, the intrinsic tryptophan fluorescence of the Trp74 and Trp114 residues of the GTPase Rab5 was used.[229] The fluorescence of these tryptophan residues changes depending on the type of nucleotide bound by Rab5: association of GTP decreases the fluorescence compared to the Rab5-GDP complex.[229] Addition of Rabex-5GEF to Rab5c accelerates the association of GTP which results in a decrease of fluorescence intensity over time. Rab5 has a strong intrinsic GTPase activity and hydrolyses about 80 % of the GTP within ten minutes.[160] To monitor solely the nucleotide exchange and not the hydrolysis of GTP, the non-hydrolysable GTP analogue GppHNp was used. In Figure 15 the nucleotide exchange is depicted at various Rabex-5GEF concentrations to confirm the activity of Rabex-5GEF. The catalytic effect of Rabex-5GEF was confirmed to be dose-dependent as expected: increasing concentrations of Rabex-5GEF led to a faster decrease of the fluorescence signal. At a level of approximately 8 RFU the reaction was saturated: all nucleotides had been exchanged for GppHNp.
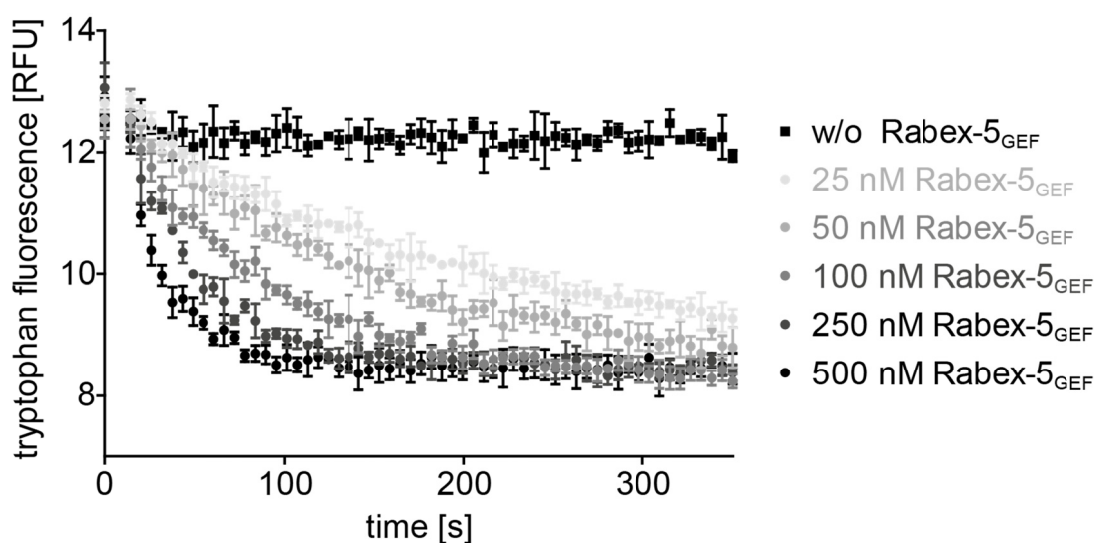
Figure 15 **Rabex-5GEF catalysed the nucleotide exchange on the small GTPase Rab5c dose-dependently.**
The nucleotide exchange was measured by monitoring the intrinsic tryptophan fluorescence of Rab5c. The x-axis shows the time [s] and the y-axis the relative fluorescence units [RFU]. The fluorescence decreased upon association of GppNHp, a non-hydrolysable analogue of GTP, with Rab5c. The intrinsic exchange activity of the GTPase is small: almost no decrease in signal was observed over 5 minutes. Rabex-5GEF, already in a very low concentration of 25 nM led to a strong decrease in fluorescence indicating nucleotide exchange was occurring. Higher Rabex-5GEF concentrations up to 500 nM accelerated the nucleotide exchange to a faster extent. At 500 nM Rabex-5GEF concentration, the maximal nucleotide exchange was observed already after ~100 seconds. The Rab5c concentration during the experiment was 1 μM; the experiment was performed in nucleotide exchange buffer with 20 mM Tris, pH 8.0, 100 mM NaCl, 2 mM MgCl$_2$ and 0.25 % Tween20.

3.2 Screening for small molecule inhibitors

The search for inhibitory small molecules targeting the Rabex-5GEF mediated Rab5c activation required a screening strategy that is designed to select molecules with the desired function. In the first subsection, the general considerations to obtain a reliable *in vitro* assay for the detection of the nucleotide exchange reaction mediated by Rabex-5GEF are presented (Section 3.2.1.1). In the following, the optimization strategy to obtain this robot-compatible assay as well as the quality control of the assay are addressed (Section 3.2.1.2 - 3.2.1.3). Subsequently, the results of screening a library of small molecules for active substances are presented (Section 3.2.2). Finally, the obtained primary hit compounds were verified by re-screening (Section 3.2.3).

3.2.1 Screening concept and assay establishment

As in most HTS approaches, the compounds were only tested in single values. Therefore, the assay was required to be robust for certainty in the interpretation of hits as well as sensitive to avoid false negatives.[230] Therefore, a stable measurement window with a reliable difference in signal between the fully active (positive control) and completely inactive (negative control) Rabex-5 was required.[228] Both, the robustness and the measurement window are quantified by the use of the Z'-factor (Section 3.2.1.3).[231]

3.2.1.1 Nucleotide exchange assay optimization for HTS

The nucleotide exchange of Rabex-5GEF on Rab5c can be monitored easily and reliably via tryptophan fluorescence as described above (Figure 15) and was used to set up the HTS suitable assay. Due to the speed limitation of the plate reader, the kinetic measurement of the reaction was suited only for detection of 24 samples at a time. To increase the sample throughput, the readout was converted from kinetic to endpoint detection which allowed testing of up to 80 compounds in parallel (Figure 16).

The change in fluorescence (ΔRFU) was defined as the difference in the fluorescence of a designated time and the fluorescence before injection of the nucleotide. The ΔRFU in absence of Rabex-5GEF was small because the intrinsic exchange activity of Rab5 was comparably slow and it was significantly increased in the reaction with Rabex-5GEF.

A schematic overview of the screening approach and the anticipated effect of active small molecules are depicted in Figure 17. In the control reactions, dimethyl sulfoxide (DMSO), the solvent of the compounds, was used instead of small molecule compounds. The positive control contained both proteins, thus the occurring nucleotide exchange reaction led to a decrease in fluorescence and a high ΔRFU (Figure 17A). The absence of Rabex-5GEF in the negative control simulated an inhibited reaction. The small ΔRFU in the negative control indicated that almost no nucleotide was exchanged (Figure 17B). An active compound (Figure 16C) was expected to disrupt the exchange activity and thereby reduce the ΔRFU to a similar level to the negative control (compare Figure 17B vs. C). The inactive compounds were expected not to interfere with the readout and to result in a similar ΔRFU as the positive control.
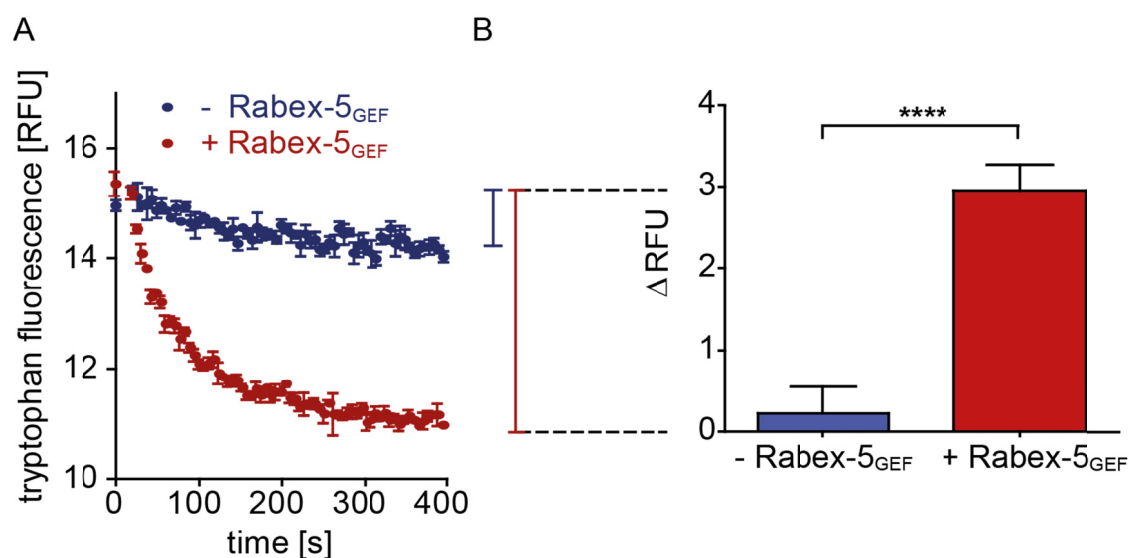
Figure 16   Conversion of the kinetic nucleotide exchange assay into a HTS-suitable screening format.
The blue curve and column represent the Rab5c samples without Rabex-5GEF while the red curve and column indicate the samples with Rab5c and Rabex-5GEF present. **A)** The kinetic readout of the nucleotide exchange assay is not suited for screening because it does not allow a high throughput of samples. **B)** The form of assay observation was changed to an endpoint readout. The change in the nucleotide binding state of Rab5c, ergo fluorescence, is now depicted as ΔRFU, defined as the change of fluorescence between the start of the measurement (before injection of nucleotide) and the measured endpoint. The significance shown in the bar graph was calculated using the unpaired t-test, p-value: ****$p < 0.0001$ (Graph Pad Prism Software).
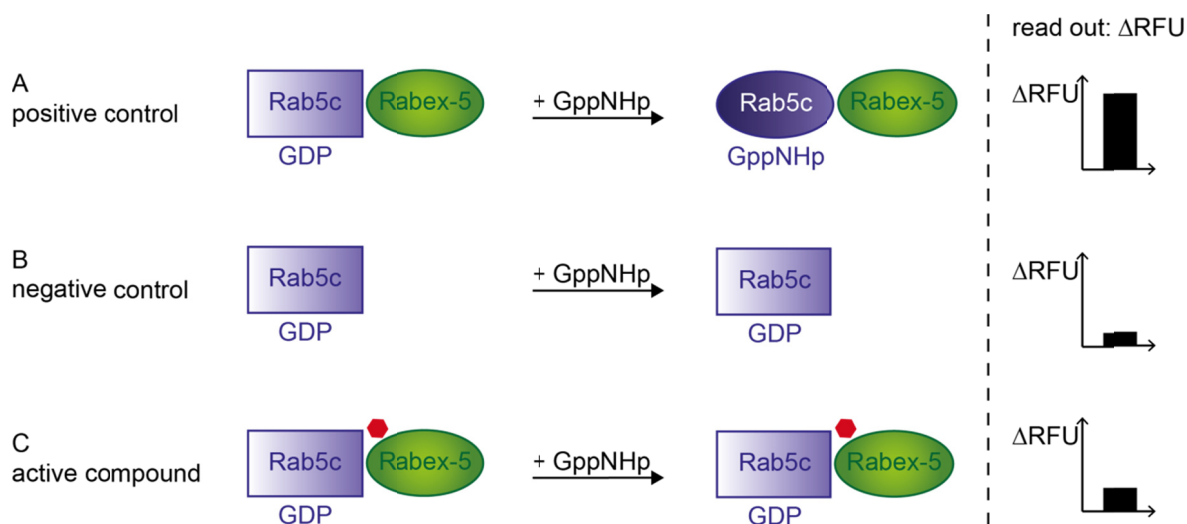
Figure 17   Planned screening approach: monitoring the Rabex-5 dependent Rab5c activation.
Schematic illustration of the concept of the screening for inhibitors of the nucleotide exchange of Rabex-5GEF. The readout is depicted as ΔRFU which is the difference of fluorescence signal before (t_0) and after (t_{170}) addition of GppNHp (left side). **A)** The positive control contains Rab5c (blue) and Rabex-5GEF (green) with DMSO but no small molecule compound and results in the activation of Rab5c and consequently in a high ΔRFU signal. **B)** The negative control of the assay which represents a completely inhibited reaction is defined by absence of Rabex-5 and contains only Rab5c and DMSO. The GTPase Rab5c stays in the inactive, GDP loaded form and thus no fluorescence change takes place wherefore the ΔRFU signal is small. **C)** An active small molecule candidate (red hexagon) would inhibit the exchange reaction resulting in a ΔRFU level comparable to the negative control.

41

3.2.1.2   Optimization of the assay conditions

Further optimization steps besides the adaption of the readout mode were necessary to achieve the above mentioned requirements for a reliable screening assay. The assay was modified regarding volume and type of the microtitre plates to obtain a small sample volume that would limit the protein and compound material needed during the screening process. The assay preparation protocol, the DMSO concentration, the presence of a detergent as well as the Rabex-5GEF concentration were optimized to increase the assay robustness. The final conditions used during the screening and the range of varying conditions that have been analysed to find the optimal screening setup are summarized in Table 2. Detailed information on the screening optimization can be found in the appendix (Section 8.4).

Several microtitre plates were tested for their impact on the protein activity and variations between the control samples. The differences between the plates were found to be negligible. Half area plates were chosen because they allowed a reduction of the total sample volume from 200 μL to 50 μL (Section 8.4, Supporting table 8). The lower sample volume allowed a restriction of the total amount of material.

Table 2   Summary of the optimization procedure for HTS suitable-assay conditions.

Step [a]	Conditions tested [b]	Conditions used[c]
Plates	– 96 well plates – half area and full area – Greiner Bio One (Germany) / Corning Inc. (USA) – black and white – low binding / medium binding	– 96 well plates – half area – Greiner Bio One (Germany) – black – medium binding
Volume	– 200, 100 and 50 μL total volume – 5 to 10 μL injection of GppHNp	– 50 μL total volume – 10 μL injection of GppNHp
Proteins	– varying Rabex-5GEF concentrations were tested – ± preloading with GDP – batches #3 and #4 were tested in comparison [d]	– 500 nM Rabex-5GEF, 1 μM Rab5c – no preloading – batch #4
Assay preparation	– variations in the order of the pipetting the assay components – assay preparation at RT / 12 °C 　– centrifugation / sonication – shaking manually or by *Varioskan* – incubations: 5 - 40 minutes at RT / ice	– order of pipetting: Rab5c – compound – Rabex-5GEF – assay preparation at 12 °C – centrifugation 30 seconds – manually shaken – 7 minutes incubation at RT
Measurement	– several intervals within 10 minutes	– 0, 60, 120, 170, 300 seconds (0 = prior to GppNHp addition) – used for analysis: 0, 170 seconds
Detergent	– 0.0025 - 2.5 % Tween20 – 0.01 - 0.25 % Igepal / TritonX100	– 0.25 % Tween20
DMSO	– 2 - 10 % – standard DMSO (Carl Roth GmbH + Co. KG, Germany) / anhydrous DMSO (Acros Organics, Belgium)	– 2 % – anhydrous DMSO (Acros Organics, Belgium)

All conditions tested during the assay optimization process are summarized in the table. **[a]** The optimized parameters are indicated. **[b]** All conditions that have been tested are listed. **[c]** The conditions that have been finally used for the screening are denoted. RT = room temperature. **[d]** Between proteins from different purification batches no difference in activity was observed (Section 8.4, Supporting table 7).

The protein concentration was chosen to obtain an optimal measurement window within a short measurement period. The measurement period was one of the limiting steps for the execution of the screening procedure and thus was intended to be as short as possible. The use of 500 nM Rabex-5GEF ensured that the maximal exchange plateau was rapidly reached.

The order of pipetting did influence the assay quality. Adding Rabex-5GEF in the first pipetting step resulted in decreased protein activity (Section 8.4, Supporting table 9). Rab5c was more stable and could be added as first assay component. In addition, it was important that the compounds were not added in the first step. The amount of DMSO (1 μL) was the smallest volume the robot could handle and the addition was more reliable with liquid already present in the well. To obtain the best Rabex-5GEF activity, Rabex-5GEF was added as the last step, following the addition of compounds. In this way, the compound should not have to compete with a preformed Rabex-5-Rab5c complex, thereby increasing the chances of identifying a hit compound.

To enable a higher throughput of compounds, the assay was supposed to be stable when pipetted by a robot.[228] Pipetting the assay with the robot introduced air bubbles that disturbed the assay readout. To circumvent that problem, the plates were centrifuged for 30 seconds after completion of the pipetting by the robot. This procedure removed the air bubbles completely (Section 8.4, Supporting table 10).

An ideal point for the readout seemed to be the moment when the reaction just approached the saturation level. At this time, the ΔRFU reached the maximal measurement window while the readout time was short. Thereby the total time needed for the measurement of one assay plate was restricted. A decrease of protein activity was observed upon measuring a complete 96 well plate, which had been prepared by the robot, compared to the manually prepared 24 well reaction (Section 8.4, Supporting table 11). To gain the desired measurement window, the endpoint readout time was adapted accordingly to 170 seconds. The nucleotide exchange reaction was quantified by the difference of fluorescence signal before and 170 seconds after starting the exchange reaction by injection of GppNHp (ΔRFU).

Non-ionic detergents are known to hinder small molecule aggregation that might lead to false positives and to suppress promiscuous inhibitor action in general.[232] Although many distinct detergents exist, predictions for a suitable amount and type of a detergent are not available due to the diversity of proteins and assays.[233] Thus, the suitable detergent had to be identified by try-and-error. Supplementation with Tween20 was investigated and at a concentration of 0.25 % Tween20 the highest exchange rate was reached in the nucleotide exchange assay (Table 3). In addition, the variation between the samples decreased. These two consequences of Tween20 addition were beneficial for the screening assay since they increased the measurement window. Higher concentrations of Tween20 were disadvantageous. Comparable results to 0.25 % Tween20 were obtained with 0.01 % Igepal or 0.05 % Triton-X100 (Section 8.4, Supporting table 12). Since both detergents did not offer further advantageous effects to the assay, Tween20 was not replaced.

Table 3 The impact of Tween20 on the Rabex-5GEF exchange rate.

Assay preparation condition	Exchange rate k_{cat}/K_m [M^{-1}s^{-1}] ± SD
w/o detergent	0.015 ± 0.003
0.0025 % Tween20	0.017 ± 0.006
0.025 % Tween20	0.025 ± 0.009
0.25 % Tween20	**0.029 ± 0.002** [a]
2.5 % Tween20	0.023 ± 0.007

Non-ionic detergent is known to have beneficial influence on HTS assays. In order to be used, it had to be tested for compatibility with the assay system. The other assay components were 1 % DMSO, 0.5 μM Rabex-5GEF, 1 μM Rab5c. The samples were incubated for 5 minutes at RT prior to the measurement. **[a]** At 0.25 % Tween20 the observed rate constant was maximal while the error, here depicted as standard deviation (SD), was minimal. This condition was chosen for the HTS assay.

Since the small molecules in the compound library were dissolved in DMSO, the DMSO tolerance of the assay was analysed. 2 - 10 % DMSO final concentration were tested for their impact on the nucleotide exchange assay. The assay volume of 50 μL and the pipetting volume limitation of 1 μL by the screening robot assigned that at least 2 % DMSO were necessary to avoid pre-dilution of the compounds. Such a pre-dilution step is undesired because additional pipetting steps in the screening procedure would increase the screening time and would waste compound material. In addition, the number of potential pipetting errors would naturally rise. The addition of 2 % DMSO decreased the exchange rate by about 33 % (Table 4). Higher concentrations affected the protein activity even stronger. Hence, a final concentration of 2 % DMSO was used because it was still tolerated by the proteins and otherwise pre-dilution of the compound would have been necessary.

Table 4 Dependency of the Rabex-5GEF exchange rate on the DMSO concentration.

DMSO	w/o	2 % (v/v)	4 % (v/v)	10 %(v/v) [a]
exchange rate k_{cat}/k_m [M^{-1}s^{-1}]	0.033	**0.022**	0.018	0.018
relative change	0 %	**33 %**	45 %	45 %

DMSO in the assay buffer decreases the exchange rate indicating that it had an inhibitory effect on the catalysed reaction. **[a]** At 10 % DMSO the fluorescence readout is also affected and bore the risk of readout disturbance.

3.2.1.3 Z' factor

The amount of false-negatives and false-positives emerging during a screening needs to be minimized. It has to be avoided to miss active compounds or to have many false-positives, which have to be retested in follow-up experiments. This can be either guaranteed by performing the HTS in adequate numbers of replicates or by using high quality assays.[231] Replicates, however, have the disadvantage of multiplying screening time, material, and costs and are thus less favourable than to optimize the assay to high quality. The Z' factor is a parameter to determine reliability and robustness of a screening assay.[231] It comprises the arithmetic mean and standard deviation of the assay controls to calculate the wideness of the measurement window. These theoretical considerations are illustrated in Figure 18A. The averages of the control samples are shown as μ1 and μ2

assuming a Gaussian distribution of the single values of both control sample populations. The measurement window is calculated according to the following formula taking into account how far both control average values are separated ($\mu2 - \mu1$) and the strengths of the scattering of the single values in each population ($3\sigma1 + 3\sigma2$).

$$Z' = 1 - \frac{3\sigma2 + 3\sigma1}{|\mu2 - \mu1|}$$

The Z' value can have a maximal value of 1 and the closer the Z' value is to 1, the better the assay. For the Rabex-5$_{GEF}$ dependent nucleotide exchange screening assay, a Z' value was calculated from five different test plates (Figure 18B), yielding a Z' value of 0.52. Any value above 0.5 is considered to indicate that the assay is reliable in a high throughput setting. The Z' of the Rabex-5$_{GEF}$-Rab5c assay was above the reliability threshold and thus the assay was considered suitable for screening.
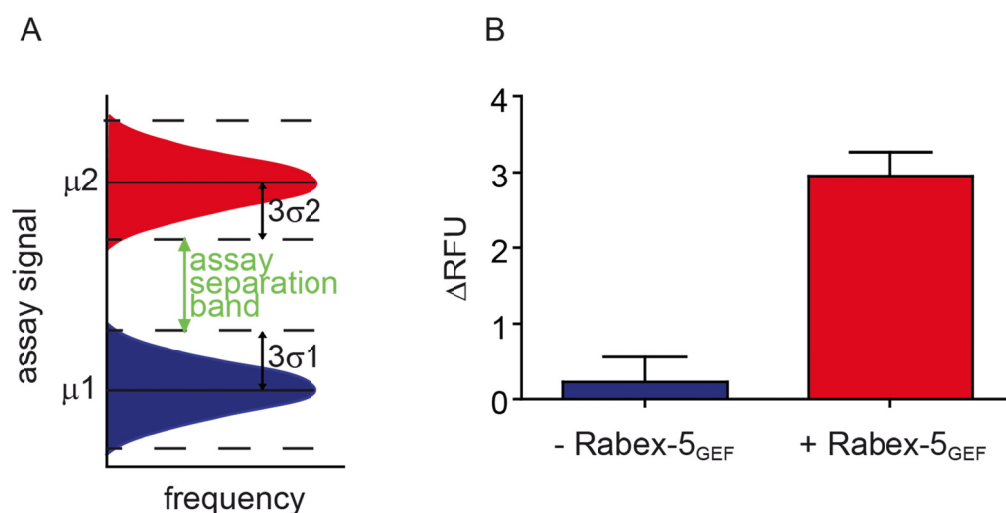
Figure 18   The Z' factor (for the Rabex-5$_{GEF}$-Rab5c screening assay).
A) The general concept of the Z' factor analysis is illustrated. The positive control is depicted in red, the negative control in blue. As every method is prone to perturbation by instrumental or human imprecisions, the measurements of the assay signal are assumed to contain a certain degree of variety according to Gaussian distribution. Three times the standard deviation (σ) covers the majority (bulk) of the sample values. The area between the two populations is considered as measurement window or assay separation band (green arrow). The larger this area the more reliable is the assay. Hits are defined as those compounds that stick out from the normal distribution which are defined by the three-fold SD (3σ). This graphic was adapted from [231]. **B)** The Z' value for the Rabex-5$_{GEF}$ screening assay. μ and σ were calculated from 15 replicates originating from five independent microtitre plates. The errors are shown as SD. The blue column represents the negative control with solely Rab5c GTPase present; the red column shows the positive control with Rab5c and Rabex-5$_{GEF}$. The obtained average values were $\Delta RFU = 0.2 \pm 0.3$ and $\Delta RFU = 3.0 \pm 0.3$ for the negative and positive control, respectively, resulting in a Z' value of 0.52.

3.2.1.4 Compound library

An in-house compound library containing about 13,000 molecules was used in this study. It mainly consists of compounds following the "Lipinski rule of five".[234] The "Lipinski rule of five" gives a rough estimate if small molecules are likely to be orally active. Poor absorption of a molecule is expected with increased likelihood when two or more of the following criteria are not complied: maximal five hydrogen bond donors, maximal ten hydrogen bond acceptors, molecular mass of maximal 500 Da, and a logP below five.[234] The logP gives the lipophilicity of a compound and is calculated as logarithm of the solute in water divided by the solute in octanol. The majority of the compounds of the in-house library has been purchased (ComGenex). The library contains additional substances which have been synthesized in the groups of *Professor Dr. M. Famulok, Professor Dr. M. Gütschow* and other groups of the University of Bonn.

3.2.2 Screening results

The compound library was screened under the established conditions (Section 3.2.1.2); the obtained data is plotted in Figure 19. The ΔRFU values for the controls and each screening sample are depicted on the y-axis. Approximately 33 % residual activity of the nucleotide exchange reaction compared to the controls (ΔRFU = 1) was chosen as the threshold for the hit definition. According to the definition, the screening yielded 73 primary hits (Figure 19, below the threshold line that is indicated in red). A complete list of all primary hits can be found in the appendix (Section 8.5).

In addition, the fluorescence intensity observed at the initial fluorescence reading of each measurement (t_0) is given on the x-axis. A shift of the bulk of the samples to the right on the x-axis compared to the controls indicated that many of the compounds changed the fluorescence signal. Most of the compounds still yielded signals in the ΔRFU range of the positive control. However, compounds with high intrinsic fluorescence seem to be more prone to drift towards extreme ΔRFU values than compounds with low auto-fluorescence characteristics (Figure 18, right side).

141 compounds had to be excluded from the analysis (data not shown) because of inaccurate pipetting by the robot. For these, low starting signals were observed suggesting that less or no Rab5c had been added. In all cases the sample volume was found to be less than 50 μL and these compounds were omitted from further investigation.
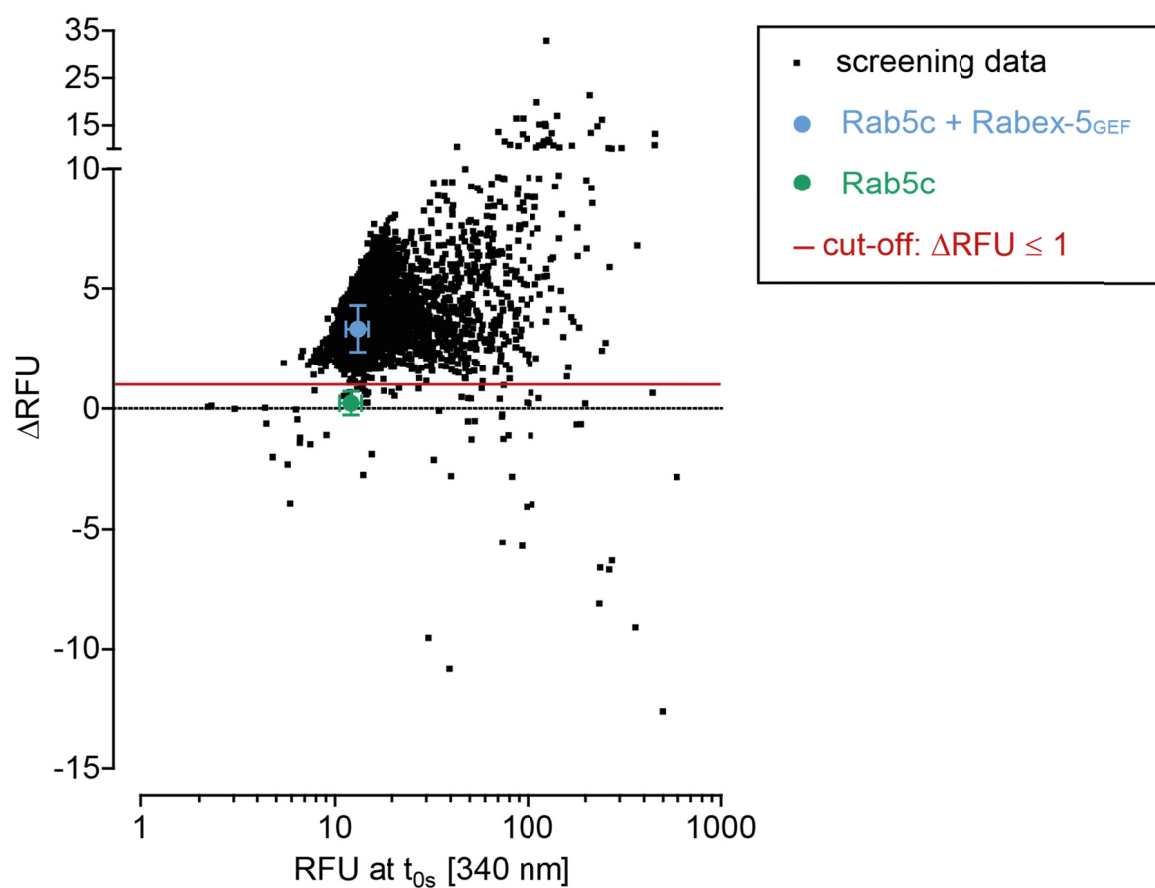
Figure 19   Result of the screening: 73 primary hits.
Result of the HTS for small molecule compounds inhibiting the nucleotide exchange of Rab5c-Rabex-5$_{GEF}$. The data of all screening samples are shown: the ΔRFU value of each compound (y-axis) is plotted against the fluorescence RFU at t_0 (x-axis). The positive control (blue, Rab5c+Rabex-5$_{GEF}$) had an average ΔRFU of 3.3 ± 1.0 and the negative control (green, Rab5c) an average ΔRFU of 0.2 ± 0.5. The cut-off to define hit compounds was set to ΔRFU = 1.0 (red line) which represents ~33 % residual exchange activity.

3.2.3 Re-screening of hit compounds

All 73 primary hits were re-screened to verify their activity. This was necessary to detect false-positive hits because the screening had been performed in single values. For the re-screening process, the screening assay was performed manually and all compounds were tested in quadruplicates. 25 compounds again showed a ΔRFU value below 1 (Figure 20; red, light red and orange data points) and were confirmed as hits.

In the primary screening the impact of the auto-fluorescence of the compounds had already become apparent. Hence, it was considered whether all primary hits that affected the fluorescence readout compared to the controls should be omitted from the analysis. To estimate the impact of intrinsic fluorescence on the nucleotide exchange assay all rescreened hits were plotted in Figure 20 with respect to their fluorescence characteristics (y-axis, RFU 340 nm) and the screening readout (x-axis, ΔRFU).
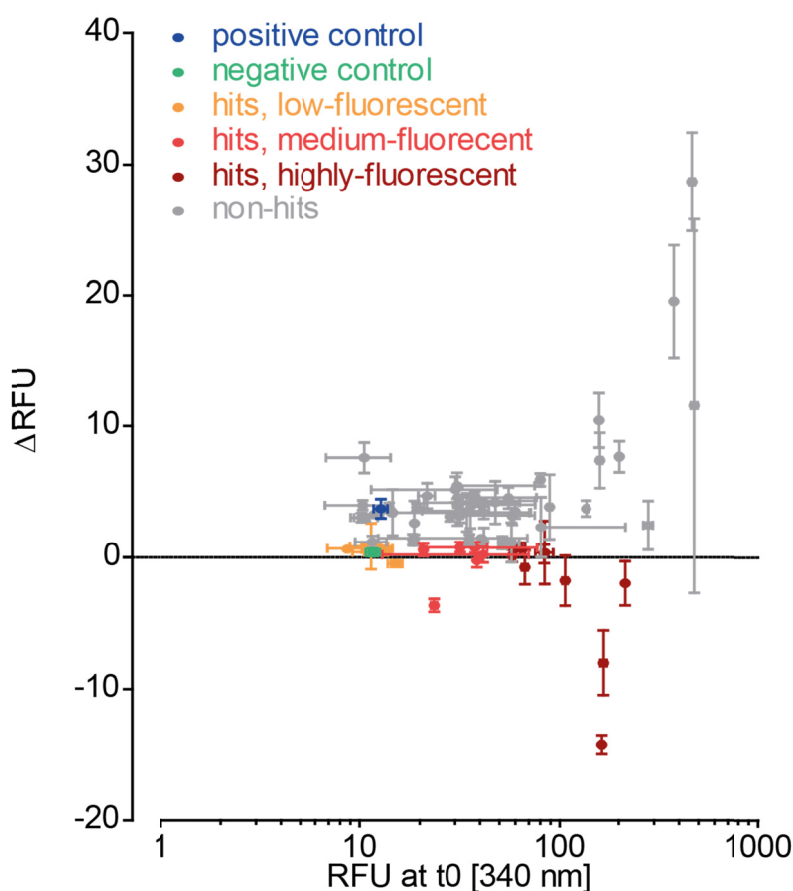
Figure 20   Results of the re-screening: 73 primary hits yielded 25 secondary hits.
The re-screened primary hits are depicted with the obtained ΔRFU on the y-axis and the intrinsic fluorescence (RFU [340 nm] at t_0) on the x-axis. The negative control containing only Rab5c is shown in green, the positive control with Rab5c and Rabex-5$_{GEF}$ is shown in blue. The hits that are confirmed are shown in orange (low-fluorescent, RFU < 20), light red (medium-fluorescent, 20 > RFU < 40) and red (highly-fluorescent, RFU > 40). The non-confirmed hits are shown in grey. 22 primary hits were classified as low-fluorescent, 21 as medium fluorescent and 30 as fluorescent. Consequently, 51 of 73 hits had at least medium fluorescence characteristics. Of the confirmed hits 9 were low-fluorescent, 6 medium-fluorescent and 10 highly-fluorescent.

3.2.3.1 Hits with high fluorescence characteristics

It was observed that about 70 % of the primary hits were auto-fluorescent (RFU [340 nm] ≥ 20). Most compounds with high auto-fluorescence (RFU [340 nm] ≥ 40) induced ΔRFU values with high standard deviations (Figure 20, red data points). This indicates a disturbance of the readout rather than actual inhibition of the nucleotide exchange. The confirmed highly fluorescent hits were analysed in a kinetic form of the nucleotide exchange assay (Section 8.5). No conclusive inhibitory compound was found among them.

3.2.3.2 Hits with low to medium fluorescence characteristics

The re-screening data of the remaining 43 low-fluorescent and medium-fluorescent hits is again shown in Figure 21 considering solely the ΔRFU signal to allow better comparison of the activity of these compounds. 15 of these 43 primary hits were confirmed in the re-screen (Figure 21, dark grey bars). They are referred to as secondary hits and comprise 20 % of the primary hits. Subsequently, the activity and specificity of the secondary hits was verified and C4.30.H05 (JH5) and K1.08.C11 (Gü321) were chosen as promising lead compounds. A detailed description of this selection process can be found in Section 3.6. The following Section 3.3 continues with the activity profile of both lead compounds. The structures of both molecules are depicted in Figure 21.
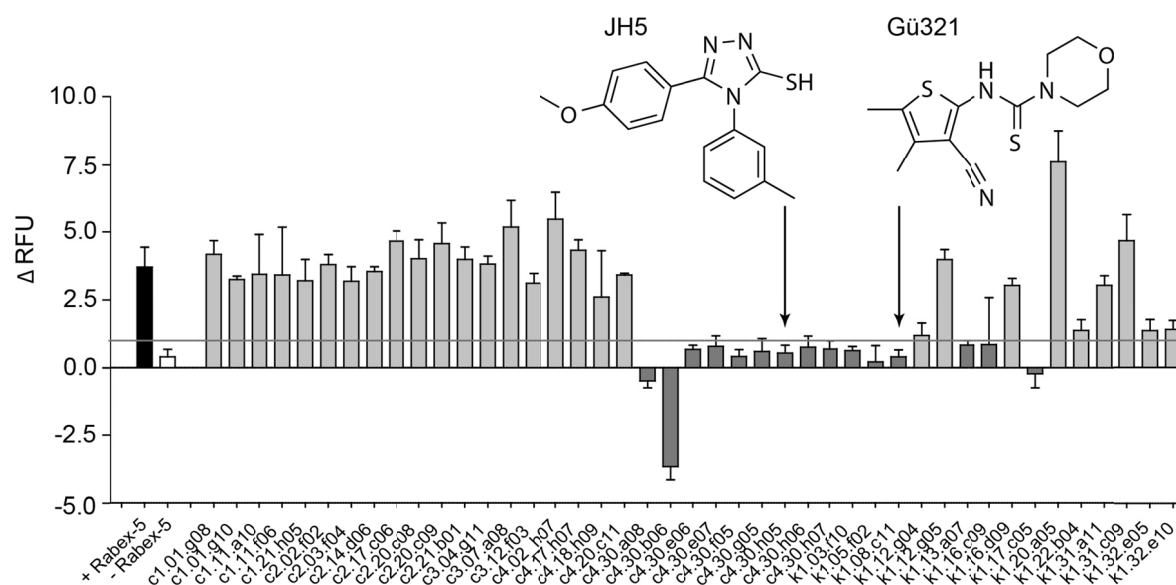
Figure 21   Re-screening of the primary hits confirmed 15 compounds as secondary hits.
The data set from Figure 20 is presented but the highly-fluorescent hits are excluded from this figure. The y-axis shows the ΔRFU readout of the re-screened compounds. The positive control (black) contained Rab5c and Rabex-5GEF with DMSO and resulted in an average ΔRFU of 3.7 ± 0.7. The negative control (white) contained only Rab5c and DMSO but no Rabex-5GEF protein and had an average ΔRFU of 0.4 ± 0.3. 15 hits (dark grey) were confirmed by having again a ΔRFU below 1 (cut-off depicted as grey line). The compounds C4.30.A08 and C4.30.B06 showed negative ΔRFU values. An explanation for this behaviour was discovered in later investigations in the kinetic assay (Section 8.5): the auto-fluorescence of these compounds led to an increase in fluorescence over time. The same behaviour was also observed when measuring the compound without proteins in buffer. Thus, this observation has its origin in the intrinsic compound fluorescence. The data are shown as mean ± SD. The compounds were investigated regarding their activity and specificity. Two lead compounds C4.30.H05 (JH5) and K1.08.C11 (Gü321) showing most promising characteristics were selected and are indicated with their structures in the upper part of the graphic.

3.3 Activity profile of JH5 and Gü321

The definition of lead compound used in this thesis is taken from *Joseph G. Lombardino* and *John A. Lowe* who defined it as "a chemical structure or series of structures that show activity and selectivity in a pharmacological or biochemically relevant screen".[235] Hence, the first step in the compound characterisation was the confirmation of their activity. The characterization of the two chosen molecules JH5 and Gü321 regarding their effect on the nucleotide exchange reaction of Rabex-5$_{GEF}$ on Rab5c is explained in Section 3.3.1. Besides that, specificity limitations are often observed for small molecules and are problematic for the latter application as probe or therapeutic.[181] Therefore, specificity towards the ArfGEF Cytohesin-2, the RabGEF DrrA, and the RhoGEF Vav-1 was analysed at this early stage of compound selection (Section 3.3.2). Additional experiments regarding the identification of the target protein, the affinity towards the target protein, and activity of the compounds under reducing conditions were performed (Section 3.3.3 - 3.3.4). JH5 was found to have more promising characteristics than Gü321 and finally, JH5 was chosen as sole lead compound.

3.3.1 Confirmation of the inhibitory activity

IC$_{50}$ (inhibitory constant 50 %) values enable comparison of the inhibitory potencies of the different compounds. The kinetic format of the Rabex-5$_{GEF}$-Rab5c nucleotide exchange assay was used for the determination of IC$_{50}$ values. For the IC$_{50}$ determination, the nucleotide exchange assay was performed with 1 μM Rab5 and 20 nM Rabex-5$_{GEF}$ yielding a linear reaction process. This allowed the calculation of the initial reaction rate and plotting of these against the logarithmic compound concentration for IC$_{50}$ calculation. To estimate the reliability of the IC$_{50}$ calculation, the 95 % confidence intervals (CI) are given. They indicate the concentration range that contains the true mean of the population with a likelihood of 95 %.

JH5[1] inhibited the nucleotide exchange of Rabex-5$_{GEF}$ in a dose-dependent fashion with an IC$_{50}$ of 0.4 μM (95 % CI 0.3 - 0.5 μM; Figure 22A, B). Gü321[2] was also active in this assay. The IC$_{50}$ of 3.7 μM (95 % CI 2.8 - 4.9 μM) indicated that this molecule was about tenfold less active than JH5 (Figure 22C, D). With the corresponding library compound an IC$_{50}$ of 2.8 μM (95 % CI 2.2 - 3.7 μM) was obtained (Section 3.6.3.2).

The fluorescent readout of the nucleotide exchange assay was observed at 290 nm/340 nm (excitation/emission). To determine whether the observed effects were due to the inhibitory activity of the compounds or solely due to their interference with the fluorescent readout, a radioactive nucleotide exchange assay was established. Radioactive GTPγ^{35}S was used as nucleotide. Rab5c and the compounds were incubated with GTPγ^{35}S in presence and absence of Rabex-5$_{GEF}$. The proteins were separated from the free nucleotide by native SDS-PAGE and the radioactive intensity was detected. In the presence of Rabex-5$_{GEF}$, increased GTPγ^{35}S binding to Rab5c was observed. In this assay,

---

[1] The synthesis and compound characterisation of JH5 was kindly performed by Dr. Jeffrey Hannam.
[2] Gü321 was kindly provided by Professor Dr. M. Gütschow.

both JH5 and Gü321 were found to inhibit the reaction dose-dependently. This confirmed their inhibitory activity on the nucleotide exchange of Rabex-5$_{GEF}$-Rab5c (Figure 23).
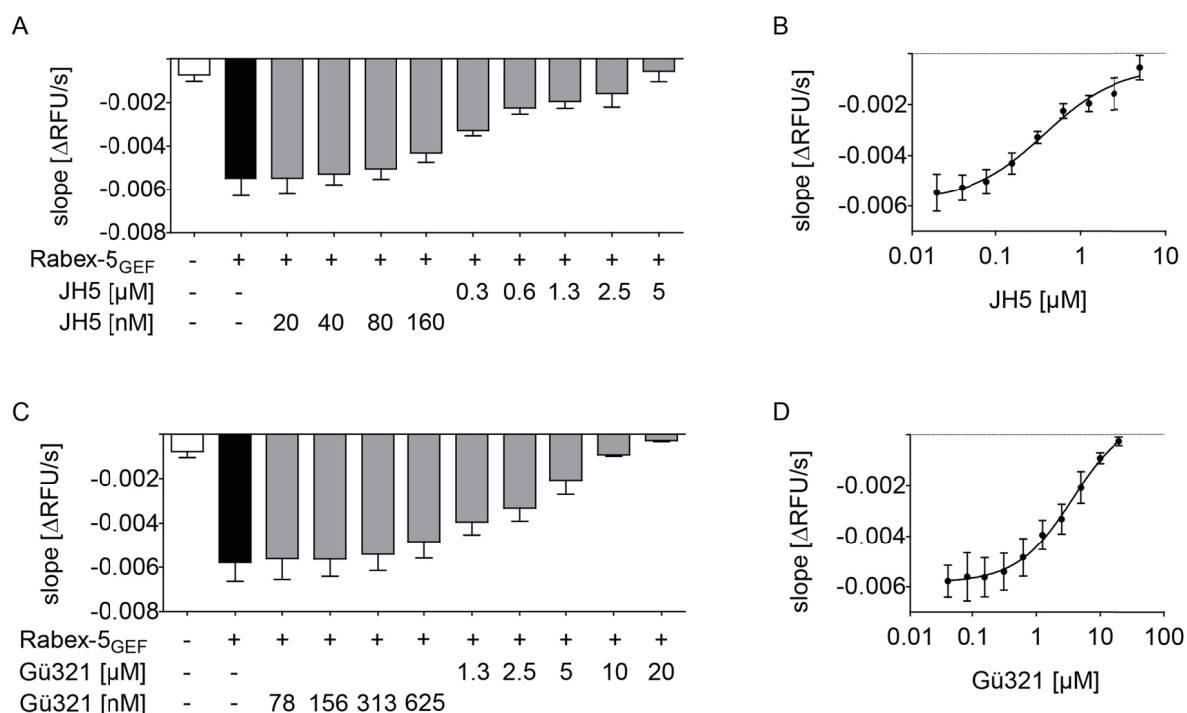
Figure 22   Inhibitory potential of JH5 and Gü321 in the Rab5c-Rabex-5$_{GEF}$ nucleotide exchange.
The IC$_{50}$ of JH5 (**A-B**) and Gü321 (**C-D**) was determined in the Rab5c-Rabex-5$_{GEF}$ nucleotide exchange assay with tryptophan-fluorescence readout. The assay was performed with 1 µM Rab5c and 20 nM Rabex-5$_{GEF}$ at 2 % DMSO. The data are depicted as column diagram (**A, C**) and as x-y-graph showing the fits which were used to obtain the IC$_{50}$ values (**B, D**). Both compounds inhibited the reaction dose-dependently. JH5 has an IC$_{50}$ of 0.4 µM (95 % CI 0.3 - 0.5 µM) and Gü321 has an IC$_{50}$ of 3.7 µM (95 % CI 2.8 - 4.9 µM). The error bars represent the SD.
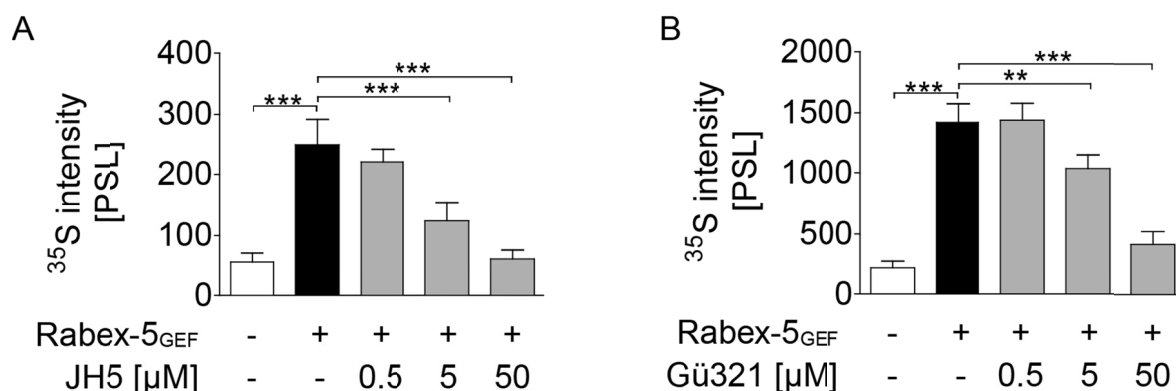
Figure 23   Inhibitory activity of JH5 and Gü321 was confirmed in a radioactive assay.
The Rabex-5$_{GEF}$ mediated nucleotide exchange on Rab5c was monitored by the association of GTPγ^{35}S to Rab5c. In all control samples DMSO was added instead of compound. **A)** JH5 inhibited the nucleotide association dose-dependently. Significant effects were observed with 5 µM and 50 µM compound. **B)** Gü321 inhibited the nucleotide exchange dose-dependently with a significant effect at 5 µM and 50 µM. However, the Gü321 inhibition was not as strong as the JH5 inhibition, verifying the results of the tryptophan fluorescence assay. Data are shown as mean ± SD from two independent experiments. The significance was calculated by the use of the one-way-ANOVA with the Tukey post-test (*GraphPad Prism* software), p-values: *p < 0.05, **p < 0.01, ***p < 0.001.

The radioactive assay was less suitable to obtain quantitative results than the tryptophan assay. The incubation time after the addition of nucleotide could not be determined as exactly as in the fluorescent assay with the *Varioskan* plate reader that injected the nucleotide. Moreover, the amount of samples that could be processed in parallel was limited to seven duplicates. Thus, only three concentrations of each compound were tested. This did not allow the calculation of IC_{50} values. Nevertheless, the radioactive assay was reliable enough to obtain qualitative results and it supported the conclusions of the IC_{50} determination. For both molecules, JH5 and Gü321, higher concentrations were needed to obtain maximal or half-maximal effects in comparison to the fluorescent assay. Rough IC_{50} value estimation from the radioactive assay data resulted in IC_{50} values of about 5 μM for JH5 and 30 - 40 μM for Gü321. The higher activity of JH5 compared to Gü321 was in line with the observations from the fluorescent assay although for both compounds the concentrations that generated half-maximal effects were higher in the radioactive assay.

3.3.2   Specificity over other nucleotide exchange reactions

With the long-term goal to use the small molecule inhibitors in a cellular environment, it is necessary to exclude that the compounds have unspecific effects. To address the specificity for Rabex-5GEF over other GEFs in functional assays, the compounds were analysed in nucleotide exchange assays with several other GEFs and GTPases. Exchange assays with the GTPase Arf1 and the GEF Cytohesin-2, the GTPase Rab1 and the GEF DrrA as well as the GTPase Rac1 and the GEF Vav-1, respectively, were performed. The readout of the Cytohesin-2-Arf1 nucleotide exchange assay was also tryptophan fluorescence. Therefore, compounds acting unspecific either due to disturbance of the readout or unspecific behaviour towards other proteins can be eliminated. In addition, the Sec7 GEF domain of Cytohesin-2 and the Vps9 domain of Rabex-5 show structural similarities.[136] Moreover, both classes of GEFs act through a very similar mechanism in the exchange reaction (Figure 24).[136] DrrA, a Rab1 GEF from *Legionella pneumophila*, is also thought to act in a manner that is comparable to Vps9.[23] The Vav-1 GEF is least related to Rabex-5 and has a DH-PH tandem domain as catalytic domain that is distinct from the structure of the Vps9 domain (Figure 24C). Therefore, this GEF was useful to see if the compound would target any nucleotide exchange reaction on small GTPases in general. Unfortunately, no other Vps9 domain proteins were available.
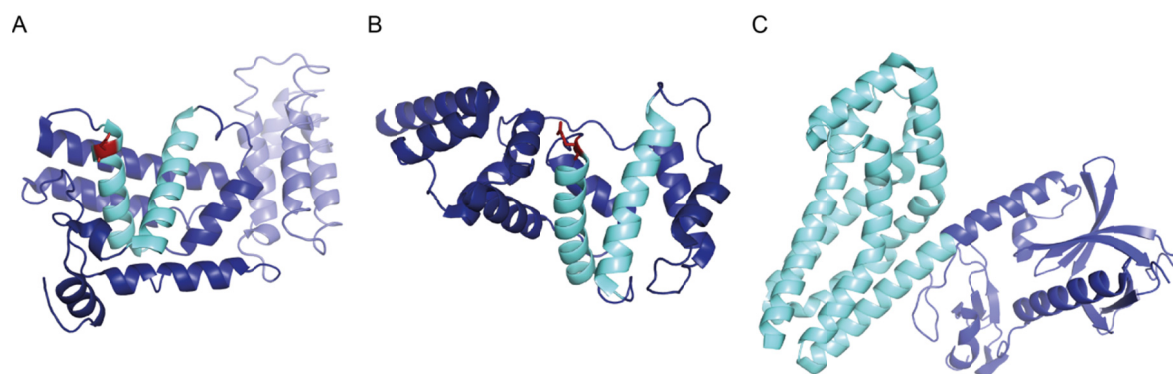
Figure 24   Structures of Rabex-5GEF, Cytohesin-2-Sec7 domain and Vav-1 DP-PH domain.
Structures of the exchange factor catalytic domains are shown with GTPase binding surface facing the front. Structural data from PDBsum (http://www.ebi.ac.uk/pdbsum/) were illustrated by the use of the PyMOL software. **A)** Rabex-5GEF (PDB-ID 2ot3), the helical bundle is depicted in light blue, the Vps9 domain in dark blue with exception of helices αV4 and αV6 (aquamarine), and the aspartate finger (Aps313) in red. **B)** The Sec7 domain of Cytohesin-2 (PDB-ID 1r8r) is illustrated in dark blue with exception of the helices that build the hydrophobic groove (aquamarine) and carry the glutamate finger (Glu156, red). **C)** The Vav-1 (PDB-ID 2vrw) DH domain is depicted in aquamarine and PH domain is illustrated in blue.

JH5 did not show any influence on the Arf-Cytohesin-2 exchange reaction upon 20 µM (Figure 25A). Furthermore, no inhibitory effect on the nucleotide exchange of DrrA and the corresponding GTPase Rab1 was observed up to 50 µM JH5 (Figure 25B). Finally, no inhibition of the Vav-1-Rac1 nucleotide exchange reaction by JH5 was monitored with a compound concentration of 0.05 - 50 µM (Figure 25C). This absent activity on the nucleotide exchange reaction of three other GEF-GTPase pairs indicated that JH5 has excellent specificity properties.

Gü321, however, inhibited the Cytohesin-2 mediated nucleotide exchange on Arf1 significantly at 20 µM compound concentration (Figure 26A). Nevertheless, Gü321 did not influence the nucleotide exchange of DrrA-Rac1 (Figure 26B) and Vav-1-Rac1 (Figure 26C). In summary, these results indicated promising specificity of JH5 for Rabex-5GEF over several other GEFs and GTPases. The specificity of Gü321 was not as pronounced as the one of JH5. Nevertheless, Gü321 distinguished the Vav-1 and the DrrA mediated nucleotide exchange which argues for some form of specificity.
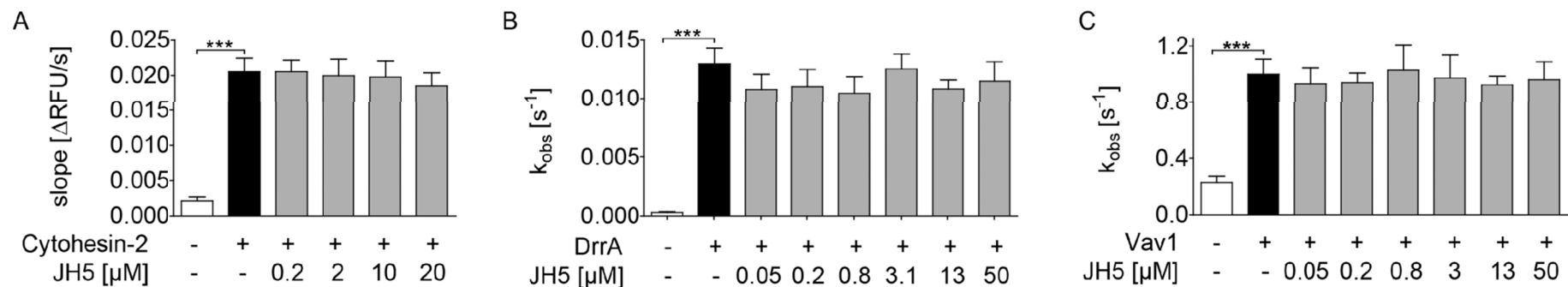
Figure 25   Specificity profile of JH5.

The specificity of JH5 was monitored in nucleotide exchange assay with Cytohesin-2 and Arf1, DrrA and Rab1, as well as Vav1 and Rac1. **A)** No inhibitory effect of JH5 was determined in the Arf1-Cytohesin-2 nucleotide exchange up to a concentration of 20 µM. A higher concentration was not tested due to solubility issues because this assay tolerates only 0.5 % DMSO. **B)** JH5 had no effect in an exchange assay with DrrA and Rab1 when using 0.05 - 50 µM of the small molecule. **C)** Finally, no inhibition of the Vav1-Rac1 nucleotide exchange was observed with up to 50 µM of JH5. Data from at least three independent experiments are plotted as mean ± SD. The significance was calculated by the use of the one-way-ANOVA with the Tukey post-test (*GraphPad Prism* software), p-values: *p < 0.05, **p < 0.01, ***p < 0.001.
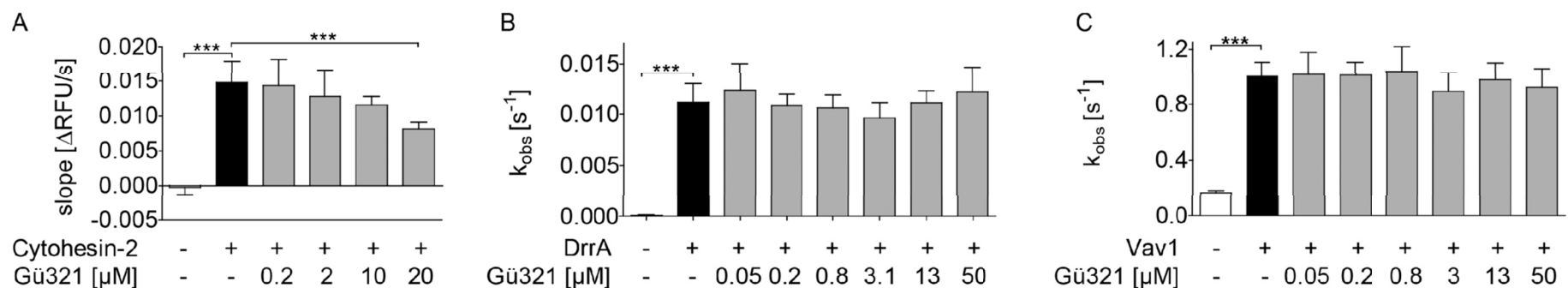
Figure 26   Specificity profile of Gü321.

The specificity of Gü321 was monitored as described in Figure 25. **A)** Inhibition of the Arf1-Cytohesin-2 nucleotide exchange was observed with Gü321, a significant impact was detected with 20 µM small molecule. Anticipating from the obtained data an IC$_{50}$ of about 20 µM can be estimated. **B)** Gü321 had no effect in an exchange assay with DrrA and Rab1 when using of 0.05 - 50 µM of the small molecule. **C)** Finally, no inhibition of the Vav1-Rac1 nucleotide exchange was observed up to 50 µM of Gü321. Data from at least three independent experiments are plotted as mean ± SD. The significance was calculated by the use of the one-way-ANOVA with the Tukey post-test (*GraphPad Prism* software), p-values: *p < 0.05, **p < 0.01, ***p < 0.001.

3.3.3   JH5 and Gü321 were inactive under reducing conditions

Several derivatives of JH5 were found in the screening which had comparable activity in the Rabex-5GEF-Rab5c assay in the low micromolar range (Section 3.6.3.1). Interestingly, there were several compounds in the library with similarity to JH5 except for lacking the thiol group at position 3 of the 1,2,4-triazole (structure: Figure 21). None of them had been identified as hit (Section 8.9). Thus, the thiol group appeared to be relevant for the function of JH5. Furthermore, it raised the question whether JH5 might be sensitive to a reducing environment. Supplementing the assay buffer with the reducing agent dithiothreitol (DTT) did not affect the Rabex-5GEF dependent nucleotide exchange reaction (Section 8.6) but diminished the activity of JH5. Already at DTT concentrations that were equimolar to JH5, the inhibition of nucleotide exchange was affected (Figure 27A). Gü321 differs in structure from JH5; nevertheless, it also has a thiol group that can be formed by tautomerization (structure: Figure 21). Gü321 was found to be as sensitive towards reducing conditions as JH5 (Figure 27B).
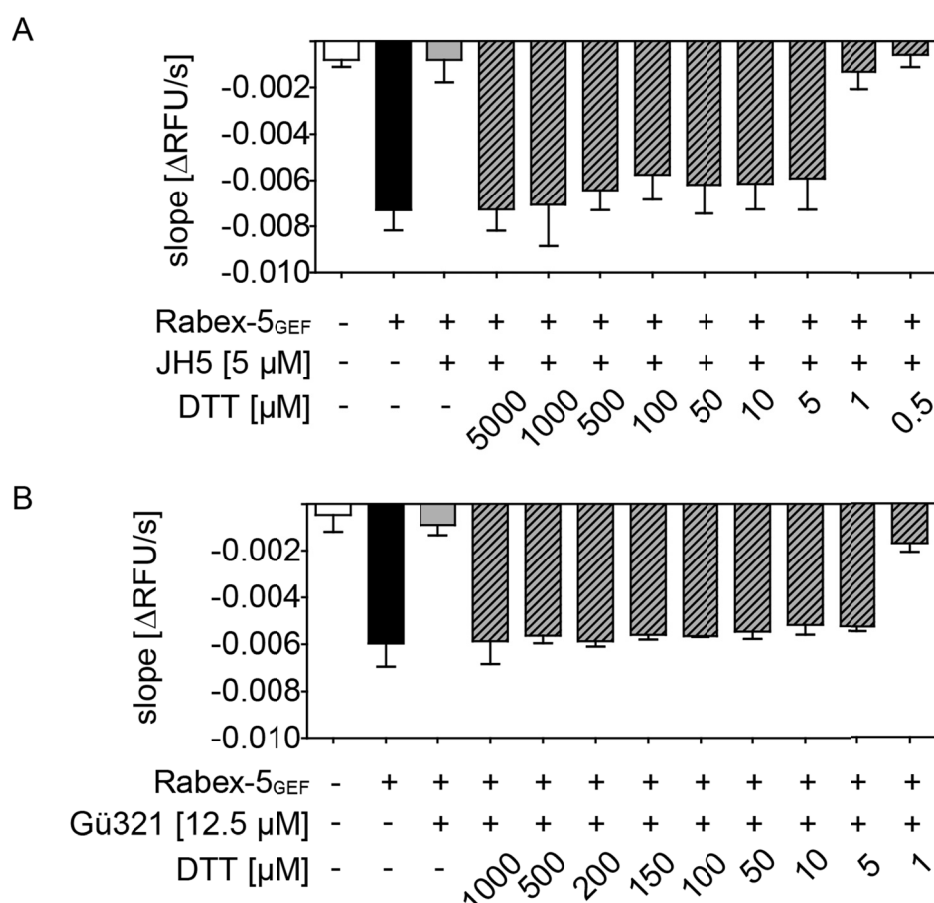
Figure 27   The presence of DTT affects the activity of JH5 and Gü321.[3]
A) The nucleotide exchange assay was performed with 1 μM Rab5, 20 nM Rabex-5GEF and constant JH5 concentration (5 μM). DTT addition at the indicated concentration completely abolished the activity of JH5 till DTT concentrations as low as 5 μM. Concentrations of 1 μM DTT or lower did not decrease the JH5 activity. **B)** The nucleotide was performed under the same conditions as in A) with 12.5 μM Gü321 as active compound. The addition of DTT resulted in the loss of Gü321 activity by using at least 5 μM DTT.

---

[3] The nucleotide exchange assay was planned by Christine Wosnitza and kindly performed by Nicole Krämer.

To investigate the sensitivity of JH5 towards DTT further, electrospray ionization mass spectrometry (ESI-MS) in absence and presence of DTT was performed. In the absence of DTT, a peak of the correct size (observed: 298.1 Da, calculated: 297.1 Da; Figure 28A) was observed. Additionally, a peak with twofold mass (observed: 593.2 Da, calculated: 592.2 Da; Figure 28B), which most likely represented the dimer of JH5, was visible. DTT treatment prior to the mass spectrometry measurement diminished this peak (Figure 28B). From this observation, two hypotheses regarding the mode of action of the compounds were derived. Since thiol groups are prone to build disulphide-bonds it was hypothesized that JH5 either was active in a disulphide-bound dimeric form or that it covalently reacted with thiol groups of cysteines in Rabex-5GEF. Both hypotheses were pursued in Section 3.4 to gain mechanistic insights.
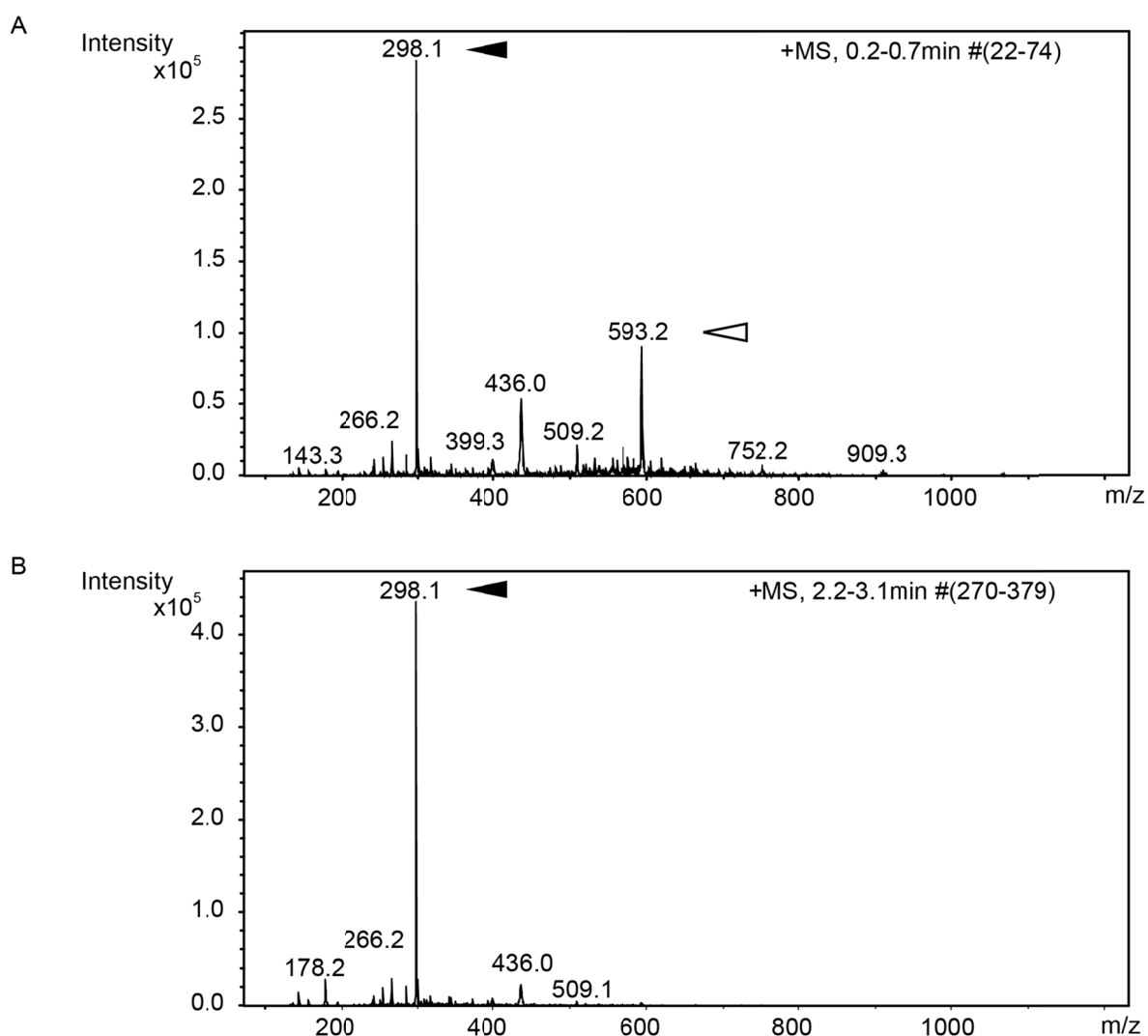
Figure 28   ESI-MS of JH5 in absence and presence of DTT.[4]
This figure shows the ESI-MS data of JH5 (10 μM) in absence and presence of 200 μM DTT. ESI-MS measurements in the positive mode generate [M+H]+ ions (M = molecule of interest). **A)** The control sample displayed a peak with calculated mass of monomer of 297.1 g/mol (found: 298.1 Da; black arrow head) and the mass of a potential dimer of a theoretical mass of 592.2 g/mol (found: 593.2 Da; white arrow head). **B)** After the treatment with DTT (15 minutesRT) the dimer peak was not detectable while the monomer peak (298.1 Da, black arrow head) remained present.

---

[4] MS measurements were performed with the kind help of Dr. Barbara Albertoni.

3.3.4 The compounds interacted with Rabex-5GEF

As Rab5c and Rabex-5GEF were present in the screening assay, both proteins, as well as the complex of both can be a target structure for compound interaction. Classical approaches to monitor bio-molecular interaction are isothermal titration calorimetry (ITC) and surface plasmon resonance (SPR). Thus, preliminary ITC and SPR measurements were performed. The SPR approach was not pursued after the preliminary tests due to poor protein stability after coupling to the sensorchip (Section 8.7). In addition, the obtained signals were very small and hard to distinguish from the background. Since no functional biotinylated compound derivative was available it was not possible to couple the compound instead of the proteins to the sensorchip. Noisy signals were observed in the ITC experiments lowering the reliability of the measurements (Section 8.7). Moreover, the ITC data reported in the literature were often obtained by using at least one of the interaction partners in the millimolar range when the expected K_d was in the micromolar range.[236, 237] The compound solubility was found to be well in the two-digit micromolar range but the millimolar range could not be reached (Section 8.8). Finally, another approach was utilized to perform binding studies: microscale thermophoresis (MST). In MST, the interactions between biomolecules are determined by monitoring the migration of a fluorescently labelled interaction partner within a temperature gradient.[238] The migration is dependent upon the hydration shell, size and charge of the molecule which are, in turn, influenced by binding events.[238, 239] Therefore, binding of molecules leads to different migration characteristics within temperature gradients. This method was chosen because smaller sample volumes and lower concentrations of the binding partners were required compared to ITC. Moreover, the analytes did not have to be immobilized on a matrix as in SPR. However, the proteins had to be labelled fluorescently to enable detection.

After the labelling procedure, both Rab5c and Rabex-5GEF were analysed for their activity (Figure 29A, B). Rabex-5GEF was found to be as active as unlabelled protein (Figure 29A). For Rab5c, however, the fluorescence measurement of the nucleotide exchange assay resulted in ambiguous data. Hence, the radioactive assay was performed and in this assay Rab5c could be loaded with the radioactive nucleotide by Rabex-5GEF. However, the radioactive signal of the labelled protein was lower than of the wild type protein suggesting reduced protein activity. This might be explained by differences in the protein concentration. Since the amount of Rab5c in each sample limits the maximal signal that can be obtained in this assay, small differences in concentration determination already have a large impact. Therefore, the natural error from concentration determination might have a dramatic impact on the analysis of these data when comparing different protein batches. Secondly, the radioactive assay was not as suitable for quantitative data acquisition as the fluorescent assay (Section 3.3.1). Nevertheless, the label might influence the activity of Rab5c but residual activity in complex with Rabex-5GEF remained. In conclusion, it is plausible that a potential interaction with the compounds could be decreased but it is unlikely that it would be completely diminished. Due to the residual activity, which was observed, the protein was considered to be suitable for MST studies.
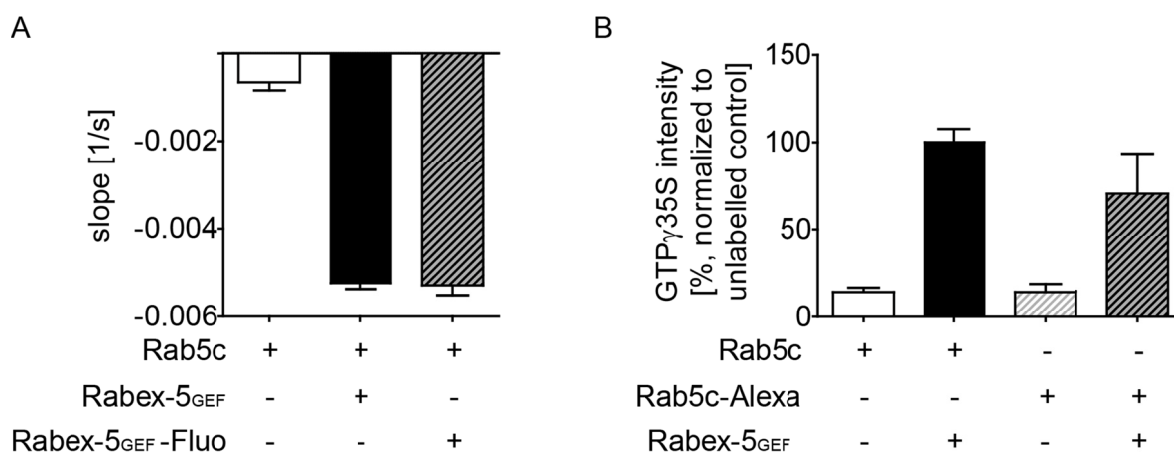
Figure 29   Activity of Rabex-5GEF and Rab5c proteins labelled with fluorescent tags.
A) The fluorescein labelled Rabex-5GEF (Rabex-5GEF-Fluo) showed expected activity in the nucleotide exchange assay. The nucleotide exchange assay with tryptophan fluorescent readout was performed as described in Figure 22. **B)** The tryptophan fluorescent based assay with labelled variants of Rab5c did not resulted in interpretable results. The RFU signal was independent of the amount of Rab5c indicating that the tryptophan fluorescence of the GTPase was disturbed. Thus, the radioactive assay was performed as depicted here (Rab5c-Alexa = Alexa647-labelled Rab5c). Although this assay was characterized by higher variations than the fluorescent assay it was considered suitable for general statements on protein activity. The intensity of GTPγ^{35}S in the sample with Rabex-5GEF and Rab5c-Alexa was lower than in the comparable sample with unlabelled Rab5c. However, the same observation was made for the samples without Rabex-5GEF indicating that the concentration of Rab5c-Alexa might have been lower than Rab5c. Although the concentration determination was carried out thoroughly prior to the experiment, small variations are natural. Comparing the nucleotide uptake from the samples with and without Rabex-5GEF the increase was sevenfold in case of the unlabelled Rab5c and fivefold in case of Rab5c-Alexa. Still, this indicates loss of protein activity. Nevertheless, the protein was in general functional and was thus used in the MST assay. Data from two independent experiments represented as mean ± SD.

JH5 bound to fluorescein labelled Rabex-5GEF with a K_d of 2.6 μM (Figure 30, red curve). This K_d matched well with the activity that was observed in the nucleotide exchange assays at a range of high-nanomolar to low micro molar compound concentrations (Section 3.3.1). Furthermore, JH5 interaction with Rabex-5GEF-Alexa647 resulted in a K_d of 2.1 μM (Section 8.7). No binding of JH5 to Rab5c was observed (Figure 30, black curve). To proof the specificity of the recorded binding, several other GEFs (Cytohesin-2, DrrA) as well as less related proteins like kinases (Erk2, Grk2) and a GTPase (Arf1) were analysed. No binding of JH5 could be detected to any of these proteins (Figure 30). These results were in line with the data obtained in the functional assay (Section 3.3.1) and supported the hypothesis that JH5 specifically targets Rabex-5GEF.

The interaction of JH5 and Rabex-5GEF was disrupted by addition of DTT above 5 μM (Figure 31). Again, the MST data observed in this experiment are supporting the results obtained in the functional assays (Section 3.3.3)
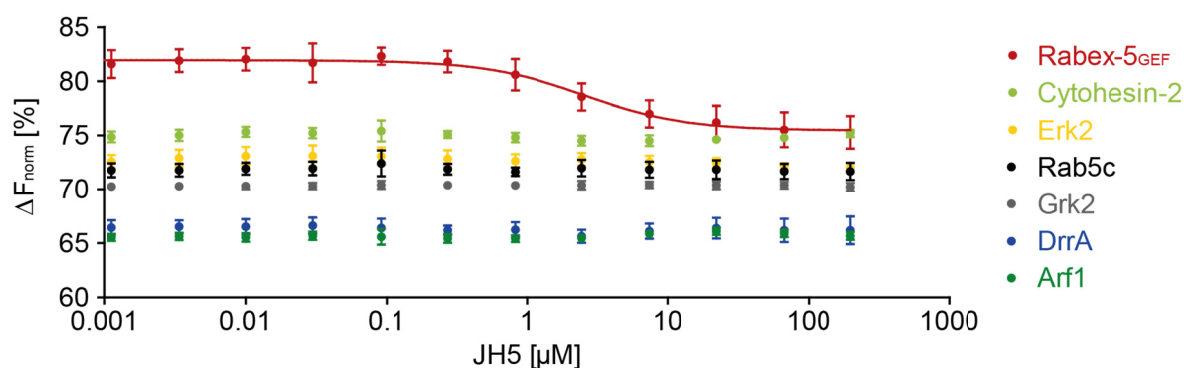
Figure 30   MST measurements indicate a specific interaction of JH5 with Rabex-5GEF.[5]
MST data were obtained under the following buffer conditions: 1 x Rabex-5 nucleotide exchange assay buffer, 500 nM BSA, 2 % DMSO. The thermophoresis (with temperature-jump), here shown as difference in normalized fluorescence [ΔF_{norm}], was plotted against the logarithmic compound concentration for the calculation of the K_d. The data from at least three independent experiments are depicted as mean ± SD. The binding of JH5 (red curve) to Rabex-5GEF was observed with a K_d of 2.6 μM (95 % CI 1.9 - 3.5 μM). No binding of JH5 to Rab5c (black curve) was detectable. MST measurements of JH5 with several proteins are depicted: for none of the control proteins binding was observed. Other GEFs that were investigated were the ArfGEF Cytohesin-2 (Sec7 domain, light green curve) and the RabGEF DrrA (blue curve). The kinases Erk2 (yellow curve) and Grk2 (grey curve) and the Arf1 GTPase (green curve) represented less related proteins and also did not interact with JH5. These results suggested that the interaction of JH5 with Rabex-5GEF was specific.
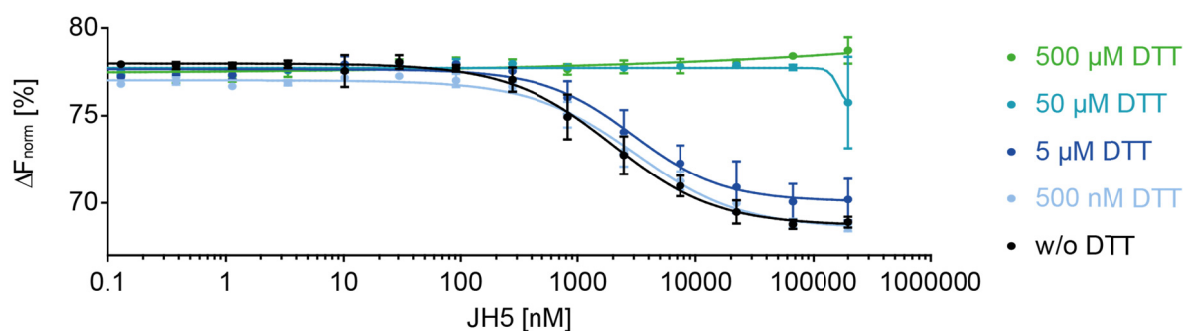
Figure 31   Negative influence of DTT on the Rabex-5GEF JH5 interaction confirmed in MST.
The MST analysis was performed as described in Figure 30. The interaction of JH5 (black curve) and Rabex-5GEF was quantified with a K_d of 2.0 μM (95 % CI 1.5 - 2.5 μM) which corresponded well with the preceding results (Figure 30). The addition of 500 μM DTT (green curve) or 50 μM DTT (turquoise curve) severely affect the interaction of JH5 and Rabex-5GEF. 5 μM DTT (blue curve) resulted in a shift of the MST curve. However, the obtained K_d of 2.9 μM (95 % CI 1.9 - 4.4 μM) was already in the range of the undisturbed interaction. With 500 nM DTT (light blue curve), the calculated K_d was 3.1 μM (95 % CI 2.4 - 4.0 μM). Data from at least two independent experiments are depicted as mean ± SD.

The interaction of Gü321 with Rabex-5GEF was analysed in MST and compared to K1.08.C11, the library stock compound. In both forms, the compound interacted with Rabex-5GEF with a K_d in the one-digit micromolar range (Figure 32). The K_d of Gü321 was with 5.0 μM (95 % CI 1.5 - 16.4 μM) slightly higher as the K_d of the library stock K1.08.C11 with 2.7 μM (95 % CI: 2.0 - 3.7 μM). Gü321 was also analysed for its interaction with Cytohesin-2. Again, an interaction was observed: the obtained K_d of 5.1 μM (95 % CI 1.9 -

---

[5] Measurements with Erk2, Grk2, DrrA, Arf1 and Cytohesin-2 were kindly performed by Nicole Krämer. All experiments were planned and analysed by Christine Wosnitza.

13.5 µM) revealed that Gü321 interacted with Rabex-5$_{GEF}$ and Cytohesin-2 Sec7 at a comparable affinity. Due to the unspecific profile of Gü321, which was observed in functional assays and binding studies, the future work was focused on JH5.
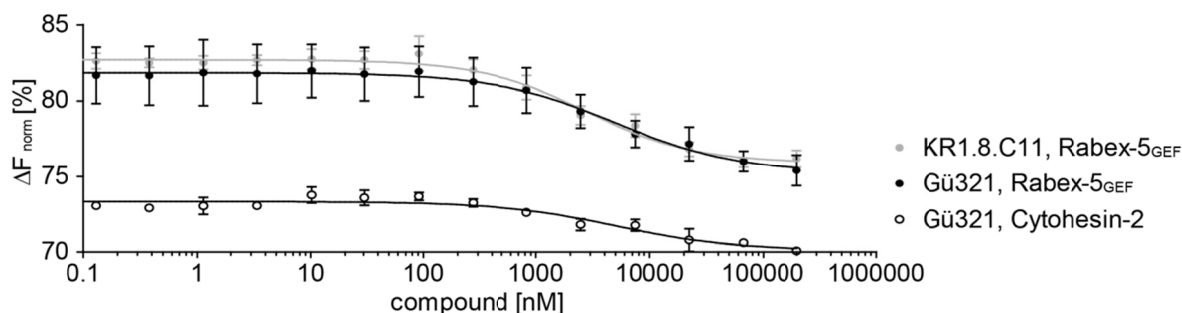
Figure 32   MST measurements of K1.8.C11 and Gü321. [6]
MST data were obtained under the same conditions as in Figure 30. K1.8.C11 revealed binding to Rabex-5$_{GEF}$ with a K_d of 2.7 µM (95 % CI: 2.0 - 3.7 µM). Gü321 had a similar affinity towards Rabex-5$_{GEF}$ with a K_d of 5.0 µM (95 % CI 1.5 - 16.4 µM). However, Gü321 also interacted with Cytohesin-2-Sec7 at a K_d of 5.1 µM (95 % CI 1.9 - 13.5 µM). This underlined the unspecific effect of Gü321 already observed in the Cytohesin-2-Arf1 nucleotide exchange assay. Data from at least two independent experiments are depicted as mean ± SD.

3.4   Mode of action of JH5 and derivatives

To determine the mode of action of JH5 it is important to know which groups of the molecule are essential to its activity. Several derivatives of JH5 were found as hits in the screening (Section 3.6.3.1). Interestingly, other library compounds with similar structures lacking the thiol group have not been identified as hits (Section 8.9). In addition, JH5 was inactive and not binding to Rabex-5$_{GEF}$ if reducing agents like DTT were present (Section 3.3.3). Thus, several thiol-modified compounds were designed to verify the hypothesis that this group is important for the inhibitory function (Section 3.4.1). Additionally, it was investigated whether JH5 can form disulphide bonds either with another JH5 molecule or with the Rabex-5$_{GEF}$ protein (Section 3.4.2).

3.4.1   Structure activity relationship study

Based on the knowledge gathered from the screening, several JH5-derivatives were re-synthesized and evaluated regarding their inhibitory potential to establish a structure activity relationship.[7] The results are summarized in Table 5.

JH5 consists of a central 1,2,4-triazole ring with a thiol group at position 3 and a phenyl substituent at position 4 and 5. The 4-phenyl carries a methyl substituent in *meta* position, and the 5-phenyl is methoxy-substituted in *para* position.

---

[6] Cytohesin-2-Sec7-FITC was a kind gift of Benjamin Weiche.
[7] The synthesis and compound characterisation were kindly performed by Dr. Jeffrey Hannam. The analytical compound data can be found in Section 8.13.

Table 5   Structure activity relationship of JH5 and derivatives.

name	R¹	R²	R³	IC₅₀ [μM][a]	95 % CI [μM][b]	Specific? [c]
JH5	4-methoxyphenyl	3-methylphenyl	-SH	0.4	0.3 - 0.5	yes
JH5-M	4-methoxyphenyl	3-methylphenyl	-S-Me	n.i.[d]		n.d.
JH5-O	4-methoxyphenyl	3-methylphenyl	-OH	n.i.[d]		n.d.
CCO	phenyl	phenyl	-OH	n.i.[e]		n.d.
CCD	phenyl	phenyl	-SH	5.8	3.2 – 10.6	yes
CCJ	4-tert-butylphenyl	cyclohexyl	-SH	1.8	1.5 – 2.3	yes
CCV	2-methylphenyl	cyclohexyl	-SH	6.6	5.0 – 8.8	yes
CCF	cyclohexyl	cyclohexyl	-SH	17.3	12.3 – 24.2	yes
JH5-E	4-methoxyphenyl	3-methylphenyl	thioester (3-methylbutanethioate)	3.0	2.0 - 4.5	no
JH5-B	4-bromophenyl	phenyl	-SH	0.3	0.2 - 0.4	yes [f]
JH5-B-dimer	4-bromophenyl	phenyl	disulfide-linked triazole (4-bromophenyl)	0.2	0.1 - 0.4	yes [f]
JH5-A	4-methylphenyl	phenyl	-SH	0.6	0.5 - 0.8	n.d.
JH5-A-dimer	4-methylphenyl	phenyl	disulfide-linked triazole (4-methylphenyl)	0.4	0.3 – 0.6	n.d.
JH5-C	3-bromophenyl	phenyl	-SH	0.7	0.5 – 0.9	n.d.
JH5-C-dimer	3-bromophenyl	phenyl	disulfide-linked triazole (3-bromophenyl)	0.6	0.4 – 0.8	n.d.
CCC	-H	/	-SH	8.1[g]	5.5 – 12.1	no
CCP	phenyl	/	-SH	3.2	2.2 – 4.8	no
CCM	H	-Me	-SH	>100		n.d.
JH5-N	4-methylphenyl	-NH₂	-SH	7.8	5.6 - 10.7	n.d.
JH5-N dimer	4-methylphenyl	-NH₂	thioether-linked triazole (4-methylphenyl, NH₂)	n.i. [d]		n.d.
CS-dimer 1	4-bromophenyl	phenyl	thioether-linked oxadiazole (4-methoxyphenyl)	n.i. [d]		n.d.

61

name	R¹	R²	R³	IC$_{50}$[μM][a]	95 % CI [μM][b]	Specific? [c]
CS-dimer 2				n.i. [d]		n.d.
CS-dimer 3				n.i. [h]		n.d.

All compounds were kindly synthesised and analysed by *Dr. Jeffrey S. Hannam*, except compounds JH5-N, CCC, CCP, CCM, JH5-B, JH5-C-dimer, and JH5-A-dimer which were obtained commercially as described in Section 8.13.3. **[a]** The activity of the compounds was monitored in the nucleotide exchange of Rabex-5$_{GEF}$ on Rab5c (tryptophan fluorescence readout). **[b]** CI: confidence interval; **[c]** The specificity rating refers to the effect of the compound in the Cytohesin-2-Arf1 nucleotide exchange assay. n.d. = not determined. Corresponding data can be found in Section 8.5 **[d]** n.i.: no inhibition of Rabex-5$_{GEF}$ mediated nucleotide exchange was found up to 50 μM (radioactive exchange assay) and no binding was observed till 200 μM (MST). **[e]** n.i.: no inhibition of Rabex-5$_{GEF}$ mediated nucleotide exchange was found up to 50 μM (tryptophan fluorescence exchange assay). **[f]** The specificity was determined in the Vav-1-Rac1 and DrrA-Rab1 nucleotide exchange assay instead of the Cytohesin-2-Arf1 assay. **[g]** The compound was inactive in the radioactive nucleotide exchange assay with Rabex-5$_{GEF}$-Rab5c up to 50 μM compound concentration. **[h]** n.i.: no inhibition of the Rabex-5$_{GEF}$ mediated nucleotide exchange was found up to 50 μM (radioactive exchange assay) and no interaction with Rabex-5$_{GEF}$ was observed in MST.

At first, it was investigated whether the thiol group at position R3 was required for activity. The modification of the thiol group either by exchange for a hydroxyl group (JH5-O) or by methylation (JH5-M) prevented the binding of these compounds to Rabex-5$_{GEF}$ (Figure 33A). Consequently, no inhibitory activity in the nucleotide exchange assay was observed with JH5-O (Figure 33B) and JH5-M (Figure 33C), suggesting that the thiol group at position 3 is required for Rabex-5$_{GEF}$ binding and inhibition.

The 3-hydroxyl analogue CCO which was additionally modified at position R1 and R2 was also found to be inactive. In contrast to JH5, the compound CCO was phenyl-substituted at the positions R1 and R2. To exclude the possibility that the observed loss of activity of CCO was caused by the substitution of the R1 and R2 position, the molecule CCD was synthesized. Regarding the positions R1 and R2 it was congeneric to CCO while sharing the R3 substituent (thiol group) with JH5. CCD was active in the one-digit micromolar range (IC$_{50}$ = 5.8 μM) showing a roughly 15-fold loss of activity compared to JH5. Nevertheless, the activity of CCD contradicted the hypothesis that CCO was inactive due to its substituents at position R1 and R2.

The comparison of CCD and JH5 suggested that the presence of a bulky group like an O-methyl in *para*-position of the R1 phenyl substituent increases the activity of the compounds. Indeed, the compounds JH5 with a *para*-hydroxymethyl-5-phenyl substituent, JH5-B with a *para*-bromo-5-phenyl substituent, and JH5-A carrying a *para*-methyl-5-phenyl substituent were found to have IC$_{50}$ values below 1 μM.

The JH5-C with the bromine in *meta*- instead *para*-position had similar inhibitory potency. Hence, a substitution in *meta*-position on the phenyl residue at R1 position may be comparable to the *para*-substitution.
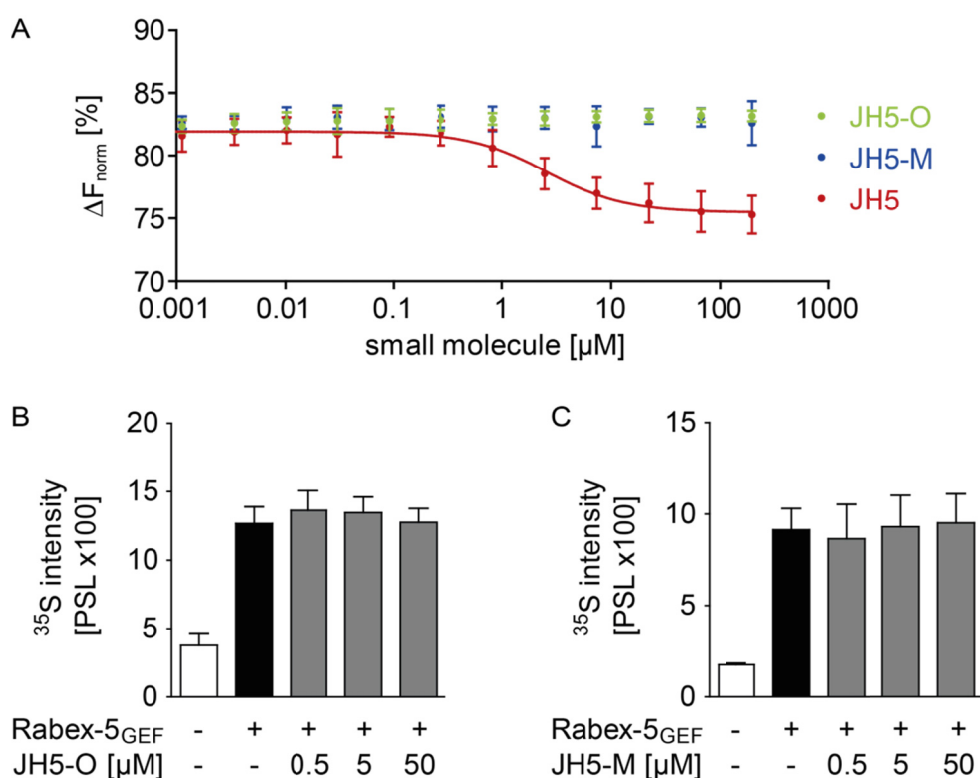
Figure 33 Thiol-free JH5 derivatives are inactive.
A) The MST data were obtained as described in Figure 30. The binding of JH5 (red curve) to Rabex-5GEF from Figure 30 was plotted as reference. JH5-O (light green) and JH5-M (blue) did not interact with Rabex-5GEF. The data from at least three independent experiments are depicted as mean ± SD. **B-C)** The Rabex-5GEF mediated nucleotide exchange on Rab5c was monitored by the association of GTPγ^{35}S to Rab5c (as described in Figure 23) because the auto-fluorescence of both molecules disturbed the tryptophan fluorescence assay. In the radioactive nucleotide exchange assay, both JH5-O (**B**) and JH5-M (**C**) were inactive up to at least 50 μM compound. Data are shown as mean ± SD from two independent experiments.

The compound CCJ with a *para-tert*-butyl-phenyl substituent at position R1 and a cyclohexyl-group at position R2 showed an about six-fold activity loss compared to JH5. This observation might be explained either by the increased size of the *para*-substituent of the R1-phenyl or by the substitution of the aromatic residue at position 4 by a cyclohexyl-group. That phenyl-substituents improve the activity of the molecule compared to a cyclohexyl-substitution can be concluded from comparison of the activity of the compounds CCD and CCF. CCD is phenyl-substituted at position R1 and R2 and has an IC$_{50}$ of 5.8 μM while the cyclohexly-substituted analogue CCF is about three-times less active (17.3 μM).

Three compounds with a cyclohexyl-moiety at the R2 position were available for direct comparison: CCJ, CCV and CCF. CCJ was the most active compound among the cyclohexyl at position R2 substituted compounds with an IC$_{50}$ value of 1.8 μM. The R1 of CCJ is a *para-tert*-butyl-4-phenyl. The *ortho*-methyl-4-phenyl compound CCV was about four-times less active than CCJ. Finally, the compound CCF with cyclohexyl substitution at position R1 and R2 was the least active compound (IC$_{50}$ = 17.3 μM). These observations suggested that the aromatic phenyl-substitution at position R2 increased the potency of the compound compared to a cyclohexyl substituent. In addition, the compound CCJ with

a *para*-substitution of the 5-phenyl group was found to be more active than the *ortho*-substituted compound (CCV). However, the substituents in *para*- and *ortho*-position were not directly comparable due to their size difference. Nevertheless, in addition to prior observations on the beneficial effect of a *para*-substituent on the 4-phenyl this conclusion seems valid.

A six-membered carbon ring in the position R2 might increase the specificity towards the Rab5c-Rabex-5GEF system: the compounds CCP and CCC, which are not substituted in that position, were found to inhibit the Cytohesin-2-Arf1 nucleotide exchange reaction.

A dimeric JH5-derivative (JH5-B-dimer) inhibited the Rabex-5GEF catalysed nucleotide exchange on Rab5c with equivalent potency as JH5. The comparable activity of all available -S-S-bridged dimers like the JH5-A-dimer, the JH5-B-dimer and the JH5-C-dimer indicated that the thiol group can be replaced by a disulphide form without significant loss or gain of activity. A similar behaviour was observed for an inhibitor of the Cholesteryl ester transfer protein which was active in its disulphide or thiol form.[240, 241] The isopropyl thioester of this compound, also known as JTT-705 (Dalcetrapib) showed similar potency as the corresponding disulphide and was used for *in vivo* assays.[241, 242] To investigate whether a likewise effect existed for JH5, an isobutyl thioester derivative of JH5 (JH5-E) was analysed in the Rabex-5GEF-dependent Rab5c activation assay (Figure 34A, B). JH5-E inhibited Rabex-5GEF with an IC_{50} of 3.0 μM which corresponds to a sevenfold loss of activity with respect to JH5 (Figure 34A). Nevertheless, this result indicated that the thiol group at position R3 can be replaced by a thioester without a complete loss of activity. The reduced activity compared to JH5 can be explained by an equilibrium between hydrolysed (equivalent of JH5) and non-hydrolysed form of JH5-E. Decreased specificity was observed for JH5-E compared to JH5 since it was also active on the nucleotide exchange of Cytohesin-2-Arf1 (Figure 34C). The fact that the other nucleotide exchange reactions (Vav-1-Rac1, DrrA-Rab1, Figure 34D, E) were not affected underlines the observation that JH5-E has similar specific characteristics as JH5.

To investigate whether a distinctly bridged dimeric JH5-derivative was active, a JH5-dimer in which the disulphide moiety was substituted by a -CH2-CH2- bridge was synthesised. However, this compound was found to be insoluble and could not be tested under the assay conditions with aqueous buffer.

A -S-CH2-S-bridged dimer (JH5-N-dimer) was modified at the position R2: the phenol-substituent was replaced by an amino-group (Figure 35A). The JH5-N-dimer did not bind to Rabex-5GEF. The corresponding monomer JH5-N had reduced affinity to Rabex-5GEF compared to JH5 but showed interaction that reached the saturation (Figure 35A). The reduced affinity of JH5-N compared to JH5 indicated that the primary amine at position R2 is less favourable for the activity of the molecules compared to an aromatic substitution.
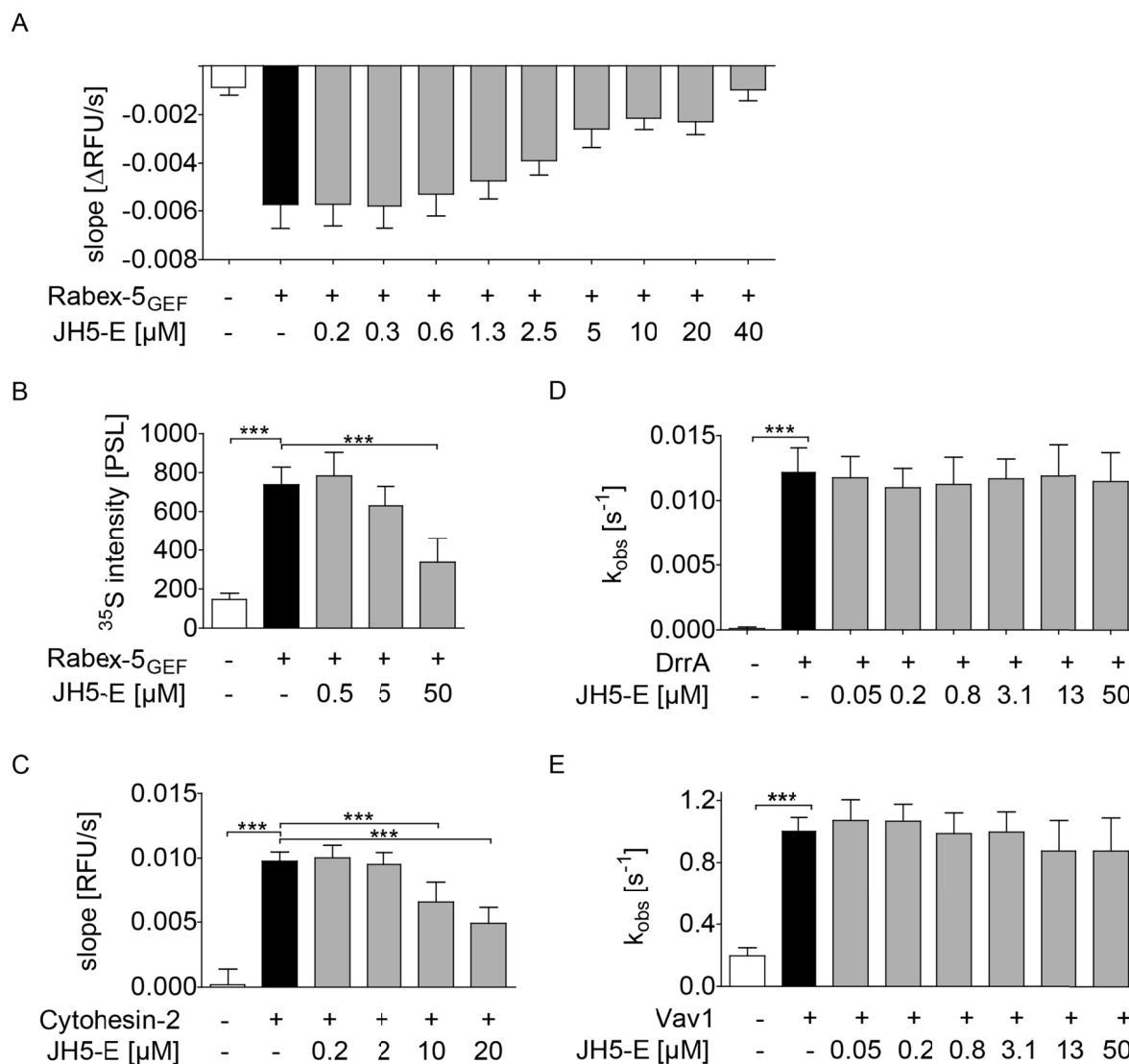
Figure 34   Characterization of JH5-E in several nucleotide exchange assays.
A) JH5-E inhibition of the Rab5c activation by Rabex-5$_{GEF}$ in the assay with fluorescent readout. An IC$_{50}$ of 3.0 µM (95 % CI 2.0 - 4.5 µM) was calculated from the dose-response curve. **B)** JH5-E inhibited the Rabex-5$_{GEF}$ dependent nucleotide association in the radioactive nucleotide exchange assay. In agreement with the IC$_{50}$ data obtained in the fluorescent assay it was found to be less active than JH5 in this assay, too. **C)** However, JH5-E was also active in the Arf1-Cytohesin-2 nucleotide exchange assay at 10 µM and 20 µM. A rough estimate of the IC$_{50}$ (considering the concentration that was needed to reach about 50 % inhibition) results in an IC$_{50}$ value of ~20 µM. **D)** JH5-E was inactive in the DrrA-Rab1 nucleotide exchange assay. **E)** JH5-E did not show any inhibitory effect in the Vav-1-Rac1 nucleotide exchange up to 50 µM. The data from at least two independent experiments are depicted as mean ± SD. The significance was calculated by the use of the one-way-ANOVA with the Tukey post-test (*GraphPad Prism* software), p-values: *p < 0.05, **p < 0.01, ***p < 0.001.

Two CH$_2$-S- bridged dimers (CS-dimer **1** / CS-dimer 2) with an oxadiazole centre on one side were found to be soluble (Section 8.8). In the tryptophan nucleotide exchange assay both molecules disturbed the fluorescent read-out (data not shown) and were thus analysed in the MST for interaction with Rabex-5$_{GEF}$ (Figure 35B). No binding to Rabex-5$_{GEF}$ was observed and no saturation level was reached up to 200 µM compound.
The CS-dimer 3, which was most closely related to JH5, was found to be soluble within certain limits (Section 8.8). This compound was analysed in the radioactive nucleotide exchange assay and no activity was observed up to 50 µM (Figure 36). Moreover, no

interaction was observed with Rabex-5GEF up to 200 µM in the MST assay (Figure 35B) and this molecule was thus considered to be inactive.
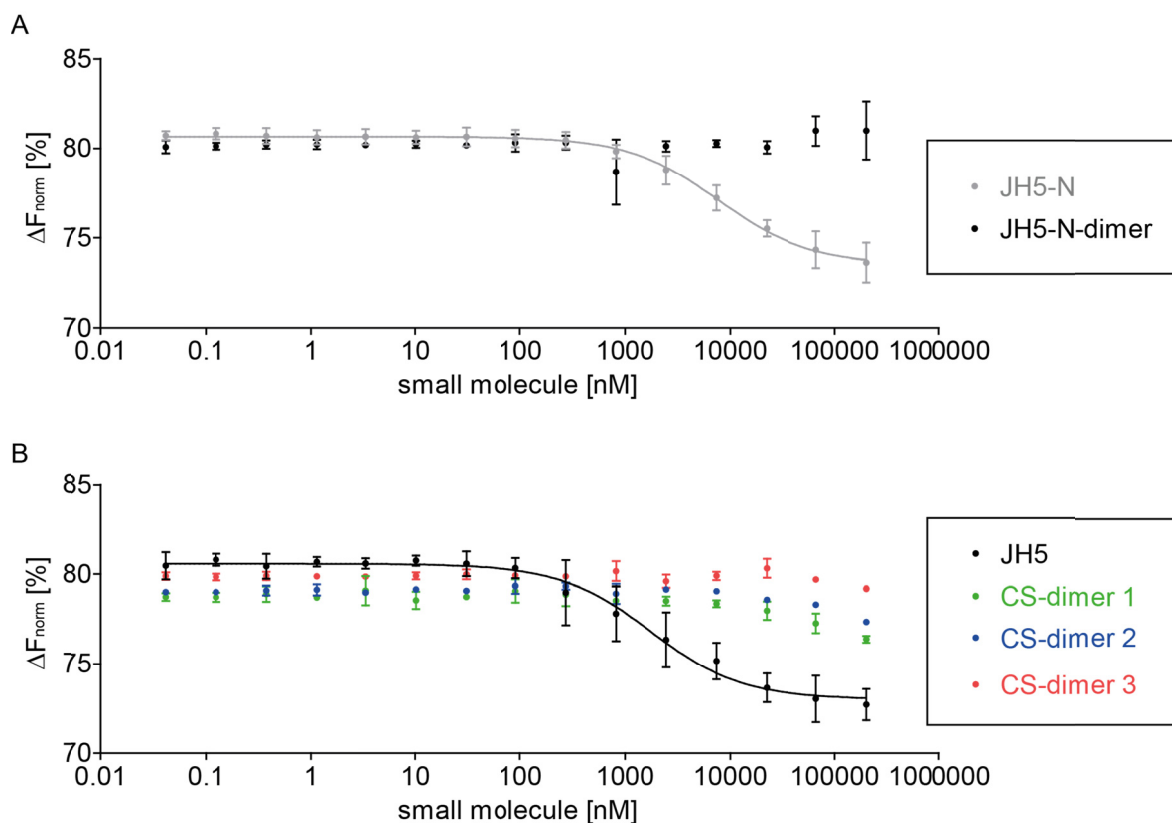
Figure 35   No interaction between stable-bridged JH5-dimer-derivatives and Rabex-5GEF.
The MST data were derived and analysed as in Figure 30. The data from three independent experiments are depicted as mean ± SD. **A)** JH5-N (grey) interacted with Rabex-5GEF and a K_d of 7.8 µM (95 % CI 5.6 - 10.7 µM) was obtained. The JH5-N-dimer (black) did not have notable affinity for Rabex-5GEF. **B)** The interaction of JH5 with Rabex-5GEF (black) served as positive control and a K_d of 1.8 µM (95 % CI 1.1 - 2.8 µM) was found to be comparable to previous MST data (Figure 30). No binding of CS-dimer 1 (green), CS-dimer 2 (blue) or CS-dimer 3 (red) to Rabex-5GEF was detectable.
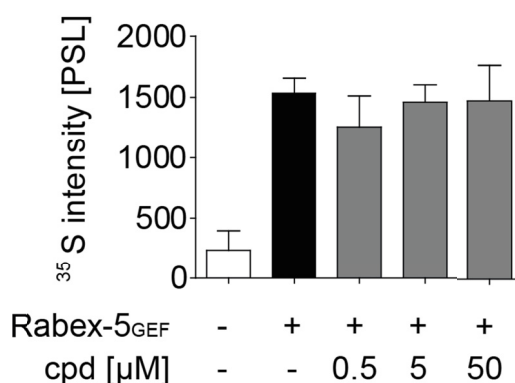
Figure 36   The CS-dimer 3 did not inhibit the Rabex-5GEF-Rab5c nucleotide exchange.
The activity of the compound (cpd) CS-dimer 3 was determined in the radioactive nucleotide exchange to avoid the disturbance of the assay readout by the auto-fluorescence of the molecule. No inhibitory activity was observed using up to 50 µM CS-dimer 3.

66

3.4.2 Investigation of the potential covalent binding of JH5 to Rabex-5GEF

For investigating the theory that JH5 can form a covalent bond with Rabex-5GEF as suggested in Section 3.3.3, a biotinylated JH5 variant should be used to label the protein and be subsequently detected on a western blot. However, the biotinylated JH5 was found to be less specific than JH5 and it showed reduced DTT sensitivity (Section 8.7). The linker and biotin might have modified JH5 to a greater extent than intended. Hence, this compound was not used in this study because the comparability with JH5 was not given.

Instead, the analysis of the potentially covalently JH5-labeled protein was investigated by mass spectrometry.[8] A mass shift of 297 Da upon addition of JH5 to the protein was expected. This shift should be measureable: similar approaches have been successfully reported in literature using a molecule of 282 Da on a ~35 kDa protein.[243] Also, the system was validated by covalently labelling Rabex-5GEF with a fluorescent compound of the size of 298.3 Da (Section 8.11).

Using matrix-assisted laser desorption/ionization-time of flight (MALDI-TOF), Rabex-5GEF was detected clearly (Figure 37A). The protein mass was detected with $z = 1$ (31471.6), $z = 2$, (15720.9) and $z = 3$ (10470.2). A second experiment (Section 8.11) resulted in the observed masses of $z = 1$ (31457.2), $z = 2$, (15750.1) and $z = 3$ (10506.2). The theoretical mass for this Rabex-5GEF protein construct was 31393.0 g/mol. No mass shift of 297 Da was visible after treatment of the protein with JH5 (Figure 37B) as it was observed by the perfect overlay of the mass spectrum with and without JH5. This observation indicated that no reaction with the compound occurred.

Figure 37C shows the mass of Rab5c with $z = 1$ (21120.5) and $z = 2$ (10555.5) as negative control. The theoretical mass of this Rab5c construct was 21035.9 g/mol. The mass spectra of the sample treated with JH5 and the DMSO samples were found as a perfect match (Figure 37C). As expected, a mass shift corresponding to the size of JH5 was not found.

For both proteins, the theoretically calculated protein mass and the observed masses showed small differences (Table 6). Since the measurement fidelity of large molecules is less exact than of small ones these mass differences were not unexpected. Salt adducts are typically observed in mass spectrometry and result in masses that are larger than the theoretically calculated values. In addition, the mass addition can be explained by the presence of modifications of the proteins as for example also observed in the MS/MS experiments (see below). Amino acids can be oxidized, e.g. cysteines can from sulfenic acids, sulfinic acids or even sulfonic acids resulting in the addition of 16, 32 or 48 Da, respectively. Other amino acids like proline or methionine can be oxidized as well. Moreover, the width of the peaks was large due to resolution limitations at this mass range and the presence of salt adducts. This allowed the calculation of the maximum of the protein mass peak while the signal was distributed around this maximum. Hence, the mass values obtained in these experiments were in the expected range of fidelity and it was possible to detect the proteins properly.

---

[8] All protein MS measurements were performed in cooperation with Dr. Marc Sylvester and PD Dr. Sebastian Franken, Institut für Biochemie und Molekularbiologie, University of Bonn.
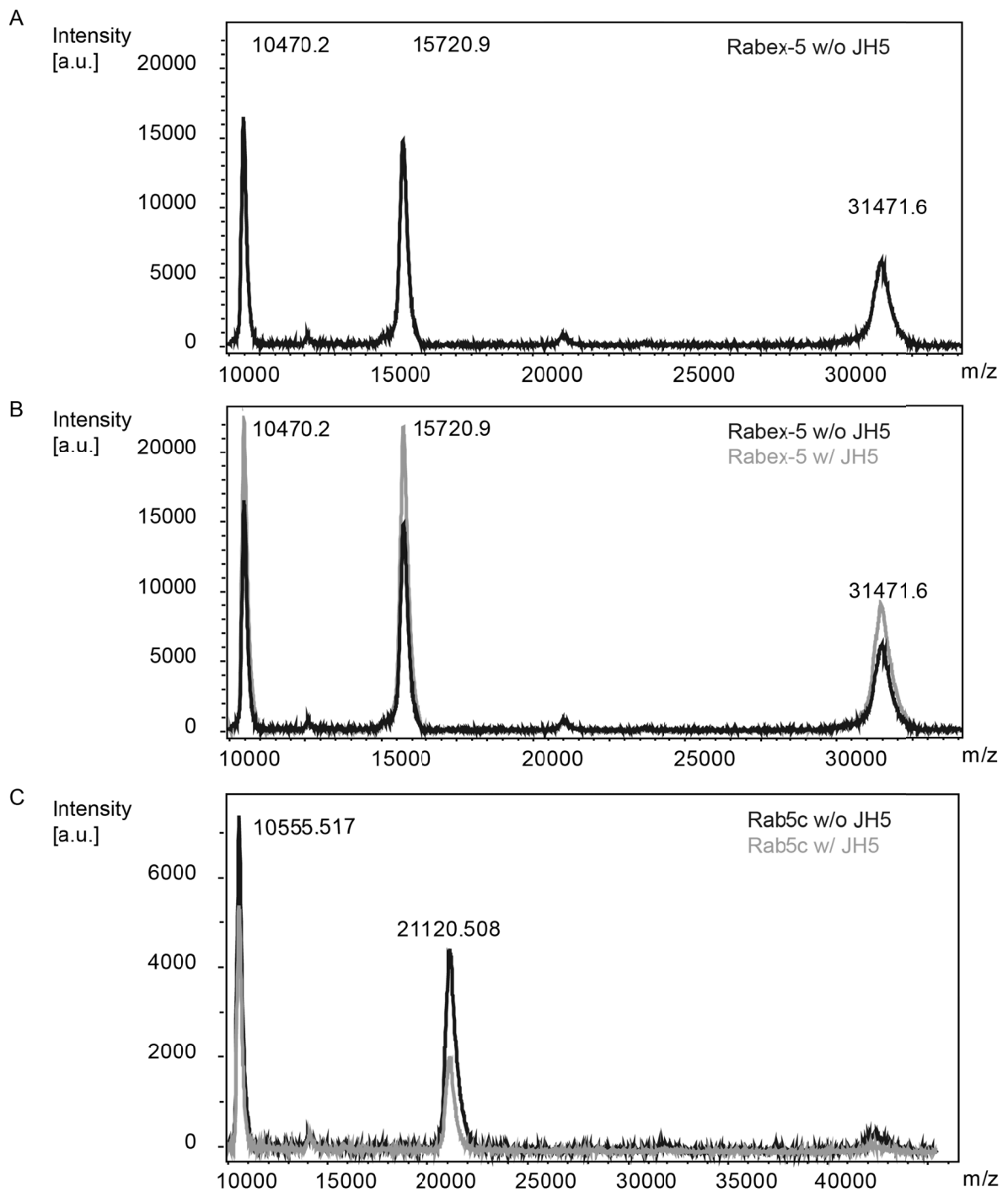
Figure 37   MS analysis of Rab5c and Rabex-5GEF protein in absence and presence of JH5.
Rab5c and Rabex-5GEF (50 μM) were incubated with JH5 (200 μM) or DMSO as control at RT. Subsequently, the sample was purified and spotted onto the target for MALDI-TOF analysis. The mass spectra with (grey) and without (black) JH5 were found as perfect overlays without any difference. Hence, no covalent modification of the proteins by JH5 was introduced. **A)** Rabex-5GEF. **B)** Rabex-5GEF ± JH5. **C)** Rab5c

Table 6   Observed protein masses in MALDI-TOF.

Protein	theoretical mass [Da]	Z	Observed masses [Da] [a]	Observed mass difference [b]
Rabex-5GEF	31393.0	1	31471.6 / 31457.2	78.6 / 64.2
		2	15720.9 / 15750.1	48.8 / 107.2
		3	10470.2 / 10506.2	17.6 / 125.6
Rab5c	21035.9	1	21120.5	84.6
		2	10555.5	75.1

[a] The observed masses for Rabex-5GEF were obtained in two independent experiments. [b] The mass difference is given with respect to the calculated total mass depending on the charge of each peak.

To investigate whether it was possible to observe a JH5 modification after the enzymatic digestion of the protein sample two additional approaches were pursued (Figure 38B, C). The analysis of digested protein has the advantage of generating smaller peptide fragments which can be determined with higher resolution in mass spectrometry.[244] In addition, it is possible to identify the amino acid sequence by tandem mass spectrometry (MS/MS).[245] The first approach included digestion of the proteins with AspN, GluC and Trypsin prior to the MS analysis to obtain these smaller fragments (Figure 38B). By the use of protein databases and MS/MS, the masses of the obtained peptides can be assigned to the protein sequence.

The modifications on Rabex-5GEF identified with the digestion approach (Figure 38B) are listed in the Supporting tables 18/19. Mainly oxidations and propionamide modifications were found. Propionamide modifications are presumably introduced during the SDS-PAGE by an undesired reaction with acrylamide. The MS data obtained for Rabex-5GEF revealed no modification of the size of JH5. However, the sequence coverage was not complete and not all cysteine-positions were covered in these measurements. Although the overall sequence coverage was high with > 80 % and would have been sufficient for approaches like protein identification the half of the cysteine-residues was unaccounted for. The sequence coverage is depicted in Figure 39.
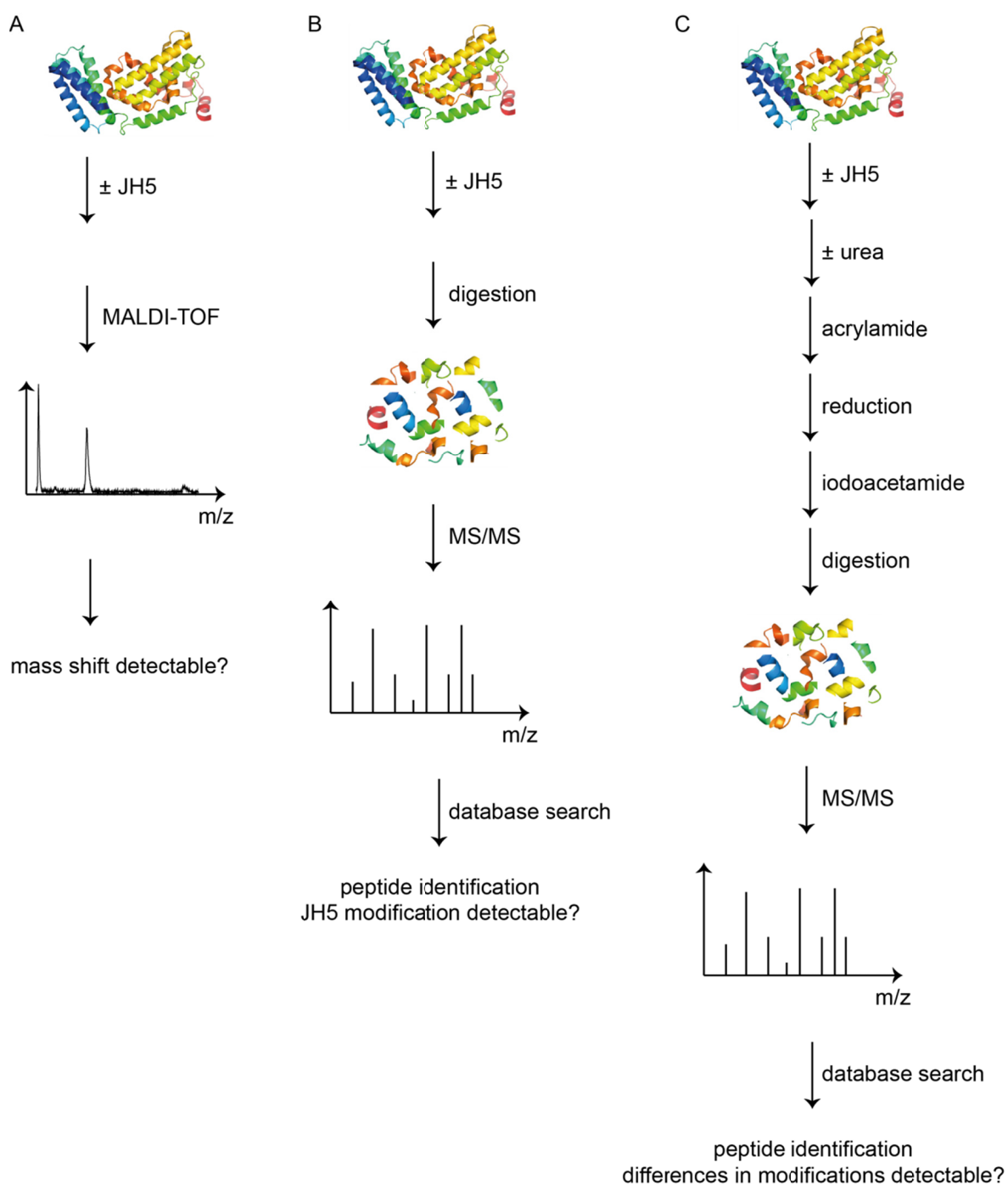
Figure 38   Illustration of the three distinct MS approaches used in this study.
A) The mass of the proteins was observed by MALDI-TOF measurements. Comparison of the mass spectra of the same protein with and without JH5 was anticipated to reveal a mass shift in case of covalent interaction of the inhibitor with the protein. **B)** The proteins were treated with digestion enzymes (e.g. Trypsin) after the incubation with the compound. The generated peptides were subjected to MS/MS. The mass spectra of the peptides were investigated for modifications in order to find a mass addition of the size of JH5. **C)** The proteins were treated with compound. Subsequently, the samples were treated with acrylamide to introduce propionamide (PA) modifications at the cysteine residues. Before, the samples had either been denatured with urea to increase the accessibility of the cysteines or had not been treated to preserve the native state. The samples were reduced to remove all previously occupied cysteines and disulphide bridges. Treatment with iodoacetamide was performed to modify the remaining cysteine-residues with a distinct label. The samples were digested and subjected to mass spectrometry as described in B). The mass spectra of the peptides were investigated for modifications.

A   JH5

MGHHHHHHGSIETDRVSKEFIEFLKTFHKTGQEIYKQTKLFLEGMHYKRDLSIEEQSE
CAQDFYHNVAERMQTRGKVPPERVEKIMDQIEKYIMTRLYKYVF**C**PETTDDEKKDLAI
QKRIRALRWVTPQML**C**VPVNEDIPEVSDMVVKAITDIIEMDSKRVPRDKLA**C**ITK**C**SK
HIFNAIKITKNEPASADDFLPTLIYIVLKGNPPRLQSNIQYITRF**C**NPSRLMTGEDGY
YFTNL**CC**AVAFIEKLDAQSLNLSQEDFDRYMSGQTSP

B   DMSO

MGHHHHHHGSIETDRVSKEFIEFLKTFHKTGQEIYKQTKLFLEGMHYKRDLSIEEQSE
CAQDFYHNVAERMQTRGKVPPERVEKIMDQIEKYIMTRLYKYVF**C**PETTDDEKKDLAI
QKRIRALRWVTPQML**C**VPVNEDIPEVSDMVVKAITDIIEMDSKRVPRDKLA**C**ITK**C**SK
HIFNAIKITKNEPASADDFLPTLIYIVLKGNPPRLQSNIQYITRF**C**NPSRLMTGEDGY
YFTNL**CC**AVAFIEKLDAQSLNLSQEDFDRYMSGQTSP

Figure 39   Sequence coverage in the MS measurements after enzymatic digestion.
The sequence coverage in the peptide identification mass spectrometry is illustrated. Identified peptide sequences are highlighted with grey background, and cysteines are shown in enlarged, bold letters. In both cases the four C-terminal cysteines (Cys172, Cys220, Cys238 and Cys239) were not among the covered sequences. **A)** The protein sample was treated with JH5 prior to the measurement. **B)** The protein sample was treated with DMSO prior to the measurement.

The last approach (Figure 38C) was based on the idea that the JH5 interaction might not withstand the process of sample generation with harsh conditions e.g. the application of the strong acid TFA. Therefore, after incubation of the protein with the compound all cysteine residues were modified by the use of acrylamide. The intention was to identify the cysteine residue to which JH5 was bound by its unavailability for alkylation. To increase the accessibility of the cysteines, the samples were incubated with urea. Alkylation with acrylamide results in propionamide (PA) modification of the cysteines. Subsequently, the samples were reduced to remove the hypothetically bound JH5 and the protein was treated with iodoacetamide to create carbamidomethyl (CaM) modifications. In theory, all cysteines that have been modified by CaM are candidates for the binding site of JH5. Alternatively, these cysteines might be engaged in disulphide bridges.

This alkylation approach (Figure 40) resulted in distinct modification profiles for all cysteines. For the sample treated with JH5 in the absence of urea (+JH5,-urea) the amount of detected peptide spectrum matches (PSMs) was lower than in all other samples. The PSMs are a measure for the reliability of the measurement. Therefore, the comparison of the +JH5,-urea sample with the other samples was not appropriate. For the other samples comparable level of PSMs were observed. This holds true for the general level as well as for individual cysteine positions (Figure 40). Comparison of both DMSO treated samples (Figure 40A, C) shows that urea treatment increased the amount of PA modifications. Hence, the accessibility of the cysteines was increased by the urea treatment as anticipated. In the urea treated JH5 and DMSO samples (Figure 40C, D) a reduction of the PA modifications on Cys132, Cys239 and Cys238 was observed in the presence of JH5 suggesting that these cysteine residues have been unavailable to the addition of PA. This implies an interaction with JH5 at the time of the reaction.
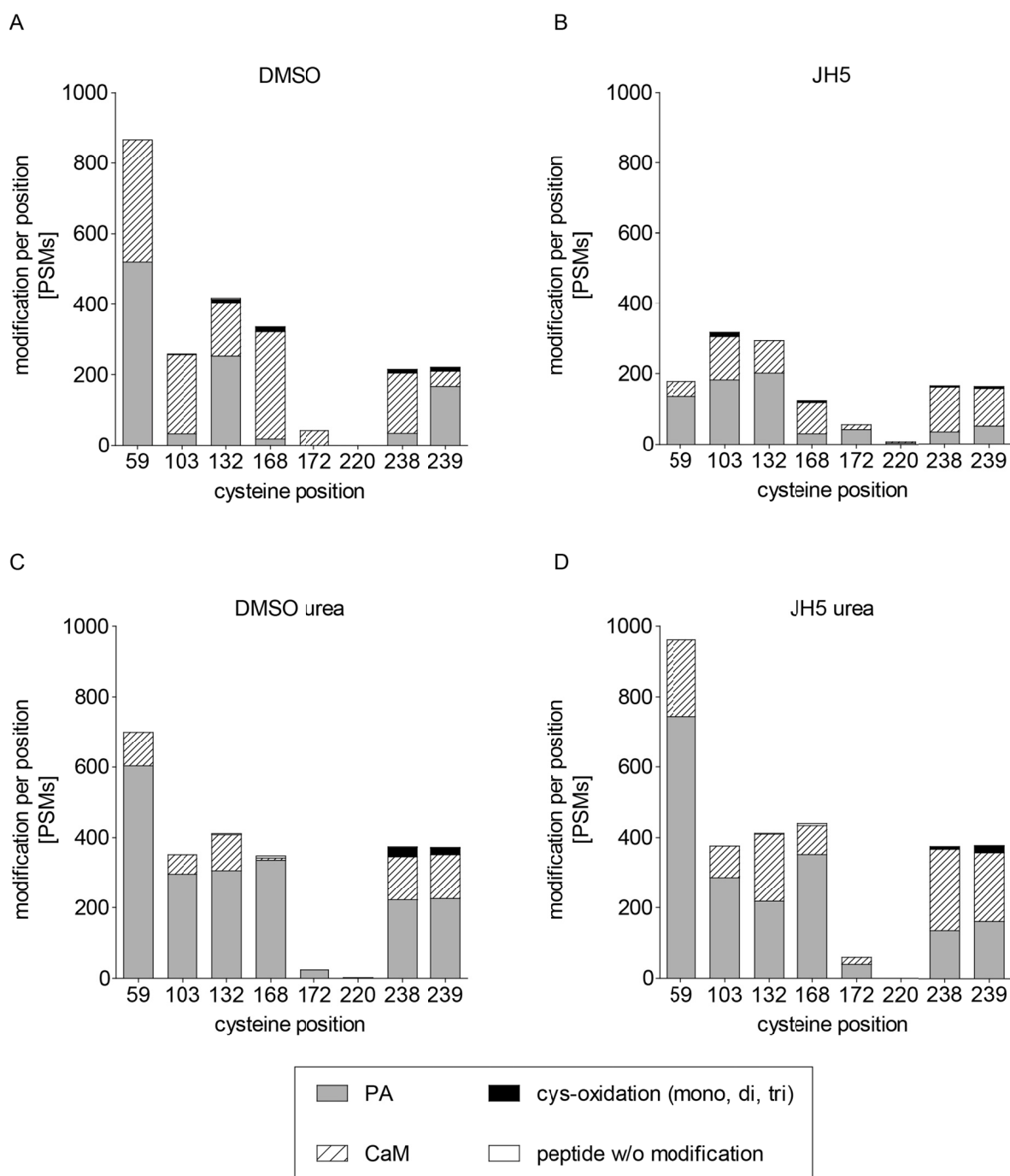
Figure 40   Alkylation modifications at Rabex-5GEF in absence and presence of JH5.
The experiment was performed in absence (**A, B**) and presence (**C, D**) of urea to denaturate the protein and to increase the accessibility of the cysteine residues. The first alkylation step was performed with acrylamide to introduce propionamide (PA) modifications at the cysteine residues. After treatment in a reducing environment to remove all disulphide bonds or potential covalent JH5 modifications, the protein was treated with iodoacetamide to introduce Carbamidomethyl (CaM) modifications. The number of identified cysteine residues is shown for all samples. In all samples, the cysteines 172 and 220 were identified with low or no PSMs. Hence, no conclusion about their modification status can be drawn. **A)** DMSO treated Rabex-5GEF in absence of urea. **B)** JH5 treated Rabex-5GEF in absence of urea: the low PSMs available for this sample indicated lower confidence in the obtained data and led to the exclusion of this condition from further consideration. **C)** DMSO treated Rabex-5GEF in presence of urea. **D)** JH5 treated Rabex-5GEF in presence of urea. Comparison of A and C indicated that the urea treatment enabled increased accessibility of the cysteines for PA modifications. Comparison of C and D indicated that the cysteines 132, 238 and 239 were less accessible for the PA modifications in the JH5 sample compared to the DMSO sample. Data from one experiment is depicted.

The mass spectrometry approach to investigate whether a cysteine-residue of Rabex-5GEF was targeted by JH5 was complemented by the use of several mutated Rabex-5GEF proteins[9] with cysteine to serine replacements (Figure 41A, B). All cysteine to serine mutants showed reduced activity but none of them had completely lost its activity (Section 8.10). The proteins were investigated for the inhibition by JH5. The Rabex-5GEFCS protein with replacement of all eight cysteines to serines was not inhibited by JH5. The Rabex-5GEFCSN protein, in which the N-terminal cysteines were replaced by serine was affected by JH5 in a comparable manner to the wildtype Rabex-5GEF. The Rabex-5GEFCSC protein with replacements of the C-terminal cysteines was only slightly inhibited by JH5. These observations indicated that one or more of the C-terminal cysteines are likely to contribute to the interaction with Rabex-5GEF. These findings are in line with the observation from the alkylation mass spectrometry approach. The cysteine residues Cys239 and Cys238 which were implicated in the interaction of JH5 with Rabex-5 belong to the cysteines at the C-terminus of Rabex-5GEF. The fact that no JH5 modification on the cysteine residues of Rabex-5GEF was identified in the peptide mass spectrometry approach might be explained by the poor sequence coverage. It was not possible to detect the C-terminal cysteine residues of Rabex-5GEF in this experiment.

---

[9] The cloning of the constructs was kindly performed by Dr. Anton Schmitz. The protein biosynthesis was kindly performed by Nicole Krämer.
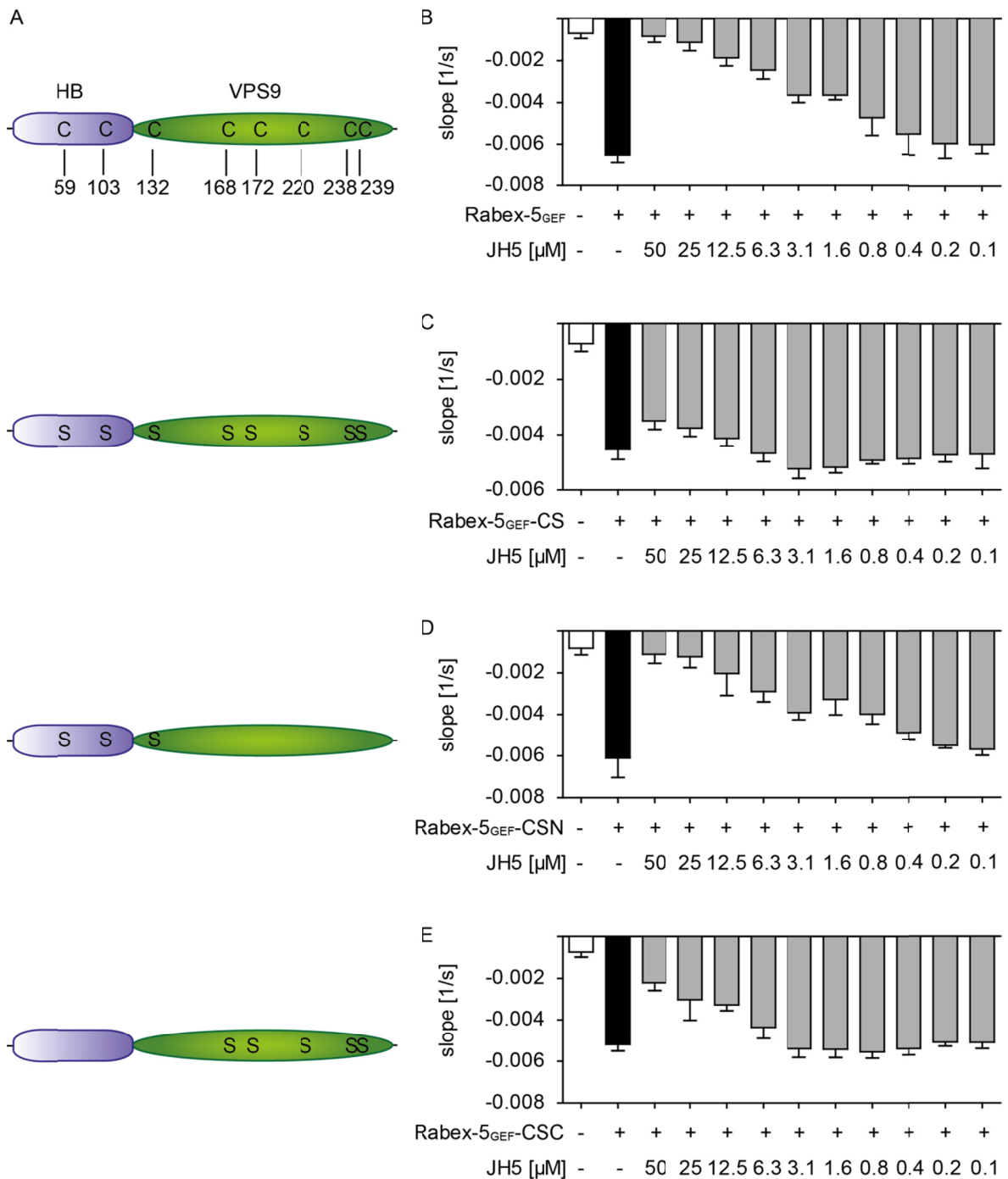
Figure 41 **Inhibitory effect of JH5 on the Rabex-5$_{GEF}$ cysteine mutant proteins.**
A) Schematic representation of the Rabex-5$_{GEF}$ cysteine position and mutant constructs. The helical bundle domain is shown in blue and the Vps9 domain in green. The cysteine positions are marked as C and the amino acid position is given underneath the wildtype protein scheme. The Rabex-5$_{GEF}$ cysteine mutants used in the study are depicted. An exchange of cysteine for serine is indicated as S. **B-E)** The activity of JH5 was determined in the nucleotide exchange assay (tryptophan fluorescence readout) with 100 nM Rabex-5$_{GEF}$, 1 µM Rab5c and 2 % DMSO. **B)** Rabex-5$_{GEF}$ was inhibited dose-dependently by JH5 with an IC$_{50}$ of 2.7 µM (95 % CI 1.8 - 3.9 µM). **C)** The Rabex-5$_{GEF}$CS was almost not affected by JH5 up to a concentration of 50 µM. Calculation of an IC$_{50}$ value resulted in a large 95 % CI: 98 µM (95 % CI 7 – 1479 µM) **D)** Rabex-5$_{GEF}$CSN was inhibited by JH5 with an IC$_{50}$ of 3.4 µM (95 % CI 2.0 - 5.7 µM). **E)** Rabex-5$_{GEF}$CSC was inhibited by JH5 with an IC$_{50}$ of 21.5 µM (95 % CI 11.8 - 39.2 µM).

3.5 Estimation of cellular applicability

The long term goal was the application of the identified Rabex-5GEF inhibitors in an intracellular environment. Preliminary experiments were performed to estimate the intracellular applicability of JH5. The observation that JH5 was inactive in a DTT containing environment (Section 3.3.3) had pointed out that this application might be challenging. In the following sections (Section 3.5.1 -3.5.5), several intracellular assays monitoring the activity of Rab5 are presented.

For several cellular assays, the overexpression of Rab5 and Rabex-5 was necessary. Rab5a but no Rab5c constructs were available from Addgene. Since, both proteins are highly homolog it was not expected that the compounds would affect the Rabex-5GEF nucleotide exchange on Rab5c selectively. An *in vitro* assay using Rab5a instead of Rab5c confirmed the activity of JH5 in the Rabex-5GEF mediated nucleotide exchange on Rab5a (Section 8.6). To use the compounds in a cellular environment, less DMSO could be used than in the *in vitro* assays. Therefore, the solubility of the compounds in RPMI medium with 0.5 % DMSO was investigated first and found to be acceptable till 100 µM (Section 8.8).

3.5.1 Intracellular Rab5 activation

Effector proteins can be used to detect activated GTPases because they are per definition proteins interacting only with the GTP from of a GTPases.[5] The Rab5 binding domain of Rabaptin-5 (R5BD) is well described as probe for Rab5 activation.[47, 246-248] The R5BD was cloned to a GST tag to enable interaction with a matrix to pull Rab5-GTP from cell lysate.[10] The scheme in Figure 42A explains the principle of the experiment. To optimize the assay system, a pull-down experiment with cell lysate that had been pre-loaded with nucleotide was performed. In addition, it was investigated whether the transfection with a Rab5-Flag construct to increase the cellular level of Rab5 protein would be beneficial. Both the Rab5-Flag and the endogenous Rab5 were pulled more effectively from the lysate when they were loaded with a non-hydrolysable nucleotide like GTPγS compared to GDP (Figure 42B). However, comparison of the Rab5 pull-down from the GDP and GTP pre-loaded cell lysates revealed no difference. The non-hydrolysable GTPγS treatment induced the strongest Rab5 pull-down. This indicated that hydrolysis occurred during assay performance in the GTP sample. The results with the endogenous Rab5 and the transfected Rab5Flag were congruent. Since no benefit from Rab5 overexpression was observed, the assay was subsequently optimized without Rab5 overexpression. Shortening the incubation time reduces the time in which hydrolysis can occur. Despite the reduction of the assay performance time to about 10 minutes in total no difference between the GDP and GTP sample was visible (Figure 42C). In conclusion, this assay format was not suitable to monitor Rab5 activation in cells and this approach was not pursued further.

---

[10] A Strep-Tag fusion protein was also available but had no advantage compared to the GST-R5BD protein. The cloning of the constructs was kindly performed by Nicole Krämer.
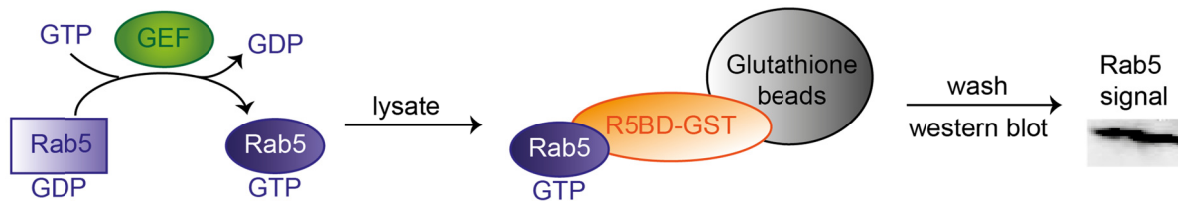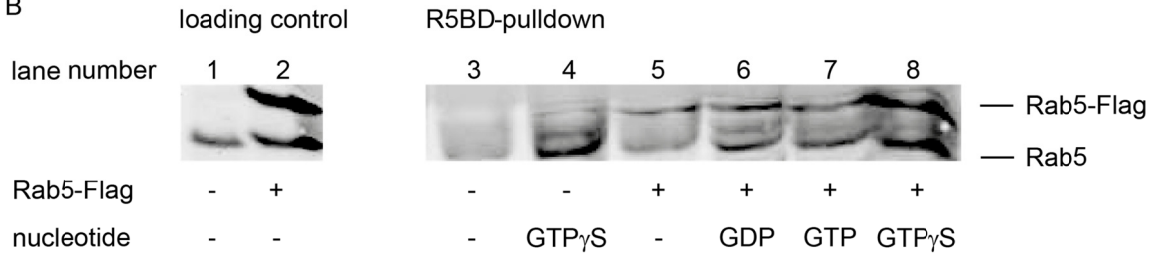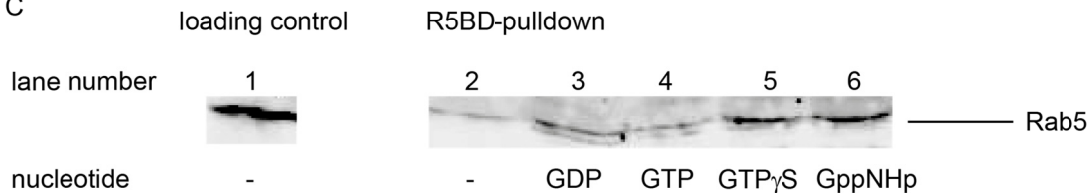
Figure 42   R5BD effector pull-down to monitor intracellular Rab5 activation.
A) The principle of the R5BD pull-down is illustrated. The activation of Rab5 (e.g. by a GEF) results in the production of Rab5-GTP. Rab5-GTP interacts with the Rab5 binding domain of the effector Rabaptin-5 (R5BD). R5BD was designed as a GST-fusion protein to allow the separation of active Rab5 from cell lysate by interaction with a Glutathione matrix. All non-binding proteins from the cytosol can be removed by washing while keeping the specifically pulled R5BD interactor Rab5. Via western blotting, the amount of Rab5 that bound to the R5BD matrix can be detected. By comparison to the total Rab5 protein level from the lysate (loading control) the amount of active Rab5 can be quantified. **B, C)** 15 % SDS-polyacrylamide gel submitted to western blotting using a Rab5 antibody for visualization. **B)** The loading control contained untreated Hek293 cell lysate. All samples submitted to transfection with Rab5-Flag are indicated below the blot. The R5BD pull-down lanes show the cell lysate that has been spiked with the indicated nucleotides (pre-loading). Comparing lane 3 and lane 4 (which contain lysate samples that have not been subjected to transfection) an increase in the Rab5 band is visible in lane 4 (non-hydrolysable GTPγS). The lanes 5 to 8 contain lysate from Rab5-Flag transfected cells. The comparison of lane 5 (no nucleotide incubation) with lane 8 (GTPγS) shows stronger Rab5 signals in the GTPγS samples than in the non-treated sample. The incubation with GTPγS increased the amount of active Rab5 that interacted with R5BD. The incubation with GDP (lane 6) and GTP (lane 7) increased the amount of active Rab5 compared to the non-preloaded sample. However, no difference between the GDP and the GTP pre-loaded sample was observed. **C)** The protocol was shortened to less than 10 minutes to lower the time in which hydrolysis is possible. In lane 1 the loading control is depicted. Lane 2 shows lysate that has not been pre-loaded with nucleotide. Lanes 3 to 6 contain lysate pre-loaded with nucleotide. The non-hydrolysable sample has the highest content of active Rab5. Again, no difference between the GDP (lane 3) and the GTP (lane 4) sample was observed.

3.5.2 EGFR-degradation

The EGF-Receptor (EGFR) endocytosis and subsequent degradation is triggered by binding of the ligand EGF to the receptor.[27] Subsequently, the EGFR is taken up by endocytosis which is a Rab5 dependent process.[158] The degradation of the receptor and EGF in the lysosomes terminates the stimulation of the signalling cascade.[27, 249, 250] *Balaji* et. al. reported that the EGFR degradation was impaired in absence of Rabex-5.[163] A concentration of 100 ng/mL EGF at which EGFR degradation should be favoured over recycling was used to maximize the amount of degraded EGFR. In addition, Rabex-5 was implicated in the transition of early-to-late endosomes which is required for the EGFR degradation.[15, 154, 155, 249]
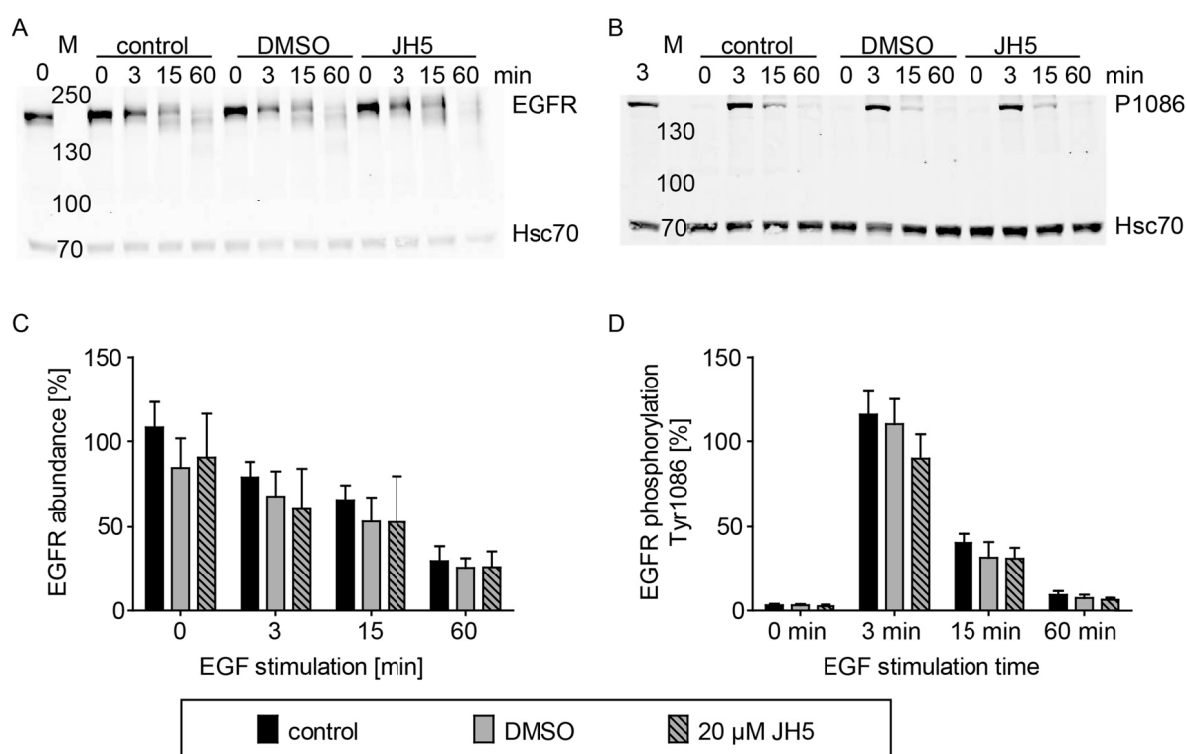
Figure 43   EGFR stimulation and degradation of HeLa cells in presence and absence of JH5.
A) A 7.5 % SDS-polyacrylamide gel was blotted (wet blot) and probed with EGFR-CT and Hsc70 antibodies. A standard sample was loaded in line 1, a size marker (M) was loaded in lane 2: the 250, 130, 100 and 70 kDa marker signals are indicated. The assay conditions were an untreated control population, a DMSO treated population and a JH5 (20 µM) population. Four distinct times (0, 3, 15, 60 minute) of EGF stimulation were chosen for each assay condition. The stimulation with EGF resulted in the decrease of the EGFR receptor level over time, longer EGF stimulation times resulted in stronger receptor degradation. By visual inspection of the blot no difference between the distinct assay conditions is detectable. **B)** The experiment was performed as described in A: the antibodies used in this blot were Phospho-Tyr1086-EGFR and Hsc70. The stimulation with EGF triggered the phosphorylation of the EGFR which is an indication of its activated status. The phosphorylation signal decreased over time, the maximal phosphorylation was observed at the shortest EGF stimulation performed (3 minute). No difference between the distinct assay conditions is detectable. **C-D)** The quantification from three independent experiments is depicted. The western blot signals were normalized with respect to background, Hsc70 signal (loading control), and standard sample. The trends that have been described in A and B were not changed by the normalization. However, the normalization enabled comparison of the distinct treated samples. No noteworthy difference between control, DMSO and JH5 sample was observed.

HeLa cells were chosen because they were known to contain Rabex-5 (15 nM, 3 mg/mL lysate).[95] This assumption was confirmed by western blotting. HeLa cells were treated either with DMSO or compound overnight, followed by EGF stimulation, cell lysis, and western blot analysis to quantify levels of EGFR (Figure 43A, C). As a control for the successful stimulation, the phosphorylation status of the receptor was analysed by western blotting with a phosphor-Tyr1086-EGFR specific antibody (Figure 43B, D). The EGF stimulation resulted in a time dependent loss of the EGFR signal. The phosphorylation signal of the EGFR was maximal at three minutes EGF stimulation and decreased at longer incubation times. DMSO and JH5 had no visible effect on the degradation of the EGFR or the phosphorylation status of the receptor.

3.5.3   Receptor endocytosis

Rab5 is known to be relevant for the endocytosis of membrane receptors (Section 1.3.3). To investigate the endocytosis of a receptor, the cells were incubated with the cognate fluorescently labelled receptor ligand. Endocytosis is temperature dependent, at 4 °C almost no receptors will be taken up.[250] The endocytosis of the Transferrin receptor, a well described marker of endocytosis,[251] as well as the endocytosis of the EGFR was monitored. A direct link for the impact of Rabex-5 on the transferrin receptor endocytosis is not known. Nevertheless, the Rabex-5 interacting partner Rabaptin-5 can delay the endocytosis of the transferrin receptor and provides an indirect connection.[48] In addition, Rab5 is known to be involved in the transferrin receptor endocytosis.[116] As described previously, Rabex-5 had been implicated in the regulation of the EGFR receptor (Figure 11).

The results of the receptor internalisation assay are depicted in Figure 44. For both receptors, it was possible to obtain a positive and a negative control by incubation of the cells at 4 °C and 37 °C, respectively. The effect of the compounds was measured at 37 °C. In case of the transferrin receptor, JH5 and JH5-E were tested. Both compounds induced a slight decrease of the endocytosis. However, these effects were not significantly distinct from the positive control. For the EGFR, the endocytosis was decreased for about 35 % by JH5. However, the control compound JH5-O which was inactive in all *in vitro* assays showed the same effect. The compounds JH5-E and JH5-M had less pronounced effects on the receptor internalization.
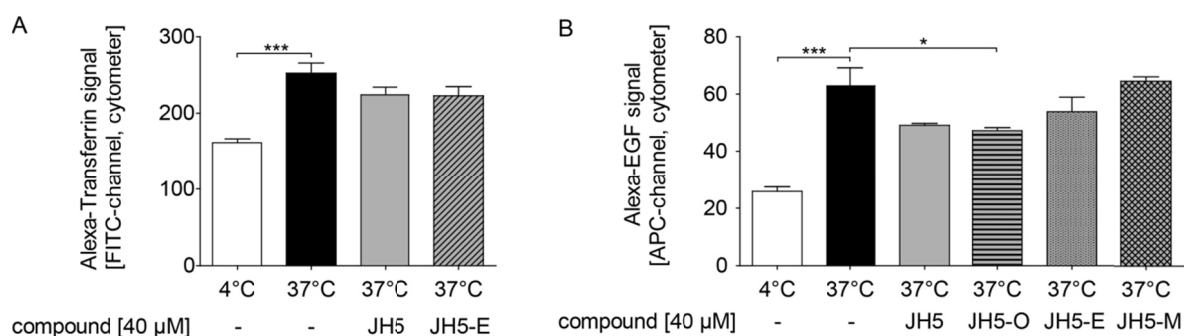
Figure 44 **Internalisation of Transferrin and EGF monitored by flow cytometry.**
The internalisation of the receptors was monitored by using fluorescently labelled ligands. The ligands were allowed to interact with the receptors on the cell surface. Subsequently, the cells were washed to remove unbound ligand. The cells were subjected to flow cytometry analysis. The fluorescence observed in the flow cytometry (x-axis) is equivalent to the amount of receptor internalized by endocytosis. **A)** The endocytosis of Alexa448-labelled Transferrin was observed by incubation of HeLa cells at 37 °C for 30 minute with labelled ligand (black column). At 4 °C the internalization process was decreased (white column) and this condition was used as negative control. The treatment of the cells with the compounds JH5 and JH5-E for two hours prior to Transferrin addition did not have a significant effect on the endocytosis of the transferrin receptor. **B)** The internalization of Alexa647-labelled EGF was observed by flow cytometry after 5 minute incubation with HeLa cells. Again, the DMSO treated cells at 4 °C (white column) or 37 °C (black column) served as negative and positive control, respectively. The treatment with JH5 prior to and during the experiment (grey column) had a slight inhibitory effect on the internalization of EGF. However, the same effect was observed with JH5-O (striped column). The effects of JH5-E (dark grey column) and JH5-M (dotted column) were less pronounced. Representative cytometry histograms to illustrate the raw data can be found in Section 8.12. The significance was calculated by the use of the one-way-ANOVA with the Tukey post-test (*GraphPad Prism* software), p-values: *$p < 0.05$, **$p < 0.01$, ***$p < 0.001$.

3.5.4 Rabex-5 dependent neurite growth

The overexpression of constitutive active Rab5 or Rabex-5 has been reported to inhibit NGF-induced neurite outgrowth.[247] Therefore, cells of the human primary glioblastoma cell line U87 were incubated with small molecules and photographed after 24 hours to monitor cell morphology and potential effects on the amount of neurites.

As controls, the cells were either not treated at all or incubated with DMSO to monitor the effect of the solvent of the compounds. Figure 45 shows three representative images of each sample. Comparing non-treated controls (Figure 45A) to DMSO treatment (Figure 45B) no difference in cell shape was visible as expected. However, the treatment of the U87 cells with the compounds JH5 (Figure 45C) and JH5-E (Figure 45D) had no effect on the overall architecture of the cells and the amount of neurites. Longer incubation times of the cells with compounds did not result in more pronounced effects. Hence, no stimulation of neurite formation by the Rabex-5GEF inhibitors was observed.
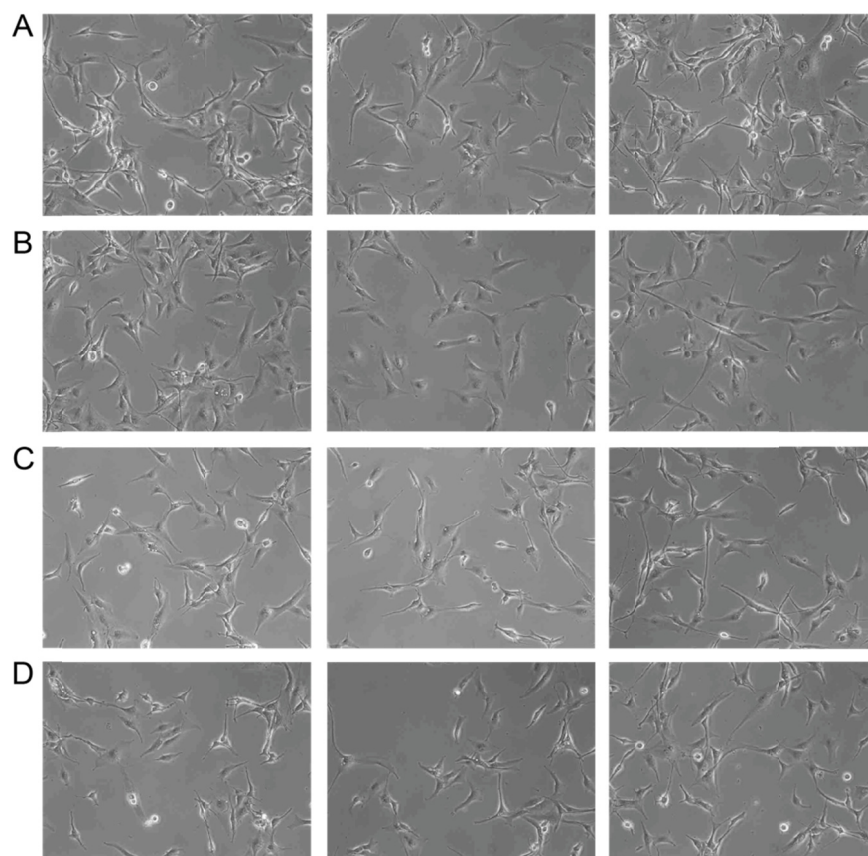
Figure 45   No effect of JH5 and derivatives on the neurite growth of U87 cells.
U87 cells have been treated for 24 hours with 50 µM compound in 0.5 % DMSO f.c. and the morphology of the cells was documented by light microscopy. No morphological differences were visible upon DMSO or compound treatment. For each condition three representative pictures have been chosen (from in total three independent experiments). **A)** Untreated U87 cells, **B)** DMSO treated U87 cells, **C)** JH5 treated U87 cells, **D)** JH5-E treated U87 cells.

3.5.5   Effects on the Rab5 dependent PI3K activity

In cooperation with the group of *Professor Dr. A. Haas* (University of Bonn), the activation of the PI3K, which is dependent on Rab5 activity, was analysed (Section 1.3.2). The amount of PI3P that had been generated on early phagosomes of murine macrophages by the PI3K was monitored. The macrophages were incubated with the compounds and subsequently, the cells were exposed to latex-beads. The cells were allowed to internalize the beads for 10 minutes before their phagosomes were isolated to probe for the PI3P level. Therefore, the 2xFYVE-GST, a well described probe for the detection of PI3P levels that is based on the FYVE motif that interacts with PI3P, was used.[100] The results of these experiments are depicted in Figure 46. As controls, the cells have been treated with DMSO and the well described PI3K inhibitor Wortmannin.[252] Macrophages incubated with DMSO showed a 2xFYVE-GST (in fluorescence units) signal of about three FU that was drastically reduced in the presence of Wortmannin. The assay revealed a decrease in the PI3P level in presence of JH5 by about 50 %. However, the negative control compound JH5-M reduced the signal to the same extend. Therefore, it is likely that the observed

effect was not due to inhibition of Rabex-5 by JH5 but rather by unspecific side effects or by interference with the assay.

In summary, in none of the above presented cellular assays an effect which indicated inhibition of Rabex-5 was observed for JH5 or JH5-E. Explanations for this findings and further experiments are suggested in Section 4.5 and the Outlook. However, these results indicated that JH5 cannot be used in an intracellular environment without further optimisation.
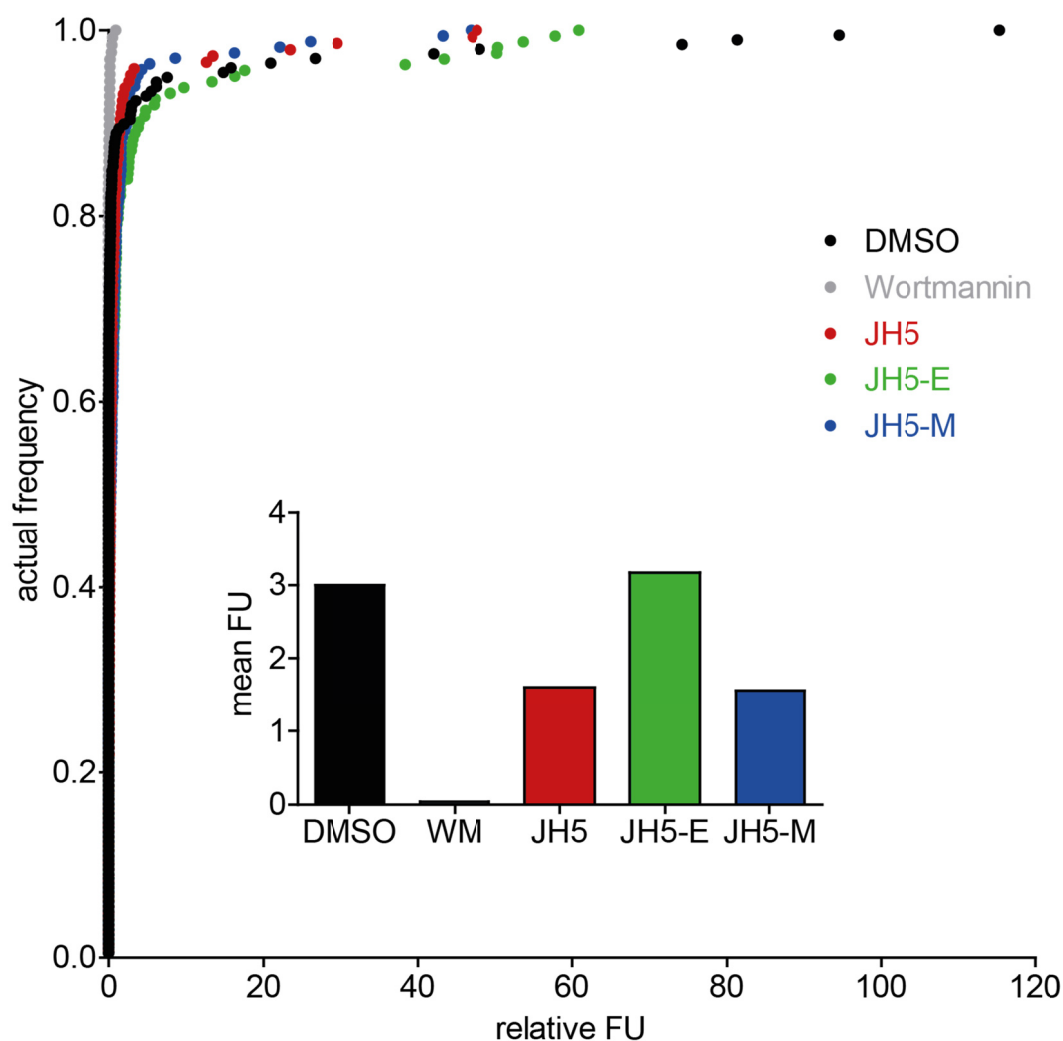
Figure 46   The impact of Rabex-5 inhibitors on the PI3P level of early phagosomes.
The level of PI3P depends on the activity of PI3K, which is a Rab5 effector. J774E macrophages (murine) were incubated for 60 minute with DMSO (black), and 100 nM Wortmannin (grey), a PI3K inhibitor, as controls or with 80 μM compound of interest (coloured). Subsequently, the cells were incubated for 10 minute with latex-beads (1 μm) in presence of the compounds. The cells were homogenised and centrifugation yielded the postnuclear supernatant by separated from the nuclei and cell debris. After normalisation of the postnuclear supernatant for the protein concentration, the lysate samples were incubated with 2 μM 2xFYVE-GST for 15 minute on ice. The early phagosomes from these supernatants were purified and the amount of bound 2xFYVE-GST was quantified as measure of the phagosomal PI3P. The raw data is presented in the x-y-graph. On the y-axis is the actual frequency of phagosomes given. These are blotted against their fluorescence intensity (in fluorescence units) on the x-axis. The bar diagram inserted in the figure gives the mean fluorescence units (FU) for each sample which represents the amount of PI3P on the phagosomes. In presence of DMSO a mean FU of about three was observed. Wortmannin decreased the level of PI3P to almost zero. JH5 (red) and JH5-M (blue) decreased the level of the mean FU by about 50 %. The compound JH5-E (green) had no effect and showed a level of mean FU of about the same level as the DMSO control. The depicted data are courtesy of Andreas Jeschke and Professor Dr. A. Haas (University of Bonn).

3.6 Screening hit verification and lead selection

JH5 and Gü321 were found to have undesired sensitivity towards reducing conditions. In addition, no cellular effect of JH5 was observed in several assays. Thus, the question whether one of the other hit compounds might have been a more appropriate choice remained. The detailed compounds selection process is revisited in this section to answer this question.

The first characteristic that all compounds were required to have was the desired activity. The inhibitory potential of the secondary hits was estimated in the kinetic form of the Rabex-5GEF- Rab5c screening assay as introduced in Section 3.1.3. The kinetic format is a continuous assay type and provides more information than the endpoint detection assay belonging to the class of stopped assays.[253] The nucleotide exchange catalysed by Rabex-5GEF was investigated in the absence and presence of 20 μM compound. For some compounds, IC_{50} values (Section 3.3.1) were determined to enable comparison.

Moreover, as indicated in Section 3.3, the specificity of the compounds was analysed. Therefore, the nucleotide exchange assays with Cytohesin-2-Arf1 and Vav-1-Rac1 (Section 3.3.2) were used.

Finally, the identity and integrity of the hit compounds had to be controlled by HPLC-MS and the corresponding data can be found in Section 8.13.3.

Dependent on their inhibitory activity, specificity, and compound quality, the hit compounds were classified either to be lead compounds or to be excluded from further investigation. The results of the classification of the secondary hit compounds are depicted in Table 8 at the end of this section. For each compound or group of compounds the characterisation will be described in the following subsections to explain the choice of the lead compounds and to investigate whether further potential compounds were found in the screening that should be considered in the light of the findings of the cellular non-applicability of JH5.

3.6.1 Compounds excluded due to non-specific effects

3.6.1.1 K1.03.F10

K1.03.F10 was active in the Rabex-5-Rab5c nucleotide exchange assay (Figure 47A). However, it was additionally active in the Cytohesin-2 mediated nucleotide exchange and the Vav-1-Rac1 nucleotide exchange. (Figure 47B, Supporting figure 13F). This observation suggested non-specific activity which was supported by several descriptions in literature. K1.03.F10 was reported as inhibitor for Cdc25 and other protein tyrosine phosphatases.[254, 255] Due to this non-specific profile, K1.03.F10 was excluded from further studies.
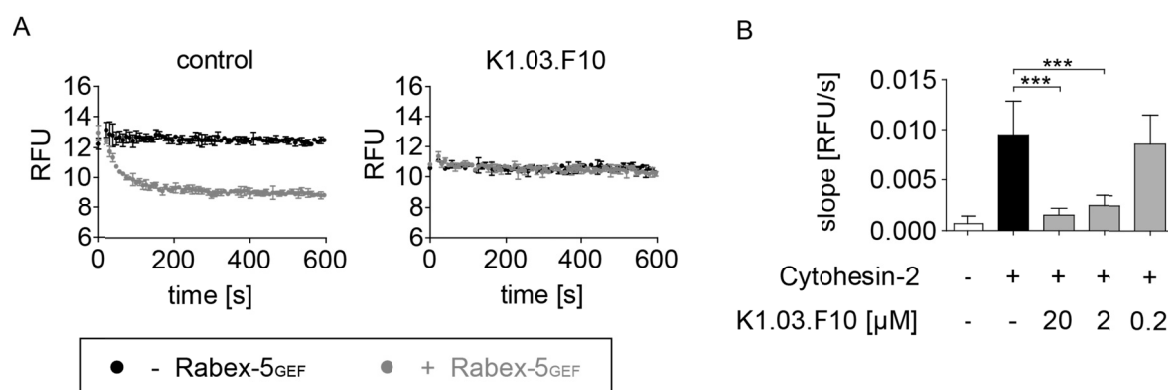
Figure 47   Unspecific effects of K1.03.F10.[11]

A) K1.03.F10 was investigated in the kinetic format of the Rabex-5$_{GEF}$ activity assay with 1 µM Rab5c and 500 nM Rabex-5$_{GEF}$. The reaction with Rab5c and water is shown in black and the reaction with Rab5c and Rabex-5$_{GEF}$ in grey. The control reaction with DMSO instead of compound is depicted on the left, the reaction with 20 µM compound from the library stock on the right side. The addition of K1.03.F10 to the nucleotide exchange reaction results in a curve with the same curve progression as in the negative control. This observation argued for the inhibitory activity of K1.03.F10. **B)** K1.03.F10 inhibited the Cytohesin-2-Arf1 nucleotide exchange in a dose-dependent manner. The data were obtained from two independent experiments and the errors are depicted as SD. The significance of the effects was tested by One-way ANOVA and Tukey's Multiple Comparison Test (*GraphPad Prism* software), p-values: *p < 0.05, **p < 0.01, ***p < 0.001.

3.6.1.2   *K1.13.A07*

The bromo-barbiturate K1.13.A07 inhibited the Rabex-5-Rab5c nucleotide exchange assay (Figure 48A). The compound had been identified before as active substance in a screening for inhibitors of the PH-domain of Cytohesin-2.[256] This indicated that it might not be a specific Rabex-5$_{GEF}$-Rab5c inhibitor. The anticipation was confirmed: K1.13.A07 was active in the Vav-1-Rac1 assay even more pronounced than in the Cytohesin-2-Arf1 assay (compare Figure 47B, C). Hence, the compound was excluded from further investigations.

3.6.1.3   *Xanthine-derivatives*

The compounds K1.16.C09 and K1.17.C05 are xanthine-derivatives. K1.16.C09 inhibited the Rabex-5$_{GEF}$ nucleotide exchange assay at a concentration of 50 µM. IC$_{50}$ calculation was challenging because no saturation was reached. Using the data of the positive and the negative control as constrains an IC$_{50}$ could be estimated and was found to be > 20 µM (Figure 49A). Moreover, this molecule was found to be active in the Cytohesin-2 nucleotide exchange. The Cytohesin-2 assay was significantly affected at 20 µM K1.16.C09 which represents activity of the compound in the same concentration range as for the Rabex-5$_{GEF}$ inhibition (Figure 49B). This behaviour indicated dramatic unspecific activity. No compelling activity of K1.17.C05 (Section 8.5) was observed in the Rabex-5$_{GEF}$-Rab5c nucleotide exchange and both compounds were eliminated from the panel of promising secondary hits.

---

[11] Franziska Wolter performed the Cytohesin-2 nucleotide exchange measurement, Christine Wosnitza planned and analysed the experiment.
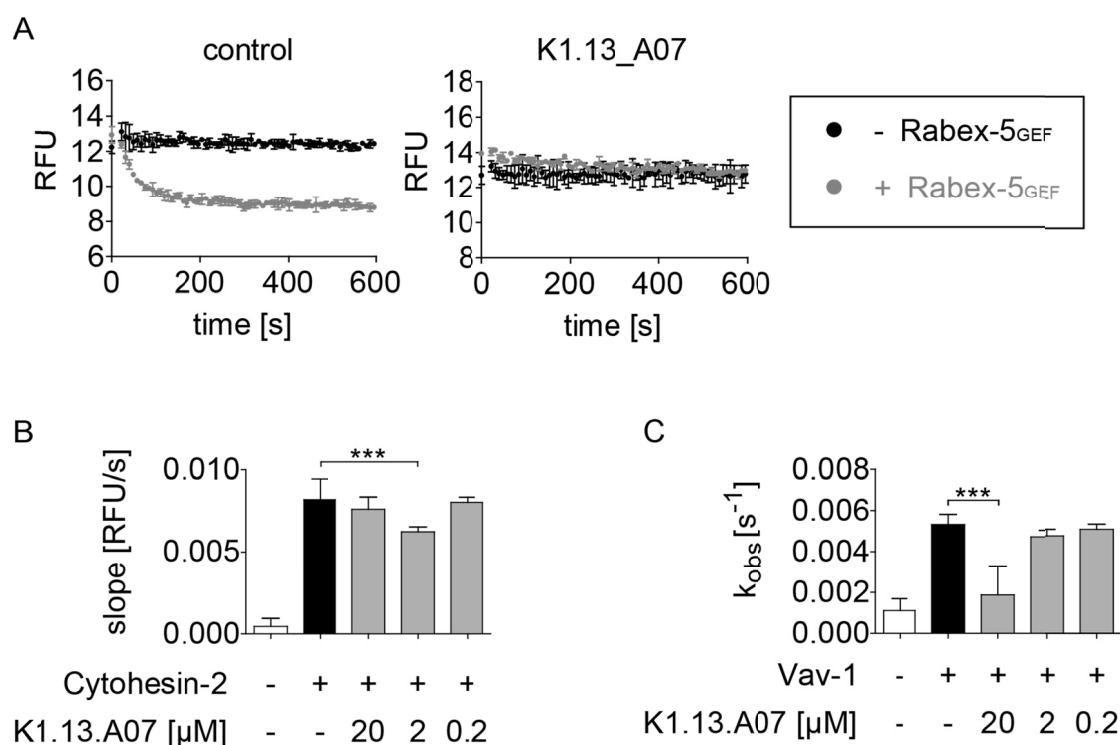
Figure 48   Unspecific effects of K1.13.A07.[12]
A) K1.13.A07 was investigated in the kinetic format of the Rabex-5GEF activity assay with 1 µM Rab5c and 500 nM Rabex-5GEF. The reaction with Rab5c and water is shown in black and the reaction with Rab5c and Rabex-5GEF in grey. The control reaction with DMSO instead of compound is depicted on the left, the reaction with 20 µM compound from the library stock on the right side. The addition of K1.13.A07 to the nucleotide exchange reaction produce the same curve progression as the negative control without Rabex-5GEF. This observation suggested inhibitory activity of K1.13.A07. **B)** K1.13.A07 inhibited the Cytohesin-2-Arf1 at 2 µM but not at 20 µM. **C)** K1.13.A07 was also active in the Rac1-Vav-1 nucleotide exchange. These results led to the decision to rate this compound "non-specific". The data was obtained in two independent experiments depicted as mean ± SD; the significance of the effects was tested by One-way ANOVA and Tukey's Multiple Comparison Test (*GraphPad Prism* software), p-values: *p < 0.05, **p < 0.01, ***p < 0.001.
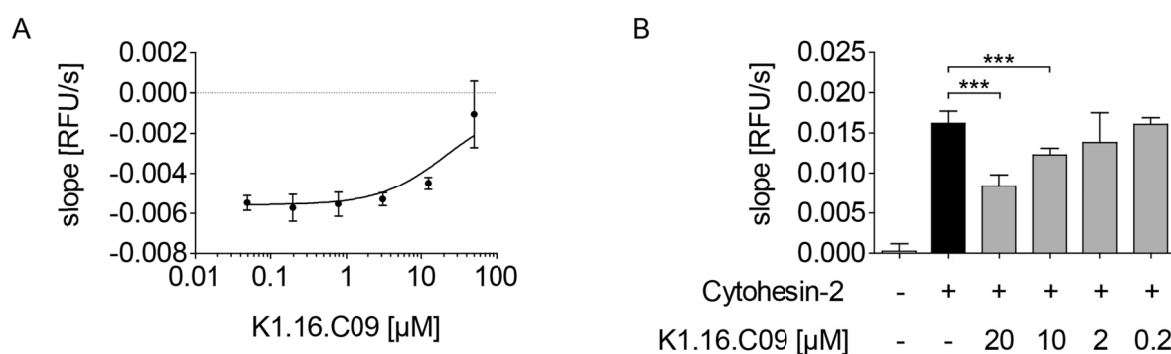
Figure 49   Unspecific effects of K1.16.C09.
A) The Rabex-5GEF mediated nucleotide exchange for IC50 determination with 20 nM Rabex-5GEF and several compound concentrations is presented. IC50 estimation was only possible if positive and negative control of the assay were used as constrains in the calculation since the saturation was not reached. The IC50 for the Rabex-5GEF nucleotide exchange was observed to be > 20 µM with K1.16.C09. **B)** The Cytohesin-2 catalysed nucleotide exchange on Arf1 with several compound concentrations is depicted. A significant inhibition of the Cytohesin-2 catalysed nucleotide exchange was obtained at 10 µM and 20 µM K1.16.C09. Data from at least three independent experiments are shown as mean ± SD. The significance was calculated by the use of the one-way-ANOVA with the Tukey post-test (*GraphPad Prism*), p-values: *p < 0.05, **p < 0.01, ***p < 0.001.

---

[12] Franziska Wolter performed the Cytohesin-2 nucleotide exchange measurement.

3.6.2 Stock and library compound differed in activity

3.6.2.1 *K1.05.F02 (Gü61)*

K1.05.F02 was active in the Rabex-5GEF mediated nucleotide exchange assay. The IC_{50} of 2.8 μM (95 % CI 2.2 - 3.7 μM) was about seven times higher than the IC_{50} of JH5 (Figure 50A). Compared with the inhibition of the Rabex-5GEF nucleotide exchange, its effect on the Cytohesin-2 mediated nucleotide exchange on Arf1 was moderate. The first significant reduction of the nucleotide exchange was observed at 20 μM (Figure 50B). The specificity of this compound is therefore lower than the specificity of the 1,2,4-triazole-3-thiols. Nevertheless, it inhibited the Rabex-5GEF-Rab5c nucleotide exchange with higher potency and was therefore considered for further analysis. Potentially, the specificity profile could be improved by SAR.

However, HPLC analysis revealed several peaks in the library compound (Section 8.13.1). The pure product of the compound was kindly provided by *Professor Dr. M. Gütschow* and will be referred to as Gü61. In comparison to the library stock, Gü61 showed a different peak pattern in HPLC (Section 8.13.1). The correct mass was found in the Gü61 sample while the library compounds mass spectrum showed several, smaller masses (Section 8.13.2). Gü61 did not possess the same inhibitory activity as K1.05.F02 (Figure 50). This was addressed in radioactive nucleotide exchange assay with Rabex-5GEF and Rab5c (Section 3.3.1) and the MST assay (Section 3.3.4). These assays revealed inhibition of the Rabex-5GEF mediated nucleotide exchange by interaction with Rabex-5GEF by K1.05.F02 (Figure 50C). For Gü61 no binding to Rabex-5GEF and consequently no inhibitory properties were observed (Figure 50D, E).

3.6.3 Compounds chosen as leads

3.6.3.1 *1,2,4-triazole-3-thiol compounds*

Nine secondary hits, namely C4.30.A08, C4.30.B06, C4.30.E06, C4.30.E07, C4.30.F05, C4.30.G05, C4.30.H05 (JH5), C4.30.H06, C4.30.H07, shared the same core structure. They consist of a central 1,2,4-triazole ring with a thiol substituent at position 3. Most of these compounds have phenyl- or cyclohexyl-groups at position 4 and 5. All members of this hit family possessed inhibitory activity in the kinetic assay. Since their properties were comparable, the compound with the most promising activity had to be assigned. Several 1,2,4-triazole-3-thiols were synthesised and were found to be active. To choose one lead compound from this group, IC_{50} values were calculated from dose-response measurements (Table 7). C4.30.H05, also referred to as JH5 in its re-synthesized form, was found to be the most active compound with an IC_{50} of 0.3 μM (95 % CI 0.2 - 0.4 μM).

The 1,2,4-triazole-3-thiol compounds with exception of C4.30.B06 were tested in the Cythesin-2 mediated nucleotide exchange (Section 8.5). All of them possessed promising specificity: only C4.30.F05 was found to be active in the Cytohesin-2 nucleotide exchange with the first significant effect at 20 μM. For C4.30.A08 a significant effect on the Cytohesin-2 nucleotide exchange was observed at 2 μM. However, this observation was

not confirmed with freshly synthesized compound. The other re-synthesized compounds were specific over Cytohesin-2. None of these small molecules were active in the Vav-1 nucleotide exchange although not all of them were tested due to limitations in the amount of library compound available at this time of the study.
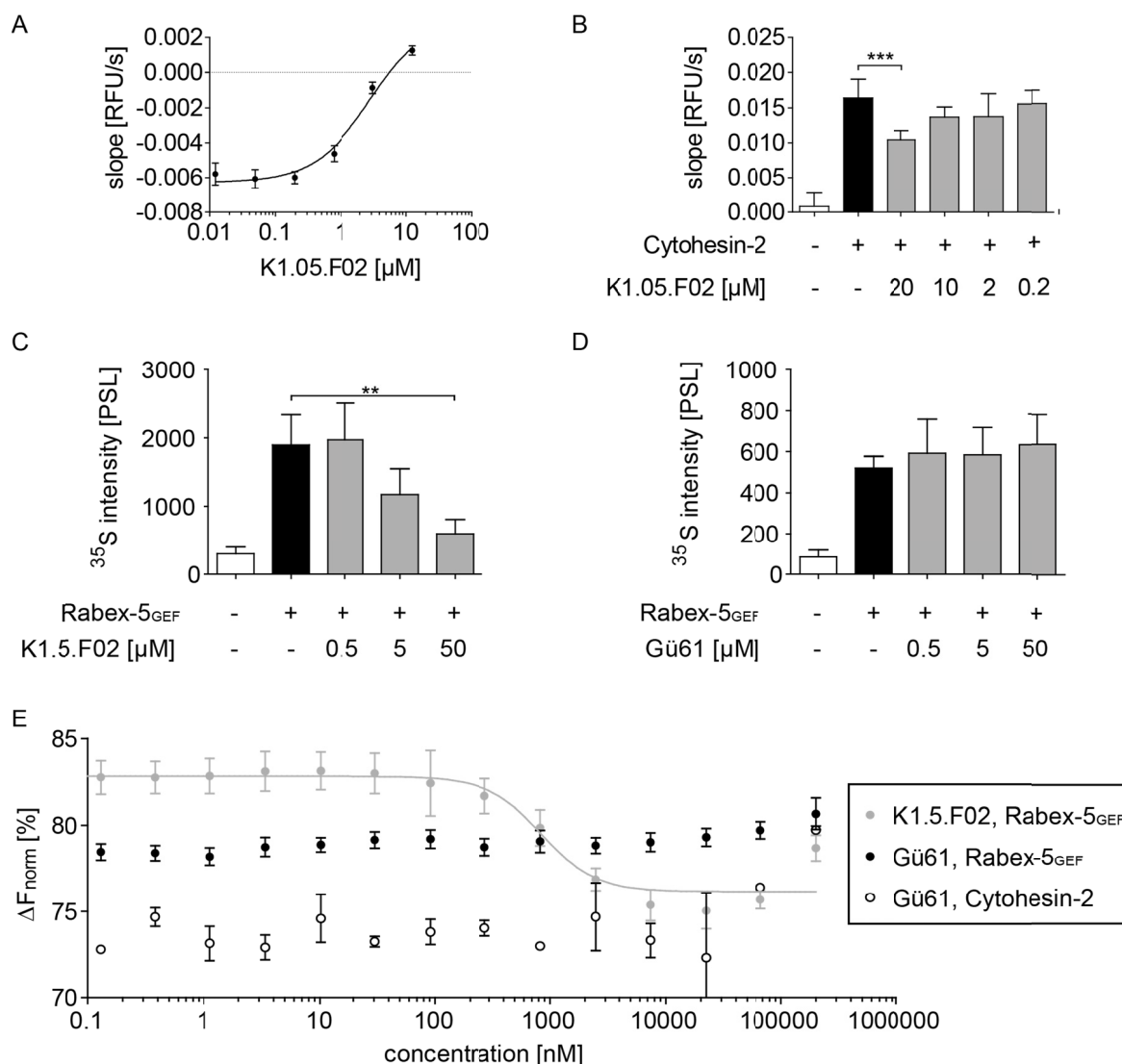
Figure 50   Comparison of K1.05.F02 (library compound) and Gü61 (stock).
A) The IC_{50} for the Rabex-5GEF nucleotide exchange inhibition with K1.05.F02 was observed to be 2.8 μM (95 % CI 2.2 - 3.7 μM). **B)** The Cytohesin-2 catalysed nucleotide exchange on Arf1 with several compound concentrations is depicted. A significant inhibition of the Cytohesin-2 catalysed nucleotide exchange was obtained at 20 μM K1.05.F02. **C, D)** Inhibition of the Rabex-5GEF catalysed nucleotide exchange assay monitored in the radioactive assay by K1.05.02 **(C)** and Gü61 **(D)** was determined in the radioactive nucleotide exchange assay. K1.05.02 revealed dose-dependent inhibition of the exchange reaction, thereby confirming the effect observed in the nucleotide exchange assay with fluorescent readout (A). Gü61 did not inhibit the nucleotide exchange. **E)** The binding of the compounds to Rabex-5GEF and Cytoehsin-2 was observed by MST. K1.05.02 bound Rabex-5GEF with a K_d of 0.9 μM (95 % CI 0.6 - 1.3 μM). The hill slope was determined to be -1.9 (95 % CI -3 - -0.6 μM). This did not support the assumption of a stoichiometry of 1:1 interaction between compound and protein. Gü61 did not bind Rabex-5GEF: this result was in line with the absence of inhibitory properties. Also, Gü61 did not bind Cytohesin-2. In conclusion, the effects of K1.05.F02 and Gü61 were not comparable. Data from at least two independent experiments represented as mean ± SD. The significance was calculated by the use of the one-way-ANOVA with the Tukey post-test (*GraphPad Prism* software), p-values: *$p < 0.05$, **$p < 0.01$, ***$p < 0.001$.

Thus, all investigations for the inhibitory properties and specificity of these compounds were promising and suggested to choose one of these structures as lead compound. The molecule JH5 was chosen because it was the most active representative of this group (Table 7).

Table 7   IC$_{50}$ values of 1,2,4-triazole-3-thiol compounds.

Compound	IC$_{50}$ [μM]	95 % CI [μM] [a]	Compound source [b]
C4.30.H05 (JH5)	0.3	0.2 - 0.4	Synthesis
C4.30.H07	0.5	0.3 - 0.7	Library compound
C4.30.E06 (JE6)	0.6	0.4 - 0.9	Synthesis
C4.30.F05 (JF5)	0.8	0.6 - 1.2	Synthesis
C4.30.H06	1.2	0.8 - 1.7	Library compound
C4.30.A08 (JA8)	1.5	0.9 - 2.3	Synthesis
C4.30.E07	1.6	1.0 - 2.4	Library compound
C4.30.G05 (CCV)	6.6	5.0 - 8.8	Synthesis

[a] 95 % CI = 95 % confidence interval. [b] The synthesis of the compounds was kindly performed by Dr. Jeffrey Hannam. The analytical data of the compounds can be found in Section 8.13.

3.6.3.2   K1.08.C11 (Gü321)

K1.08.C11 was active in the Rabex-5$_{GEF}$ kinetic assay and its IC$_{50}$ was with 2.6 μM (95 % CI 2.0 - 3.3 μM) about eight times weaker than JH5 (Figure 51A). It also had activity in the Cytohesin-2 nucleotide exchange (Figure 51B) but it did not inhibit the Vav-1 mediated nucleotide exchange on Rac1 (Section 8.5). In fact, the specificity of K1.08.C11 is not as excellent as observed for JH5. However, at this stage of the study, it was considered to be acceptable since Cytohesin-2 is closer related to Rabex-5 than Vav-1. Moreover, its structure differed from the 1,2,4-triazole-3-thiol compounds and provided the advantage of a potentially distinct mode of action compared to JH5.
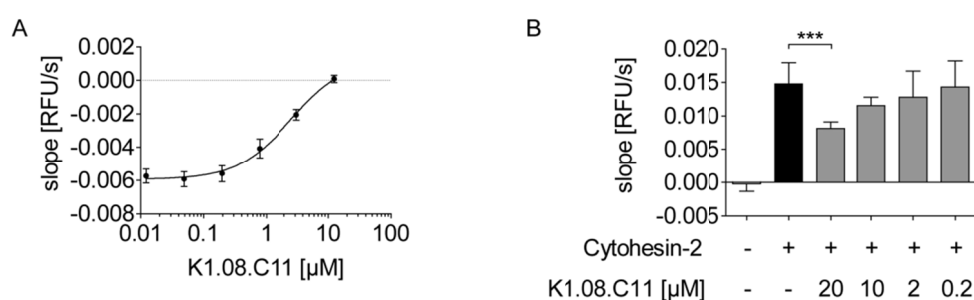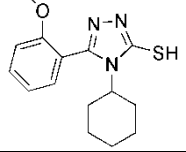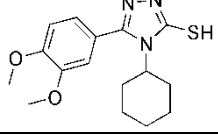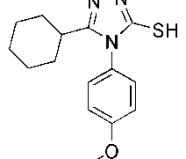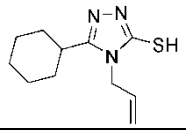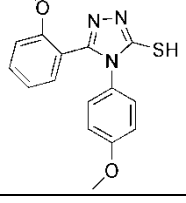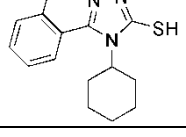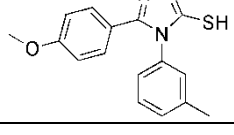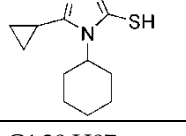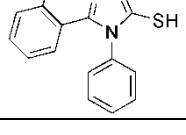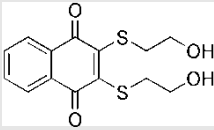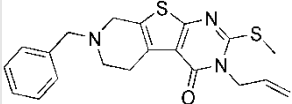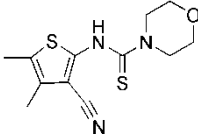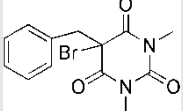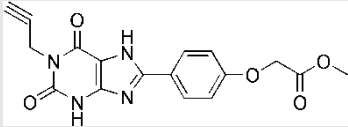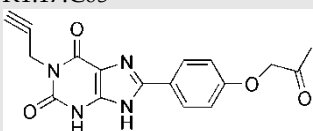
Figure 51   K1.08.C11 affects the Rabex-5$_{GEF}$ and Cytohesin-2 nucleotide exchange.
A) The Rabex-5$_{GEF}$ mediated nucleotide exchange for IC$_{50}$ determination with 20 nM Rabex-5$_{GEF}$ and several compound concentrations is presented. The IC$_{50}$ for the Rabex-5$_{GEF}$ nucleotide exchange was observed to be 2.6 μM (95 % CI 2.0 - 3.3 μM) with K1.08.C11. **B)** The Cytohesin-2 catalysed nucleotide exchange on Arf1 with several compound concentrations is depicted. A significant inhibition of the Cytohesin-2 catalysed nucleotide exchange was obtained at 20 μM K1.08.C11. Data from at least three independent experiments are shown was mean ± SD. The significance was calculated by the use of the one-way-ANOVA with the Tukey post-test (*GraphPad Prism* software), p-values: *p < 0.05, **p < 0.01, ***p < 0.001.

Table 8   Selection of the lead compounds after rescreening.

Compound	Nucleotide exchange		
	Rabex-5GEF-Rab5c [a]	Cytohesin-2-Arf1 [b]	Rac1-Vav-1 [c]
C4.30.A08	active	active (2 μM - library) inactive (synthesis)	inactive
C4.30.B06	active [d]	n.d.	n.d.
C4.30.E06	active	inactive (library & synthesis)	inactive
C4.30.E07	active	inactive (library)	n.d.
C4.30.F05	Active	inactive (library) active (20 μM - synthesis)	inactive
C4.30.G05	Active	inactive (library & synthesis)	inactive
C4.30.H05 (JH5)	active [e]	inactive (library & synthesis)	inactive
C4.30.H06	Active	inactive (library)	n.d.
C4.30.H07	Active	inactive (library)	n.d.

Compound	Nucleotide exchange		
	Rabex-5GEF-Rab5c [a]	Cytohesin-2-Arf1 [b]	Rac1-Vav-1 [c]
K1.03.F10	active	active (2 µM - library)	active
K1.05.F02	active	active (20 µM - library) inactive (stock)	n.d.
K1.08.C11 (Gü321)	active	active (20 µM- library & stock)	inactive
K1.13.A07 (Gü783)	active	active (2 µM - library)	active
K1.16.C09	active	active (20 µM - library)	n.d.
K1.17.C05	Inactive	n.d.	n.d.

This table summarizes the results obtained in the process of compound validation. Table elements that are highlighted in light grey represent results that led to the decision to exclude the compound from further studies. n.d. = not determined. **[a]** The activity of the compounds on the Rabex-5GEF-Rab5c assay was monitored in a kinetic form of the screening assay using 20 µM compound (for the corresponding data see Section 8.5). **[b]** The concentrations given represent the lowest concentration at which a significant effect was observed in the Cytohesin-2-Arf1 nucleotide exchange. The significance was calculated using the ANOVA with Tukey Post Test calculation (*GraphPad Prism* software). For the corresponding data see Section 8.5. **[c]** The corresponding data to the Vav-1-Rac1 nucleotide exchange can be found in Section 8.5. **[d]** C4.30.B06 caused an increase of the fluorescence signal in the kinetic assay. This is likely due to compound intrinsic properties since the same behaviour is observed in buffer only. Due to the fact that other hits with similar structure were more promising, C4.30.B06 was not analysed further. **[e]** C4.30.H05 (JH5) was found to be the most promising hit compound due to the lowest IC_{50} (Table 7).

4 DISCUSSION

Small molecule inhibitors are powerful tools to study functions of proteins *in vivo*. In this thesis, a small molecule inhibitor targeting the GEF Rabex-5 was intended to be identified. The molecules JH5 and Gü321 were discovered in an *in vitro* assay monitoring the nucleotide exchange on the GTPase Rab5c catalysed by Rabex-5GEF. Their characterisation regarding activity and specificity revealed that JH5 was the strongest candidate in the tested compound library. Therefore, its structure activity relationship, mode of action, and cellular applicability were analysed.

4.1 Rabex-5GEF and Rab5c protein production and evaluation

The first step in the project was the successful *in vitro* production and evaluation of the proteins of interest. The purification procedure for Rabex-5GEF and Rab5c was shortened in comparison to the reported protocol from *Delprato et al.* [136] to be more appropriated for the purification of a large batch of active protein. 50 mg of pure Rabex-5GEF and 65 mg Rab5c were obtained from two litre bacterial culture: enough to perform the screening assay as well as the post-screening verification. Another difference to the original protocol [136] was the type of affinity chromatography used for the Rab5c purification. *Delprato et al.* used GST-tagged Rab5c but the construct had later on been sub-cloned to avoid the necessary cleavage step of the GST tag (*Anna Delprato*, personal communication). That the presence of the His-tag has little influence on the protein activity became apparent as the activities of the proteins lay in the range reported in the literature.

The intrinsic Rab5a and Rab5c exchange activity was described to be slow: *Tall* et.al. observed about 20 % nucleotide exchange for Rab5a and roughly 30 - 40 % nucleotide exchange for Rab5c over 30 minutes.[81] The yeast homolog of Rab5, Vps21p, has been reported to have a stronger intrinsic activity (~50 % in 30 minutes).[257] The intrinsic activity of Rab5c was measured in the nucleotide exchange assay based on the tryptophan fluorescence of the GTPase (Section 3.1.3). Here, a decrease of fluorescence of 12 - 25 % over ten minutes was observed (calculated from the RFU data in Figure 15 and 16). Furthermore, a measurement spanning two hours revealed an intrinsic exchange activity of about 50 % within 30 minutes (Section 8.3). Thus, the intrinsic nucleotide exchange activity of the Rab5c protein was found to be consistent with the observed intrinsic nucleotide exchange rates from literature.

To compare enzyme activity of Rabex-5GEF, the ratio of k_{cat}/K_m was used. k_{cat} is the catalytic constant for the conversion of substrate to product and K_m the Michealis constant. Although it is under discussion whether this ratio is useful to compare the efficiency of different enzymes because the rate is partially depending on the reaction conditions,[258] it was a valid measure in this study as the same proteins were used under similar conditions. *Delprato et al.* [136] determined 2.3×10^4 $M^{-1}s^{-1}$ as k_{cat}/K_m compared to the here observed ratio of 5.7×10^4 $M^{-1}s^{-1}$ ($\pm 0.3 \times 10^4$ $M^{-1}s^{-1}$) as plotted in Supporting figure 16 (Section 8.3). The slight differences in the k_{cat}/K_m ratio can be explained by minor

differences in the assay preparation, e.g. the presence of Tween20. Moreover, the increased protein activity observed here might be due to the shortened protein purification protocol that treated the proteins more gently. In summary, a dose-dependent nucleotide exchange for GppNHp on Rab5c by Rabex-5GEF was shown in the expected range of reaction efficiency. Thus, the aim of producing a sufficient amount of active protein for the screening was achieved and was used to establish the *in vitro* screening assay.

4.2 Screening for small molecule inhibitors

4.2.1 Screening approach

Screening compound libraries is a fairly new discipline flourishing since the early 1990s.[176, 259] Although widely used, there is no standardized concept: the screening approaches differ in assay design and formats, readout techniques, library design, etc. However, one unifying idea is the "magic triangle of HTS": time, cost and quality are considered in most approaches.[259] The advantage of an assay monitoring the protein activity over assays aiming for the detection of interaction is that binding of a small molecule to the target protein not necessarily leads to inhibition. There are several examples of screenings to identify protein binding molecules, e.g. by using fragment based lead discovery (FBLD) or aptamer-displacement assay based on luminescent oxygen channelling (ADLOC), in which more compounds were found to bind the target than to inhibit the protein function.[192, 260, 261] Furthermore, many methods for detecting the interaction of small molecules with proteins are based on labelled proteins, e.g. fluorescence polarization, small molecule microarrays, or fluorescence correlation spectroscopy.[262] This is due to the fact that reactions with either labelled proteins or compounds are often more sensitive and better to observe.[263] The drawbacks of label introduction are extra synthetically efforts and the risk of changing the properties of the molecule by the coupling reaction.[181] Thus, an additional advantage of the Rabex-5GEF-Rab5c screening approach, besides being a functional assay, is that the proteins were not altered by addition of a fluorescent label. A potential disadvantage of the Rabex-5GEF-Rab5c nucleotide exchange assay was the presence of two proteins which allows the identification of inhibitors of Rab5c, Rabex-5GEF or the complex of both. This question had to be evaluated in the compound characterisation process. Nevertheless, since no Rab5 inhibitor is known to date both proteins were attractive targets for small molecules.

Ideally, screening assays are easy to perform (also described as "mix and read"), and do not require expensive components.[182, 228] Both criteria were met by the Rabex-5GEF-Rab5c screening assay. Only addition steps and no disadvantageous washing steps had to be performed. However, the centrifugation step had to be performed manually and should be automated or optimized for screening larger libraries with this assay in the future. Finally, the assay was cost efficient since only the proteins from one purification batch, buffer components, nucleotide and comparably cheap assay plates were required.

4.2.2   Assay establishment

In the process of assay optimization, the evaluation of detergent and DMSO compatibility were the most important steps. Non-ionic detergents have been used to avoid aggregation of small molecules, to decrease the identification of promiscuous inhibitors, and to keep membrane proteins in solution.[232, 233] The presence of 0.25 % Tween20 increased the exchange rate and decreased the variation between the samples providing an increased measurement window (Section 3.2.1). The interaction of protein with polystyrol, the material of the assay plates, was described to be most efficiently blocked by presence of detergent in concentrations above the critical micelle concentration.[264] 0.25 % Tween20 is above its critical micelle concentration of 0.06 mM (about 0.01 % (v/v)) according to manufacturer's specifications. Hence, it is likely that the detergent diminished the interaction of the proteins with the assay plate to form a homogeneous protein population and increase protein activity. The presumed formation of a homogeneous protein population in the presence of 0.25 % Tween20 explains also the low variation between distinct samples. Other assay systems have been reported that suffered a reduction of the enzymatic activity upon use of detergent concentrations above the critical micelle concentration.[265] Since this was not the case for the Rabex-5$_{GEF}$-Rab5c nucleotide exchange assay, 0.25 % Tween20 was chosen for the screening assay. The fact that the assay not only allowed the presence of a detergent but was improved by its presence highlights the beneficial choice of 0.25 % Tween20 as detergent. It was anticipated that less promiscuous inhibitors would be identified during the screening procedure compared to an assay without Tween20. As discussed in Section 4.7 this hypothesis was found to be valid.

The presence of DMSO, even at concentrations below 3 %, may affect protein folding, and enhance protein aggregation or denaturation.[266] Nevertheless, DMSO is used as the solvent of the library compounds. Hence the screening assay has to tolerate at least small amounts of DMSO. At all tested concentrations (2 % - 10 %), the addition of DMSO disturbed the nucleotide exchange activity. Since 77 % residual protein activity was sufficient for the screening assay the desired DMSO concentration of 2 % could be used.

The Z' value is a measure of robustness of a screening assay.[231]A Z'-value of 0.52 was obtained with the Rabex-5$_{GEF}$-Rab5c screening assay. It indicated that the assay is in general suitable for a screening. A higher value was not obtained by further optimisation of incubation times, temperature during assay preparation and incubation, or distinct detergent choice. The limitation of assay optimization potential can be explained by the small separation band between the positive and the negative control: in the Supporting figure 15 (Section 8.3) the maximal signal of nucleotide exchange was demonstrated in a Rabex-5$_{GEF}$-Rab5c assay. In the screening assay this maximal signal was already reached. Thus, all optimization steps could only aim for the minimization of errors. Potentially, using a higher concentration of Rab5 could have increased the range between Rab5c-GDP and Rab5c-GppNHp. Since the assay had already reached a good robustness, DMSO and detergent tolerance this hypothesis was not pursued further.

4.2.3 Screening results

In target based approaches using *in vitro* assays with purified proteins, the screening of libraries with 10,000 to 1,000,000 compounds yields usually about 10 to 100 primary candidate hits.[175] This corresponds to up to 1 % of the library. The same rates might apply for cellular assays, for example, in the Ras-inhibitor screening yielding the MPC compounds (Section 1.5.2) about 1 % primary hits were found.[200] The primary hit range is even higher in screenings using a focused library which is based on one parental structure.[181] For instance, more than 10 % primary hits were found in a phenotype based Ras inhibitor screening using a small focused library with a parental compound that was known for Ras-Raf inhibition.[203] In other screenings with the same compound library as used in this thesis, assays with Z′ values of about 0.7 had resulted in 0.5 - 0.9 % primary hits.[256, 260] Thus, it was expected that the described screening assay with a lower Z′ value might yield more hits. However, the yield of only 73 primary hits (0.6 % of the library) confirmed that the choice not to spend further time on assay optimization was advisedly. Moreover, the here obtained hit rate of 0.6 % fits the general expectations received by literature study.

4.2.4 Re-screening of hit compounds

The re-screening process was performed manually and all primary hits were tested in quadruplicates. Hits, showing high intrinsic fluorescence (RFU > 40) were either not confirmed in the re-screen or not considered to be worth pursuing after analysis in the kinetic assay. Therefore, it would have been possible to shorten the analysis of the screening data by introduction of a second cut off excluding all compounds with intrinsic fluorescence (Figure 52). Thereby, the sensitivity of the assay towards fluorescence variation is taken into account. If it had been applied directly after the screening it would have reduced the number of hits to 43 primary hits (0.3 %). This second hit definition would have reduced the amount of compounds that have to be analysed after the screening process and therefore would have been time efficient. In future screening approaches using fluorescence readout in the UV range this second threshold could be applied. Considering the results of this re-screening process it seems unlikely that promising structures would be missed by omitting all fluorescent hits. Certainly, this threshold for fluorescence is artificial but it contributes to the classification of the compounds and appears to be accurate enough to reduce the number of fluorescence artefacts.

The observation that compounds can interfere with the fluorescent readout of an assay was not unexpected. In screening assays using fluorescence readouts it was observed that several primary hits have to be excluded due to their fluorescence characteristics. For example, in a study using fluorescence polarization to monitor ligand interaction at GPCRs about 2 % initial hits were found, most of them fluorescence artefacts.[267] For fluorescence polarization assays it is known that the readout can be compromised by intrinsic fluorescence of small molecules when compound fluorescence and assay signal are at the same order of magnitude.[268] The same applied for the fluorescent readout of the

Rabex-5GEF-Rab5c assay. The auto-fluorescence of the compounds can disturb this assay because UV fluorescence was used as read-out wavelength. The UV fluorescence range is known to be the characteristic absorbance range for many small molecules.[269] Compounds with high auto-fluorescence were observed to change the starting fluorescence and to produce higher variations in the ΔRFU values. For several compounds, the auto-fluorescence resulted in unreliable ΔRFU values outside of the range of the controls (Figure 19/20). This illustrated the side effect of the assay using a fluorescent readout in the UV wavelength range. However, the use of a radioactive nucleotide exchange assay in the lead characterization process ensured that the compounds were not merely fluorescence artefacts (Section 3.3.1). Nevertheless, compared to the radioactive assay, the handling of the tryptophan fluorescence assay was more convenient. In the radioactive assay the number of samples that can be processed in parallel was limited to seven duplicates. Thus, this assay would have been an unfavourable alternative starting point for the establishment of a screening assay.

In general it might be indicated to avoid screening with assays of fluorescence readout in the UV-range. For a nucleotide exchange assay, for example one could have used fluorescent nucleotides. This was not pursued here because preliminary tests with boron-dipyrromethene(BODIPY)-GDP were found to be not promising. It was considered to be less time consuming to eliminate fluorescent artefacts after the screening than establishing a nucleotide exchange assay with a fluorescent nucleotide. Finally, the identified hits would have been tested in any case in an independent, non-fluorescent assay after the screening.

It is common that the majority of primary hits are false positives which are not confirmed in the re-screening.[270] False positives might be avoided by increasing the amount of data collected for each compound. However, replicates or full dose-dependency curves are very time and material consuming.[181] In conclusion, the choice between high quality data and the amount of compounds that can be tested will always have to be balanced in any HTS approach. In case of the Rabex-5GEF assay it was decided to test the compounds in single values since this option was in due proportion to time and effort.

The rate of false positive hits was about 66 %. The initial hypothesis that the false positives are caused by fluorescence disturbances, was not confirmed. The hits were examined according to their intrinsic fluorescence level and the amount of false positives revealed comparable rates (Table 9). This finding indicates that the false positive hits are likely to be caused by assay-related characteristics while the fluorescence of the compounds played a minor role. In addition, overestimation of the activity of compounds can occur if precipitated material is transferred to the assay and solubilized there.[271] Also, false positives might arise from aggregating compounds,[232] although the presence of Tween20 in the assay should prevent compound aggregation. Inaccurate robot function, which had become apparent as 141 samples had to be excluded due to incorrect sample volume, might be suspected to contribute to the false positives. However, several successful test-runs had been performed to ensure that even the small volume of 1 μL was reliably dispensed. In addition, manual inspection of all assay plates has been performed and contradicts massive robot malfunction.
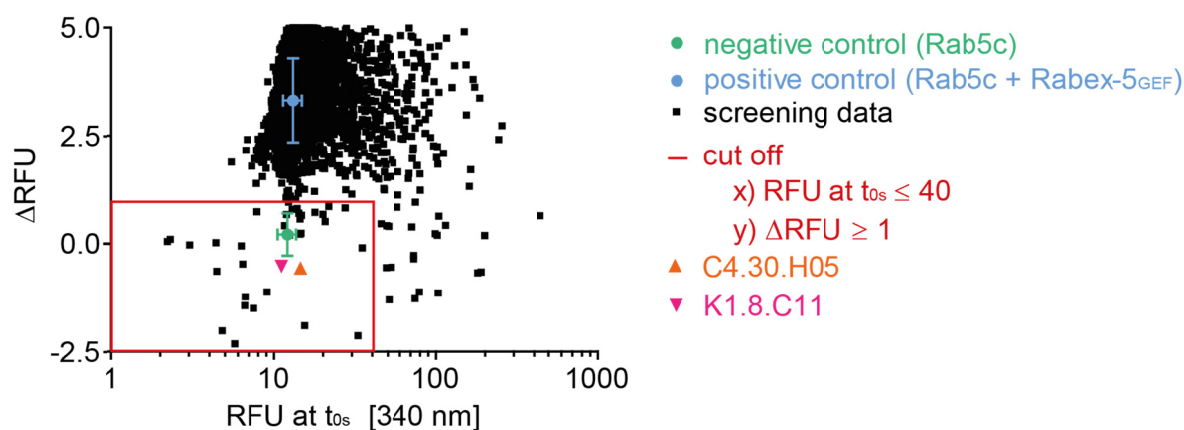
Figure 52   Retrospect illustration of the screening result.
The screening results are depicted as described in Figure 19. Compared to Figure 19, only parts of the screening data are presented to focus on the ΔRFU range of successful compounds and controls. This depiction shows that the two most promising compounds obtained from this screening approach were detected very close to the negative control. They do not have strong auto-fluorescence that disturbs the readout. This argues to apply very strict cut-offs since the promising compounds yielded screening values close to the relevant control.

Table 9   Number of false positive primary hits identified in the re-screening.

	Amount of primary hits	Amount of secondary hits	False positive primary hits
Total	73	25	66%
Low fluorescent	22	9	59%
Medium fluorescent	21	6	71%
High fluorescent	30	10	67%

The compounds were grouped according to the intrinsic compound fluorescence. Low-fluorescent: RFU < 20, medium fluorescent: 20 > RFU < 40, high fluorescent: RFU > 40.

4.3   Activity profile of JH5 and Gü321

The compounds JH5 and Gü321 were chosen as lead compounds due to their activity in both Rabex-5$_{GEF}$ mediated nucleotide exchange assays: the one with fluorescent and the one with radioactive readout. This argued against the possibility that these compounds are solely fluorescence artefacts. It was observed that both molecules were needed in slightly higher concentrations in the radioactive assay than in the tryptophan assay. This might be due to a combinatorial effect of inhibition and fluorescence interference observed in the tryptophan assay. More likely, it was caused by the simple fact that the assay conditions differed and IC$_{50}$ values from distinct assays are in general not directly comparable.[272] The radioactive assay with an endpoint detection format and the kinetic tryptophan fluorescence assay used for the IC$_{50}$ determination were distinct. Moreover, the radioactive assay allowed the processing of very few samples in parallel and complete dose-response curves were not recorded. The notion that IC$_{50}$ values are assay-dependent was underlined by the observation that the Rabex-5$_{GEF}$ concentration in the tryptophan fluorescence based assay has a direct impact on the compound inhibition. When it was performed with higher Rabex-5$_{GEF}$ concentrations, increased amounts of JH5 were needed

to observe inhibition (Section 8.6). This might indicate that the compounds are targeting Rabex-5GEF rather than Rab5c as described before for other cases like the small molecule inhibiting SOS-mediated nucleotide exchange activity.[192] The hypothesis that JH5 interacts with Rabex-5GEF was supported by the MST data. No binding to Rab5c was detected.

All MST and functional assay data of this study complemented each other convincingly as it will be discussed in the following subsections. Hence, although being a fairly new method, MST was found to be well suited for the investigation of protein-small molecule interaction.

4.3.1 Gü321 was excluded from further investigations

Gü321 was about tenfold less active than JH5. Nevertheless, even such a higher IC50 was still promising since the value was in the low micromolar range. Despite of the activity in the Rabex-5GEF nucleotide exchange assay, Gü321 was excluded from further investigation at this point of the study. It was found to inhibit the Cytohesin-2 mediated Arf1 activation. This effect was confirmed in MST experiments and the impact observed in MST was even more drastic than in the functional assay. The fact that Gü321 acted non-specific was not entirely surprising because specificity limitations are a general observation when applying small molecules.[181] The lower activity on Rabex-5GEF combined with a less favourable specificity might have been tolerated. However, Gü321 was as sensitive towards supplementation with the reducing agent DTT as JH5. The intracellular environment is known to be reducing and the fact that JH5 and Gü321 are inactive in the presence of DTT might pose a challenge to the intracellular application of these small molecules.[27] Finally, no further investigation of Gü321 was pursued because it did not have any advantage over JH5 regarding its activity and specificity while sharing this challenging feature.

4.3.2 JH5 specifically inhibits Rabex-5GEF

The interaction of JH5 with Rabex-5GEF was observed in MST using fluorescein-labelled and Alexa-647-labelled protein. Alexa-647 labelled Rabex-5GEF was also bound by JH5 and at the same time JH5 did not interact with other fluorescently labelled proteins. These findings argue for an interaction of JH5 with Rabex-5GEF and not with the fluorescent label. Even more important, the MST data corroborated the specificity of JH5 over several other proteins. The result is in line with the data of the functional assays using other GEFs and GTPases (Section 3.3.2). Ultimately, the DTT sensitivity of JH5 was observed in MST and confirmed these results from the Rabex-5GEF nucleotide exchange assay.

It seems valid to conclude that JH5 exerts its inhibitory effect on the Rabex-5GEF mediated Rab5c activation by binding to Rabex-5GEF. The affinity of JH5 for Rabex-5GEF is among the strongest compared to the already reported GEF inhibitors which have activities in the mid to upper micromolar range (Table 1). [192, 214, 215, 218]

Although the mechanisms of GEF domains function are relatively similar,[23] it was possible to identify the small molecule JH5 that can selectively inhibit Rabex-5GEF nucleotide exchange but does not interfere with Vav-1, DrrA and Cytohesin-2 nucleotide exchange. Due to the similarity in the catalytic mechanism, Cytohesin-2 and DrrA represent quite rigorous controls. Nevertheless, how well JH5 might discriminate between Rabex-5 and other Vps9 domain containing RabGEFs remains to be investigated. Certainly, a high specificity of JH5 for Rabex-5GEF over other proteins can be concluded from the fact that JH5 can discriminate GEFs with similar enzymatic mechanisms as Rabex-5. Of course it is possible that JH5 targets other proteins which have not been tested here and which do not necessarily have to be GEFs. To investigate this question compound-centric chemical proteomics could be performed.[273] In this approach the compound is conjugated to a matrix and incubated with a biological sample, e.g. cell lysate.[273-275] After the elution of the captured proteins the sample is submitted to mass spectrometry analysis.[273] Admittedly, this approach requires a biotinylated-JH5 or another JH5 derivative that can be coupled to a matrix without loss of activity. Alternatively, Drug Affinity Responsive Target Stability (DARTS) could be applied that utilizes the stabilising effect of small molecules interaction on its target protein to isolate binders from complex protein mixtures.[276] A biotinylated JH5 derivative was available but not used in this study since it did not show the same properties as the unmodified JH5 (Section 8.7). Since the cellular applicability of JH5 was not proven at this time of the study, the synthesis of another biotinylated JH5 molecule as well as further specificity investigations for off-targets were omitted. If in the future effects in cellular assays would indicate crucial off-target effects, these investigations should be pursued.

4.4 Mode of action of JH5

By comparing the activity of JH5 and several derivatives, hypotheses concerning the structure activity relationship (SAR) were established. In general it is expected that a molecule possesses substituents that show a flat (continuous) SAR and others that have a steep (discontinuous) SAR.[277] Regarding modifications at the thiol group at position R3 the SAR was observed to be steep. Exchange of the sulphur for oxygen and modifications like the thiomethyl that prevent the regain of a thiol group blunted the activity of the molecules. The molecules required a thiol-group, a disulphide or a hydrolysable thio-ester at position 3 of the 1,2,4-triazole core. The importance of this substituent was underlined by the finding that reducing conditions abrogated the activity of JH5.

However, regarding the triazole substituents at position R1 and R2 the SAR was rather continuous. Although the substitution of the aromatic residues by cyclohexyl- or NH2-groups was found to reduce the activity of the molecules, the effects were not as drastic as the modifications of the thiol that blunted the activity.

No gain in potency was observed with the molecules analysed in this study compared to the screening hit JH5. Compounds with a *para*-phenol group at position R1 were found to be equipotent to JH5. The synthesis of further *para*-substituted-phenol derivatives should

increase the understanding of the SAR. Importantly, further *para*-substituted derivatives could yield more potent compounds because this substitution at position R1 appeared to influence the activity of the compounds positively. To establish the relationship between the size of the *para*-phenyl substituent, e.g. to compare methyl-groups in *para*-position with *tert*-butyl substituents, a CCJ-derivative carrying a phenyl-group at position R2 would be enlightening.

The hypothesis that a dimer-shaped molecule, which fits into a corresponding binding pocket, is the active component was tested by the synthesis of several dimeric molecules. Four kinds of bridges between the triazole-cores were used: $-CH_2-CH_2-$, $-CH_2-S-$ $-CH_2-S-CH_2-$, and $-S-S-$. All molecules containing a $-CH_2$-group in their bridge were found to be less soluble than the $-S-S$-molecules. The $-S-S$-molecules JH5-B-dimer, JH5-C-dimer and JH5-A-dimer were found to be as active as their corresponding monomers. The $-CH_2-S-$, the $-CH_2-S-CH_2-$, and the $-CH_2-CH_2-$ bridged molecules should be stable under reducing conditions in contrast to the $–S-S$-bridged dimers. The $-CH_2-CH_2$-molecule was not soluble enough to be analysed in presence of the assay buffer. The $-CH_2-S-$ and the $-CH_2-S-CH_2-$ molecules were soluble enough to be tested. However, they did not interact with Rabex-5GEF. For the $-CH_2-S-CH_2$-bridged compound JH5-N-dimer it has to be considered that the length of the bridge was increased. This might affect the activity negatively since the two triazole centres and their substituents of both sides of the dimer will be a distinct distance. The impact of that modification cannot be read from the obtained data. However, this consideration was not relevant in case of the $-CH_2-S$-bridged CS-dimer 1 and CS-dimer 2. Here, it cannot completely be ruled out that the modification of the triazole ring and the lack of a substituent at position R2 were responsible for the inactivity of both CH2-S-bridged dimers. To compare these molecules properly, diazole-monomers should be analysed.

Of all CH2-S-bridged dimers, the CS-dimer 3 showed maximal similarity with JH5. Nevertheless, it was found to be inactive. Since the solubility of this molecule decreased over time in DMSO as well as in aqueous solutions (Section 8.8) all experiments with this compound were performed directly after solubilizing. It is possible that compound concentrations in the higher micromolar range might be accompanied by solubility problems. Nevertheless, if this stable, dimeric form of JH5 should have activity emerging from its shape its potency should be increased since dimerization in solution is not required anymore. Hence, rather lower IC_{50} and K_d values were expected for this molecule at a concentration range that should not be accompanied by problems in solubility. Finally, all soluble, stable-bridged dimer-derivatives are inactive, which strongly argues for a monomeric mode of action or for the requirement of the disulphide rather than demand for an overall dimeric shape of the molecule.

The observation that JH5 was inactive under reducing conditions and that thio-ester and disulphide groups could replace the thiol group at position 3 of the 1,2,4-triazole centre showed parallels to the report on the compound JTT-705.[241] For this inhibitor, a cysteine residue of the target protein was suggested to be important for the activity of the compounds. Hence, it was hypothesized that JH5 might interact with a cysteine in

Rabex-5GEF, e.g. by the formation of a covalent bond. This hypothesis was investigated by the use of Rabex-5GEF cysteine to serine mutants and by mass spectrometry approaches.

The cysteine mutated Rabex-5GEF proteins were found to have distinct sensitivity towards JH5. The Rabex-5GEFCS protein without any cysteine residue was not inhibited by JH5 arguing for a contribution of one or more cysteine residues to the interaction of JH5 and Rabex-5GEF. Rabex-5GEF CSN (three N-terminal cysteines exchanged for serine) was targeted by JH5 with a similar potency as the wild type Rabex-5. Rabex-5GEF CSC (five C-terminal cysteines exchanged for serine) was only slightly inhibited by JH5. In summary, diminished activity of JH5 was observed for proteins lacking the C-terminal cysteines.

No JH5-sized mass shift was observed in MALDI-TOF measurements analysing Rabex-5GEF and Rab5c as well as in ESI-MS measurements of peptides originating from Rabex-5GEF. The observation that no JH5 addition to Rab5c was found by MALDI-TOF measurements was expected due to the results of the MST measurements. However, the fact that no addition was observed with Rabex-5GEF, argued against a covalent interaction of JH5 with this protein. This observation contradicts the results from the nucleotide exchange assays using the Rabex-5GEF cysteine mutants.

The sequence coverage obtained in the peptide mass spectrometry approach (Figure 39) did include four of the eight cysteines. However, all four C-terminal cysteines were not covered in the identified peptides. Hence, no conclusion on the contribution of these cysteines could be drawn from this experiment. Regarding the identified cysteines, a contribution to the interaction with JH5 seemed rather unlikely.

In the light of the results with the cysteine mutant proteins it is tempting to speculate that either the Cys238 and/or Cys239 significantly contribute to the JH5 interaction with Rabex-5GEF. Both cysteines were found to be less alkylated by acrylamide in presence of JH5 in the mass spectrometry alkylation approach which indicated that these positions might be occupied by JH5. The observation that Rabex-5GEFCSC was not as resistant to JH5 as the Rabex-5GEFCS protein indicates a potential minor involvement of one of the N-terminal cysteines. A possible candidate might be Cys132 since a distinct pattern in the alkylation approach was observed for this position. Nevertheless, the main contribution to the interaction with JH5 is likely provided by the C-terminal cysteine residues. However, since the experiment was performed without replicates, careful interpretation is required in whether this result supports the hypothesis of these cysteines participating in the binding site of JH5.

The contradicting result from the MALDI-TOF mass spectrometry does not absolutely exclude that a covalent reaction product between JH5 and Rabex-5GEF is involved in the inhibition mechanism. The modification may represent a reactive intermediate or it may be acid-labile. Admittedly, it is possible that the experimental conditions in the MALDI-TOF experiment might have disturbed the interaction. In general, the sample preparation and MS measurements include harsh conditions, e.g. the treatment with the strong acid TFA, formic acid as well as high temperatures.

By increase of the sequence coverage, e.g. by use of additional digestion enzymes, the visualization of the important cysteine residue(s) can be approached. In addition, single

cysteine to serine exchanges can provide mutated Rabex-5GEF variants that may elucidate the mode of action of JH5.

4.5   Estimation of cellular applicability

With the long term goal of using the identified Rabex-5GEF inhibitor as tool to investigate Rabex-5 biology it was of interest whether the compound was applicable in an intracellular environment. JH5 and its derivative JH5-E were inactive under reducing conditions. Since the cytosol is known to be a reducing environment [27] the intracellular application of the compounds was challenged. In order to estimate the intracellular potential of the compounds several assay systems were used. This was due to the fact that no direct Rabex-5 activity assay was available. To monitor the Rabex-5 activity, the Rab5 activity was always used as readout.

The approach using the Rab5 binding site of its effector Rabaptin-5 for the quantification of the level of intracellular active Rab5 resembled the *in vitro* nucleotide exchange assay the most. However, in this system no difference between the positive control (Rab5-GTP) and the negative control (Rab5-GDP) was observed. This was likely due to hydrolysis of the GTP during the assay preparation. The use of non-hydrolysable nucleotide showed that the assay system in general worked. The observation of Rab5 hydrolysis in the pull-down assay was not unexpected since Rab5 is known to have a fast hydrolysis rate.[160] In literature the R5BD assay has often been described using Rab5 mutants that are locked in one nucleotide state.[246-248] Consequently, this setup counteracts the fast hydrolysis rate of Rab5 and provides stable signals. The use of these mutants was not useful for the investigation of the compounds effect. Due to the fact that the potential effects of the compounds on the activity of Rabex-5 would not affect Rab5 mutants, the use of wildtype Rab5 was necessary. The protocol was shortened regarding the time for lysate preparation and incubation according to the protocols of an analogue Rac assay (Cytoskeleton, Inc.) which had been successfully applied by the author before. This modification among other optimization steps was supposed to increase the difference in the Rab5-GDP and the Rab5-GTP signal. However, this modification of the protocol was not successful. Since the difference between the negative and the positive control could not be observed the compounds were not tested in this assay system. Obviously, several other Rab5 effector proteins are known that can bind active Rab5 (Section 1.1.2). However, the main contribution to the low difference between the GDP and the GTP control was probably the fast hydrolysis of GTP to GDP by Rab5 and in this case the use of a different effector protein would not be indicated.

Monitoring the degradation of the EGFR was considered to be a suitable experiment to detect Rabex-5 activity. Rabex-5 has been implicated in this process as described in Section 1.4.3.[141, 163] However, no effect of JH5 on the receptor degradation was observed. Since the HeLa cells contained Rabex-5, the absence of an effect was unlikely to be due to missing target protein.[95] Repetition of the experiments with modified conditions, e.g.

shorter incubation times with higher concentrated compound or a change of the cell line, did not result in more pronounced effects of the compounds.

In the internalization assay, the reduction of endocytosis of the EGFR by JH5 was promising at the first sight. However, the *in vitro* inactive control JH5-O had the same effect. This argued for a Rabex-5 independent effect caused by the presence of the compounds.

Rabex-5 was reported to inhibit the outgrowth of neurites as described in Section 3.5.4. The cells used in the cited study [247] were PC12 cells which have been derived from a pheochromocytoma of the rat adrenal medulla. Compared to the cited literature, the used U87 cells which were used here have been derived from a glioblastoma. Should the Rabex-5 effect be cell specific this would explain the lack of an inhibition by JH5. Hence, it might be more promising to modify the conditions and repeat the experiment in PC12 cells. However, *Mori* et. al. reported that the number of dendrites was not affected in a Rabex-5 knockout in murine hippocampal neuronal cultures while the length and the outgrowth of the dendrites was decreased.[138] These observations indicate that Rabex-5 influences the neurite outgrowth in several cell-types although not necessarily with the same outcome. More likely, the involvement of several other factors in the regulation of neurite outgrowth, e.g. the RhoGEF Trio, could weaken the effect by a potential Rabex-5 inhibition.[278] The small molecule ITX3 could be used in combination with a Rabex-5 inhibitor to unravel the role of the distinct GEFs.[218]

The PI3P level on early endosomes and phagosomes is dependent on Rab5 activity. The addition of JH5 decreased the level of PI3P as expected for a Rabex-5 inhibitor. However, the same effect as for JH5 was observed with JH5-M. This strongly argues for an effect that is independent of Rabex-5 since JH5-M is one of the inactive compounds *in vitro*. In general, compounds applied at higher concentrations have been described to be prone to the induction of nonspecific effects.[181] In this assay 80 μM of each compound was used which can explain nonspecific effects. The read-out of this approach is indirect on several levels: the activity of PI3K destines the level of PI3P while the PI3K activity depends on active Rab5 levels which are among other things dependent on Rabex-5 activity. Hence, the level of PI3P might be influenced by several other factors. Therefore, this approach might not be ideal for the investigation of Rabex-5 inhibition. The level of PI3P on early endosomes and phagosomes was kindly analysed in two further biochemical assay systems by *Andreas Jeschke* (group of *Professor Dr. A. Haas*). Nevertheless, both assay systems were found to be unsuitable to estimate the effect of the compounds (Section 8.12).

In summary, these results do not support the assumption that JH5 inhibits Rabex-5 in living cells. Since Rab5 has several different functions for which the relevant GEF is not exactly known each assay by itself cannot proof the absence of an effect of JH5. For a proof of principle of the compounds activity in cells these indirect readouts are problematic. In absence of an effect the question remains whether the assay system was not suitable. Nevertheless, none of the results supported the intracellular applicability of JH5. This is likely due to the fact that JH5 is not working in a reducing environment. Nevertheless, another obstacle for the compound might be the uptake into the cells. To determine cell

permeability, the compound could be monitored by fluorescent detection in confocal microscopy.[279-281] However, unless the fluorescence of the compound can be used, the modification of the molecule to enable visualization might change the compounds characteristics and data interpretation has to be performed carefully. Introduction of radioactive isotopes into the compound of interest should change of their characteristics to a lesser extent. However, these approaches suffer from increased synthesis and security efforts. Alternatively, the parallel artificial membrane permeability assay (PAMPA), in which two aqueous compartments are separated by phospholipid-coated filters to monitor the passive transport of small molecules, can be applied.[282, 283] Finally, assays monitoring the transport over cellular monolayers by LC-MS measurements can be used which have the advantage of considering additionally paracellular transport for intestinal absorption, transporter proteins, and metabolic enzymes.[284]

Finally, the cells could be permeabilized, e.g. by a-toxin or digitonin, to enable the compound to enter the cells.[285] Should an effect be observed under these conditions the compounds applicability could be optimized by targeted delivery or further efforts for a second generation of Rabex-5 inhibitors might focus on the cell permeability of the inhibitor.[286, 287] The thiol group of JH5 might even pose an advantage to be used in disulphide bond-based bio-conjugation as strategy for delivery.[288] To increase the cell permeability by medicinal chemistry, the introduction of groups that increase the hydrophobicity can be helpful while extremely acidic groups have a contrary effect as observed for caspase inhibitors.[289]

4.6   Hit verification and lead definition

The verification of the hit compounds and the selection of lead compounds was based on the activity of the compounds in the Rabex-5GEF-Rab5c nucleotide exchange as well as their specificity. Since active small molecules are likely to have unspecific effects [181, 273] the effects of the compounds on nucleotide exchange reactions with distinct GEFs and GTPases was included in the compound selection process. Several of the secondary hit molecules were found to be active in the Cytohesin-2-Arf1 (and the Vav-1-Rac1) nucleotide exchange, for instance the compounds K1.03.F10, K1.13.F07, and K1.16.C09. This underlines the importance of rigid selection criteria in order to avoid the investigation of compounds that would have been excluded later due to their unspecific effects.

Most of the hit compounds were sole representatives of one structural motif. However, it has been reported that compounds with structural similarity are likely to be active in the same biological setup.[290] It even has been suggested to increase the amount of similar compounds in a diversity oriented library to increase the chances of hit identification since false positives are always an issue.[291] Moreover, to consider similarities of compounds seems to be beneficial in the classification of hits.[270] Hence, the group of 1,2,4-triazole-3-thiol compounds that shared one core structure and had comparable activity in the Rabex-5GEF-Rab5c nucleotide exchange assay were promising candidates for genuine

inhibitors. Of them, only C4.30.F05 and C4.30.A08 were found active in the Cytohesin-2 nucleotide exchange with the first significant effect at 20 μM or 2 μM, respectively. For C4.30.A08 the unspecific effect was not confirmed when using re-synthesised compound. The effects are very small when considering the inhibition was at maximum 25 %. In conclusion, the effect on the Cytohesin-2 nucleotide exchange was comparably weak.

An often described problem is that compounds in freshly prepared stock solutions are more active than after storage in DMSO.[271] For K1.05.F02 the contrary was observed. The fresh product of K1.05.F02 (Gü61)[13] was inactive. It is likely that the active compound in the library stock is a degradation product. Degradation of compounds stored in DMSO is not unprecedented.[292] Degradation of compounds is believed to be facilitated by oxygen, humidity and light,[293, 294] and should be counteracted by atmosphere controlled compound storage.[295] This idea of active degradation products in the K1.05.F02 solution was supported by the observation of several minor peaks in the HPLC chromatogram. It would be possible to identify a degradation product that serves as active compound in HTS from the library stock by analytical methods and re-synthesis.[296] However, the identification of this active compound would be very time consuming and was designated to be beyond the scope of this work. Moreover, the activity to specificity ratio of the compound was not as promising as for the 1,2,4-triazole-3-thiols and thus K1.05.F02/Gü61 was excluded from further study.

K1.16.C09 and K1.17.C05 are xanthine-derivatives and might function by competition with GTP. However, these compounds were excluded from analysis due to minor and unspecific activity, and no further investigation regarding a potential inhibitory mechanism was pursued.

After the selection process, two hit structures were left for detailed analysis: JH5 and Gü321. Gü321 was later on excluded due to specificity limitations while JH5 was characterized in detail. In summary, JH5 was the most potent and specific inhibitor identified in this screening.

4.7   JH5 as inhibitor of the Rabex-5 mediated Rab5 activation

There are numerous theories about the properties that render a small molecule either a promising or an unsuitable candidate. For example, several signs for the unintentional aggregation-based inhibitory mechanism of an inhibitor have been defined by *Brian Shoichet and co-workers*.[297] Among them is the disturbance of activity or interaction by the addition of non-ionic detergent or BSA to *in vitro* measurements, the observation of an unusual steep dose-response curve leading to a Hill coefficient larger than one, or the formation of particles of 50 to 1000 nm size.[297-299] Aggregation of drugs is not in all cases problematic: for example, there are several drugs available that are thought to be bioavailable due to intensified uptake in the gastrointestinal environment in the

---

[13] This compound was kindly provided by Professor Dr. M. Gütschow.

aggregated state.[300] Although aggregating compounds might sometimes facilitate their bioavailability, the absence of typical signs for an aggregation based inhibitory mechanism is in general considered an advantage. For instance, it was reported that the aggregation inhibition mechanism involves unfolding of the protein.[301] Also, these compounds are not very well suited for lead-optimization due to their flat structure activity relationships.[297] Although the investigation of aggregation was not the main focus of this work since detergent was present in the screening assay and the identification of aggregation inhibitors was not to be expected, some of these issues have been addressed. The detergent Tween20 was present in all performed assays including the screening assay leading to the identification of JH5 (Section 3.2.1.2). Therefore, JH5 can be considered active in the presence of detergent (Section 3.3.1). Also, the addition of BSA in MST assays which was supposed to block unspecific binding [299] did not disturb the K_d of the Rabex-5$_{GEF}$-JH5 interaction (Section 3.3.4 and 8.7). Finally, the Hill slope determined in the K_d calculation as well as the IC$_{50}$ determination indicated an expected slope of about one (Section 3.3). All these observations argue against the possibility that JH5 acts via an aggregation-based mechanism. Hence, the strategy of avoiding the identification of promiscuous inhibitors by the presence of detergent in the screening assay as described in Section 3.2.1 had been successful.

Furthermore, small molecules are often found to have non-specific effects,[181] especially on closely related proteins due to structural or functional overlap as for example observed for kinase inhibitors.[302, 303] In this work, all specificity investigations using distinct GEF proteins in nucleotide exchange assays and a variety of proteins in MST emphasise the specific action of JH5 (Section 3.3.2 and 3.3.4). As indicated in Section 4.3.2, a proteome wide specificity analysis as well as the investigation of other Vps9 domain proteins is pending. Nevertheless, the absence of inhibitory effects on several other GEF-GTPase pairs which have a high degree of homology to Rabex-5-Rab5c underlines the promising specificity characteristics of JH5.

5 OUTLOOK

5.1 JH5 future perspectives

In spite of its excellent specificity, the sensitivity of JH5 towards reducing conditions (Section 3.3.3) and the current absence of a proof of activity in cells (Section 3.5) challenges the use of JH5 as tool to elucidate Rabex-5 biology. In fact, either the presented cellular assays were not as appropriate for monitoring Rabex-5 activity as anticipated from literature or JH5 requires further improvement before it can be successfully applied in a cellular environment.

There are several additional experiments to monitor Rab5-Rabex-5 activity in cells. The overexpression of active Rab5 or Rabex-5 increases the size of the early endosomes and the effect is dependent on the GEF activity of Rabex-5.[70, 143] Recently, the activity the localisation of the small GTPase Rab17 in dendrites of mouse hippocampal neurons was reported to be dependent on Rabex-5.[138] Should JH5 inhibit the nucleotide exchange with Rabex-5GEF and Rab17 *in vitro*, this cellular application might be suited to test JH5. Since Rabex-5 forms oligomers with Rabaptin-5, EEA1 and SNAREs to stabilize the Rab5 microdomain, these interactions could be analysed, e.g. by confocal laser scanning microscopy.[99] Also by the use of microscopic methods, Mon-1 recruitment to the early endosomes, the transition of Rab5 to Rab7 endosomes as well as the disassembly of the nuclear envelope could be monitored.[15, 133, 154] Moreover, the production of recycling vesicles is negatively regulated by the Rabaptin-5/Rabex-5 complex and its inhibition should stimulate the formation of vesicles which can be monitored.[304] Finally, the GEF activity of Rabex-5 was described to be relevant for the localization of Rab5 on early endosomes.[63]

Medicinal chemistry can be used to improve the oral activity of the compound and, in this case, the intracellular applicability.[305] The structure activity relationship (SAR) study revealed that the thiol group of JH5 was found to be essential for its function (Section 3.4.1). It is likely that the thiol group is responsible for the sensitivity towards DTT. Since all available compounds that lack a sulphur-containing group had no activity this hypothesis could not be tested. However, the replacement of the thiol-group by a thio-ester or a disulphide is possible without noteworthy loss of activity. Nevertheless, these compounds share the sensitivity towards DTT. Thus the performed SAR did not result in improved compounds at this point. The use of a thio-ester (JTT-705) to improve the bioactivity compared to a corresponding thiol- or disulphide-compound was described in literature.[241] This compound was reported to be active *in vivo*.[242] However, the target protein Cholesteryl ester transfer protein is located in serum and not in an intracellular environment.[241] Hence, this example of modification to improve the bioavailability of disulphide/thiol compounds could not be applied for the Rabex-5GEF inhibitor. Instead, further SAR efforts should be inspired by irreversible inhibitors targeting cytosolic proteins.[306-309]

The other functional groups of JH5 were also investigated. It was discovered that aromatic substituents at the position 4 and 5 of the 1,2,4-triazole core have beneficial effects on the

compounds activity. It was hypothesized that a *para*-substitution at the phenyl-substituent at position R1 can boost the activity of the compounds compared to phenyl compounds (Section 4.4). However, the number of available compounds was not sufficient to verify the exact properties that these substituents require. Nevertheless, the obtained results can be used to guide future SAR efforts. For instance, several larger *para*-substituents are indicated to be investigated.

Full clarification of the mode of action of JH5 is anticipated from the use of further cysteine to serine mutants of Rabex-5GEF and additional mass spectrometry measurements (Section 4.4). It should be possible to narrow down the contributing cysteine residues. The efforts in the identification of the binding site would very likely be positively influenced by the availability of a co-crystal structure of Rabex-5GEF and JH5. Moreover, structural information on the interaction of JH5 and Rabex-5GEF would also shed light on the inhibitory mechanism. X-ray crystallization efforts have already been initiated.[14] Also, structural elucidation can be performed by NMR spectroscopy. An alternative, although less precise, possibility of binding site identification is the activity-based protein profiling concept.[310, 311] Here, a probe consisting of the inhibitor, a reactive group, and a tag for detection is used to identify the target proteins of the inhibitor.[310] In general this concept is used to map all protein targets of a covalent inhibitor.[312] In addition, this approach has been successfully applied in the identification of conserved catalytic residues in the active sites of several enzymes.[313] It works comparably in the identification of protein-ligand interaction sites and should be applicable to define the area of inhibitor binding by identification of modified amino acids.[314, 315] Therefore, in addition to identifying the proteins of the proteome that interact with JH5, the binding side might be unravelled. Should the suggested covalent mode of action of JH5 be confirmed in the future (Section 3.4.2) a JH5-derivative with a detection tag would provide a suitable JH5-probe for activity-based protein profiling. Nevertheless, also without a covalent binding mode, the JH5 inhibitor could be used as recognition unit of the activity-based probe. In that case, JH5 has to be modified additionally with a reactive group for stable interaction with the protein.[310, 316] Finally, the use of radioactively labelled JH5 and subsequent enzymatic digestion might reveal the peptide of Rabex-5GEF which is involved in the interaction with JH5.[306]

These potential information about the mode of action and binding site of JH5 might contribute to the advanced understanding of the interaction between small molecules and proteins.[317] The intended identification of the binding site of JH5 can further support the identification of a small molecule binding pocket. The knowledge on such binding pocket can provide a starting point to model potential inhibitors to this protein cavity. Protein cavities are required for the binding of molecules and their identification will support the generation of improved inhibitors.[317] These cavities can provide a cleft for ligand-binding with multiple interaction possibilities on a small area which is required for strong binding.[318] One example of successful identification of a small molecule binding pocket was provided by two independently performed fragment based screens targeting Ras (Section 1.5.2.1).[192, 193]

---

[14] The experiments have been and will be performed by Benjamin Weiche.

The information on the JH5-Rabex-5GEF interaction site obtained in these suggested experiments could be used for the virtual screening of a second generation of Rabex-5 inhibitors with more promising characteristics regarding the intracellular application.[319] But even if no additional information on the Rabex-5GEF-JH5 interaction should be available, the knowledge of structural data on Rabex-5GEF provides a protein model to be used in a virtual screening.[136, 146] Virtual screening efforts have been described to be more fruitful if information of the mode of action of the compound as well as extensive SAR are available.[277] Nevertheless, the successful performance of a virtual screening in absence of extensive SAR is also possible.[320] An example is generation of inhibitory molecules for the GEF Cytohesin-2 from the parental inhibitor SecinH3: *Stumpfe et al.* successfully identified second generation inhibitors and showed that the identified molecules revealed a high degree of structural diversity from the parental inhibitor.[321] This underlines the potential of virtual screening as an approach to identify improved inhibitors that differ from the parental structures. In the case of Rabex-5 inhibitors this approach is anticipated to yield molecules that will lack the thiol group.

5.2 Considerations for future screening approaches

5.2.1 Screening concept

Certainly, future screening strategies aiming for the identification of cellular applicable small molecule inhibitors would benefit from insights of this study. In particular, a secondary cellular screen should be carried out at an early time point. If no cellular screening assay might be available, the buffer conditions could be optimized to mimic cytosolic conditions for cytosolic proteins. This is due to the fact that early focus towards intracellular application is essential. The compound activity in cells can be hampered on several levels. First, not all compounds are cell permeable.[322-325] Second, there are compounds that are not specific enough on cellular level.[325-327] Third, as observed in this work (Section 3.3.3 and 3.5), there are compounds that are inactive under conditions that differ from the system they were identified in. For inhibitors with the final goal of intracellular application a direct cellular screening or an intracellular second screen should be very useful.[328] Thereby, all compounds with solubility problems as well as other disadvantageous features (e.g. limited cell permeability or toxicity) would be excluded.[328] To investigate the intracellular applicability early on, a suitable cellular assay is required to be used as secondary screen and follow up strategy to detect the compounds potency for *in vivo* application. Although this idea might be challenging, because it requires two stable, reliable assays instead of one, future screening projects will surely benefit from this stringency. An example for a successful application of this proceeding can be found in the screening for Ras inhibitors resulting in the identification of Sulindac derivatives.[203] Although the compounds targeting the Ras-Raf interaction were only active in the two-digit micromolar concentration range a cellular effect was observed in addition to the *in vitro* inhibition of the Ras-Raf interaction.[202, 203]

5.2.2 Library considerations

The appropriate storage and composition of the compound library was described to be as important as the HTS performance itself and should influence the choice of the library in future screenings.[294] For instance, it has been realized that the solubility of small organic molecules is often poor in aqueous solutions.[271, 329] Automated compound quality controls were suggested to optimize screening results because it was demonstrated that there can be a significant difference between the actual compound concentration in the assay buffer and the theoretical concentration predicted from the stock solutions.[330] The library stocks are stored in DMSO at -80 °C to preserve instable compounds. In general, only compound precipitation is expected when storing compound solutions under cold conditions.[271] As the DMSO freezes, the compound concentration in the remaining liquid part increases while the temperature is low. This favours crystallization ergo precipitation. Freeze-thaw cycles should be reduced to a minimum as they in the long-term favour loss of compound.[331] Moreover, lowering the library compounds stock concentration was shown to prevent compound precipitation: Compound storage at 1 mM in DMSO at -70 °C allowed stable compound storage over years.[332] In addition, a mixture of DMSO, Glycerol and water (45:45:10) instead of using pure DMSO as solvent can counteract precipitation.[332] At first sight, the reduction of the stock concentration has the disadvantage of limiting the concentration of compound usable in the assay, e.g. to 20 µM for 2 % DMSO or 5 µM for 0.5 % DMSO. However, it has also been reported that lower compound concentrations in the screening (5 µM instead of 30 µM) will reduce the rate of false-positive promiscuous inhibitors dramatically (from 19 % to 1.4 %).[232] Thus, low concentration storage and usage of compounds provides more benefits than disadvantages.

Careful composition of libraries instead of merely increasing the amount of compounds has been suggested to the scientific community.[28, 271] The use of a focused library in comparison to a diversity-oriented library can only be useful if parental structures are available that are the basis of the focused library.[181] However, since for most GEF proteins no inhibitory structures are available for these targets the use of focused libraries is impossible. Molecules that belong to the group of "privileged scaffolds", i.e. several molecules with distinct biological targets sharing the same scaffold, were suggested to increase the quality of the compound collection.[333] These molecules are often inspired from natural substances.[333] Admittedly, restricting the library to privileged scaffolds bears the risk that no compound will be identified. Since protein-protein interfaces differ to a great extent, except when considering close homologues, this risk is especially high for these kinds of targets.[334] In summary, the library and the storage conditions of the compounds do have an impact on the outcome of screening approaches and should be considered from the beginning.

6 CONCLUSION

Small molecules have been shown to be valuable tools for the investigation of protein functions. [178, 179] GEFs are ideal target proteins for small molecules because they regulate GTPases. These are, due to their switching functions, key factors in signalling events and transport processes. [3, 7, 41, 190, 208] Often, a variety of GEFs are targeting the same GTPase.[79] Therefore, it would be of immense interest to elucidate the differences between these closely related GEFs in GTPase activation and biological effects. However, GEFs for the same GTPase often share the same catalytic domain structure (e.g. the Rab5 GEFs contain a Vps9 domain) and therefore it is difficult to target them specifically.[79] Moreover, the interfaces between small GTPases and GEFs are usually very large [7] and thus it is challenging to disturb these interactions by small molecules.[317, 334] Nevertheless, a toolbox of specific inhibitors for several Rab5GEFs, e.g. Rabex-5, would boost the unravelling of the complex interaction networks around Rab5. The application of these specific, cell applicable compounds would facilitate the understanding of the interplay of these GEFs and their exact functions in the regulation of Rab5.

Therefore, the challenging aim of the identification and characterization of Rabex-5 inhibitory molecules was approached and partly achieved during this work. The screening for small molecule inhibitors targeting the Rabex-5 nucleotide exchange was successfully performed by the use of an *in vitro* assay (Section 3.1 and 3.2). Thorough *in vitro* characterisation was performed for two molecules of which the compound JH5 showed excellent activity and specificity (Section 3.3). Albeit the differences between the catalytic mechanisms of distinct GEFs are relatively small, it was possible to identify a small molecule that can selectively inhibit Rabex-5 but not Cytohesin-2, DrrA or Vav-1 (Section 3.3.2). JH5 consists of a central 1,2,4-triazole core with a thiol substituent at position 3 and aromatic residues at position 4 and 5. The structure activity relationship of JH5 was investigated and revealed the major importance of the thiol group (Section 3.4). The experiments undertaken to unravel the mode of action of the compound suggested a mechanism that involved one or more cysteine residues of the GEF domain of Rabex-5 (Section 3.4.2). Nevertheless, final proof for a covalent interaction between JH5 and Rabex-5 should be gained in the future. Although the exact mechanism of inhibition is yet to be elucidated, the low micromolar affinity of JH5 for its target protein Rabex-5GEF and its high specificity over other GEFs make it a promising tool for further studying the role of Rabex-5 in controlling Rab5 activity. However, the transition of small molecule *in vitro* use to *in vivo* application was found to be challenging (Sections 3.3.3 and 3.5). Small molecules are generally thought to be easy applicable in cellular environments.[175, 180, 185] Nevertheless, there are several examples of small molecules not matching these criteria and JH5 was found among them.[322-325] Careful composition of libraries as well as early investigation of cellular applicability in the compound characterization process might circumvent this challenge in future screening approaches.

Being the first inhibitor of the nucleotide exchange of Rab5-Rabex-5, the discovery of JH5 proves that RabGEFs are suitable targets for the development of specific small molecule

inhibitors. Although JH5 is unlikely to be suitable for intracellular application, it is a promising lead compound due to its excellent specificity (Section 3.3.2).

The synthesis of additional JH5 derivatives will deepen the understanding of the structure activity relationship of JH5 and might comprise a molecule with improved activity in reducing environment. In addition, these findings should provide further insights into the mode of action and give invaluable information for *in silico* approaches. The use of additional Rabex-5GEF mutants, improved mass spectrometry measurements, activity-based protein profiling, and structural elucidation approaches as outlined in Section 5 should shed light on the mode of action of JH5 as well as its binding site. These insights will support *in silico* predictions. As lead compound, JH5 will serve for the identification of second generation Rabex-5 inhibitors, e.g. by modelling approaches using information of the assumed small molecule binding pocket. *In silico* screenings may provide inhibitory molecules without the problematic sensitivity towards reducing conditions. In fact, it is anticipated that these *in silico* approaches maybe combined with an improved HTS can reveal even more potent Rabex-5 inhibitors in the near future.

These second generation compounds may finally provide the opportunity to elucidate the complex role of Rabex-5 in early endosomal biology. Their application may shed light on the spatial and temporal regulation of the Rabex-5 activity in Rab5 microdomain assembly, Rab5 localization and membrane receptor signal integration. Also, the suggested role of Rabex-5 in early-to-late endosome transition could be explored. Finally, if highly specific second generation Rabex-5 inhibitors can be obtained, the complex interplay of the distinct Rab5 GEFs can be investigated in detail.

7 MATERIAL & METHODS

7.1 Material

7.1.1 Equipment

Equipment, type	Manufacturer, location, country
Agarose gel camera, UV-transilluminator	Bio-Rad Laboratories, Inc., Hercules, CA, USA
Agarose gel running chamber	In-house construction, University of Bonn, Germany
Analytical balance	Sartorius AG, Göttingen, Germany
Autoclave	Systec, Wettenberg, Germany
Balance	Sartorius AG, Göttingen, Germany
blot chamber, semi dry	PHASE Gesell. für Phorese, Analytik und Separation mbH, Lübeck, Germany
Blot shaker (orbital)	IKA, Staufen, Germany
Blot shaker (vertical)	Lab4you GmbH, Berlin, Germany
Centrifuges	Beckman Coulter, Inc., Pasadena, CA, USA Eppendorf AG, Hamburg, Germany
counting chamber, Neugebauer improved	Marienfeld, Lauda Königshofen, Germany
Drigalski spatula	In-house construction
Electrophoresis power supply	Consort, Turnhout, Belgium
Eppi racks	Carl Roth GmbH + Co. KG, Karlsruhe, Germany
Flow cytometer, BD FACSCanto II	BD Biosciences, San Jose, CA, USA
FPLC, ÄKTA	GE Healthcare Life Science, Chalfont St Giles, Great Britain
French Press	Thermo Scientific, Waltham, MA, USA
Gel dryer	Bio-Rad Laboratories, Inc., Hercules, CA, USA
Heating block	Bachofer, Reutlingen, Germany
Heating chamber	Binder GmbH, Tuttlingen, Germany
HPLC column, C18 Zorbax reverse phase column 4.6x150 mm	Agilent Technologies, Inc., Santa Clara CA, USA
HPLC, Agilent 1100	Agilent Technologies, Inc., Santa Clara CA, USA
Image eraser	raytest Isotopenmessgeräte GmbH, Straubenhardt, Germany
Incubator - shaking (bacteria), Innova4430	Eppendorf AG, Hamburg, Germany
Incubator (mammalian cells)	Heraeus, Hanau, Germany
ITC, N-ITC III	Calorimetry Sciences Corporation, Lindon, UT, USA
Liquid Scintillation counter, Winspectral, 1414	PerkinElmer, Waltham, MA, USA
Magnetic stirrer	IKA, Staufen, Germany
Microscope + camera, AG Sandhoff	Carl Zeiss AG, Oberkochen, Germany
Microscope, Axiovert25	Carl Zeiss AG, Oberkochen, Germany
Microwave	Bosch, Gerlingen-Schillerhöhe, Germany
MS	BRUKER AXS Inc., Madison, WI, USA
MST-instrument, Monolith NT.115	NanoTemper, München Germany
MST-instrument, Monolith NT.LabelFree	NanoTemper, München Germany
Multichannel pipette	Eppendorf AG, Hamburg, Germany
Multipette	Eppendorf AG, Hamburg, Germany
Odyssey scanner	LI-COR, Lincoln, NE, USA
Over-head-tumbler	Heidolph, Schwabach, Germany
PCR Thermocycler	Biometra, Göttingen, Germany
Peristaltic pump	LKB Bromma Mettler Toledo GmbH, Gießen, Germany
pH-meter	Inolab, Weilheim, Germany
Phosphorimager screens and equipment	raytest Isotopenmessgeräte GmbH, Straubenhardt, Germany
Phosphorimager, FLA-3000 and equipment	FUJIFILM Corporation, Tokyo, Japan

Equipment, type	Manufacturer, location, country
Pipette-boy	Brand GmbH + Co. KG, Wertheim, Germany
Pipettes	Eppendorf AG, Hamburg, Germany
Plate reader, EnSpire®	PerkinElmer, Waltham, MA, USA
Plate reader, NanoQuant - infiniteM200	Tecan, Männedorf, Switzerland
Plate reader, Varioskan	Thermo Scientific, Waltham, MA, USA
Power-supply	Consort, Turnhout, Belgium
Refrigerator and freezer, 4°C, -20°C, -80°C	AEG, Nürnberg, Germany Thermo Scientific, Waltham, MA, USA
Screening robot, Freedom Evo	Tecan, Männedorf, Switzerland
SDS-PAGE casting equipment	Bio-Rad, Hercules, CA, USA
SDS-PAGE electrophoresis chamber	Bio-Rad, Hercules, CA, USA
Sonication manifold and water bath	Bandelin, Berlin, Germany
SpeedVac, Concentrator 5301	Eppendorf AG, Hamburg, Germany
SPR, Biacore	GE Healthcare Life Science, Chalfont St Giles, Great Britain
Sterile hood (bacteria)	Heraeus, Hanau, Germany
Sterile hood (mammalian cells)	Heraeus, Hanau, Germany
Superdex200 gel filtration column (26/60 high load)	GE Healthcare Life Science, Chalfont St Giles, Great Britain
Thermomixer, GFL Thermomixer, Eppendorf	GFL, Burgwedel, Germany Eppendorf AG, Hamburg, Germany
UV-Vis-photo-spectrometer, BioMate 3	Thermo Scientific, Waltham, MA, USA
VersaDoc 5000 CCD camera	Bio-Rad, Hercules, CA, USA
Vortexer	NeoLab, Heidelberg, Germany
Water bath	GFL, Burgwedel, Germany
Water purification system	Werner, Leverkusen, Germany
Wet blot system, Criterion Blotter	Bio-Rad, Hercules, CA, USA

7.1.2   Glass ware

Glass ware	Manufacturer, location, country
Baffled flask	Schott, Mainz, Germany
Beaker	Schott, Mainz, Germany
Erlenmeyer flask	Schott, Mainz, Germany
Glass bottles	Schott, Mainz, Germany
Glass plates for PAGE	Baack, Schwerin, Germany
Graduated cylinder	Faust, Meckenheim, Germany
Pasteur pipettes	VWR International GmbH, Darmstadt, Germany
Pipettes	Hirschmann, Eberstadt, Germany

7.1.3   Chemicals

Reagent, specification	Manufacturer, location, country
Acetic acid	Merck KGaA, Darmstadt, Germany
Acetonitrile, LC-MS-grade	Sigma-Aldrich (Fluka), St. Louis, MO, USA
Acrylamide-, Bisacrylamide-solution (37.5:1)	Carl Roth GmbH + Co. KG, Karlsruhe, Germany
Agarose	Lonza, Basel, Switzerland Merck KGaA, Darmstadt, Germany
Alexa Fluor 647 NHS-ester	Life Technologies Corporation (Invitrogen), Carlsbad, CA, USA
APS	Carl Roth GmbH + Co. KG, Karlsruhe, Germany
Biotin	Sigma-Aldrich Corporation, St. Louis, MO, USA
Boric acid	Grüssing GmbH Analytika, Filsum, Germany

Reagent, specification	Manufacturer, location, country
Bradford reagent	Bio-Rad, Hercules, CA, USA
Bromophenol blue	Merck KGaA, Darmstadt, Germany
CHAPS	Sigma-Aldrich (Fluka), St. Louis, MO, USA
Chloroform	Merck KGaA, Darmstadt, Germany
ComGenex compound library	ComGenex, Budapest, Hungary
Coomassie, Page blue™ protein staining solution	Thermo Scientific, Waltham, MA, USA
Coomassie brilliant blue G-250	AppliChem GmbH, Gatersleben, Germany
Anhydrous DMSO	Acros Organics, Thermo Fisher Scientific, Geel, Belgium
DTT	Carl Roth GmbH + Co. KG, Karlsruhe, Germany
ECL reagent, Detection Reagents a) Luminol Enhancer Solution, b) Peroxide Solution	Thermo Scientific (Pierce), Waltham, MA, USA
EDTA	AppliChem GmbH, Gatersleben, Germany
Ethanol	Merck KGaA, Darmstadt, Germany
Ethidium bromide	Carl Roth GmbH + Co. KG, Karlsruhe, Germany
FITC	Sigma-Aldrich (Fluka), St. Louis, MO, USA
Glutathione	Carl Roth GmbH + Co. KG, Karlsruhe, Germany
Glycerol	Grüssing GmbH Analytika, Filsum, Germany
Glycine	AppliChem GmbH, Gatersleben, Germany
HCCA	Marc Sylvester, Institute of Biochemistry and Molecular Biology (IBMB), University of Bonn
HCl	VWR International GmbH, Darmstadt, Germany
Hepes	AppliChem GmbH, Gatersleben, Germany Carl Roth GmbH + Co. KG, Karlsruhe, Germany
hydrogen peroxide	Merck KGaA, Darmstadt, Germany
Igepal	Sigma-Aldrich (Fluka), St. Louis, MO, USA
Imidazole	Carl Roth GmbH + Co. KG, Karlsruhe, Germany
IPTG	Carbolution Chemicals GmbH, Saarbrücken, Germany
Isopropanol	VWR International GmbH, Darmstadt, Germany
Methanol	VWR International GmbH, Darmstadt, Germany
$MgCl_2$	Acros Organics, Thermo Fisher Scientific, Geel, Belgium
NaCl	Grüssing GmbH Analytika, Filsum, Germany
NaOH	Grüssing GmbH Analytika, Filsum, Germany
NH_4HCO_3	AppliChem GmbH, Gatersleben, Germany
NHS-Fluorescein	Thermo Scientific (Pierce), Waltham, MA, USA
Phenol	Carl Roth GmbH + Co. KG, Karlsruhe, Germany
Protease-Inhibitor Mix HP	SERVA Electrophoresis GmbH, Heidelberg, Germany
SDS	AppliChem GmbH, Gatersleben, Germany Carl Roth GmbH + Co. KG, Karlsruhe, Germany
Sodium orthovanadate	AppliChem GmbH, Gatersleben, Germany
TEMED	Carl Roth GmbH + Co. KG, Karlsruhe, Germany
Trifluoroacetic acid	Sigma-Aldrich (Fluka), St. Louis, MO, USA
Tris	Carl Roth GmbH + Co. KG, Karlsruhe, Germany
Triton X-100	Merck KGaA, Darmstadt, Germany
Tween20	AppliChem GmbH, Gatersleben, Germany Carl Roth GmbH + Co. KG, Karlsruhe, Germany
Urea	AppliChem GmbH, Gatersleben, Germany
Xylene blue	Merck KGaA, Darmstadt, Germany
β-mercaptoethanol	Carl Roth GmbH + Co. KG, Karlsruhe, Germany Sigma-Aldrich Corporation, St. Louis, MO, USA

7.1.4   Consumables

Product	Manufacturer, location, country
96 well plates, flat, black, medium binding	Greiner Bio One, Frickenhausen, Germany
96 well plates, flat, transparent	Carl Roth GmbH + Co. KG, Karlsruhe, Germany
96 well plates, half area, flat, black, medium binding	Greiner Bio One, Frickenhausen, Germany
Amberlite® XAD®-2	Supleco Analytical, Bellefonte, PA, USA
Amicon filters	Millipore, Billerica, MA, USA
Blotting paper	Macherey-Nagel GmbH & Co. KG, Düren, Germany
Capillaries, Hirschmann	Hirschmann, Eberstadt, Germany
Capillaries, Monolith™ NT.LabelFree Standard Treated Capillaries	NanoTemper, München, Germany
Cell culture dishes and flasks	TPP, Trasadingen, Switzerland
Centrifugation tubes (15 mL / 50 mL)	Techno Plastic Products AG (TPP), Trasadingen, Switzerland Greiner Bio One, Frickenhausen, Germany Faust, Meckenheim, Germany
Cotton swabs	Braun, Kronberg, Germany
Dialyse cassettes	Thermo Scientific, Waltham, MA, USA
Dialyse tubes	Spectrum Laboratories, Inc., Rancho Dominguez, CA, USA
Disposable columns	Bio-Rad Laboratories, Inc., Hercules, CA, USA
Disposable cuvettes	Carl Roth GmbH + Co. KG, Karlsruhe, Germany
Flow cytometer tubes	BD Biosciences, San Jose, CA, USA
Gloves	Peske, Aindlingen-Arnhofen, Germany
Gloves	Rösner-Mautby Meditrade GmbH, Kiefersfelden, Germany
Glutathione Sepharose 4B	GE Healthcare Life Science (Amersham), Chalfont St Giles, Great Britain
Hollow needles	Carl Roth GmbH + Co. KG, Karlsruhe, Germany
Membrane filters 45 µm, 25 mm	Sigma-Aldrich, St. Louis, MO, USA
Monomeric Avidin Agarose	Thermo Scientific, Waltham, MA, USA
Nap columns (NAP-5, -10)	GE Healthcare Life Science, Chalfont St Giles, Great Britain
Ni-NTA-agarose	Qiagen, Hilden, Germany
Nitrocellulose membrane; Protran	Schleicher & Schuell BioScience GmbH, Dassel, Germany
Parafilm	Faust, Meckenheim, Germany
PCR tubes, 0.2 mL	Sarstedt, Nümbrecht, Germany
Petisdishes for LB-agar plates	Faust, Meckenheim, Germany
pH paper	Macherey-Nagel GmbH & Co. KG, Düren, Germany
Pipette Tips	Peske, Aindlingen-Arnhofen, Germany
Reaction tubes (1.5 mL / 2 mL)	Sarstedt, Nümbrecht, Germany
Scalpel blades	Labomedic GmbH, Bonn, Germany
Scintillation vials; 20mL / 6 mL	PerkinElmer, Waltham, MA, USA
Sensor chips (CM5)	GE Healthcare Life Science, Chalfont St Giles, Great Britain
Serological pipettes	Faust, Meckenheim, Germany
Sterile filters (syringe filter / bottle top)	Merck Millipore, Billerica, MA, USA
Sterile pipettes	TPP, Trasadingen, Switzerland
Streptactin Superflow High Capacity	Qiagen, Hilden, Germany
Syringes	Braun, Kronberg, Germany
Tips for multipette; Combitips plus	Eppendorf AG, Hamburg, Germany
ZipTip® C18	Merck-Millipore, Billerica, MA, USA

7.1.5   Nucleic acids

7.1.5.1   Plasmids[15]

Plasmid	Cloning sites	Resistance	Tag	Insert [original description of plasmid]
pET19mod	NdeI XhoI	Amp	6xHis	DrrA [DrrA, aa340-533]
pGEX-5X-3	SalI NotI	Amp	GST	R5BD739-862 [Rabaptin-5, human, aa739-862]
pGEX-5X-3	SalI NotI	Amp	GST	R5BD789-862 [Rabaptin-5, human, aa789-862]
pET15b	NdeI BamH1	Amp	6xHis	Rab5a17-184 [Rab5a, human, aa17-184]
pcDNA5/ FRT/TO	unknown	Amp Hyg	3x Flag	Rab5a FL [Rab5a, human, FL][335]
pDL2	BamHI SalI	Amp	10xHis	Rab5c [Rab5c, murine, aa18-185]
pASK IBA 45plus	SacII XmaI	Amp	Strep 6xHis	Rabaptin-5 [Rabaptin-5, human, FL]
pGEX-5X-3	XmaI XhoI	Amp	GST	Rabaptin-5 [Rabaptin-5, human, FL]
pDL2	BamHI SalI	Amp	6xHis	Rabex-5$_{GEF}$ [Rabex-5, human, aa132-391]
pCMV3Tag2a	PstI SalI	Kana Neo	3x c-myc	Rabex-5 FL [Rabex5 isoform2, human, FL]

7.1.5.2   Primer for QuikChange and Cloning

Target	Forward	Reverse
pGEX-5X-3-R5BD739-862	5' GCGTCGACGCTTCTATTT CTAGCCTAAA 3'	5' CCCGCGGCCGCTCATGTCTCAG GAAGCTGGT 3'
pGEX-5X-3-R5BD789-862	5' GCGTCGACGCTAAGGCT ACCGTTGAACA 3'	5' CCCGCGGCCGCTCATGTCTCAG GAAGCTGGT 3'
pET15b-Rab5a17-184	5' GGTCTCAGTCCATATGA AAATATGCCAGTTCAA 3'	5' GTTAGCAGCCGGATCCTTAATT CTTTGGCAATT 3'
pDL2-Rab5c; quikchange	5' GGAGAGCACAATTGGAGCGGCTTTCCTCACACAGAC 3' 5' GTCTGTGTGAGGAAAGCCGCTCCAATTGTGCTCTCC 3'	
pASK-IBA-45plus-Rabaptin-5	5' AATTCCGCGGTTATGGC GCAGCCGGGCC 3'	5' GGGGCTCGAGTCATGTCTCAGG AAGCTGGTTAATGTCTGTCAG 3'
pGEX-5X-3-Rabaptin-5	5' AATACCCGGGAAATGGC GCAGCCGGGCC 3'	5' GGTTCTCGAGTCATGTCTCAGG AAGCTGGTTAATGTCTGTCAG 3'
pCMV3Tag2a-Rabex-5 FL	5' GGACCGAGCCTGCAGAT GAGCCTT AAGTCTGAA 3'	5'CCCCTCGAGGTCGACTCATCCT GC ATAAACTTG 3'

---

[15] For vector maps and insert sequences see appendix (Section 8.1)

7.1.5.3   Sequencing primer

Target vector	Forward primer	Reverse primer
pET19mod-DrrA	T7 (GATC) TAATACGACTCACTATAGGG	T7 terminator could be used
pGEX-5X-3-R5BD739-862	pGEX-5 (GATC) CTGGCAAGCCACGTTTGG	/
pGEX-5X-3-R5BD789-862	pGEX-5 (GATC) CTGGCAAGCCACGTTTGG	/
pET15b-Rab5a17-184	T7 (GATC) TAATACGACTCACTATAGGG	/
pcDNA5/FRT/TO-Rab5a-FL	CMV-F (GATC) CGCAAATGGGCGGTAGGCGTG	BGH-rev (GATC) TAGAAGGCACAGTCGAGG
pDL2-Rab5c	T7 (GATC) TAATACGACTCACTATAGGG	pRSET-RPnew (GATC) GGGTTATGCTAGTTATTGC
pASK-IBA-45plus-Rabaptin-5	pASK45-forward GAGTTATTTTACCACTCCCT Rabaptin849-65 CCAGTTAAAACATACGTGG	pASK45-reverse AAATGTCGCACAATGTGCG
pGEX-5X-3-Rabaptin-5	pGEX5FP (GATC) AACGTATTGAAGCTATCCC Rabaptin849-65 CCAGTTAAAACATACGTGG	pBR1 (GATC) CGAAAAGTGCCACCTGAC
pDL2-Rabex-5GEF	T7 (GATC) TAATACGACTCACTATAGGG	pRSET-RPnew (GATC) GGGTTATGCTAGTTATTGC
pCMV3Tag2a-Rabex-5 FL	T3 (GATC) AATTAACCCTCACTAAAGGG	T7 (GATC) TAATACGACTCACTATAGGG

7.1.6   Nucleotides

Nucleotide	Manufacturer, location, country
dNTPs	Larova GmbH, Teltow, Germany
GppNHp	Jena Biosciences GmbH, Jena, Germany
GTPγS	Jena Biosciences GmbH, Jena, Germany
GTPγ^{35}S	PerkinElmer, Waltham, MA, USA
mantGDP	Jena Biosciences GmbH, Jena, Germany
NTPs	Larova GmbH, Teltow, Germany

7.1.7   Standards and Kits

Product	Manufacturer, location, country
DNA marker	Peqlab Biotechnologie GmbH, Erlangen, Germany
GLISA Lysis buffer	Cytoskeleton, Inc., Denver, CO, USA
NucleoBond® Xtra Midi/Maxi Kits	Macherey-Nagel GmbH & Co. KG, Düren, Germany
NucleoSpin Extract II	Macherey-Nagel GmbH & Co. KG, Düren, Germany
NucleoSpin® Plasmid Kit	Macherey-Nagel GmbH & Co. KG, Düren, Germany
Page ruler prestained protein marker	Thermo Scientific (Fermentas), Waltham, MA, USA
PCR clean-up kit	Macherey-Nagel GmbH & Co. KG, Düren, Germany
QuikChange site directed mutagenesis kit	Agilent Technologies Inc. (Stratagene), Santa Clara CA, USA
Venor™GeM Mycoplasma Detection Kit	Sigma-Aldrich Corporation, St. Louis, MO, USA

7.1.8   Enzymes and Proteins

Enzyme / protein	Manufacturer, location, country
BamHI	New England Biolabs, Ipswich, MA, USA
BSA	AppliChem GmbH, Gatersleben, Germany
BSA; RNase free	Merck KGaA (Calbiochem), Darmstadt, Germany
CIAP	Promega Corporation, Madison, WI, USA
DNase I	Roche, Basel, Switzerland
EGF	PeproTech, Rocky Hill, NJ, USA
EGF-Conjugate AlexaFluor647	Life Technologies Corporation (Invitrogen), Carlsbad, CA, USA
HGF	PeproTech, Rocky Hill, NJ, USA
JIP4	Gift from Benjamin Weiche, AK Famulok
Lysozyme	Sigma-Aldrich, St. Louis, MO, USA
Milk powder, Sucofin	TSI GmbH & Co.KG, Zerven, Germany
NdeI	New England Biolabs, Ipswich, MA, USA
NotI	New England Biolabs, Ipswich, MA, USA
Pfu Polymerase	In house production, Nicole Krämer; AK Famulok
Pfu Ultra Polymerase	Agilent Technologies Inc. (Stratagene), Santa Clara CA, USA
PstI	New England Biolabs, Ipswich, MA, USA
Rab1	Gift from Dr. Aymelt Itzen, MPI Dortmund (currently: TU München)
Reverse Transcriptase; Superscript II	Life Technologies Corporation (Invitrogen), Carlsbad, CA, USA
Ribonuclease Inhibitor; RNasin	Promega Corporation, Madison, WI, USA
SacII	New England Biolabs, Ipswich, MA, USA
SalI	New England Biolabs, Ipswich, MA, USA
T4 DNA Ligase	New England Biolabs, Ipswich, MA, USA
T7 RNA-Polymerase	In house production, Nicole Krämer; AK Famulok
Taq Polymerase	In house production, Nicole Krämer; AK Famulok
Transferrin Conjugate AlexaFluor488	Life Technologies Corporation (Invitrogen), Carlsbad, CA, USA
XhoI	New England Biolabs, Ipswich, MA, USA
XmaI	New England Biolabs, Ipswich, MA, USA

7.1.9   Antibodies

7.1.9.1   Primary antibodies

Antibody target	Species	dilution	Manufacturer, location, country (product number)
EGFR-CT	abbit	1:500	Santa Cruz Biotechnology, Inc., Santa Cruz, CA, USA (sc-03)
Hsc70	mouse	1:10,000	Enzo Life Sciences, Inc. Farmingdale, NY, USA (clone N27F3-4, ADI-SPA-820)
Phospho-EGFR (Thy1086)	rabbit	1:1000	Epitomics - an Abcam Company, Burlingame, CA, USA (1139-1)
Rab5a, D11	mouse	1:1000	Santa Cruz Biotechnology, Inc., Santa Cruz, CA, USA (sc-46692)
Rab5a, S19	rabbit	1:500	Santa Cruz Biotechnology, Inc., Santa Cruz, CA, USA (sc-309)
Rabex-5	mouse	1:1000	BD Biosciences, San Jose, CA, USA (612558)
Rabex-5	rabbit	1:1000	Cell Signaling Technology, Inc., Beverly, MA, USA (cloneD21F12, 7622)

7.1.9.2   Secondary antibodies

Antibody target	Species	Dilution	Manufacturer, location, country (product number)
Anti-goat (680 nm fluorophore conjugated)	donkey	1: 20,000	LI-COR, Lincoln, NE, USA (IRDye®680)
Anti-mouse (800 nm fluorophore conjugated)	goat	1:20,000	Thermo Scientific, Waltham, MA, USA (35521)
Anti-rabbit (800 nm fluorophore conjugated)	goat	1:20,000	Thermo Scientific, Waltham, MA, USA (35571)
Anti-rabbit (HRP-conjugated)	goat	1:10,000	Santa Cruz Biotechnology, Inc., Santa Cruz, CA, USA (sc-2005)

7.1.10   Cell culture

7.1.10.1   Culture medium

Reagent	Manufacturer, location, country
Agar	Carl Roth GmbH + Co. KG, Karlsruhe, Germany
Ampicillin	AppliChem GmbH, Gatersleben, Germany
Chloramphenicol	Sigma-Aldrich, St. Louis, MO, USA
DMEM	PAA Laboratories GmbH, Pasching, Austria
FCS	Lonza, Basel, Switzerland
Kanamycin	AppliChem GmbH, Gatersleben, Germany
LB Broth	Carl Roth GmbH + Co. KG, Karlsruhe, Germany
OptiMEM	Gibco®, Life Technologies Corporation (Invitrogen), Carlsbad, CA, USA
PBS	Gibco®, Life Technologies Corporation (Invitrogen), Carlsbad, CA, USA
RPMI	Gibco®, Life Technologies Corporation (Invitrogen), Carlsbad, CA, USA
SOC	Stratagene (supplied with cells)
Sodium pyruvate	Sigma-Aldrich Corporation, St. Louis, MO, USA
Trypsin EDTA	PAA Laboratories GmbH, Pasching, Austria
Tryptone	Sigma-Aldrich, St. Louis, MO, USA
Yeast extract	Sigma-Aldrich (Fluka), St. Louis, MO, USA

7.1.10.2   Bacterial strains

Strain	Genotype	Supplier, location, country
BL21-CodonPlus (DE3)-RIL strain	E. coli B F– ompT hsdS(rB– mB–) dcm+ Tetr gal λ(DE3) endA Hte [argU ileY leuW Camr]	Agilent Technologies Inc. (Stratagene), Santa Clara CA, USA
XL1 blue	recA1 endA1 gyrA96 thi-1 hsdR17 supE44 relA1 lac [F´ proAB lacIqZΔM15 Tn10 (Tetr)]	AK Famulok (Volkmar Fieberg)
XL10 gold competent cells	TetrD(mcrA)183 D(mcrCBhsdSMR-mrr)173 endA1 supE44 thi-1 recA1 gyrA96 relA1 lac Hte [F´proAB lacIqZDM15 Tn10 (Tetr) Amy Camr	Agilent Technologies Inc. (Stratagene), Santa Clara CA, USA

7.1.10.3   *Mammalian cell lines*

Cell line	Description	Culture medium	Supplier, location, country
Hek293	Human embryonic kidney cell line	DMEM + 10 % FCS	ATCC, Manassas, VA, USA
HeLa	Human cervical cancer cell line	RPMI + 10 % FCS	ATCC, Manassas, VA, USA
Sk-BR-3	Human adenocarcinoma cell line	RPMI + 10 % FCS	ATCC, Manassas, VA, USA
U87	Human glioblastoma cell line	RPMI + 10% FCS + 110 µg/mL sodium pyruvate	ATCC, Manassas, VA, USA

7.1.11   Software

Software type	Manufacturer, location, country
Adobe Illustrator CS	Adobe Systems, San Jose, CA, USA
AIDA Biopackage	raytest Isotopenmessgeräte GmbH, Straubenhardt, Germany
Chem Office 2002	PerkinElmer, Waltham, MA, USA
GraphPad Prism®	GraphPad Software, Inc., La Jolla, CA, USA
Quantity One® 1-D analysis software	Bio-Rad, Hercules, CA, USA

7.2   Handling of compounds

7.2.1   HPLC

The purity of the compounds was analysed by HPLC on an Agilent 1100 with an analytical C18 Zorbax reverse phase column (4.6 x 150 mm) using gradient conditions according to Table 10. Compounds and impurities were detected by absorption at 254 nm. The mobile phase was formed by a gradient of water and acetonitrile (ACN) and was applied at a flow of 1 mL/min.

Table 10   Gradient for the analysis of compounds purity by HPLC.

Time [min]	Water [%]	ACN [%]
0	90	10
5	90	10
35	10	90
40	10	90
42	90	10
52	90	10

Flow: 1 mL/min.

7.2.2   MS

The samples for MS analysis were diluted in LC-MS grade ACN. The molecular mass of the small molecules was detected on a Bruker Esquire HCT spectrometer with atmospheric pressure interface-electrospray ionisation (API-ESI) using direct infusion at 240 µL/min. The detection parameters are presented in Table 11.

Table 11   Parameters for the MS analysis of compounds.

Parameter	Value
Scan modus	Standard-Enhanced, positive
Neb	30 psi
Dry gas	10 l/min
Dry temp	330 °C
Smart Target	200 000
Scan	300 to 1500 m/z
Averages	5
Target mass	300

7.2.3   Determination of solubility by absorption measurement

The solubility of the compounds was determined by absorption measurements. The wavelength of maximal absorption of the compound of interest was identified via an absorption scan using the *NanoQuant* plate reader. A serial dilution of the compound was prepared in the buffer/solvent of interest and absorption was detected.[336] The samples were incubated at the temperature and indicated times. The samples were centrifuged for 15 minutesat 20.000 g and the supernatant was transferred to a fresh tube. Again, the absorption of the supernatant was determined and plotted against the compound concentration. A linear curve was expected; a decrease in the signal after the incubation indicated that precipitation or aggregation of the small molecule had occurred.

7.2.4   Compound storage

To prevent precipitation by repeated freeze-thaw cycles the compounds were stored at RT in the dark. Storage at -20 °C in aliquots was found to be more suitable condition for long time storage.

7.3   Nucleic acid manipulation

7.3.1   PCR

Polymerase chain reaction (PCR) is used for the amplification of DNA templates.[337] The reactions were performed in a PCR-thermocycler according to the protocol illustrated in Table 12 and Table 13.

Aliquots (5 µL) were taken and visualized on agarose gels (Section 7.3.2) to monitor the amplification. The negative control without template served for control of contamination or unspecific amplification. All PCR products for cloning were purified using the PCR clean-up kit. This purification was performed according to manufacturer's protocol except for dilution of NT buffer 1:1 with water and elution of DNA in 50 µL water.

Table 12   PCR reaction scheme for Rabaptin-5 cloning.

Reagent	Volume	Stock	Final concentration
Ultra Pfu reaction buffer	5 µL	10 x	1 x
dNTPs	0.2 µL (0.5 µL)	25 mM	100 µM (250 µM)
Primer 3′	0.5 µL	100 µM	1 µM
Primer 5′	0.5 µL	100 µM	1 µM
Template	x µL		e.g. 60 ng Rabaptin-5 cDNA
Pfu Ultra	0.25 µL (1 µL)	2.5 u/µL	0.63 u (2.5 u)
Water	ad 50 µL		

Table 13   PCR cycle scheme for Rabaptin-5 cloning.

Temperature	Time	Repeats
95°C	2 min	Initial denaturation, no repeat
95°C	1 min	
65°C	45 s	30 cycles
72°C	5 min	
72°C	10 min	Final elongation, no repeat

7.3.2   Agarose gel electrophoresis

Linear nucleic acids were separated and analysed using non-denaturing agarose gels as described in the *Current Protocols in Molecular Biology*.[338] The procedure was slightly adapted from the original protocol. For visualization under UV light, the gels were stained by ethidium bromide, a nucleic acid intercalating dye. The percentage of the agarose gel was adjusted between 1 and 2.5 % (w/v) depending on the length of the nucleic acid of interest. The agarose was melted in 0.5 x TBE buffer by heating in the microwave until it was completely dissolved. 100 µg/L (w/v) ethidium bromide was added to the warm agarose gel just prior to casting the gel. The samples were mixed 1:1 with agarose gel electrophoresis loading buffer and loaded onto the solid gel. The nucleic acids were separated on the gel at 125 – 150 V for 15 - 30 minutes in a chamber with 0.5 x TE buffer and 10 µg/L (w/v) ethidium bromide. The nucleic acids were visualized under UV light and the size was estimated by comparison with the DNA or RNA size marker.

Buffer	Composition
DNA agarose loading buffer (2x)	50 % Glycerol (v/v) 50 mM Tris pH 8.0 50 mM EDTA Bromophenol Blue Xylenecyanol (instead of adding the single dyes, a small amount of 6x loading buffer supplied with the DNA marker, can be added)
0.5 x TBE buffer	45 mM Tris 22 mM boric acid 1 mM EDTA, pH 8.0

7.3.3 Restriction digestion and 5'dephosphorylation

DNA fragments can be inserted into the plasmid vector of choice by generation of appropriate sticky ends. Therefore, the PCR product for the insert had to be treated with the same restriction enzymes as the plasmids. For plasmid and insert digestion, 1 - 3 µg DNA were incubated in the enzyme specific 1 x buffer (supplied by enzyme manufacturer) with 100 µg/mL BSA and 10 - 30 u of each of the restriction enzymes. The reaction was incubated for 4 - 17 hours at 37 °C followed by inactivation of enzymes at 65 °C for 20 min.

5' dephosphorylation of digested plasmid DNA prevents re-ligation of the plasmids and was performed with the CIAP enzyme. The digested plasmid was mixed with 1 µL CIAP enzyme (20 u/µL) directly after the restriction digestion and incubated for 30 minutes at 37 °C. The enzyme was inactivated by heating 10 minutesat 75 °C. The digest of the plasmid was monitored on a 1 % agarose gel. The purification was performed with the PCR clean-up kit as described in Section 7.3.1.

7.3.4 Ligation with T4 DNA ligase

The linearized plasmid and the digested insert were ligated with T4 DNA ligase. 50 - 125 fmoles plasmid DNA were mixed with the insert DNA in different plasmid / insert ratios (1:2, 1:3) in 1 x T4 DNA Ligase buffer according to manufactures' instructions. 1 µL of T4 DNA ligase (20 u/µL) was added to a reaction of 40 µL total volume and the samples were incubated o/n at 16 °C. To control the reaction, samples without the insert or the ligase were prepared. 20 µL of the ligation reaction were used for the transformation of 50 µL competent Top10 *E.coli* cells.

7.3.5 Site-directed mutagenesis

The QuikChange (Stratagene) technique was used for site-directed mutagenesis and performed according to manufacturers' protocol. The reaction was mixed as indicated in Table 14 and incubated in a thermocycler according to Table 15. Subsequently, 1 µL of DpnI (10 u/µL) endonuclease, which specifically targets methylated and hemimethylated DNA, was added to the reaction to digest the parental DNA template. XL10 gold *E.coli* cells were transformed with the endonuclease treated reaction (Section 7.3.6.1).

Table 14   Reaction scheme for the QuikChange reaction.

Reagent	Volume	Stock	Final concentration
Reaction buffer	5 µL	10 x	1 x
DNA template			20 ng
5' primer	1.1 µL	10 µM	0.22 µM (=125 ng)
3' primer	1.1 µL	10 µM	0.22 µM (=125 ng)
dNTP mix	1 µL		
Pfu Turbo DNA Polymerase	1 µL	2.5 u/µL	2.5 u
Water	ad 50 µL		

Table 15   Cycle conditions for the QuikChange reaction.

Step	Temperature	Time	Repeats
Initial denaturation	95 °C	1 min	No repeat
Denaturation	95 °C	30 s	
Annealing	55 °C	1 min	16 cycles
Elongation	68 °C	7 min	

7.3.6   Transformation of *E.coli*

7.3.6.1   *XL10 gold ultracompetent cells*

25 µL cells were thawed on ice and incubated with 1.5 µL of the supplied β-ME solution for 10 minuteson ice. Then, 1 µL of the QuikChange reaction was added to the cells and they were incubated for 30 minutes on ice. The heat shock was performed at 42 °C for 45 seconds and the cells were placed back on ice for two minutes. 500 µL SOC medium were added and the cells were incubated for 90 minutes at 37 °C shaking in an *Eppendorf*-thermomixer at 800 rpm. Afterwards they were plated on LB-agar plates with the appropriate antibiotics and incubated o/n at 37 °C.

Antibiotic	Stock concentration		Final concentration
Ampicillin	100 mg/mL (in ethanol, stored at -20 °C)		100 µg/mL
Chloramphenicol	34 mg/mL (in ethanol, stored at -20 °C)		34 µg/mL – 50 µg/mL

7.3.6.2   *XL1 blue E.coli*

After thawing on ice, 100 µL cells were incubated with an appropriate amount of plasmid DNA for 20 minutes. The heat pulse was performed for 60 seconds at 42 °C and the cells were incubated on ice for 3 minutes. The *E.coli* cells were mixed with 800 µL LB-medium and incubated for 1 hour at 37 °C shaking at 800 rpm in a thermomixer. The mixture was centrifuged at 14,000 rpm for 3 minutes to concentrate the cells and approximately half of the supernatant was decanted. After resuspension, the cells were plated on LB-agar plates supplemented with the appropriate antibiotics and incubated o/n at 37 °C.

7.3.6.3   *Top10 competent cells*

50 µL cells were thawed on ice for 20 minutes and incubated for further 20 minutes with 20 µL of the ligation reaction. The heat-shock was performed for 45 seconds at 42 °C and the cells were immediately placed back on ice for 2 minutes. 400 µL LB-medium were added and the cells were incubated for 90 minutes at 37 °C and 10 % rotation in a GFL-thermomixer. Cells were plated on LB-agar plates containing the appropriate antibiotics. The agar plates were incubated o/n at 37 °C.

7.3.7 Isolation of plasmid DNA from *E.coli*

Plasmids were prepped from bacteria by the use of the NucleoSpin® Plasmid Kit (5 mL culture volume) or NucleoBond® Xtra Midi/Maxi Kits (larger culture volumes). Therefore, the cultivated *E.coli* were harvested by centrifugation at 4 °C and 4,500 *g*. Lysis, binding of the DNA to the supplied silica column, and washing steps were performed according to manufacturers' protocol. Using the NucleoSpin® Plasmid Kit, the DNA was eluted in 50 µL water, for the larger kits in 100 - 200 µL water.

7.3.8 Determination of DNA concentration

The concentration of nucleic acid solutions was calculated from the measured absorption at 260 nm (Abs [260 nm]). For the determination of the absorption an UV-spectrophotometer or the *NanoQuant* plate reader was used. After subtraction of the blank, the concentration (c) was calculated using the law of Lambert-Beer which has the following equation:

$$\text{Abs [260 nm]} = c \bullet \varepsilon \bullet l$$

l = length of cuvette; e = extinction coefficient

Simplified, it was assumed that if the Abs [260nm] equals 1, the concentration of dsDNA is 50 µg/mL and of RNA is 40 µg/mL.

7.3.9 DNA sequencing

Plasmids were prepped from bacterial culture by the use of the NucleoSpin® Plasmid Kit (Section 7.3.7) and the DNA concentration was measured (Section 7.3.8). After choosing the appropriate primer (Section 7.1.5.3) the samples were sent to the GATC biotech AG (Konstanz, Germany) for sequencing. The results were analysed by comparison with expected sequence.

7.4 Protein biosynthesis and purification

7.4.1 Cultivation of *E.coli* and preparation of glycerol stocks

E.coli bacteria were cultivated in LB-medium as described in the *Current Protocols in Molecular Biology* with the appropriate antibiotics at 37 °C in a shaking incubator with 130 - 150 rpm agitation.[339] For expression of Rabex-5GEF and Rab5c the cells were cultivated in 2xTY medium.[136] Cell growth was determined by measurement of the OD_{600}. The glycerol stocks were produced by mixing a sample of the cell culture with the equal volume of glycerol medium and freezing them at -80 °C.

Medium	Components
2xTY medium	16 g Tryptone 10 g Yeast Extract 5 g NaCl ad 1 L with water Autoclave
LB medium	20 g LB broth ad 1 L with water
LB agar plates	LB medium, supplemented with 15 g/L agar
Glycerol medium	50 mM Tris, pH 7.8 300 mM NaCl 40 % Glycerol

7.4.2 Protein biosynthesis and purification

7.4.2.1 *Transformation of BL21-CodonPlus® (DE3)-RIL competent cells*

For the biosynthesis of proteins the *E.coli* strain BL21-CodonPlus® (DE3)-RIL was used. This strain has the advantage of supplying additional copies of specific tRNA genes that are rare in *E. coli* (arginine, isoleucine, and leucine) and thereby enhance the level of protein expression. 100 µL cells were thawed on ice, mixed with 1 µL plasmid DNA (mini-prep, about 100 ng) and incubated further 20 minutes on ice. The heat shock was performed for 1 minute at 42 °C and the cells were chilled on ice for 3 minutes. 800 µL LB-medium or SOC-medium was added and the cultures were shaken for 60 - 90 minutes at 37 °C and 800 rpm in an *Eppendorf*-thermomixer. The bacteria were plated on LB plates supplemented with the appropriate antibiotics and incubated at 37 °C o/n. For BL21 (DE3) + RIL cells, the agar plates were additionally supplemented with Chloramphenicol. Single clones were picked from the plate for further use.

7.4.2.2 *Induction of gene expression*

The induction of gene expression depends on the promoter under which the expression is carried out. For most of the plasmids used in this study the gene expression can be induced with IPTG. IPTG releases the lac repressor from the lac operon so that the genes under the lac promoter can be expressed. It has the advantage over the natural inductor lactose that it cannot be metabolized by the bacteria and is therefore kept at a constant concentration. AHT can be used for induction of tet-promoter controlled protein expression. It has a stronger affinity to the promoter than tetracycline and thus can be used at concentrations that are less antibiotic.

To obtain a 2 L culture, 100 - 200 mL pre-culture was inoculated from glycerol stocks and cultivated o/n.[339] The main culture was inoculated with the pre-culture and grown at the appropriate temperature till the OD_{600} reached 0.4 - 0.5. IPTG or AHT were added and the bacteria were further cultivated for the indicated times before harvest. The conditions that were used for the different constructs are indicated in Table 16.

Table 16   Conditions for gene induction.

Construct	Temperature	Induction time	Induction (OD$_{600}$ ≠ 0.4 - 0.5)
pET19mod-DrrA	20°C	5 hrs	IPTG, 0.2 mM
pGEX-5X-3-R5BD739-862	27°C	o/n	IPTG, 1 mM (OD$_{600}$ = 0.8)
pGEX-5X-3-R5BD789-862	27°C	o/n	IPTG, 1 mM (OD$_{600}$ = 0.8)
pET15b-Rab5a17-184	27°C	o/n	IPTG, 1 mM
pDL2-Rab5c	20°C	16 hrs	IPTG, 0.05 mM
pASK-IBA-45plus-Rabaptin-5	21°C	o/n	AHT, 600 ng/ml
pGEX-5X-3-Rabaptin-5	37°C	5 hrs	IPTG, 0.1 mM
pDL2-Rabex-5$_{GEF}$	20°C	16 hrs	IPTG, 0.05mM

7.4.3   Preparation of cell lysate

7.4.3.1   *Cell harvest*

The cultivated bacteria were harvested by centrifugation at 8000 g and 4 °C for 20 - 30 minutes. The supernatant was discarded and pellets were frozen at -80 °C until they were used for protein purification.

7.4.3.2   *E.coli cell lysis*

For the purification of proteins from *E.coli*, the cells were lysed with French Press. To do so, the frozen cell pellet was resuspended in lysis buffer by vortexing until it was completely dissolved. The cell solution was sucked into the French Press chamber and released under a defined pressure (1200 - 1400 psi) through a small hole, thereby disrupting the cells. The lysate was cleared by centrifugation at 20,000 - 48,000 g at 4 °C (Table 17).

Buffer	Composition
Lysis buffer DrrA	50 mM Tris 300 mM NaCl
Lysis buffer Rabex-5$_{GEF}$	50 mM Tris, pH 7.8 at 4 °C 50 mM NaCl 0.1 % β-Mercaptoethanol
Lysis buffer Rab5c / Rab5a	50 mM Tris, pH 7.8 at 4 °C 50 mM NaCl 0.5 mM MgCl$_2$ 0.1 % β -Mercaptoethanol
Lysis buffer R5BD / GST-Rabaptin-5	25 mM Hepes, pH 7.4 100 mM NaCl 5 mM MgCl$_2$ 1 mM DTT
Lysis buffer Strep-Rabaptin-5	50 mM Tris pH 8.0 50 mM NaCl

7.4.4 Affinity chromatography

Affinity chromatography was used for the separation of fusion proteins carrying an affinity tag from all proteins not containing the affinity tag. The His-tag contains six or ten histidine amino acids and binds Ni NTA resin by complexing nickel ions immobilized on the matrix beads.[340] Glutathione S-transferase (GST) is a small protein that preferably binds to glutathione and was the second type of affinity tag used in this study.[341] Elution of the bound protein is achieved with a competitor: imidazole for his-tag proteins and glutathione for GST-fusion proteins, respectively.

Table 17   Lysate preparation and affinity chromatography.

Construct	Clearance of lysate	Tag	Incubation time on beads	Further protocol steps
pET19mod-DrrA	30 min 48,000 g	His	4 hrs, 4 °C	− Increase concentration − Dialysis to storage buffer (o/n, 4 °C)
pGEX-5X-3-R5BD739-862	15 min 48,000 g	GST	2 hrs, 4 °C	/
pGEX-5X-3-R5BD789-862	15 min 48,000 g	GST	2 hrs, 4 °C	/
pET15b-Rab5a17-184	40 min 20,000 g	His	1 hr, 4 °C	− Increase concentration − Gel-filtration − Increase concentration
pDL2-Rab5c	40 min 48,000 g	His	1 hr, 4 °C	− Increase concentration − Gel-filtration − Increase concentration
pASK-IBA-45plus-Rabaptin-5	15 min 27,000 g	Strep	/	/
pGEX-5X-3-Rabaptin-5	10 min 27,000 g	GST	o/n, 4 °C	− In case of elution further purified by − Gel-filtration
pDL2-Rabex-5GEF	40 min 48,000 g	His	1 hr, 4 °C	− Increase concentration − Gel-filtration − Increase concentration

7.4.4.1   Nickel affinity chromatography

The protein supernatant of a 2 L - culture was incubated for one hour at 4 °C under agitation with 5 mL Ni-NTA resin in a head-top-tumbler. Subsequently, the beads were transferred to a disposable column, and the supernatant was removed with a peristaltic pump. The flow-through (containing all unbound protein) was collected as well as the wash fraction (at least 100 times of the bead volume). For elution, one column volume elution buffer was mixed with the beads by adding the buffer, closing the column with a lit, patting it till beads were resuspended and subsequent collection of the eluate. This process was repeated using elution buffer with increasing imidazole concentrations; each imidazole concentration elution buffer was used two to three times.

Buffer	Composition
Wash buffer Rab5c / Rab5a	50 mM Tris, pH 8.5 at 4 °C 500 mM NaCl 10 mM Imidazole 0.5 mM MgCl$_2$ 0.1 % β-Mercaptoethanol
Elution buffer Rab5c / Rab5a	50 mM Tris, pH 8.5 at 4 °C 150 mM NaCl 0.5 mM MgCl$_2$ 10 / 30 / 60 / 100 / 150 / 200 / 300 mM Imidazole
Wash buffer Rabex-5GEF	50 mM Tris, pH 8.5 at 4 °C 500 mM NaCl 10 mM Imidazole 0.1 % β-Mercaptoethanol
Elution buffer Rabex-5GEF	50 mM Tris, pH 8.5 at 4 °C 150 mM NaCl 10 / 30 / 60 / 100 / 150 / 200 / 300 mM Imidazole

7.4.4.2 *Glutathione affinity chromatography*

1.33 mL of the Glutathione Sepharose 4B 75 % slurry were prepared for purification of protein supernatant of a 1 L culture by transferring to a falcon tube and sedimentation via centrifugation at 500 g for 5 min. The supernatant was carefully decanted and the sepharose was washed by addition of 10 mL cold GST-bead preparation buffer. Addition of 2 mL cold GST-bead preparation buffer resulted in a 50 % slurry (the 50 % slurry may be stored at 4 °C for up to one month). The 50 % slurry was mixed with the protein supernatant and incubated in the overhead tumbler o/n at 4 °C. The beads were transferred to a disposable column in the cold room and liquid was allowed to pass the column by gravity flow. The sepharose column was washed with 30 times the column volume of wash buffer. Elution of the protein was obtained by adding three times one column volume of the elution buffer and incubating 10 minutesat RT.

Buffer	Composition
GST-bead preparation buffer	25 mM Hepes, pH 7.4 5 mM MgCl$_2$ 1 mM DTT
Wash buffer R5BD / GST-Rabaptin-5	25 mM Hepes, pH 7.4 100 mM NaCl 5 mM MgCl$_2$
Elution buffer R5BD / GST-Rabaptin-5	25 mM Hepes, pH 7.4 100 mM NaCl 5 mM MgCl$_2$ 10 mM glutathione (reduced)

7.4.4.3 *Strep-Tactin affinity chromatography*

2 mL 50 % slurry Strep-Tactin Superflow High Capacity were pipetted into a disposable column at 4 °C while avoiding the trapping of air bubbles. After the storage buffer drained out by gravity flow, the column was equilibrated with 2 mL wash buffer and the lysate was loaded onto the column. After the complete lysate had entered the gel bed, the column was washed five times with 1 mL wash buffer. The protein was eluted by adding six times 0.5 mL elution buffer.

Buffer	Composition
Wash buffer Strep-Rabaptin-5	50 mM Tris pH 8.0 50 mM NaCl
Elution buffer Strep-Rabaptin-5	100 mM Tris pH 8.0 50 mM NaCl 5 mM Desthiobiotin

7.4.5 Gel filtration with FPLC

Proteins can be separated according to their size by gel filtration. The porous column material allows small molecules to enter the holes. In conclusion, they need more time to pass through the material and leave the column later than larger molecules. A Superdex200 column was used in the FPLC system to purify proteins. The Superdex200 column was equilibrated with 1.5 times column volumes storage buffer. In the meantime, the protein eluate from the affinity chromatography was pooled and concentrated with Amicon filters. The flow was reduced to 2.5 mL / min, the sample was loaded and the run was performed till one column volume had passed the Superdex200 column. Fractions of 1 - 5 mL size were collected and monitored for high UV absorbance at 280 nm. Fractions with high UV absorption were pooled, if necessary concentrated with Amicon filters, and analysed by SDS-PAGE.

Buffer	Composition
Storage buffer Rabex-5$_{GEF}$	50 mM Tris, pH 7.8 at 4 °C 100 mM NaCl Filtered and degased
Storage buffer Rab5c / Rab5a	50 mM Tris, pH 7.8 at 4 °C 100 mM NaCl 5 mM MgCl$_2$ Filtered and degased
Storage buffer R5BD / GST-Rabpatin-5	50 mM Tris pH 8.0 50 mM NaCl
Storage buffer Strep-Rabpatin-5	25 mM Hepes, pH 7.4 100 mM NaCl 5 mM MgCl$_2$

7.4.6 Exchange of buffer and protein storage

To exchange the buffer of a protein solution desalting columns (on the FPLC) or dialysis was used. For use of FPLC desalting columns, the protein solution was loaded onto the equilibrated desalting column and eluted with desired buffer. For dialysis, the protein solution was incubated in a dialysis tube o/n in an excess of the desired buffer. The membrane of the tube holds back the proteins but allows exchange of the buffer. Purified proteins were aliquoted, snap-frozen in liquid nitrogen, and stored at –80 °C.

7.5 Handling and analysis of proteins

7.5.1 Desalting and buffer exchange

For buffer exchange of protein samples, NAP columns were used that function according to the principle of gel filtration (described in Section 7.4.5). The columns were equilibrated with the desired buffer. Then, the samples were loaded and the sample was eluted according to the manufacturers' protocol.

7.5.2 Increase the concentration of protein samples

Amicon filters have an ultracel regenerated cellulose membrane with appropriate cut-offs to separate proteins and buffer. The concentration increase is achieved by centrifugation according to the manufacturers' protocol (3000 - 5000 rpm for falcons; $4,000 - 10,000\,g$ for 0.5 mL tubes). The membrane holds the protein back while the buffer volume is reduced. During the concentration process, the samples were mixed by inverting the tube every 5 minutes. This avoids precipitation of the protein at high concentrations because the steep gradient that forms in the filter is disturbed.

7.5.3 Determination of protein concentration

7.5.3.1 *Absorption*

The concentration of protein solutions can be calculated from the absorption at 280 nm using the law of Lambert-Beer (Section 7.3.8). For absorption measurements the photometer or the *NanoQuant* plate reader were used. As blank the appropriate buffer was used.

7.5.3.2 *Bradford assay*

The Bradford Assay has been designed to determine protein concentrations using the absorption of the Coomassie® Brilliant Blue G-250 that binds basic and aromatic amino acid residues.[342] The absorption maximum of the free dye (465 nm) shifts towards 595 nm upon encountering the protein.

The Bradford reagent was diluted 1:5 in water. 150 µL of Bradford solution were mixed with 2 µL of the protein in a 96-well plate. Subsequently, the absorbance at 595 nm was measured (*Varioskan* or *EnSpire* plate reader). For the determination of the protein concentration in lysates, these were pre-diluted 1:10. For quantification, a BSA standard was used (167 µg/mL – 3 mg/mL) and the standard curve was fitted using a quadratic polynomial equation.

7.5.3.3 *Precision Red™ Advanced Protein Assay*

For determination of the protein concentration 5 µL lysate (in general 1:4 diluted) were mixed with 295 µL of the precision red reagent in a 96 well plate. The plate was read out at 600 nm using the *NanoQuant* plate reader. The concentration of the cell lysate was calculated according to the following equation:

$$c \text{ [mg/mL]} = A \text{ [600 nm]} \bullet DF \bullet 7.5$$

DF = dilution factor, c = concentration, A = absorption, 7.5 = correction value

7.5.4 SDS-PAGE

Glycine SDS polyacrylamide gels were used to separate and analyse proteins according to the protocol of *Laemmli*.[343, 344] SDS (sodium dodecyl sulphate), an anionic detergent, was used to denaturate the proteins and charge them negatively. The negative charge corresponds to the protein length which allows separation dependent on the size of the protein. The gel consists of a stacking gel on top of a separating gel.

The percentage of the separating gel was adjusted between 6 % and 15 % according to molecular weight of the proteins. The gel mixture was prepared from appropriate amount of stock solutions (Table 18). Then, the polymerization was initiated by addition of APS and TEMED. The solution was cast between two glass plates held apart by spacers of 0.75 or 1 mm thickness. A thin layer of isopropanol was added to smooth the top of the separating gel. The stacking gel was cast after the polymerisation of the separating gel was complete. A comb was inserted to create wells for sample loading. After complete polymerization, the comb was removed and the gel was placed in a running chamber filled with cold 1 x Laemmli running buffer.

The protein samples were mixed with SDS-loading buffer and heated to 95 °C for 5 minutes. They were loaded onto the gel and a protein marker (3 µL) was used as size reference. The gel was run at 150 - 200 V until the bromophenol blue from the loading buffer reached the bottom of the gel. The gel was removed from glass plates and either stained with Coomassie blue (0.75 mm gels) or used for western blotting (1 mm gels) as described in Section 7.8.7.

Table 18   Stock solutions for SDS-PAA-gels.

Solution	Composition	Amount per 500 mL
Laemmli separating solution (4x)	1.5 M Tris, pH 8.8 14 mM SDS	90.86 g Tris 2 g SDS Set pH to 8.8
Laemmli stacking solution (4x)	0.5 M Tris, pH 6.8 14 mM SDS	30.3 g Tris 2 g SDS Set pH to 6.8
Laemmli running buffer (5x)	125 mM Tris 960 mM Glycine 17 mM SDS	7.6 g Tris 36 g Glycine 2.5 g SDS

Buffer	Composition	Amount per 200 mL
SDS-PAGE-loading buffer (6x), used for western blot	49.5 mM Tris pH 6.8 30 % Glycerol 15 % w/v SDS 600 mM DTT Bromophenol blue	140 mL 4x stacking buffer 60 mL Glycerol 30 g SDS 18.6 g DTT (reduced) 24 mg Bromophenol blue
SDS-PAGE-loading buffer (4x), used for Coomassie stained gels	250 mM Tris, pH 8.0 40 % Glycerol 8 % w/v SDS 25 % v/v β-ME Bromophenol blue	50 mL 1 M Tris, pH 8.0 80 mL Glycerol 16 g SDS 40 mL β-ME Bromophenol blue

Table 19   Composition of SDS-PAA-gels.

1 gel	Separating gel						stacking gel 4%
	6 %	7.5 %	8 %	10%	12.5 %	15 %	
Acrylamide mix (30 %)	1000 µL	1250 µL	1333 µL	1667 µL	2083 µL	2500 µL	213 µL
Water	2712 µL	2462 µL	2379 µL	2045 µL	1629 µL	1212 µL	975 µL
Separating buffer (4 x)	1250 µL						-
Stacking buffer (4 x)	-						400 µL
APS (10 % w/v)	8 µL						2 µL
TEMED	30 µL						10.4 µL

2 gels	Separating gel						stacking gel 4%
	6 %	7.5 %	8 %	10%	12.5 %	15 %	
Acrylamide mix (30 %)	2000 µL	2500 µL	2667 µL	3333 µL	4167 µL	5000 µL	427 µL
Water	5424 µL	4924 µL	4757 µL	4091 µL	3257 µL	2424 µL	1948 µL
Separating buffer (4 x)	2500 µL						-
Stacking buffer (4 x)	-						800 µL
APS (10 % w/v)	16 µL						4 µL
TEMED	60 µL						20.8 µL

4 gels	Separating gel						stacking gel 4%
	6 %	7.5 %	8 %	10%	12.5 %	15 %	
Acrylamide mix (30 %)	4000 µL	5000 µL	5333 µL	6667 µL	8333 µL	10000 µL	853 µL
Water	10848 µL	9848 µL	9515 µL	8181 µL	6515 µL	4848 µL	3897 µL
Separating buffer (4 x)	5000 µL						-
Stacking buffer (4 x)	-						400 µL
APS (10 % w/v)	31 µL						8 µL
TEMED	120 µL						41.6 µL

7.5.5   Staining of PAA-gels

7.5.5.1   *Coomassie stain*

The protocol for this staining was modified from *Current Protocols in Molecular Biology*.[345] The gels were stained in Coomassie solution for about 30 minutes under agitation. Subsequently, the gel was rinsed and incubated in destaining solution until the protein bands became distinct. A paper towel added to the destaining solution helped to remove the dye which was not bound to the proteins. The gels were scanned using the *Odyssey Scanner*. For preservation, the gel was placed onto a piece of blotting paper and heated for two hours at 80 °C under vacuum on a gel dryer.

Solution	Composition
Destaining solution	300 mL methanol 100 mL acetic acid 600 mL water
Coomassie solution	Destaining solution with 700 mg/L Coomassie brilliant blue G-250

7.5.5.2   *Coomassie stain for in gel digest (MS)*

The PageBlue™ can detect protein in the range of 5 to 500 ng and is about ten-times more sensitive than traditional Coomassie staining methods. The gels were stained according to manufacturer's protocol by being washed three times with water (10 min) and stained for 60 minutes in ready to use PageBlue™ protein staining solution. The gel was incubated in water o/n without agitation and was subsequently washed in fresh water until the bands became distinct. The bands of interest were cut with a surgical blade and treated according to the trypsin digest protocol (Section 7.7.4.1.2).

7.6   Nucleotide exchange assays

Nucleotide exchange assays were used to monitor the activity of GEF proteins. Therefore, the exchange of GDP for GTP (or equivalent) on their corresponding GTPase is measured.

7.6.1   Tryptophan fluorescence assays

The tryptophan fluorescence of the GTPase that changes upon GTP binding is used as readout.

7.6.1.1   *Rab5-Rabex-5GEF nucleotide exchange assay*

Rabex-5GEF can catalyse the nucleotide exchange on the GTPases Rab5a and Rab5c. The assay was performed as described before with slight modifications in buffer and readout for the screening assay.[136] The Rabex-5 nucleotide exchange buffer (5 x) was prepared, filtered through a 0.45 µm membrane and degassed. Rabex-5GEF was used in

concentrations between 20 nM and 0.5 µM, Rab5 at a constant concentration (1 µM). The compounds were added in DMSO to a final concentration of 2 % DMSO. Proteins and compounds / DMSO were incubated for 5 minutes at RT before starting the measurement by injection of GppNHp (100 µM final concentration (f.c.)). GppNHp was used as nucleotide because it cannot be hydrolysed by the GTPase. The reaction is measured using the *Varioskan* plate reader at 290 nm excitation and 340 nm emission wavelengths. The slit width was 12 nm.

DMSO is hygroscopic and absorbs water if not stored properly. In the context of the nucleotide exchange assay this was important because the presence of DMSO decreased the exchange rate and thus exact reproducible amounts of DMSO were required. To ensure the purity, anhydrous DMSO (analytical grade, Acros Organics, Belgium) was purchased. Additionally, DMSO was taken from the storage bottle under argon. This setting worked most reliable for the nucleotide exchange assay and was used in all assays during the re-screening process and after.

Table 20   Protocol of the nucleotide exchange assay with Rabex-5GEF-Rab5c.

Reagent (working concentration)	Final concentration	Volume	Protocol step (plate reader)	Wavelength
Rab5 (2.5µM) in 2.5 x buffer	1 µM	20 µL		
Compound in DMSO (100 %)	2 % DMSO	1 µL		
Rabex-5GEF (50 nM) in water	20 nM	20 µL		
			5 min incubation at RT Mix reaction manually	
			Fluorescence measurement (*Varioskan*), t=0	290 nm / 340 nm
GppNHp (500 µM) in water	100 µM	10 µL	Injection by dispenser	
			Kinetic loop: fluorescence measurement (*Varioskan*), 100 repeats over ten minutes	290 nm / 340 nm

Buffer	Composition
Rabex-5 nucleotide exchange buffer (1 x)	20 mM Tris, pH 8.0 at RT 100 mM NaCl 2 mM MgCl$_2$ 0.25 % Tween20

7.6.1.2   *Cytohesin-2-Arf1 nucleotide exchange assay*

The GEF Cytohesin-2 can catalyse the nucleotide exchange on the GTPase Arf1. To increase the measurement window the GTPase was pre-loaded with GDP. The assay was performed with slight modifications as described before.[346] The Sec7 domain of Cytohesin-2 was used in this assay at a final concentration of 14.4 nM and Arf1 at 1.8 µM. The pre-loading procedure (Table 21) was performed just prior to the nucleotide exchange assay (Table 22). After mixing the proteins and the compounds/DMSO the measurement

was started by injection of GTP (100 μM f.c.). The reaction was measured using the *Varioskan* plate reader at 290 nm / 340 nm.

Table 21   Pre-loading of Arf1 with GDP.

Reagent (working concentration)	Final concentration	Mixture (30 wells)	Protocol step
PBS (1 x)	1 x	1346.7 μL	
Δ17Arf1 (471 μM)	7.15 μM	22.8 μL	
EDTA, pH 8 (500 mM)	2 mM	6.0 μL	
GDP (1000 μM)	80 μM	120.0 μL	
			Incubate 15 min at 37 °C (10 % shaking in *GFL*-thermomixer)
MgCl₂ (1000 mM)	3 mM	4.5 μL	
			Incubate 5 min at 37 °C (10 % shaking in *GFL*-thermomixer)
			Use directly for nucleotide exchange

Table 22   Protocol of the Cytohesin-2-Arf1 nucleotide exchange assay.

Reagent (working concentration)	Final concentration	Volume	Protocol step (plate reader)	Wavelength
PBS, 3 mM MgCl₂		89 μL		
Compound in DMSO (100 %)	0.5 % DMSO	1 μL		
Cytohesin-2 (72 nM)	14.4 nM	40 μL		
Arf-Mix, preloaded (7.15 μM)	1.8 μM	50 μL		
			Fluorescence measurement (*Varioskan*), t=0	290 nm / 340 nm
GTP (500 μM)	100 μM	20 μL		
			Kinetic loop: fluorescence measurement (*Varioskan*), 100 repeats	290 nm / 340 nm

7.6.2   BodipyGDP assays

The fluorescence of BodipyGDP is quenched when free in solution but its fluorescence intensity increases upon binding to the GTPase.

7.6.2.1   *DrrA-Rab1 nucleotide exchange*

The GTPase Rab1 (final 50 nM) was incubated in exchange buffer (25 mM Hepes pH 8.0, 50 mM NaCl, 5 mM MgCl₂, 0.05 % Tween20) with 50 μM DrrA and the compound (1 % DMSO final) in a total volume of 40 μL. After 5 minutes incubation at RT the exchange reaction was initiated by addition of 10 μL BodipyGDP (2.5 μM, Jena Biosciences, Germany). The fluorescence was read over 10 minutes at 500 / 520 nm (*Varioskan* plate reader). For analysis, the nonlinear Fit-One Phase association (*GraphPad Prism* software) was used. For the negative control, the mean plateau of the positive control was used as constrain. The IC_{50} was calculated from plotting the k_{obs} versus the logarithmic compound concentration.

Table 23   Protocol of the DrrA-Rab1 nucleotide exchange assay.

Reagent (working concentration)	Final concentration	Volume	Protocol step (plate reader)	Wavelength
Rab1 (125 nM) in 2.5 x buffer	50 nM	20 µL		
Compound / DMSO (50 %)	1 % DMSO	1 µL		
DrrA (125 µM) in water	50 µM	20 µL		
			5 min incubation at RT	
			Fluorescence measurement (*Varioskan*), t=0	500 nm / 520 nm
GppNHp (2.5 µM) in water	0.5 µM	10 µL	Injection by dispenser	
			Kinetic loop: fluorescence measurement (*Varioskan*), 100 repeats	500 nm / 520 nm

7.6.2.2   *Vav1-Rac1 nucleotide exchange assay*

This exchange process is catalysed by the GEF protein Vav1. The protocol was kindly provided by *Björn Niebel* and had been adapted from *Niebel, 2011*.[260] Vav1 was used at 150 nM and Rac1 at 5 µM. The final buffer was 1 x PBS, 1 mM $MgCl_2$ and 0.001 % Tween20. The compounds were added in DMSO to a final concentration of 1 % DMSO. The proteins and compounds / DMSO were incubated for 10 minutes at RT before starting the measurement by injection of BodipyGDP (50 nM f.c.). The reaction was measured using the *Varioskan* plate reader at 500 nm excitation and 520 nm emission wavelengths. The exchange reaction was analysed by fitting the kinetic with the One Phase Decay model (*GraphPad Prism* software) and plotting obtained k_{obs} values against logarithmic inhibitor concentrations.

Table 24   Protocol of the Vav-1-Rac1 nucleotide exchange assay.

Reagent (working concentration)	Final concentration	Volume	Protocol step (plate reader)	Wavelength
Rac1 (5 µM) in 1.25 x buffer	1 µM Rac1	20 µL		
Compound in DMSO (50 %)	1 % DMSO	1 µL		
Vav1 (375 nM) in 1.25 x buffer	150 nM	20 µL		
			10 min incubation at RT	
			Shake 10 s (*Varioskan*)	
			Fluorescence measurement (*Varioskan*), t=0	290 nm / 340 nm
GppNHp (500 µM) in water	100 µM	10 µL	Injection by dispenser (13%)	
			Kinetic loop: fluorescence measurement (*Varioskan*), 100 repeats every 20 s	290 nm / 340 nm

7.6.3   Radioactive Rabex-5GEF-Rab5c nucleotide exchange assay

In this assay, a radioactive, non-hydrolysable nucleotide (GTPγ^{35}S) is used for the readout of the nucleotide exchange. The same reaction buffer was used as in Section 7.6.1.1. Proteins and compounds were mixed according to Table 25. Proteins and compounds / DMSO were incubated for 5 minutes at RT before adding GTPγ^{35}S. The reaction was further incubated for 5 minutes at RT. Then, loading buffer was added and samples were transferred to a 15 % native PAA-gel. The PAA gel was prepared with slight modifications in the Tris buffer compared to the suggested procedure from *Current Protocols in Molecular Biology*.[347] The gel was run for 7 hours at 15 mA and 50 V in an ice bath. The gel was removed from the glass plates and wrapped in saran wrap. It was incubated with a phosphorimaging screen for detection o/n before the phosphorimager readout and data analysis with the Aida-Software. The radioactive intensity signals were normalized to the total amount of radioactivity per sample, which was monitored by scintillation counting. For scintillation counting an aliquot of each sample was mixed with 1 mL scintillation cocktail. Each sample was processed three times for 3 minutes.[16]

Table 25   Protocol of the nucleotide exchange assay with Rabex-5GEF-Rab5c.

Reagent (working concentration)	Protocol step	Volume
Rab5c (2.5 µM)		15 µL
Compound / DMSO (100 %)		0.75 µL
Rabex-55GEF (1.3 µM)		15 µL
	5 min incubation at RT	
GTPγ^{35}S (1250Ci/mmol, 12.5mCi/ml, diluted 1:50)		7.5 µL
	5 min incubation at RT	
Coomassie loading buffer (5x)		7.5 µL
	A) sample was loaded onto native PAA-gel B) sample was mixed with 1 mL scintillation cocktail (6 mL vials) for quantification of absolute radioactivity	5 µL each

Reagent	Native PAA separating gel (15 %)	Native PAA stacking gel (5 %)
Water	2.5 mL	2.75 mL
Bis-acrylamide mix (30 %)	5.0 mL	0.67 mL
1.5 M Tris, pH 9.2	2.5 mL	0.5 mL
APS (10 % w/v)	100 µL	16 µL
TEMED	10 µL	7 µL

Buffer	Composition
Coomassie loading buffer (5x)	6.7 mg Coomassie G-250 3 mL Glycerol 7 mL water

---

[16] As GTPγ^{35}S is a very volatile molecule it was not possible to use the filter retention method to analyse the incorporation of ^{35}S into Rab5c. It was also not possible to use Ni-NTA columns for binding of the protein via their His tags and subsequent scintillation-count of the eluate.

7.7 Molecular interaction analysis

7.7.1 Microscale thermophoresis (MST)

7.7.1.1 General introduction to MST

In MST, a fairly new immobilization free technique for the analysis of interaction between biomolecules, the movement of molecules within an optically generated temperature gradient is used to analyse binding events.[238] The thermophoretic movement is dependent on the hydration shell, charge and size of the molecules.[238] Interactions generally alter size, stability or conformation of the molecules leading to changes in the hydration shell and thus in the thermophoretic movement. The temperature gradient is induced by an IR-Laser which is strongly absorbed by water causing movement of the molecules.[348] The thermophoretic movement and its changes are detected by the fluorescence signal of one interaction partner while the other ligand is unlabelled. Ideally, the fluorescent interaction partner is kept at a constant concentration while the concentration of the unlabelled interaction partner is varied.

7.7.1.2 Labelling of proteins with fluorescent groups

As fluorescent dyes for the labelling of proteins, Fluorescein-NHS-ester, Fluorescein isothiocyanate (FITC), and Alexa Fluor®647-NHS-ester were used. If necessary, the storage buffer of the protein was replaced by Hepes buffer (25 mM Hepes, 100 mM NaCl, 5 mM $MgCl_2$, pH 7.3 at 10 °C) using NAP5 columns (Section 7.5.1). The reactive dye was added in three fold excess over the protein. 100 µL protein-dye-mix were incubated with 10 µL $NaHCO_3$ (1 M, pH 8.3 w.c.) for 60 - 90 minuteson ice. The excess of the dye was removed by NAP5 columns.

7.7.1.3 MST measurement

The fluorescently labelled proteins (100 nM f.c.) were mixed with a serial dilution of the compound of interest. The samples were filled into capillaries and incubated for 5 minutes in the Monolith NT.115 MST instrument before starting the capillary scan to localize the capillaries and to confirm the quality of the samples. Irregular capillary features indicated that the protein might stick to the capillary wall which is disadvantageous. For those samples, the assay preparation had to be modified because this irregularity in fluorescence is likely to produce artefacts. Immediately after the capillary scan, the measurement was started with 50 % LED, 60 % Laser, 30 / 30 s Laser on / off. As buffer the 1 x Rabex-5 activity reaction buffer (Section 7.6.1.1) was supplemented with 500 nM BSA.

7.7.1.4 Data analysis

Thermophoresis (including temperature jump) was calculated from the ratio of cold fluorescence (3 seconds interval) to hot fluorescence at the equilibrium (3 seconds interval, Figure 53A). The temperature jump was calculated from fluorescence ratios hot fluorescence right after switching on the laser to cold fluorescence (Figure 53B).

Thermophorsis or temperature jump data were plotted against the compound concentration All measurements were analysed regarding thermophoresis with jump unless indicated otherwise. Sigmoidal binding curves were fitted to obtain the K_d using the *GraphPad Prism* Software, 4 parameter-equation

$$Y = Bottom + (Top-Bottom) / (1+10^{((LogEC50-X)\bullet Hill Slope)}$$

wherein EC_{50} is the equivalent parameter for K_d.
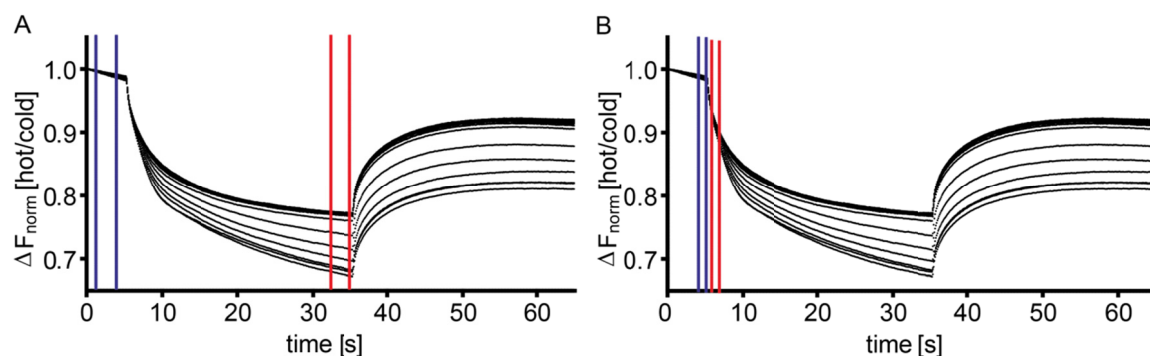
Figure 53   Curser settings for MST data analysis.
Curser settings are shown in blue for cold fluorescence and red for hot fluorescence. **A)** Curser settings used for thermophoresis with jump analysis. Normalized hot fluorescence (3 seconds interval) is divided by normalized cold fluorescence (3 seconds interval). **B)** Curser setting for the analysis of temperature jump was used according to Nanotemper definition.

7.7.2   ITC measurements

The protein was dialysed into ITC buffer o/n at 4 °C The compound was diluted in this dialysis buffer after dialysis of the protein. The protein concentration was determined and DMSO was added to the protein solution in comparable amounts to the compound-buffer solution to obtain equal buffer conditions in both the protein and the compound solution. The cells of the ITC were rinsed with the dialysis buffer and the protein was filled into the sample cell. The reference cell was filled with dialysis buffer. The compound solution was filled into the syringe and the syringe was assembled into the ITC. The sample was stirred at 25 °C until a stable baseline was reached (about two hours) prior to starting the injection mode. For analysis, a compound in buffer measurement was performed and subtracted as baseline. The data was fitted using the independent equation of the *NanoAnalyze* software.

7.7.3   Size exclusion chromatography

For analysis of natural protein complexes, size exclusion chromatography (SEC) was performed using an in-house prepared 5 mL SEC column on the HPLC system.[349] The column was equilibrated with the desired buffer and proteins were injected to monitor the retention times of the single proteins. For analysis of complex formation, the proteins were mixed and incubated for 10 minutes at RT prior to injection. For analysis of the exact protein content of the peaks, fractions were collected and precipitated with trichloroacetic

acid (TCA, 5 % f.c.) by incubation for 30 minutes on ice with subsequent 10 minutes centrifugation at 4 °C and 20,000 g. The pellet was resuspended in 1.5 M Tris, pH 9.2 and SDS-PAGE loading buffer (4 x) for analysis by SDS-PAGE with subsequent Coomassie stain.

7.7.4 Detection of covalent binding via mass spectroscopy

7.7.4.1 *Analysis of undigested protein using MALDI-TOF*

7.7.4.1.1 *Preparation of samples for MALDI-TOF*

The protein (5 µM / 50 µM) was incubated with JH5 (100 µM) or DMSO as control in 1 x Rabex-5 nucleotide exchange buffer and incubated for one hour at RT. To remove the majority of the Tween20 from the buffer, 50 mg Amberlite® XAD®-2 beads were prepared for each sample by equilibration in 2 x 500 µL methanol, 2 x 500 µL water and 1 x 500 µL Rabex-5 nucleotide exchange buffer (w/o Tween20). The equilibration was obtained by incubation for 1 - 3 minutes at RT and sedimentation at 1,000 g in a table-top centrifuge. The samples were incubated with the beads o/n at 4 °C in an over-head tumbler. The protein solution was recovered by centrifugation for 5 minutes at 500 g and carefully transferring the supernatant to a fresh tube. If necessary, this step was repeated to remove all residues of the Amberlite® XAD®-2 beads. Purification by ZipTips further increased the quality and concentration of the samples. Therefore, the ZipTip was prepared by wetting the ZipTip two times with ACN by carefully pipetting ACN up and emptying the solution onto a clean paper towel. To equilibrate the ZipTip it was washed twice the same way in 0.1 % trifluoroacetic acid (TFA). 10 µL of the protein samples was acidized with 1 µL of 1 % TFA and carefully loaded on the ZipTip membrane by pipetting up and down for ten times. The ZipTip was washed three times with 0.1 % TFA and the protein was eluted in 5 µL 0.1 % TFA / 50 % ACN. The sample was dried in the speed vac and resuspended in 5 µL 0.1 % formic acid (FA). 1 µL of the sample was mixed with 1 µL of α-Cyano-4-hydroxycinnamic acid (HCCA) matrix and spotted onto the target. Data acquisition and analysis was performed by Marc Sylvester (Institute of Biochemistry and Molecular Biology (IBMB), University of Bonn).

7.7.4.1.2 *DACM labelling of the proteins*

To verify if a mass-shift of the size of the compounds would be visible, the proteins were labelled with the fluorescent dye N-(7-dimethylamino-4-methylcoumarin-3-yl))-maleimide (DACM) which has with 298.3 g/mol approximately the same molecular weight as JH5. A 25 mM DACM solution was prepared and the proteins were incubated with different amounts of DACM (1:1, 1:3, 1:10) and incubated for two hours at RT in the dark. As buffer, the nucleotide exchange buffer w/o Tween20 was titrated to a pH of 7.0. The proteins were supposed to be purified with NAP columns from excess of dye, however, the DACM precipitated and was removed by centrifugation. As an excess of DACM led to precipitation of the protein, the samples with the equimolar amount of dye were used for the MS measurements. The labelling of the protein was verified by

measurement of the absorption at 381 nm. The protein samples were treated as described above (Section 7.7.4.1.1).

7.7.4.2   Protein treatment protocol for MS

5 μM Rabex-5GEF were incubated with 200 μM JH5 for 30 to 60 minutes at RT. The nucleotide exchange assay was performed to confirm the successful inhibition of Rabex-5GEF. In case of intended alkylation,[350] the samples (100 μL) were incubated with urea (48 mg) and Tris buffer (10 μL, 1 M, pH 8.5) for 10 minutes at RT. The alkylation was performed with 3.6 % acrylamide final concentration for 2 hours at RT. The samples were purified with G25 columns and submitted to non-reducing SDS-PAGE. The samples were cut from the gel and digested as described in the next section. However, the alkylated samples were additionally reduced and treated with iodoacteamide prior to the digestion.

7.7.4.3   Trypsin-digested protein samples for MS

The protocol was kindly provided by *Marc Sylvester* and is adapted from *Shevchenko et al* and *Rosenfeld et al*.[351, 352] 100 mM Ammonium bicarbonate (NH_4HCO_3) solution was freshly prepared and used the same day. Protein samples were prepared by SDS-PAGE (non-reducing). The bands of interest were cut from the gel with a clean blade and transferred to a clean tube. The gel slices were crushed with a pipette tip and washed with 50 % ACN (100 μL) for 1 minute. The supernatant was discarded and 100 % ACN (100 μL) was added and the samples were incubated for 5 minutes to shrink the gel pieces. The supernatant was discarded followed by washing with 50 % ACN for about 5 minutes. In case of Coomassie residues, an optional washing step with 100 mM NH_4HCO_3 was added. The gel pieces were shrunken completely with 50 - 100 μL ACN (100 %) for 5 minutes. The supernatant was discarded and the gel pieces were dried for 10 minutes in the speedvac. 20 μL trypsin solution (20 ng/μL in 50 mM NH_4HCO_3, 9 % ACN) were added. After gel had taken up the trypsin solution 50 μL NH_4HCO_3 were added. The samples were incubated o/n at 37 °C. The supernatant was transferred to a fresh tube and dried in the speedvac. The samples were stored at -20 °C till analysis. Data acquisition and analysis was performed by Marc Sylvester (Institute of Biochemistry and Molecular Biology (IBMB), University of Bonn). For most experiments, the digesting procedure was performed by Marc Sylvester.

7.8   Mammalian cell culture

7.8.1   Cultivation of mammalian cell lines

The cells were grown at 37 °C and 5 % CO_2 and passaged every 2 - 3 days when they reached a maximal confluency of 70 % to 90 %.[353] Therefore, the cells were rinsed with PBS and detached from the culture flask. All cells were detached by the use of Trypsin-EDTA solution except for Hek293 cells which were treated with PBS + 5 mM EDTA. The cells were incubated with the detachment solution for a few minutes at 37 °C and full culture medium was added. The cells were separated by pipetting and an appropriate

amount of cells were plated in a culture flask. The culture medium and the cell lines were used as described in Section 7.1.10.3.

7.8.2   Testing for mycoplasma

The mycoplasma test was performed with culture medium that had been incubated with the cells for at least 48 hours. The test was performed according to the manufacturers' protocol and is illustrated in Table 26 and Table 27.

Table 26   Reaction mix for the mycoplasma test PCR.

Reagent	Volume
Reaction buffer, 10 x	2.5 μL
dNTP-primer mix	2.5 μL
Internal control DNA	2.5 μL
Cell culture supernatant	2.0 μL
Polymerase	0.2 μL
Water	ad 25 μL

Table 27   Cycle conditions for the mycoplasma test PCR.

Step	Temperature	Time	Repeats
initial denaturation	94 °C	2 min	No repeat
Denaturation	94 °C	30 s	
Annealing	55 °C	30 s	40 cycles
Elongation	72 °C	30 s	

7.8.3   Transfection with DNA plasmids

Transfection allows the uptake of foreign nucleic acids into mammalian cells. This is achieved by the use of cationic lipids that are able to form liposomes. Furthermore, they can form complexes with nucleic acids which can interact with the cell membrane due to their positive charges and can be taken up by the eukaryotic cells via endocytosis.[354]

The cells were seeded in an appropriate culture dish and incubated in standard culture medium with FCS o/n at 37 °C and 5 % CO_2 (day 1). On the following day (day 2) the cells were transfected with plasmid DNA and metafectene according to manufacturers' protocol. In order to do so, the DNA resuspended in medium without FCS was added to the metafectene pre-mixed in the same amount of FCS-free medium. The complete reaction mix was incubated 20 minutes at RT, and then drop-wise added to the cells in full medium. On the subsequent day, the cells were starved in RPMI + 0.1 % FCS (day 3) and cultured till used for the desired experiment on day 4.

Cell type	Number of cells seeded	culture size	Nucleic acid	medium for dilution	Transfection reagent
Hek293	$1.3 * 10^6$	6 cm dish	Plasmid, 3.2 μg	DMEM, 200 μL	Metafectene, 9.6 μL
Hek293	$3.5 * 10^6$	10 cm dish	Plasmid, 8.6 μg	DMEM, 500 μL	Metafectene, 25.7 μL

7.8.4 Stimulation with EGF

The cells were starved in the appropriate culture medium with 0.1 % FCS o/n so that they were about 80 % confluent at the time of stimulation. One hour before the stimulation the starvation medium was refreshed to remove growth factors produced by the cells. Only 50 % of the normal volume of medium was added at this time to minimize the amount of growth factors required. Then, the cells were stimulated with EGF (100 ng/mL f.c.) for the indicated time by adding the growth factor directly to the culture medium.[163] The cells were harvested immediately to the end of the desired stimulation time.

Cell type	Number of cells seeded[17]	culture size	Total volume
HeLa	$0.35 - 0.7 * 10^6$	6 cm dish	4 mL
HeLa	$0.72 - 1.00 * 10^6$	10 cm dish	12 mL
Sk-BR-3	$1.00 * 10^6$	6 cm dish	4 mL

7.8.5 Preparation of cell lysates

7.8.5.1 Standard lysis for western blotting

For the preparation of lysates the cells were harvested by scraping in ice cold PBS and subsequently transferred to a pre-chilled tube. The cells were sedimented by centrifugation at 500 g for 5 minutesin a cooled centrifuge (4 °C). The supernatant was discarded and the pellet was resuspended in an appropriate amount of 1 x lysis buffer.[355] The cells were incubated for 20 minutes on ice followed by clarification of the lysate by centrifugation for 20 minutes at 14,000 g and 4 °C. The supernatant was transferred to a new tube and the protein concentration was determined by Bradford analysis. The protein concentration was normalized and lysates were diluted with water if necessary. The lysate samples were mixed with SDS-PAGE-loading buffer (6x), heated for 5 - 10 minutesat 95 °C and loaded onto SDS-PAA-gels.

Buffer	Composition
5 x Lysis buffer	100 mM Tris, pH 7.5 750 mM NaCl 5 mM EDTA 5 mM EGTA *Mix Tris, NaCl, EDTA and EGTA and set pH* 12.5 mM sodium pyrophosphate 5 mM β-glycerophosphate 5 mM sodium vanadate 5 % (v/v) Triton X-100

---

[17] The number of cells ideal for the experiment was dependent on the FCS batch used at the time of the experiment.

7.8.5.2 *Lysis according to the GLISA protocol*

For the pull-down assays with effector proteins rapid processing of the samples at 4 °C is necessary. This is due to the fact that GTP bound to GTPases is prone to hydrolysis during and after cell lysis. The fast lysis protocol from the GLISA assay (Cytoskelton, Inc) was used for effector pull-down assays. At the time of harvest, cells were placed on ice and all media was aspirated. The cells were immediately rinsed with an appropriate volume of ice-cold PBS (e.g. 1 mL for a 6 cm dish) and the PBS was thoroughly aspirated while keeping the plates embedded in ice. An optimized volume (e.g. 130 µL for a 6 cm dish) of lysis buffer supplemented with protease inhibitor cocktail (100 x stock, 1 x final concentration) was added. The cells were scraped off the culture dish while the dish was kept embedded in ice. The lysate was transferred to a pre-chilled tube and immediately centrifuged in a cooled (4 °C) centrifuge at 10,000 *g* for 1 min. The supernatant was transferred to a fresh, pre-chilled tube and snap frozen. Prior to freezing, a 12 - 20 µL aliquot of each sample was taken for determination of protein concentration using the Precision Red™ Advanced Protein Assay (Cytoskeleton, Inc).

7.8.6 R5BD pull-down targeting active Rab5

The effector protein pull-down approach allows quantification of activated GTPase within cell lysate. Therefore, the lysate will be incubated with an appropriate effector protein which will only bind its corresponding GTPase loaded with GTP. The activation status of the GTPase can be monitored by comparing the total amount of the GTPase found in the cell lysate with the amount of GTPase that can be fished from the lysate with the effector protein. This indirectly monitors the activity of the corresponding GEF protein.

7.8.6.1 *In vitro assay setup*

The matrix was prepared by washing 160 µL 25 % GST-R5BD789-862[246] sepharose slurry (650 µM / 100 % slurry) with 10 times the column volume (400 µL) in Hepes exchange buffer. For sedimentation before and after the washing step the beads were centrifuged for 5 minutesat 500 *g*. Resuspension of the beads in one column volume (40 µL) yielded 80 µL of 50 % slurry.

The nucleotide exchange assay was set up according to Table 28 using the 1 x Rabex-5 nucleotide exchange buffer (Section 7.6.1.1) and incubated 5 minutesat RT before starting the reaction by addition of GppHNp. After 2 minutesthe reaction was stopped by placing all samples on ice. During the 2 minutesreaction time, 15 µL samples were taken as loading control and mixed directly with 5 µL 4 x SDS-PAGE loading buffer. The stopped reaction was immediately diluted in 900 µL Hepes exchange buffer, mixed with the prepared R5BD-slurry and incubated for 30 minutes at 4 °C in an overhead-tumbler. The sepharose beads were washed in 200 µL Hepes exchange buffer and the supernatant was discarded. The sepharose was resuspended in 20 µL 4 x SDS-PAGE loading buffer, heated to 95 °C and used for western blotting.

Table 28   Nucleotide exchange assay for R5BD pull-down.

Assay step	Assay component (working concentration)	Final concentration	Amount (µL)				
Nucleotide exchange	Rab5c (2.5 µM) in 2.5 x buffer	1 µM	0	40	0	40	40
	Rabex-5 (e.g. 250 nM) in water	100 nM	0	0	40	40	40
	Compound in DMSO (100 %)	1 % DMSO	2	2	2	2	2
	Water		80	40	40	0	20
	0.5 mM GppNHp in water	100 µM	20	20	20	20	0
Pull-down	50 % slurry (3.25 nmoles R5BD)		10	10	10	10	10

Buffer	Composition
Hepes Exchange Buffer (1x)	25 mM Hepes pH 7.4, 100 mM NaCl, 5 mM $MgCl_2$, 0.25 % Tween

7.8.6.2   *Pull-down from cell lysate*

The Hek cells from a 10 cm dish were lysed according to GLISA lysis protocol and 500 µg lysate per sample was either directly submitted to pull-down or loaded *in vitro* with nucleotides (Table 29). The R5BD sepharose was in general prepared as described above (Section 7.8.6.1) with exception to be diluted to a final concentration of 10 % slurry. The pull-down reaction was incubated for 30 minutes at 4 °C under agitation. Subsequently, the sepharose beads were washed in 200 µL Hepes exchange buffer and the supernatant was discarded. The samples were resuspended in 23 µL 2 x SDS PAGE loading buffer of which 20 µL were submitted to western blotting.

Table 29   Protocol for in vitro loading with nucleotides and R5BD pull-down from lysate.

Assay step	Assay component (working concentration)	Final concentration	Protocol step	Control	Nucleotide loading
In vitro loading with nucleotide	Cell lysate			500 µg	500 µg
	EDTA (500 mM)	37.5 mM			10 µL
	Nucleotide (10 mM)	375 µM			5 µL
	Water			ad 165 µL	ad 133 µL
			Incubation 3 min at 30 °C		
	$MgCl_2$ (1 M)	194 mM			32
			Incubation 1 min on ice		
Pull-down	Beads 10 % slurry (3.25 nmoles R5BD)			55 µL	55 µL

7.8.7   Immunoblotting

For the detection, analysis and quantification of proteins in cell lysates immunoblots were performed. The protein concentration of the lysate was determined using either the Bradford assay (Section 7.5.3.2) or the Precision Red™ Advanced Protein Assay (Section 7.5.3.3). The lysates were normalized according to their protein concentration and run on 1 mm thick SDS-PAA gels (Section 7.5.4). Instead of staining the gels, the proteins

were transferred onto a nitrocellulose membrane by either semi-dry blotting or wet blotting technique as described below. After blotting, the membrane was blocked for either one hour at RT or o/n at 4 °C in 5 % BSA or 5 % milk depending on the optimal conditions for the desired antibody (Section 7.1.9.1). This was followed by incubation with the desired antibody dilution (Section 7.1.9.1) in the same blocking reagent o/n at 4 °C. The membranes were washed three times for about 5 minutes with TBST and incubated roughly one hour at room temperature with the secondary antibodies (Section 7.1.9.2). After washing three times with TBST the blots were either read out using the *Odyssey scanner* or enhanced chemiluminescence (ECL) reaction was performed in case of HRP-secondary antibodies. Therefore, each 500 μL of ECL reagent A and ECL reagent B were mixed and incubated on the blot for 2 minutes before monitoring the ECL signal with the *VersaDoc 5000 CCD camera*. The protein bands were quantified using the *QuantityOne* software.

7.8.7.1 *Semi-dry blotting*

To transfer the proteins from the SDS-PAA gel onto a nitrocellulose membrane the technique of discontinuous blotting described by Kyhse-Andersen [356] was used with slight modifications in the buffer system. Therefore, the gel was stacked between different layers of blotting papers, equilibrated in the indicated buffer (Table 30). The transfer was achieved by applying a constant power of 2 mA/cm^2 gel (6 x 9 cm gel: 108 mA) for 45 minutesat RT.

Buffer	composition	Amount per litre
Cathode buffer, semi-dry	25 mM Tris, pH 9.4 40 mM Glycin	3.03 g Tris 3 g Glycine *KOH to set pH*
Anode buffer I, semi-dry	300 mM Tris, pH 10.4	36.3 g Tris *HCl to set pH*
Anode buffer II, semi-dry	25 mM Tris, pH 10.4	3.03 g Tris *KOH to set pH*
Cathode buffer, wet blot, 10 x	250 mM Tris 1920 mM glycine	30.3 g Tris 144 g glycine
10 x TBS	200 mM Tris pH 7.6 1.36 M NaCl	
1 x TBST	20 mM Tris pH 7.6 136 mM NaCl Tween20 0.1% v/v	100 mL 10x TBS 1 mL Tween20
5 % BSA/milk (w/v)	5 g BSA/milk per 100 mL TBST *BSA can be supplemented with 0.02 %* *Thimerosal for long term storage*	50 g BSA/milk Diluted in 1 x TBST

7.8.7.2 *Wet blotting*

2 L of cold 1 x cathode buffer, which is a methanol-free variant of the Towbin buffer, were prepared for one wet blot tank.[357] The gel was equilibrated in cathode buffer: for each blot two pieces of blotting paper (10 x 7 cm) and one piece of nitrocellulose membrane

(10 x 7 cm) were soaked in cold cathode buffer together with two sponges per gel holder. The blot was assembled in the gel-holder while being completely immersed in cold cathode buffer. The cathode side of the gel-holder (black) was positioned on the bottom, upon which a sponge, one piece of blotting paper, the PAA gel, the nitrocellulose membrane, the second piece of blotting paper, the second sponge, and the anode part of the gel holder (red) were pilled (Table 30). During the assembly all air bubbles were completely removed. The gel-holder was placed into the blotting tank, filled with cold cathode buffer and supplemented with one cool pack (-80 °C) and a magnetic stir bar. The blotting procedure was performed at 100 V and 2000 mA for 60 minutesat 4 °C.

Table 30   Assembly of the semi dry and the wet (tank) transfer systems for blotting.

Semi dry transfer system	Wet (tank) transfer system
Cathode	
3 blotting papers in Cathode buffer	Sponge
Gel in Cathode buffer	blotting paper
nitrocellulose membrane in Anode II buffer	Gel
2 blotting papers in Anode II buffer	nitrocellulose membrane
1 blotting paper in Anode I buffer	blotting paper
	Sponge
Anode	

7.8.8   Transferrin and EGF internalization assay

The protocol was kindly provided by *Katia Schöler*. 100,000 HeLa cells were seeded per 6-well (day 1) on a 6-well plate and cultivated for 24 hours. The cells were starved o/n with 0.1 % FCS and treated with the compounds for 2 hours (day 3) prior to the transferrin treatment. They were washed once with 2 mL PBS and incubated with 300 µL transferrin solution (50 µg/mL Alexa488-Transferrin in PBS, supplemented with the compound at desired concentration in 2 % DMSO) that had been shortly centrifuged before use to remove aggregates. The incubation with transferrin was performed for 30 minutes at either 37 °C or on ice under agitation. After the incubation, the cells were washed three times with 2 mL PBS (the cells incubated at 4 °C cells were kept on ice during that step) and detached by addition of 0.5 mL Trypsin-EDTA solution for several minutes at 37 °C. The reaction was stopped by addition of 2 mL RPMI + 10 % FCS and cells were transferred to flow cytometry tubes for centrifugation.

For the EGF internalization assay, HeLa cells were prepared as described for the transferrin assay. Sk-BR-3 cells were treated similarly, however, 400,000 cells were seeded per 6-well. After compound treatment, the cells were incubated with Alexa647-EGF (100 ng/mL, supplemented with compound) for the indicated times at either 4 °C or 37 °C. The cells were washed once with cold RPMI (1 mL), twice with 2 mL acetic acid (0.2 M, pH 4.5 titrated with acetic acid), and once with cold RPMI (2 mL). They were detached with 0.5 mL Trypsin/EDTA at 37 °C. The reaction was stopped with 1 mL RPMI + 10 % FCS and transferred to flow cytometry tubes. This EGF internalization protocol was inspired by reported procedures.[103, 358, 359]

7.8.9   Flow cytometry

After the desired treatment, the cells were collected by centrifugation at $300\,g$ for 5 minutes, resuspended in 200 μL PBS by pipetting and vortexed immediately prior to flow cytometry analysis. The flow cytometry analysis was performed on the *BD FACSCanto II* with the parameters as indicated in Table 31. For each sample 10,000 events were recorded at medium flow rate,while the sit flush was on.

Table 31   Parameters for flow cytometry analysis.

Parameter	FCS	100 V
	SSC	335 V
	FITC	346 V
Threshold	FSC	5000
Laser	Blue laser current	1.3 (measured & reference)
	Blue laser power	20.38 (measured & reference)
	Red laser power	16.09 (measured), 18.00 (reference)
	Violet laser power	59.13 (measured), 59.11 (reference)

8 APPENDIX

8.1 Plasmids

8.1.1 pDL2-Rab5c and pDL2-Rabex-5GEF
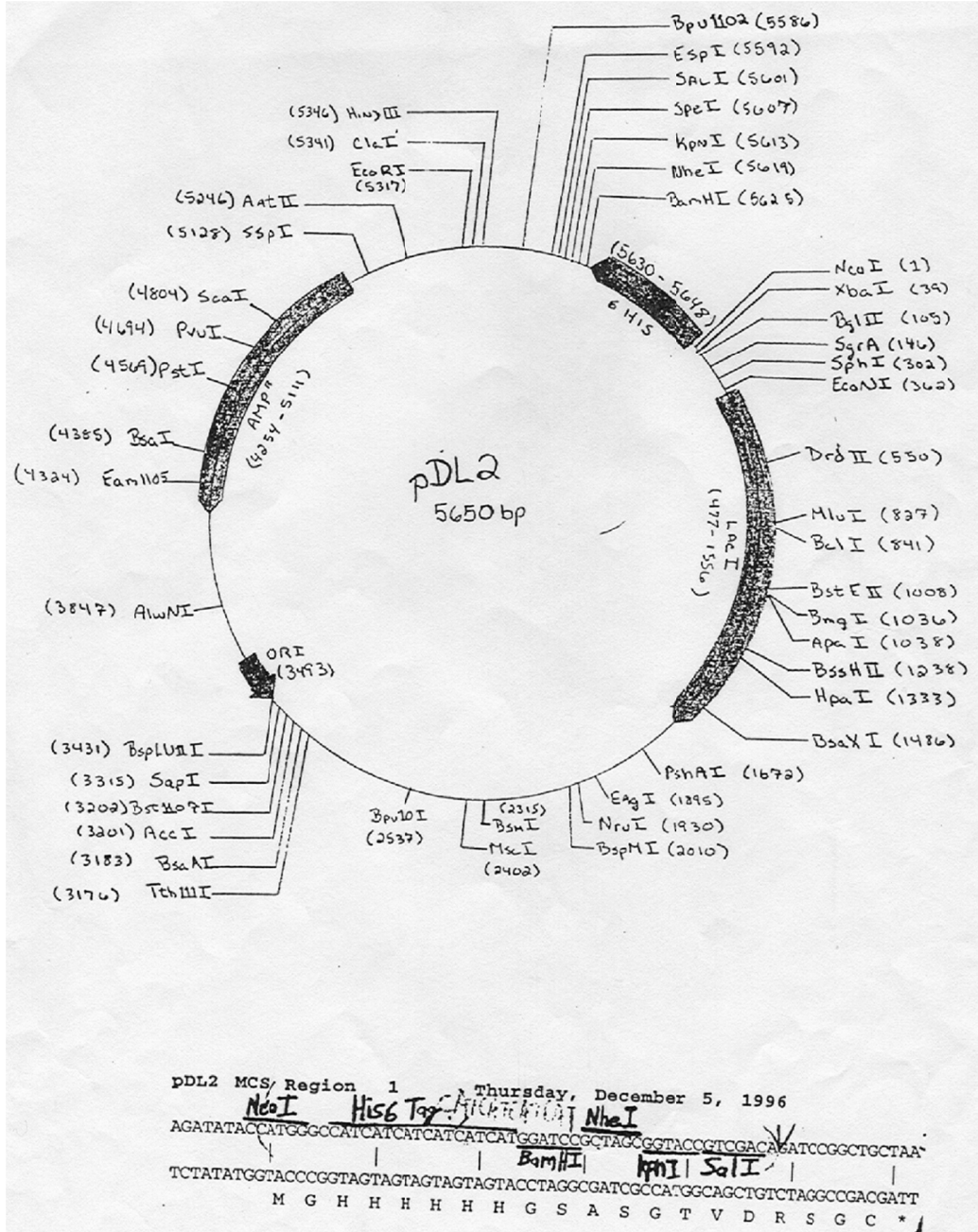
Supporting figure 1   pDL2 plasmid vector map.

```
ATCGGTGATGTCGGCGATATAGGCGCCAGCAACCGCACCTGTGGCGCCGGTGATGCCGGCCACGATGC
GTCCGGCGTAGAGGATCGAGATCTCGATCCCGCGAAATTAATACGACTCACTATAGGGGAATTGTGAG
CGGATAACAATTCCCCTCTAGAAATAATTTTGTTTAACTTTAAGAAGGAGATATACCatgGGCcatca
tcatcatcatcatGGATCCATTGAAACGGATAGAGTGTCTAAGGAGTTCATAGAATTTCTCAAGACCT
TCCACAAGACAGGCCAAGAAATCTATAAACAGACCAAGCTGTTTTTGGAAGGAATGCATTACAAAAGG
GATCTAAGCATTGAAGAACAGTCAGAGTGTGCTCAGGATTTCTACCACAATGTGGCCGAAAGGATGCA
AACTCGTGGGAAAGTGCCTCCAGAAAGAGTCGAGAAGAATAATGGATCAGATTGAAAAGTACATCATGA
CTCGTCTCTATAAATATGTATTCTGTCCAGAAACTACTGATGATGAGAAGAAAGATCTTGCCATTCAA
AAGAGAATCAGAGCCCTGCGCTGGGTTACGCCTCAGATGCTGTGTGTCCCTGTTAATGAAGACATCCC
AGAAGTGTCTGATATGGTGGTGAAGGCGATCACAGATATCATTGAAATGGATTCCAAGCGTGTGCCTC
GAGACAAGCTGGCCTGCATCACCAAGTGCAGCAAGCACATCTTCAATGCCATCAAGATCACCAAGAAT
GAGCCGGCGTCAGCGGATGACTTCCTCCCCACCCTCATCTACATTGTTTTGAAGGGCAACCCCCCACG
CCTTCAGTCTAATATCCAGTATATCACGCGCTTCTGCAATCCAAGCCGACTGATGACTGGAGAGGATG
GCTACTATTTCACCAATCTGTGCTGTGCTGTGGCTTTCATTGAGAAGCTAGACGCCCAGTCTTTGAAT
CTAAGTCAGGAGGATTTTGATCGCTACATGTCTGGCCAGACCTCTCCCtaaGTGAGTCGACAGATCCG
GCTGCTAACAAAGCCCGAAAGGAAGCTGAGTTGGCTGCTGCCACCGCTGAGCAATAACTAGCATAACC
CCTTGGGGCCTCTAAACGGGTCTTGAGGGGTTTTTTGCTGAAAGGAGGAACTATATCCGGATATCCCG
CAAGAGGCCCGGCAGTACCGGCATAACCAAGCCTATGCCTACAGCATCCAGGGTGACGGTGCCGAGGA
TGACGATGAACGCATTGTTAGATTTCATACACGGTGCCTGACTG


T7-promotor    start     his-tag     BamHI     Rabex-5     stop     SalI
```

Supporting figure 2   pDL2-Rabex-5 (aa132-391) DNA sequence.
The DNA sequence presented here is the result of sequencing and includes the full insert sequence. The Rabex-5GEF construct did not show any mutations with respect to the NCBI database entry (NM_014504.2).

```
TATCATGCCATACCGCGAAAGGTTTTGCGCCATTCGATGGTGTGTCCGGGATCTCGACGCTCTCCCTTATGC
GATTCCTGCATTAGGAAGCAGCCCAGTAGTAGGTTGAGGCCGTTGAGCACCGCCGCCGCAAGGAATGGTG
CATGCAAGGAGATGGCGCCCAACAGTCCCCCGGCCACGGGGCCTGCCACCATACCCACGCCGAAACAAGC
GCTCATGAGCCCGAAGTGGCGAGCCCGATCTTCCCCATCGGTGATGTCGGCGATATAGGCGCCAGCAACC
GCACCTGTGGCGCCGGTGATGCCGGCCACGATGCGTCCGGCGTAGAGGATCGAGATCTCGATCCCGCGAA
ATTAATACGACTCACTATAGGGGAATTGTGAGCGGATAACAATTCCCCTCTAGAAATAATTTTGTTTAAC
TTTAAGAAGGAGATATACCatgGGCcatcatcatcatcatcatcatcatcatcatGGATCTCTGGTGCCG
CGCGGATCCAAGATCTGTCAGTTTAAGCTGGTCCTATTGGGCGAGTCTGCCGTGGGCAAGTCCAGCCTGG
TCCTCCGCTTTGTCAAGGGGCAGTTCCATGAGTACCAGGAGAGCACAATTGGAGTGGCTTTCCTCACACA
GACTGTCTGCTTAGACGATACAACGGTCAAGTTTGAGATCTGGGACACAGCTGGCCAAGAGCGCTATCAC
AGCCTGGCCCCGATGTACTATCGGGGGGCCCAAGCAGCCATTGTGGTCTATGACATCACCAACACAGATA
CATTTGCACGGGCTAAGAATTGGGTGAAGGAGTTACAGAGGCAGGCCAGCCCCAACATCGTCATTGCACT
AGCGGGGAACAAAGCAGACCTGGCCAGCAAGAGAGCTGTGGAGTTTCAGGAAGCACAAGCCTATGCAGAT
GACAACAGCTTGCTCTTCATGGAGACGTCTGCCAAGACTGCAATGAACGTGAATGAAATTTTCATGGCAA
TAGCTAAGAAGCTTCCCAAGAATtaaGTGAGTCGACAGATCCGGCTGCTAACAAAGCCCGAAAGGAAGCT
GAGTTGGCTGCTGCCACCGCTGAGCAATAACTAGCATAACCCCTTGGGGCCTCTAAACGGGTCTTGAGGG
GTTTTTTGCTGAAAGGAGGAACTATATCCGGATATCCCGCAAGAGGCCCGGCAGTACCGGCATAACCAAG
CCTATGCCTACAGCATCCAGGGTGACGGTGCCGAGGATGACGATGAGCGCATTGTTAGATTTCATACACG
GTGCCTGACTGCGTTAGCAATTTAACTGTGATAAACTACCGCATTAAAGCTTATCGATGATAAGCTGTCA
AACATGAGAATTCTTGAAGACGAAAGGGCCTCGTGATACGCCTATTTTTATAGGTTAATGTCATGATAAT
AATGGTTTCTTAGACGTCAGGTGGCACTTTTCGGGGAAATGTGCG


T7-promotor    start     his-tag     BamHI     Rab5c     mutation
stop     SalI
```

Supporting figure 3   DNA sequence pDL2-Rab5c (aa18-185) – original.
The DNA sequence presented here was the result of sequencing and includes the full insert sequence. The Rab5c sequence contained two mutations in comparison to the sequence given in the NCBI data base (NCBI Reference Sequence: NM_024456.4) of which the first mutation at the nucleotide 87 (nt87) was a silent mutation. However, the second mutation (nt176) resulted in an Ala64Val mutation (the aa notation refers to the full-length Rab5c protein) from alanine to valine.

151

```
GAATCGTGAGTCTGGCTTGGTCACCCACGCGGAACCGTCTGATAAGAGACAACGCATACTTGCGGACATC
GTATAACGTACTGGTTTCACATTCACCAGCTGAATTGACTCTCTCCCGGCGCTATCATGCCATACCGCGA
AAGTTTTGCGCCATTCGATGGTGTCCGGGATCTCGACGCTCTCCCTTATGCGACTCTGCATTAGGAAGCA
GCCCAGTAGTAGGTTGAGGCCGTTGAGCACCGCCGCCGCAAGGAATGGTGCATGCAAGGAGATGGCGCCC
AACAGTCCCCCGGCCACGGGGCCTGCCACCATACCCACGCCGAAACAAGCGCTCATGAGCCCGAAGTGGC
GAGCCGATCTTCCCCATCGGTGATGTCGGCGATATAGGCGCCAGCAACCGCACCTGTGGCGCCGGTGAT
GCCGGCCACGATGCGTCCGGCGTAGAGGATCGAGATCTCGATCCCGCGAAAT```TAATACGACTCACTATAG
G```GGAATTGTGAGCGGATAACAATTCCCCTCTAGAAATAATTTTGTTTAACTTTAAGAAGGAGATATACC**a**
**tg**GGCcatcatcatcatcatcatcatcatcatcatGGATCTCTGGTGCCGCGC**GGATCC**AAGATCTGTCA
GTTTAAGCTGGTCCT**A**TTGGGCGAGTCTGCCGTGGGCAAGTCCAGCCTGGTCCTCCGCTTTGTCAAGGGG
CAGTTCCATGAGTACCAGGAGAGCACAATTGGAGTGGCTTTCCTCACACAGACTGTCTGCTTAGACGATA
CAACGGTCAAGTTTGAGATCTGGGACACAGCTGGCCAAGAGCGCTATCACAGCCTGGCCCCGATGTACTA
TCGGGGGGCCCAAGCAGCCATTGTGGTCTATGACATCACCAACACAGATACATTTGCACGGGCTAAGAAT
TGGGTGAAGGAGTTACAGAGGCAGGCCAGCCCCAACATCGTCATTGCACTAGCGGGGAACAAAGCAGACC
TGGCCAGCAAGAGAGCTGTGGAGTTTCAGGAAGCACAAGCCTATGCAGATGACAACAGCTTGCTCTTCAT
GGAGACGTCTGCCAAGACTGCAATGAACGTGAATGAAATTTTCATGGCAATAGCTAAGAAGCTTCCCAAG
AATtaaGTGA***GTCGAC***AGATCCGGCTGCTAACAAAGCCCGAAAGGAAGCTGAGTTGGCTGCTGCCACCGC
TGAGCAATAACTAGCATAACCCCTTGGGGCCTCTAAACGGGTCTTGAGGGGTTTTTTGCTGAAAGGAGGA
ACTATATCCGGATATCCCGCAAGAGGCCCGGCAGTACCGGCATAACCAAGCCTATGCCTACAGCATCCAG
GGTGACGGTGCCGAGGATGACGATGAGCGCATTGTTAGATTTCATACACGGTGCCTGACTGCGTTAGCAA
TTTAACTGTGATAAACTACCGCATTAAAGCTTATCGATGATAAGCTGTCAAACATGAGAATTCTTGAAGA
CGAAAGGGCCTCGTGATACGCCTATTTTTATAGGTTAATGTCATGATAATAATGGTTTCTTAGACGTCAG
GTGGCACTTTTCGGGGAAATGTGCG


*T7-promotor*        **start**        his-tag        **BamHI**        Rab5c        **mutation**
stop        ***SalI***
```
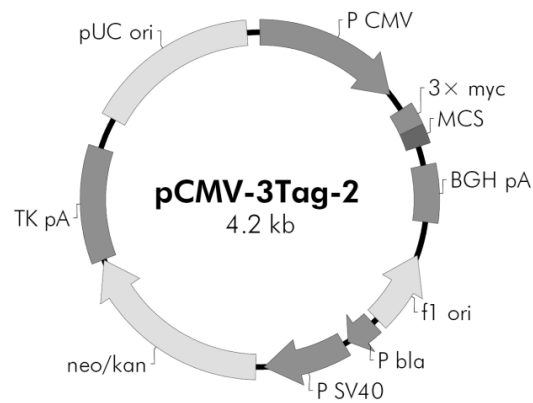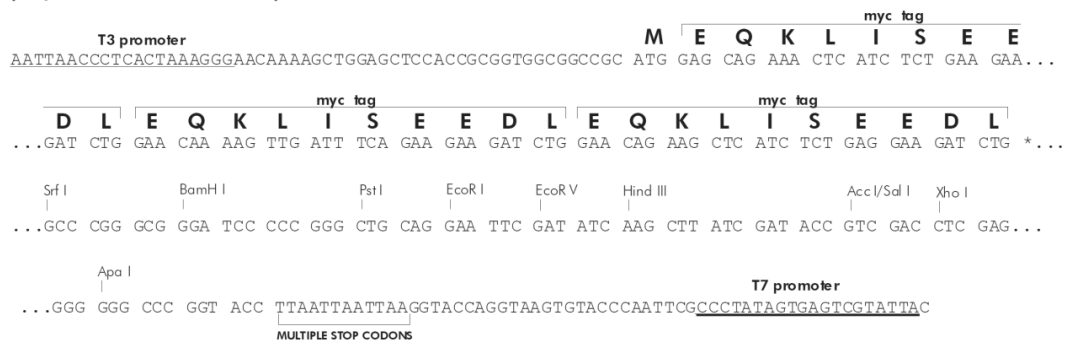
Supporting figure 4   DNA sequence pDL2-Rab5c (aa18-185) – mutation removed.[18]

The DNA sequence presented here was the result of sequencing and includes the full insert sequence. The Rab5c sequence contained two mutations in comparison to the sequence given in the NCBI data base (NCBI Reference Sequence: NM_024456.4).The Ala64Val mutation was removed by site-directed mutagenesis and the correct sequence was confirmed by sequencing. Self-evidently, the correct form of Rab5c was the only construct used in this study.

8.1.2   pCMV3Tag2a-Rabex-5-FLplasmid[19]

Supporting table 1   pCMV-3Tag-2 plasmid specifications.

Feature	Nucleotide Position
CMV promoter	1–602
T3 promoter and T3 primer binding site [5′ AATTAACCCTCACTAAAGGG 3′]	620–639
3× c-myc tag	678–767
multiple cloning site	768–842
T7 promoter and T7 primer binding site [3′ CGGGATATCACTCAGCATAATG 5′]	886–907
BGH polyA signal	922–1148
f1 origin of ss-DNA replication	1287–1593
bla promoter	1618–1742
SV40 promoter	1762–2100
neomycin/kanamycin resistance ORF	2135–2926
HSV-thymidine kinase (TK) polyA signal	2930–3385
pUC origin	3514–4181

---

[18] Named clone 8 (QC) in labbook of Christine Wosnitza

[19] Cloning was kindly performed by Nicole Krämer.

pCMV-3Tag-2 Multiple Cloning Site Region
(sequence shown 620–907)

* In pCMV-3Tag-2A, no bases inserted; in pCMV-3Tag-2B, A inserted; in pCMV-3Tag-2C, AA inserted

Supporting figure 5   **Map and multiple cloning site of the pCMV-3Tag-2 vector.**

```
aattaaccctcactaaagggaacaaaagctggagctccaccgcggtggcggccgcatggagcagaaactc
atctctgaagaagatctggaacaaaagttgatttcagaagaagatctggaacagaagctcatctctgagg
aagatctggcccgggcgggatcccccgggctgcagatgagccttaagtctgaacgccgaggaattcatgt
ggatcaatcggatctcctgtgcaagaaaggatgtggttactacggcaaccctgcctggcagggtttctgc
tccaagtgctggagggaagagtaccacaaagccaggcagaagcagattcaggaggactgggagctggcgg
agcgactccagcgggaggaagaagaggcctttgccagcagtcagagcagccaaggggcccaatccctcac
attctccaagtttgaagaaaagaaaaccaacgagaagacccgcaaggttaccacagtgaagaaattcttc
agtgcatcttccagggtcggatcaaagaaggaaattcaggaagcaaaagctcccagtccttccataaacc
ggcaaaccagcattgaaacggatagagtgtctaaggagttcatagaatttctcaagaccttccacaagac
aggccaagaaatctataaacagaccaagctgttttttggaaggaatgcattacaaaagggatctaagcatt
gaagaacagtcagagtgtgctcaggatttctaccacaatgtggccgaaaggatgcaaactcgtgggaaag
tgcctccagaaagagtcgagaagataatggatcagattgaaaagtacatcatgactcgtctctataaata
tgtattctgtccagaaactactgatgatgagaagaaagatcttgccattcaaaagagaatcagagccctg
cgctgggttacgcctcagatgctgtgtgtccctgttaatgaagacatcccagaagtgtctgatatggtgg
tgaaggcgatcacagatatcattgaaatggattccaagcgtgtgcctcgagacaagctggcctgcatcac
caagtgcagcaagcacatcttcaatgccatcaagatcaccaagaatgagccggcgtcagcggatgacttc
ctccccaccctcatctacattgttttgaagggcaaccccccacgccttcagtctaatatccagtatatca
cgcgcttctgcaatccaagccgactgatgactggagaggatggctactatttcaccaatctgtgctgtgc
tgtggctttcattgagaagctagacgcccagtctttgaatctaagtcaggaggattttgatcgctacatg
tctggccagacctctcccaggaagcaagaagctgagagttggtctcctgatgcttgcttaggcgtcaagc
aaatgtataagaacttggatctcttgtctcagttgaatgaacgacaagaaaggatcatgaatgaagccaa
gaaactggaaaaagacctcatagattggacagatggaattgcaagagaagttcaagacatcgttgagaaa
tacccactggaaattaagcctccgaatcaaccgttagcagctattgactctgaaaacgttgaaaatgata
aacttcctccaccactgcaacctcaagtttatgcaggatgagtcgacctcgagggggggcccggtacctt
aattaattaaggtaccaggtaagtgtacccaattcgccctatagtgagtcgtattac
```

PstI   <u>Rabex-5-FL</u>   *SalI*

Supporting figure 6   **pCMV3Tag2a-Rabex-5-FL insert sequence.**
The DNA sequence presented here was the result of sequencing and includes the full insert sequence.

8.1.3   pcDNA5/FRT/TO-Rab5-FL

Supporting table 2   pcDNA5/FRT/TO-Rab5-FL plasmid specifications.[20] [335]

Gene/insert name	Rab5A
Insert size	647
Species	*Homo sapiens*
Fusion protein or tag	3xFlag
Terminal	C terminal on insert
Vector backbone	pcDNA5/FRT/TO
Backbone manufacturer	Invitrogen
Vector type	Mammalian Expression
Backbone size w/o insert (bp)	5137
5' sequencing primer	CMV-F
3' sequencing primer	BGH-rev
Bacterial resistance	Ampicillin
High or low copy	High Copy
Selectable markers	Hygromycin

```
GTCGACGAGCTCGTTTAGTGAACCGTCAGATCGCCTGGAGACGCCATCCACGCTGTTTTGACCTCCATAG
AAGACACCGGGACCGATCCAGCCTCCGGACTCTAGCGTTTAAACTTAAGCTTGGTACCGAGCTCGGATCC
ATGGCTAGTCGAGGCGCAACAAGACCCAACGGGCCAAATACTGGAAATAAAATATGCCAGTTCAAACTA
GTACTTCTGGGAGAGTCCGCTGTTGGCAAATCAAGCCTAGTGCTTCGTTTTGTGAAAGGCCAATTTCATG
AATTTCAAGAGAGTACCATTGGGGCTGCTTTTCTAACCCAAACTGTATGTCTTGATGACACTACAGTAAA
GTTTGAAATATGGGATACAGCTGGTCAAGAACGATACCATAGCCTAGCACCAATGTACTACAGAGGAGCA
CAAGCAGCCATAGTTGTATATGATATCACAAATGAGGAGTCCTTTGCAAGAGCAAAAAATTGGGTTAAAG
AACTTCAGAGGCAAGCAAGTCCTAACATTGTAATAGCTTTATCGGGAAACAAGGCCGACCTAGCAAATAA
AAGAGCAGTAGATTTCCAGGAAGCACAGTCCTATGCAGATGACAATAGTTTATTATTCATGGAGACATCC
GCTAAAACATCAATGAATGTAAATGAAATATTCATGGCAATAGCTAAAAAATTGCCAAAGAATGAACCAC
AAAATCCAGGAGCAAATTCTGCCAGAGGAAGAGGAGTAGACCTTACCGAACCCACACAACCAACCAGGAA
TCAGTGTTGTAGTAACGGCGGCCGCGACTACAAAGACCATGACGGTGATTATAAAGATCATGACATCGAC
TACAAGGATGACGATGACAAGTGACTCGAGTCTA
```

Rab5a-FL   **silent mutation**

**Supporting figure 7   pcDNA5/FRT/TO-Rab5-FL DNA insert sequence.**
The DNA sequence presented here was the result of sequencing and includes the full insert sequence.

---

[20] Plasmid and plasmid information obtained from Addgene, Cambridge, MS, USA

8.1.4   pET15b-Rab5a(aa17-184)

pET-15b sequence landmarks

T7 promoter	463-479
T7 transcription start	452
His•Tag coding sequence	362-380
Multiple cloning sites	
(*Nde* I - *Bam*H I)	319-335
T7 terminator	213-259
lacI coding sequence	(866-1945)
pBR322 origin	3882
bla coding sequence	4643-5500
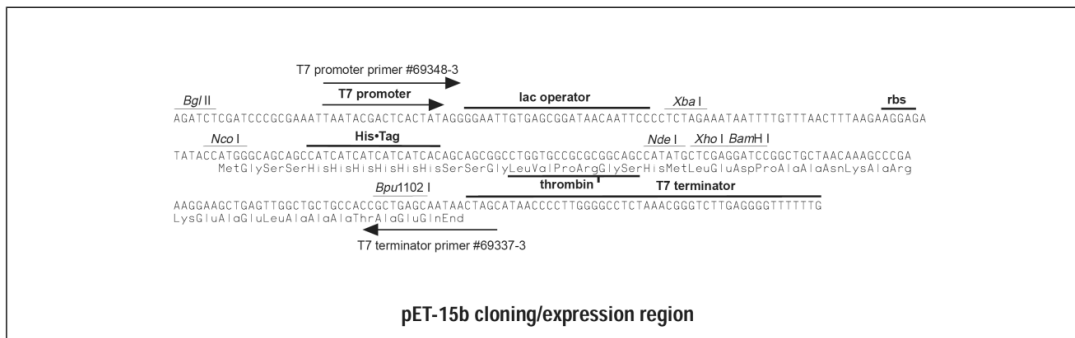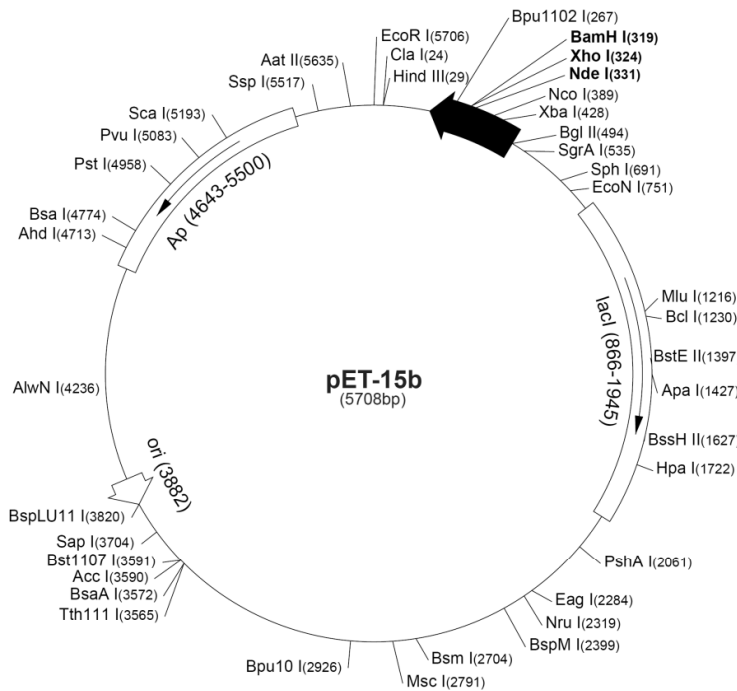
**Supporting figure 8   Map and multiple cloning site of the pET-15b vector.**

```
TTTTGTTtACTTtAAGAAGGAGATATACCATGGGCAGCAGCCATCATCATCATCATCACAGCAGCGGCC
TGGTGCCGCGCGGCAGCCATATGAAAATATGCCAGTTCAAACTAGTACTTCTGGGAGAGTCCGCTGTTG
GCAAATCAAGCCTAGTGCTTCGTTTTGTGAAAGGCCAATTTCATGAATTTCAAGAGAGTACCATTGGGG
CTGCTTTTCTAACCCAAACTGTATGTCTTGATGACACTACAGTAAAGTTTGAAATATGGGATACAGCTG
GTCAAGAACGATACCATAGCCTAGCACCAATGTACTACAGAGGAGCACAAGCAGCCATAGTTGTATATG
ATATCACAAATGAGGAGTCCTTTGCAAGAGCAAAAAATTGGGTTAAAGAACTTCAGAGGCAAGCAAGTC
CTAACATTGTAATAGCTTTATCGGGAAACAAGGCCGACCTAGCAAATAAAAGAGCAGTAGATTTCCAGG
AAGCACAGTCCTATGCAGATGACAATAGTTTATTATTCATGGAGACATCCGCTAAAACATCAATGAATG
TAAATGAAATATTCATGGCAATAGCTAAAAAATTGCCAAAGAATTAAGGATCCGGCTGCTAACAAAGCC
CGAAAGGAAGCTGAGTTGGCTGCTGCCACCGCTGAGCAATAACTAGCATAACCCCTTGgGGCCTCTAnA
CGGGTCTTGAGGgGTTtTTTGCTGAAAGGAGGAACTATATCCGGATATCCCGCAAGAGGCCCGGCAGTA
CCGGCATAACCAAGCCTATGCCTACAGCATCCAGgGTGACGGTGCCGAGGATGACGATGAGCGCATTGT
TAGATTTCATACACGGTGCCTGACTGCGTTAGCAATTTAACTGTGATAAACTACCGCATTAAAGCTTAT
CGATGAT
```

His-tag   **NdeI**   Rab5a   ***BamHI***

Supporting figure 9   pET15b-Rab5a (aa17-184) DNA insert sequence.
The DNA sequence presented here was the result of sequencing and includes the full insert sequence.

155

8.1.5   pET19mod-DrrA plasmid map
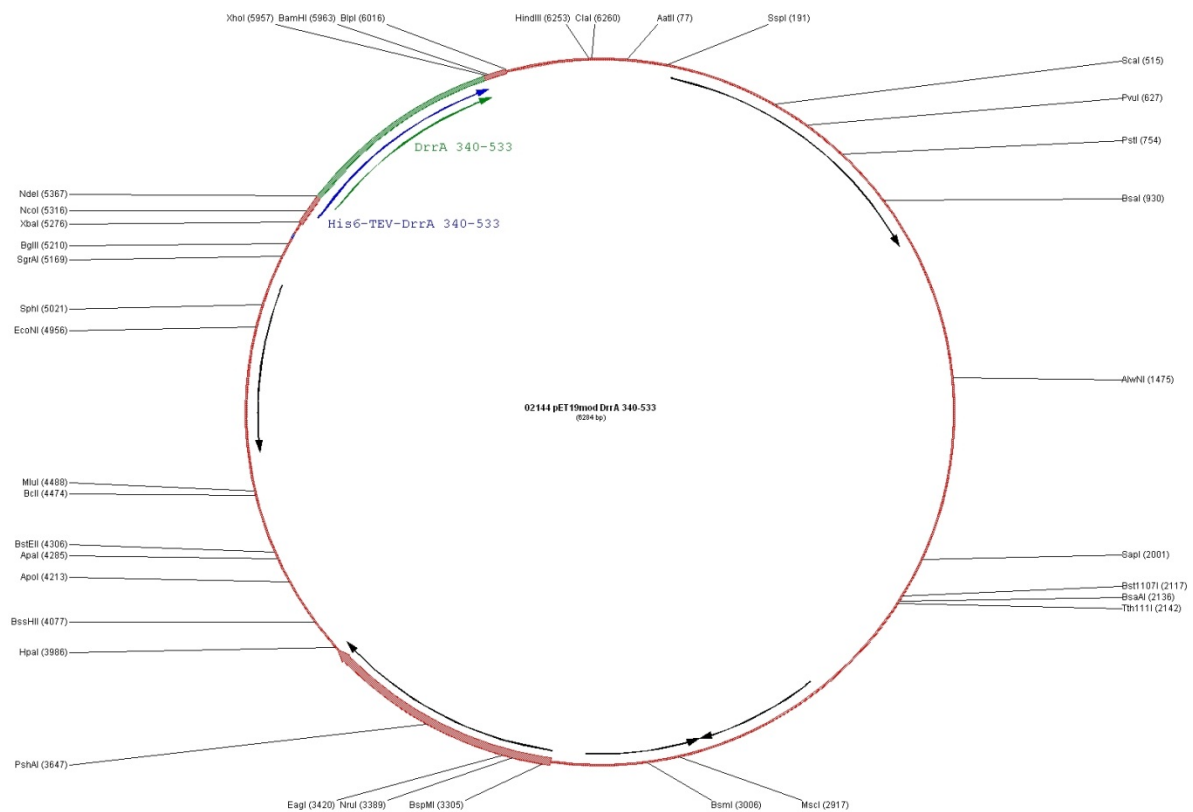
Supporting figure 10   Map of the pET19mod-DrrA plasmid. [21]

8.2   Protein sequences and parameter

8.2.1   Predicted Vps9 domain containing proteins

SMART database report on Vps9 domain containing proteins as at November 2012 with Protein identification entry of the UniProtKB (http://www.uniprot.org/):

```
A1A4T0,  A8K3R3,  B3KMF1,  B3KMM3,  B3KN67,  B3KT35,  B3KTX2,  B4DN44,
B4DPG5,  B4DW96,  B4DZM7,  B7Z310,  E7EM96,  E7EPJ1,  E7ERJ8,  E9PFK9,
E9PNR2,  F6V054,  F8W9S7,  H0YJ83,  H3BM58,  H3BQI2,  H7BYE7,  Q13671,
Q14C86,  Q3HKR1,  Q59FL5,  Q5CZ74,  Q60I27,  Q6NSK7,  Q6ZRC2,  Q6ZS11,
Q86U22,  Q8TB24,  Q8WYP3,  Q96NW4,  Q96Q42,  Q9UJ41,  Q9Y2B5
```

---

[21] The plasmid was kindly provided by Professor Dr. Aymelt Itzen, MPI Dortmund, currently TU München

8.2.2 Rabex-5GEF (aa132-391)

```
MGHHHHHHGSIETDRVSKEFIEFLKTFHKTGQEIYKQTKLFLEGMHYKRDLSIEEQSECAQDFYHN
VAERMQTRGKVPPERVEKIMDQIEKYIMTRLYKYVFCPETTDDEKKDLAIQKRIRALRWVTPQMLC
VPVNEDIPEVSDMVVKAITDIIEMDSKRVPRDKLACITKCSKHIFNAIKITKNEPASADDFLPTLI
YIVLKGNPPRLQSNIQYITRFCNPSRLMTGEDGYYFTNLCCAVAFIEKLDAQSLNLSQEDFDRYMS
GQTSP
```

Supporting figure 11   **Rabex-5GEF (aa132-391) protein sequence.**

Supporting table 3   **Rabex-5GEF (aa132-391) protein parameter.**

Parameter	Value
Number of amino acids	269
Molecular weight	31393.0
Theoretical pI	6.56

Protein parameters were computed using the online software ProtParamTool of the Expasy-Server (http://web.expasy.org/cgi-bin/protparam/protparam).

Supporting table 4   **Rabex-5GEF (aa132-391) amino acid composition.**

Amino acid	Absolute number	Relative amount
Alanine	12	4.5 %
Arginine	15	5.6 %
Asparagine	9	3.3 %
Aspartic acid	18	6.7 %
Cysteine	8	3.0 %
Glutamine	13	4.8 %
Glutamic acid	21	7.8 %
Glycine	9	3.3 %
Histidine	10	3.7 %
Isoleucine	22	8.2 %
Leucine	18	6.7 %
Lysine	22	8.2 %
Methionine	10	3.7 %
Phenylalanine	12	4.5 %
Proline	13	4.8 %
Serine	14	5.2 %
Threonine	17	6.3 %
Tryptophan	1	0.4 %
Tyrosine	11	4.1 %
Valine	14	5.2 %
Pyrrolysine	0	0.0 %
Selenocysteine	0	0.0 %

8.2.3 Rab5c (aa18-185)

```
MGHHHHHHHHHHGSLVPRGSKICQFKLVLLGESAVGKSSLVLRFVKGQFHEYQESTIGAAFLTQTV
CLDDTTVKFEIWDTAGQERYHSLAPMYYRGAQAAIVVYDITNTDTFARAKNWVKELQRQASPNIVI
ALAGNKADLASKRAVEFQEAQAYADDNSLLFMETSAKTAMNVNEIFMAIAKKLPKN
```

Supporting figure 12   **Rab5c (aa18-185) protein sequence.**

Supporting table 5   Rab5c (aa18-185) protein parameter.

Parameter	Value
Number of amino acids	188
Molecular weight	21035.9
Theoretical pI	8.50

Protein parameters were computed using the online software ProtParamTool of the Expasy-Server (http://web.expasy.org/cgi-bin/protparam/protparam).

Supporting table 6   Rab5c (aa18-185) amino acid composition.

Amino acid	Absolute number	Relative amount
Alanine	23	12.2 %
Arginine	7	3.7 %
Asparagine	8	4.3 %
Aspartic acid	8	4.3 %
Cysteine	2	1.1 %
Glutamine	10	5.3 %
Glutamic acid	10	5.3 %
Glycine	10	5.3 %
Histidine	12	6.4 %
Isoleucine	9	4.8 %
Leucine	15	8.0 %
Lysine	13	6.9 %
Methionine	5	2.7 %
Phenylalanine	9	4.8 %
Proline	4	2.1 %
Serine	11	5.9 %
Threonine	11	5.9 %
Tryptophan	2	1.1 %
Tyrosine	6	3.2 %
Valine	13	6.9 %
Pyrrolysine	0	0.0 %
Selenocysteine	0	0.0 %

```
 Murine     1 MAGRGGAARPNGPAAGNKICQFKLVLLGESAVGKSSLVLRFVKGQFHEYQESTIGAAFLT

 Human      1 MAGRGGAARPNGPAAGNKICQFKLVLLGESAVGKSSLVLRFVKGQFHEYQESTIGAAFLT

              ************************************************************

 murine    61 QTVCLDDTTVKFEIWDTAGQERYHSLAPMYYRGAQAAIVVYDITNTDTFARAKNWVKELQ

 Human     61 QTVCLDDTTVKFEIWDTAGQERYHSLAPMYYRGAQAAIVVYDITNTDTFARAKNWVKELQ

              ************************************************************

 murine   121 RQASPNIVIALAGNKADLASKRAVEFQEAQAYADDNSLLFMETSAKTAMNVNEIFMAIAK

 human    121 RQASPNIVIALAGNKADLASKRAVEFQEAQAYADDNSLLFMETSAKTAMNVNEIFMAIAK

              ************************************************************

 murine   181 KLPKNEPQNAAGAPGRTRGVDLQESNPASRSQCCSN

 human,   181 KLPKNEPQNATGAPGRNRGVDLQENNPASRSQCCSN

              ********** ***** ******* ***********
```

Supporting figure 13   Alignment of Rab5c human and murine isoforms.
The alignment was computed using the SIM tool on the expasy-server (http://web.expasy.org/sim/) and showed that the two forms of Rab5c differ only in three amino acids. 98.6% identity in 216 residues overlap; Score: 1094.0; Gap frequency: 0.0%.

8.2.4 Arf1

The Arf1 sequence was expressed from the pCMV-Arf1-NΔ17 plasmid. The *Homo sapiens* protein with a deletion of the 17 N-terminal amino acids was expressed as fusion protein with an N-terminal His tag:

```
MGSSHHHHHHSSGLVPRGSHMCMRILMVGLDAAGKTTILYKLKLGEIVTTIPTIGFNVETVEYKNI
SFTVWDVGGQDKIRPLWRHYFQNTQGLIFVVDSNDRERVNEAREELMRMLAEDELRDAVLLVFANK
QDLPNAMNAAEITDKLGLHSLRHRNWYIQATCATSGDGLYEGLDWLSNQLRNQK
```

8.2.5 Cytohesin-2

The sequence of the *Homo sapiens* Cytohesin-2-Sec7-domain was expressed with an N-terminal His tag from the pET15-ARNO-Sec7 plasmid:

```
MGSSHHHHHHSSGLVPRGSHMEANEGSKTLQRNRKMAMGRKKFNMDPKKGIQFLVENELLQNTPEE
IARFLYKGEGLNKTAIGDYLGEREELNLAVLHAFVDLHEFTDLNLVQALRQFLWSFRLPGEAQKID
RMMEAFAQRYCLCNPGVFQSTDTCYVLSFAVIMLNTSLHNPNVRDKPGLERFVAMNRGINEGGDLP
EELLRNLYDSIRNEPFKIPEDDGNDVTHS
```

8.2.6 DrrA

The DrrA aa340-533 sequence from *Legionella pneumophila* was expressed with an N-terminal His tag from the pET19mod-DrrA plasmid:

```
MGHHHHHHAENLYFQGHMVTRIENLENAKKLWDNANSMLEKGNISGYLKAANELHKFMKEKNLKED
DLRPELSDKTISPKGYAILQSLWGAASDYSRAAATLTESTVEPGLVSAVNKMSAFFMDCKLSPNER
ATPDPDFKVGKSKILVGIMQFIKDVADPTSKIWMHNTKALMNHKIAAIQKLERSNNVNDETLESVL
SSKGENLSEYLSYK
```

8.2.7 Erk2

The Erk sequence from *Rattus norvegicus* was expressed with an N-terminal His tag from the pETHis6ERK2 plasmid:

```
MAHHHHHHAMAAAAAGPEMVRGQVFDVGPRYTNLSYIGEGAYGMVCSAYDNLNKVRVAIKKISPFE
HQTYCQRTLREIKILLRFRHENIIGINDIIRAPTIEQMKDVYIVQDLMETDLYKLLKTQHLSNDHI
CYFLYQILRGLKYIHSANVLHRDLKPSNLLLNTTCDLKICDFGLARVADPDHDHTGFLTEYVATRW
YRAPEIMLNSKGYTKSIDIWSVGCILAEMLSNRPIFPGKHYLDQLNHILGILGSPSQEDLNCIINL
KARNYLLSLPHKNKVPWNRLFPNADSKALDLLDKMLTFNPHKRIEVEQALAHPYLEQYYDPSDEPI
AEAPFKFDMELDDLPKEKLKELIFEETARFQPGYRS
```

8.2.8 Grk2 (beta adrenergic receptor kinase 1)

This construct includes the N-terminus until aa184 of *Homo sapiens* beta-adrenergic receptor kinase 1 in a pGEX1lambdaT plasmid. The protein has an N-Terminal GST-Tag.

8.2.9 JIP4

The *Homo sapiens* JIP4 (aa406-476) sequence (after TEV digestion):

```
GAMDWWFMGREVENLILENTQLLETKNALNIVKNDLIAKVDELTCEKDVLQGELEAVKQAKLKLEE
KNRELEEELRKA
```

8.2.10 Rac1

The *Homo sapiens* Rac1 (aa1-192) sequence was expressed with an N-terminal GST tag which was cleaved off to yield the following protein:

```
GSMQAIKCVVVGDGAVGKTCLLISYTTNAFPGEYIPTVFDNYSANVMVDGKPVNLGLWDTAGQEDY
DRLRPLSYPQTDVFLICFSLVSPASFENVRAKWYPEVRHHCPNTPIILVGTKLDLRDDKDTIEKLK
EKKLTPITYPQGLAMAKEIGAVKYLECSALTQRGLKTVFDEAIRAVLCPPPVKKRKRKCLLL
```

8.2.11 Vav-1

The Vav-1 (aa189–575) sequence from *Homo sapiens* was expressed with an N-terminal GST tag which was cleaved off to yield the following protein (pGEX-2T-TEV-Vav-1-189-575 plasmid):

```
SMTEYDKRCCCLREIQQTEEKYTDTLGSIQQHFLKPLQRFLKPQDIEIIFINIEDLLRVHTHFLKE
MKEALGTPGAANLYQVFIKYKERFLVYGRYCSQVESASKHLDRVAAAREDVQMKLEECSQRANNGR
FTLRDLLMVPMQRVLKYHLLLQELVKHTQEAMEKENLRLALDAMRDLAQCVNEVKRDNETLRQITN
FQLSIENLDQSLAHYGRPKIDGELKITSVERRSKMDRYAFLLDKALLICKRRGDSYDLKDFVNLHS
FQVRDDSSGDRDNKKWSHMFLLIEDQGAQGYELFFKTRELKKKWMEQFEMAISNIYPENATANGHD
FQMFSFEETTSCKACQMLLRGTFYQGYRCHRCRASAHKECLGRVPPCGRHGQDFPGTM
```

8.3 Protein purification and verification

A

B
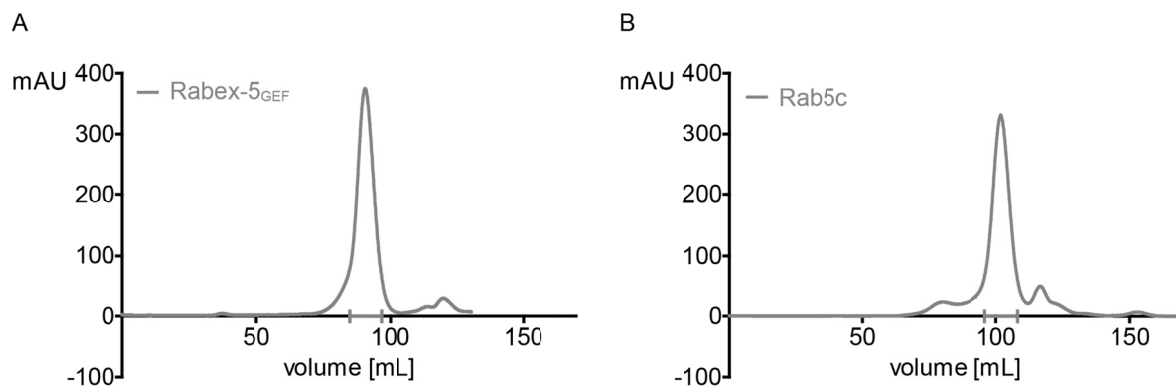
Supporting figure 14   **Gel-filtration of Rabex-5GEF and Rab5c on Superdex200.**
A) Rabex-5GEF chromatogram using a column of 120 mL total volume. The protein eluted at 90 mL volume. The fractions that are indicated by grey bars on x-axis were collected and concentrated. **B)** Rab5c chromatogram using a column of 120 mL total volume. The protein eluted maximal at 101 mL. The fractions that are indicated by grey bars on x-axis were collected and concentrated.
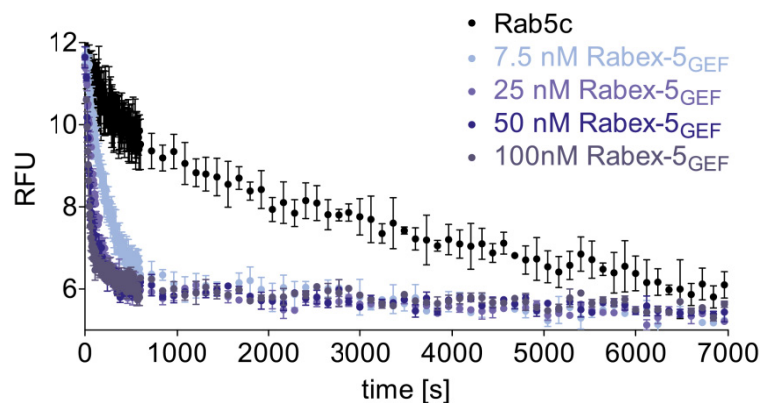
Supporting figure 15   **Nucleotide exchange of Rabex-5GEF on Rab5c[22]**
The intrinsic nucleotide exchange activity of Rab5c was determined over two hours in comparison with Rabex-5GEF. After two hours in all samples the nucleotide exchange was complete. The intrinsic nucleotide exchange activity of Rab5c was estimated to be at 50 % after 30 min. The addition of Rabex-5GEF at concentrations between 7.5 nM and 100 nM resulted in completed nucleotide exchange after roughly 10 minutes.

---

[22] Measurements were planned and analysed by Christine Wosnitza and kindly performed by Nicole Krämer
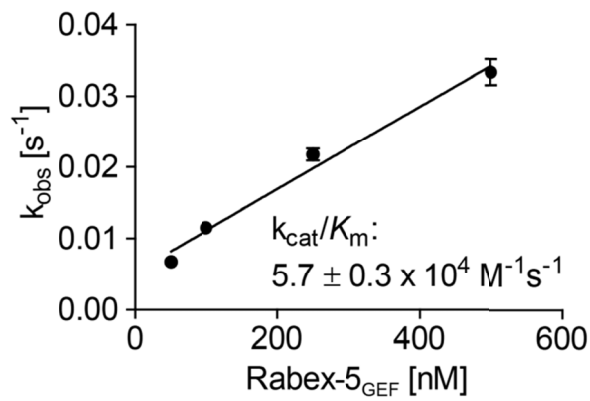
Supporting figure 16   **Rabex-5GEF nucleotide exchange rate.**

The observed rate constant (k_{obs}) was plotted against the Rabex-5GEF concentration and fitted according to the following equation: k_{obs} = (k_{cat}/K_m) [Rabex-5GEF] + k_{intr}. k_{intr} is the intrinsic exchange activity. The k_{cat}/K_m constant with 5.7 (+/- 0.3) x 10^4 $M^{-1}s^{-1}$ lies in a similar range as reported in literature (2.3 x 10^4 $M^{-1}s^{-1}$). [136]
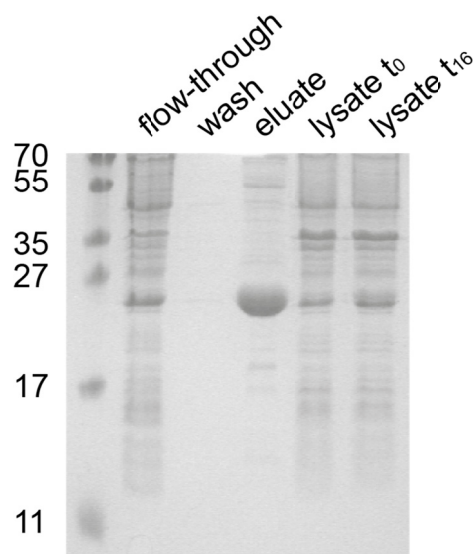
Supporting figure 17   **DrrA protein purification.**

15 % SDS PAA gels stained with Coomassie Brilliant Blue showing samples of all fractions of the protein biosynthesis and purification procedure. Protein biosynthesis was monitored in cell lysate before induction (lysate t_0 lane 4) and after 5 hours induction (lysate t_5 lane 5). Lane 1 shows the flow-through from the affinity chromatography, lane 2 the wash fraction and lane 3 the eluate.

8.4   Screening assay optimization process

These optimization procedures were performed to establish conditions with the highest measurement window and accuracy. Thus, the error was intended to be very small. Furthermore, it was of interest whether introduce changes in the procedure had negative impact on the protein activity. Hence, conditions with decreased exchange rate were excluded from further optimization steps. Since the tests were not always performed under exact conditions, e.g. DMSO concentration, protein batch etc. varied the control exchange rates differ between several setups.

Supporting table 7   **Comparison of protein batches regarding Rabex-5$_{GEF}$ exchange rate.**

Protein batch	exchange rate k_{cat}/k_m $[M^{-1}s^{-1}]$ ± SD
Protein batch #3	0.019 ± 0.002
Protein batch #4	0.020 ± 0.000

Between two protein batches no significant differences were found.

Supporting table 8   **Impact of mitrotitre plates on the Rabex-5$_{GEF}$ exchange rate.**

Microtitre plate	exchange rate k_{cat}/k_m $[M^{-1}s^{-1}]$ ± SD
96 well plate, 1% DMSO	0.026 ± 0.004
96 well half area plate, 1% DMSO	0.027 ± 0.004

There was no difference in the nucleotide exchange rate and accuracy between the different plates. Thus, the half area plates were chosen to minimize the material needed for the screening.

Supporting table 9   **Impact of the order of pipetting on the Rabex-5$_{GEF}$ exchange rate.**

Order of pipetting	exchange rate k_{cat}/k_m $[M^{-1}s^{-1}]$ ± SD
Rab5c-DMSO-Rabex-5$_{GEF}$	0.046 ± 0.004
Rabex-5$_{GEF}$-DMSO-Rab5c	0.009 ± 0.004

The order of pipetting had no impact on the sample variation but on general protein activity. The use of only 1 % DMSO explains the comparably high exchange rate in the first setup. Rab5c was observed to be more stable than Rabex-5$_{GEF}$. Thus, the first pipetting order was chosen for the screening.

Supporting table 10   **Impact of centrifugation on the assay performance.**

Assay preparation condition	ΔRFU ± SD
Centrifugation	2.6 ± 0.4
No centrifugation	2.4 ± 0.3

The pipetting procedure with the pipetting robot introduced air bubbles that disturbed the readout of the measurement. Centrifugation removed the air bubbles. A comparison with and without centrifugation confirmed that the centrifugation process did not affect the nucleotide exchange assay. This test was performed already under final screening conditions. Thus, ΔRFU is given instead of exchange rate.

Supporting table 11   Impact of assay preparation time and temperature.

Assay preparation condition	exchange rate k_{cat}/k_m [$M^{-1}s^{-1}$] ± SD
24 wells pipetted manually, RT	0.021 ± 0.002
96 wells pipetted by robot, RT	0.011 ± 0.001
96 wells pipetted by robot, 12 °C	0.011 ± 0.001

A loss of protein activity was observed upon assay preparation with the pipetting robot. It was assumed that this was due to the prolonged time required for the addition of proteins and compounds to 96 wells. To counteract this loss of activity, the assay plates were cooled to 12 °C during these pipetting steps. However, cooling of the assay plates did not improve the exchange rate.

Supporting table 12   Impact of Triton X-100 and Igepal on the Rabex-5GEF exchange rate.

Assay preparation condition	exchange rate k_{cat}/k_m [$M^{-1}s^{-1}$] ± SD
0.25 % Tween20,	0.051 ± 0.004
0.01 % Triton X-100	0.040 ± 0.004
0.05 % Triton X-100	0.048 ± 0.011
0.25 % Triton X-100	0.003 ± 0.002
0.01 % Igepal	0.051 ± 0.004
0.05 % Igepal	0.048 ± 0.009
0.25 % Igepal	0.041 ± 0.020

None of the tested detergent conditions improved the protein activity and decreased the sample variation further than Tween20. Hence, Tween20 was not replaced in this assay.

Supporting table 13   Comparison of incubation times.

Incubation time [a]	exchange rate k_{cat}/k_m [$M^{-1}s^{-1}$] ± SD
5 min	0.019 ± 0.002
10 min	0.017 ± 0.001
20 min	0.018 ± 0.001
40 min	0.005 ± 0.000

The activity of the proteins depends on the incubation time of the proteins in the assay mix before measurement. To enable the centrifugation step and to allow a smooth screening performance the incubation time was set to seven minutes. Incubation times of 5 to 20 minutes gave comparable results. **[a]** Incubation time after mixing the assay components. At the end of the incubation time the measurement was started.

Supporting table 14   Impact of the mixing procedure on the Rabex-5GEF exchange rate.

Mixing procedure	exchange rate k_{cat}/k_m [$M^{-1}s^{-1}$] ± SD
Manual, gentle mixing; 5 min incubation	**0.024 ± 0.001 [a]**
No mixing; 5 min incubation	0.036 ± 0.017
Automatic mixing by *Varioskan* plate reader; 5 min incubation	0.014 ± 0.000 [b]
Manual, gentle mixing; 35 min incubation	0.012 ± 0.002

Several modes of mixing and incubation times were compared. **[a]** Best results were obtained with gentle, manual mixing and five minutes assay incubation. **[b]** Automated mixing decreased the variations between the samples, however, severely affected the protein activity.

Supporting table 15   Protein tolerance to storage time on ice before use.

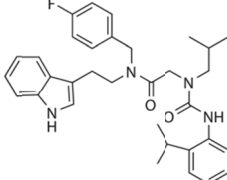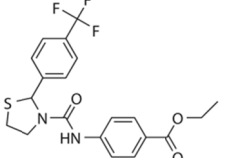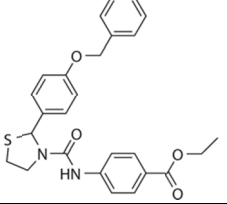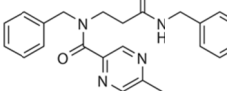| Protein storage on ice for	exchange rate k_{cat}/k_m [$M^{-1}s^{-1}$] ± SD
60 min	0.025 ± 0.002
120 min	0.025 ± 0.002
180 min	0.029 ± 0.004
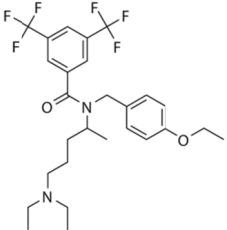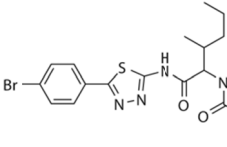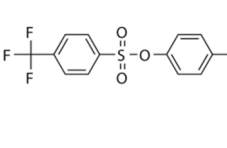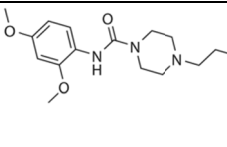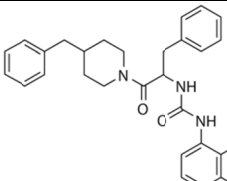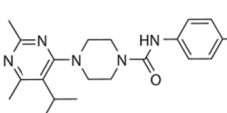
Protein aliquots can be stored on ice for at least 180 minutes without loss of activity.

8.5   Hit verification

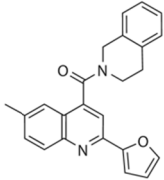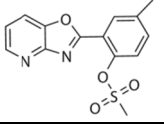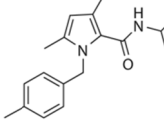**Supporting table 16   List of primary hit compounds from the screening.**
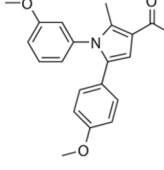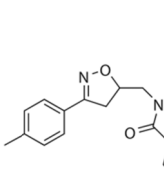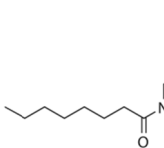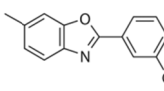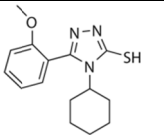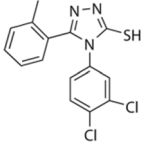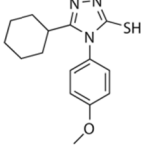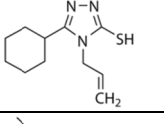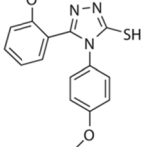
ID	Structure	RFU [340 nm]	Classification	Secondary hit
CG1.01_G08		> 20 RFU < 40 RFU		
CG1.01_G10		< 20 RFU		
CG1.11_A10		> 20 RFU < 40 RFU		
CG1.11_F06		< 20 RFU		
CG1.17_G08		< 40 RFU		
CG1.17_H06		< 40 RFU		
CG1.18_H09		< 40 RFU		
CG1.21_B07		> 20 RFU < 40 RFU		
CG1.21_H05		> 20 RFU < 40 RFU		
CG1.23_H01		< 40 RFU		
CG2.01_E01		< 40 RFU		
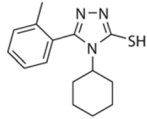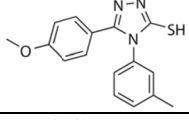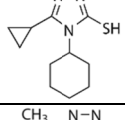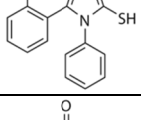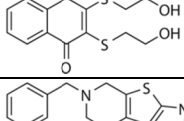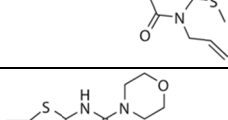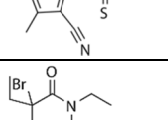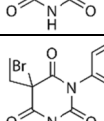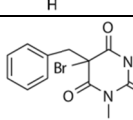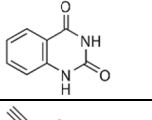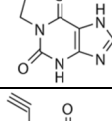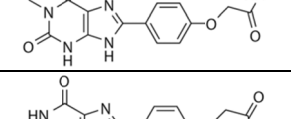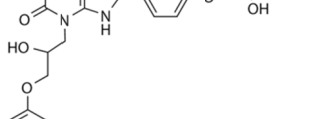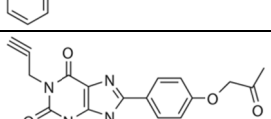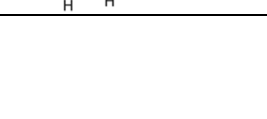
ID	Structure	RFU [340 nm]	Classification	Secondary hit
CG2.02_F02		< 20 RFU		
CG2.03_F04		> 20 RFU < 40 RFU		
CG2.11_F02		< 40 RFU		
CG2.12_C07		< 40 RFU		
CG2.12_G07		< 40 RFU		
CG2.14_D06		> 20 RFU < 40 RFU		
CG2.17_C06		> 20 RFU < 40 RFU		
CG2.18_B01		< 40 RFU		
CG2.18_C03		< 40 RFU		
CG2.20_C08		> 20 RFU < 40 RFU		

ID	Structure	RFU [340 nm]	Classification	Secondary hit
CG2.20_C09		> 20 RFU < 40 RFU		
CG2.20_D01		< 40 RFU		
CG2.20_F01		< 40 RFU		
CG2.21_B01		< 40 RFU		
CG2.24_F06		< 40 RFU	C	
CG3.04_G11		< 20 RFU		
CG3.05_E03		< 40 RFU	C	
CG3.07_A08		> 20 RFU < 40 RFU		
CG3.10_G09		< 40 RFU		
CG3.12_F03		> 20 RFU < 40 RFU		
CG3.22_A09		< 40 RFU		
CG4.02_H07		> 20 RFU < 40 RFU		

ID	Structure	RFU [340 nm]	Classification	Secondary hit
CG4.09_E07		< 40 RFU		
CG4.11_H10		< 40 RFU		
CG4.12_F11		< 40 RFU		
CG4.17_H07		> 20 RFU < 40 RFU		
CG4.18_H09		< 20 RFU		
CG4.20_C11		< 20 RFU		
CG4.28_E05		< 40 RFU	B (best of fluorescent compounds)	
CG4.30_A08		< 20 RFU	A	X
CG4.30_B06		> 20 RFU < 40 RFU	B (fluorescent drift)	X
CG4.30_E06		< 20 RFU	A	X
CG4.30_E07		> 20 RFU < 40 RFU	A	X
CG4.30_F05		< 20 RFU	A	X

ID	Structure	RFU [340 nm]	Classification	Secondary hit
CG4.30_G05		> 20 RFU < 40 RFU	A	X
CG4.30_H05		< 20 RFU	A	X
CG4.30_H06		> 20 RFU < 40 RFU	A	X
CG4.30_H07		< 20 RFU	A	X
KR1.03_F10		< 20 RFU	A	X
KR1.05_F02		> 20 RFU < 40 RFU	A	X
KR1.08_C11		< 20 RFU	A	X
KR1.12_G04		< 20 RFU		
KR1.12_G05		< 20 RFU		
KR1.13_A07		< 20 RFU	A	x
KR1.15_C05		< 40 RFU		
KR1.16_C09		< 20 RFU	A	x
KR1.16_D09		< 20 RFU		
KR1.17_A06		< 40 RFU	C	
KR1.17_C05		> 20 RFU < 40 RFU	A	x

ID	Structure	RFU [340 nm]	Classification	Secondary hit
KR1.19_B04		< 40 RFU	C	
KR1.20_A05		< 20 RFU		
KR1.22_B04		> 20 RFU < 40 RFU		
KR1.22_E11		< 40 RFU	C	
KR1.22_F11		< 40 RFU		
KR1.23_A10		< 40 RFU		
KR1.23_D10		< 40 RFU	C	
KR1.27_F04		< 40 RFU	C	
KR1.31_A11		< 20 RFU		
KR1.31_C09		> 20 RFU < 40 RFU		
KR1.32_E05		< 20 RFU		
KR1.32_E10		< 20 RFU		
KR1.32_F07		< 40 RFU	C	

The compound name and the structure are given in this table for all primary hit compounds. Furthermore the fluorescence readout at 340 nm is given for each molecule [RFU, 340 nm]. The compounds that were confirmed in the re-screening process were analysed in the kinetic Rabex-5GEF nucleotide exchange assay (Section 8.5). Compounds showing promising inhibitory properties were rated "A", compounds showing inhibitory properties less promising were rated "B". Finally, all compounds showing mainly fluorescence disturbance were rated "C" and excluded from all further consideration. All hits rated "A" were considered as secondary hits and analysed further. Compound CG4.30_B06 was rated "B" and considered secondary hit because it shared the structural core with several other secondary hit compounds. However, due to the presence of more promising compounds with the same core structure CG4.30_B06 was not investigated in more detail.
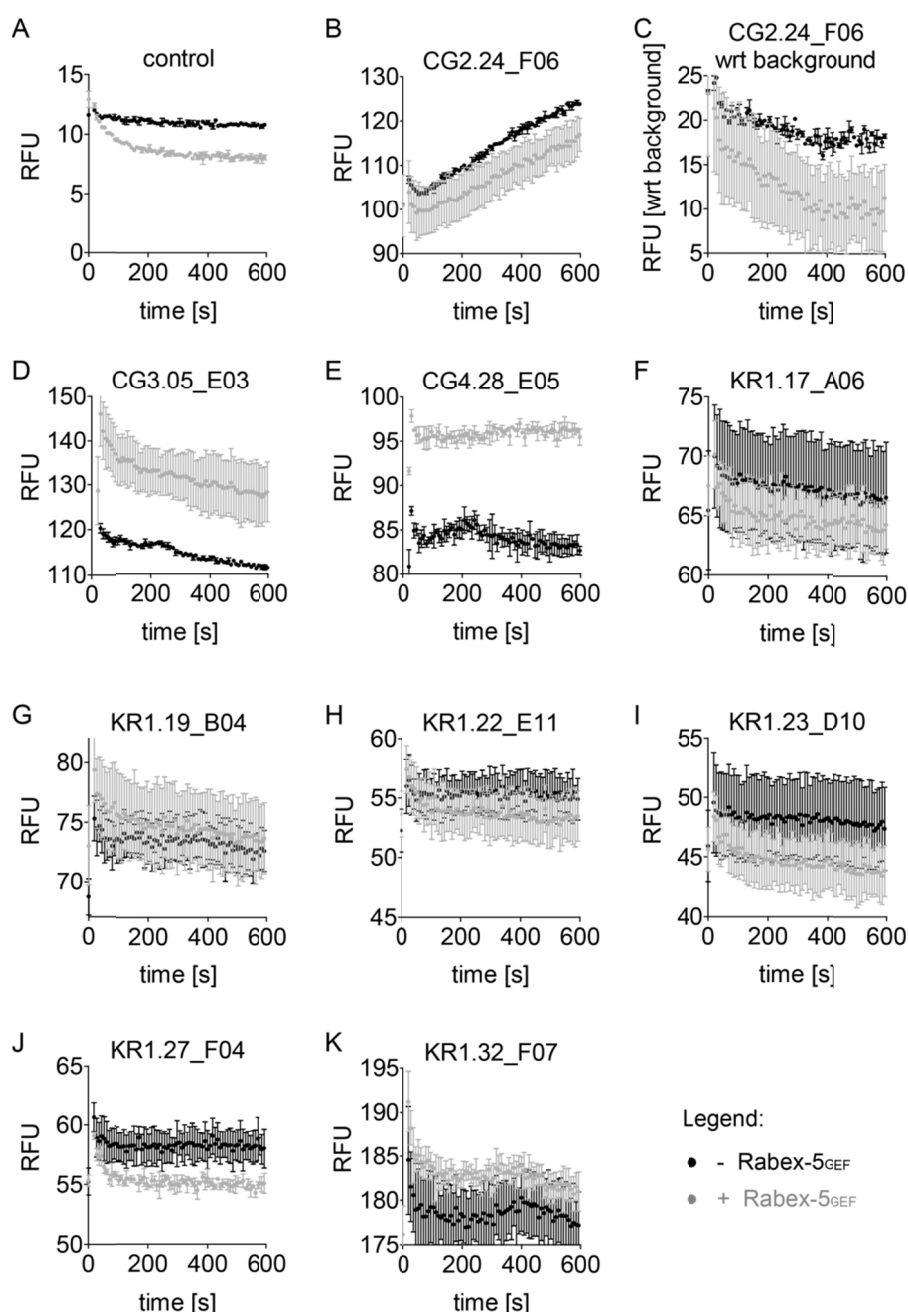
Supporting figure 18   Activity of fluorescent hits.
The confirmed hits were monitored in the kinetic format of the Rabex-5GEF activity assay. The reaction without Rabex-5GEF is shown in black and with Rabex-5GEF in grey as indicated in the legend. **A)** Control reaction with DMSO instead of compound. **B - K)** 20 μM compound from the library stock. All tested compounds belong to the group of highly-fluorescent hits. The compounds except for C4.28.E05 were rated as fluorescent artefacts because for all of them the decrease in fluorescence in the Rabex-5GEF sample is stronger than in the Rab5c control. **E)** C4.28.E05 was the only compound that might be considered as a hit. However, the fluorescence disturbed the read-out dramatically by its increase in fluorescence and no clear analysis was possible. This compound was rated a confirmed hit "class B" and not analysed further because of the presence of other compounds with more promising characteristics. **C)** The same compound as shown in B but here wrt to compound background. In this sample a decrease in fluorescence (as expected for a sample with active Rabex-5GEF) was observed indicating that the increase in B might have been due to compound fluorescence. In summary, all highly fluorescent hits were excluded from further analysis and hence high fluorescent hits could have also been excluded directly after the screening with the same outcome.
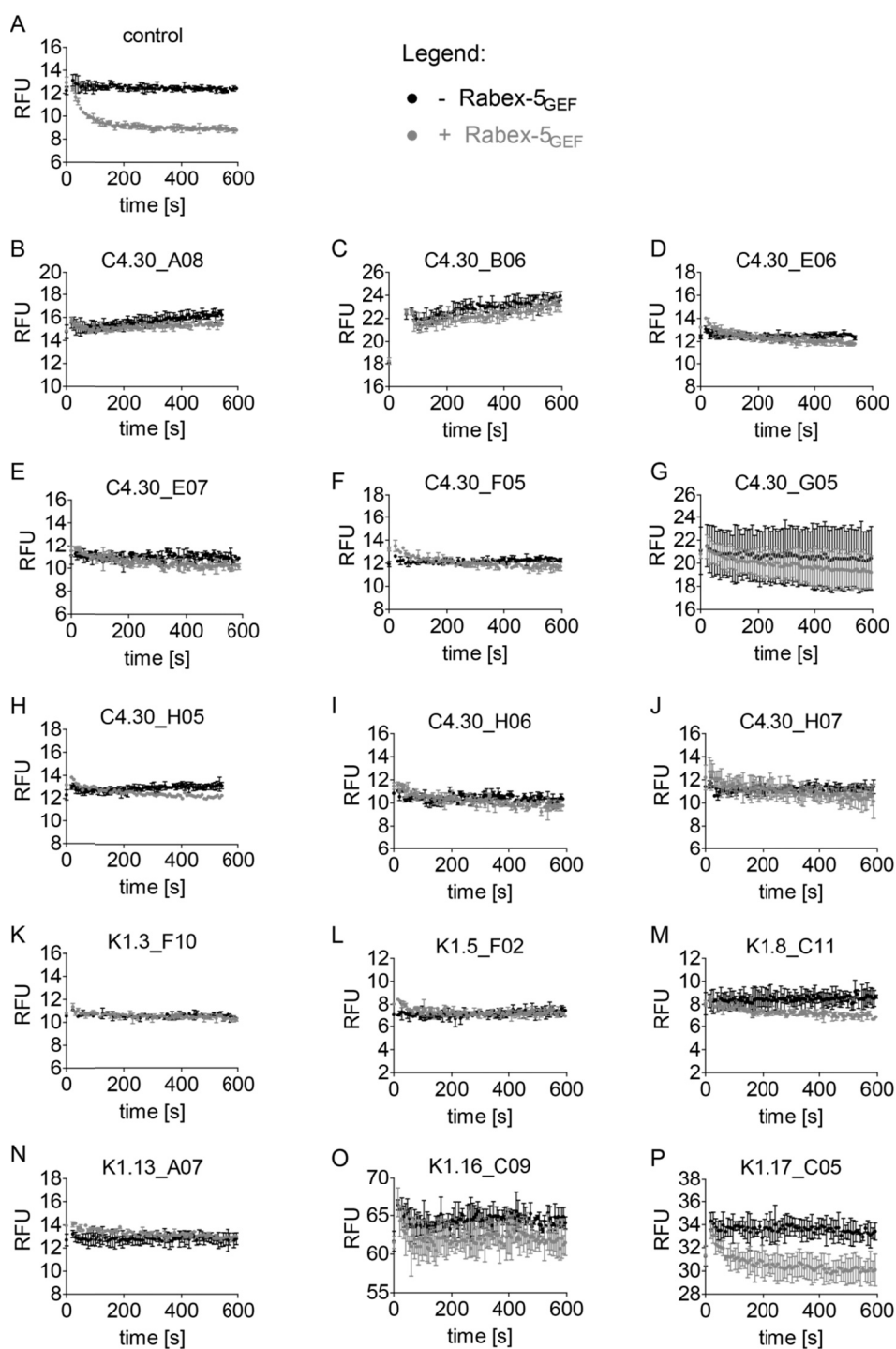
Supporting figure 19   Activity of low-to-medium fluorescent hits.
The confirmed hits were investigated in the kinetic format of the Rabex-5$_{GEF}$ activity assay. The reaction without Rabex-5$_{GEF}$ is shown in black and with Rabex-5$_{GEF}$ in grey as indicated in the legend. **A)** Control reaction with DMSO instead of compound. **B – P)** 20 µM compound from the library stock were tested in the nucleotide exchange assay. All tested compounds belong to the group of low- or medium-fluorescent hits. The compounds B-O were considered confirmed hits because they all reduce the nucleotide exchange of Rabex-5$_{GEF}$ on Rab5. **P)** K1.17_C05 was excluded from further studies due to minor effect on the nucleotide exchange. In general, 500 nM Rabex-5$_{GEF}$ were used in this assay. However, some compounds (C4.30.E07, C4.30.H06, C4.30.H07, K1.05.F02, K1.08.C11, K1.16.C09) were tested at a later stage of this study and were tested with 20 nM Rabex-5$_{GEF}$ since at this time, this was the concentration used in assays for IC$_{50}$ determination.
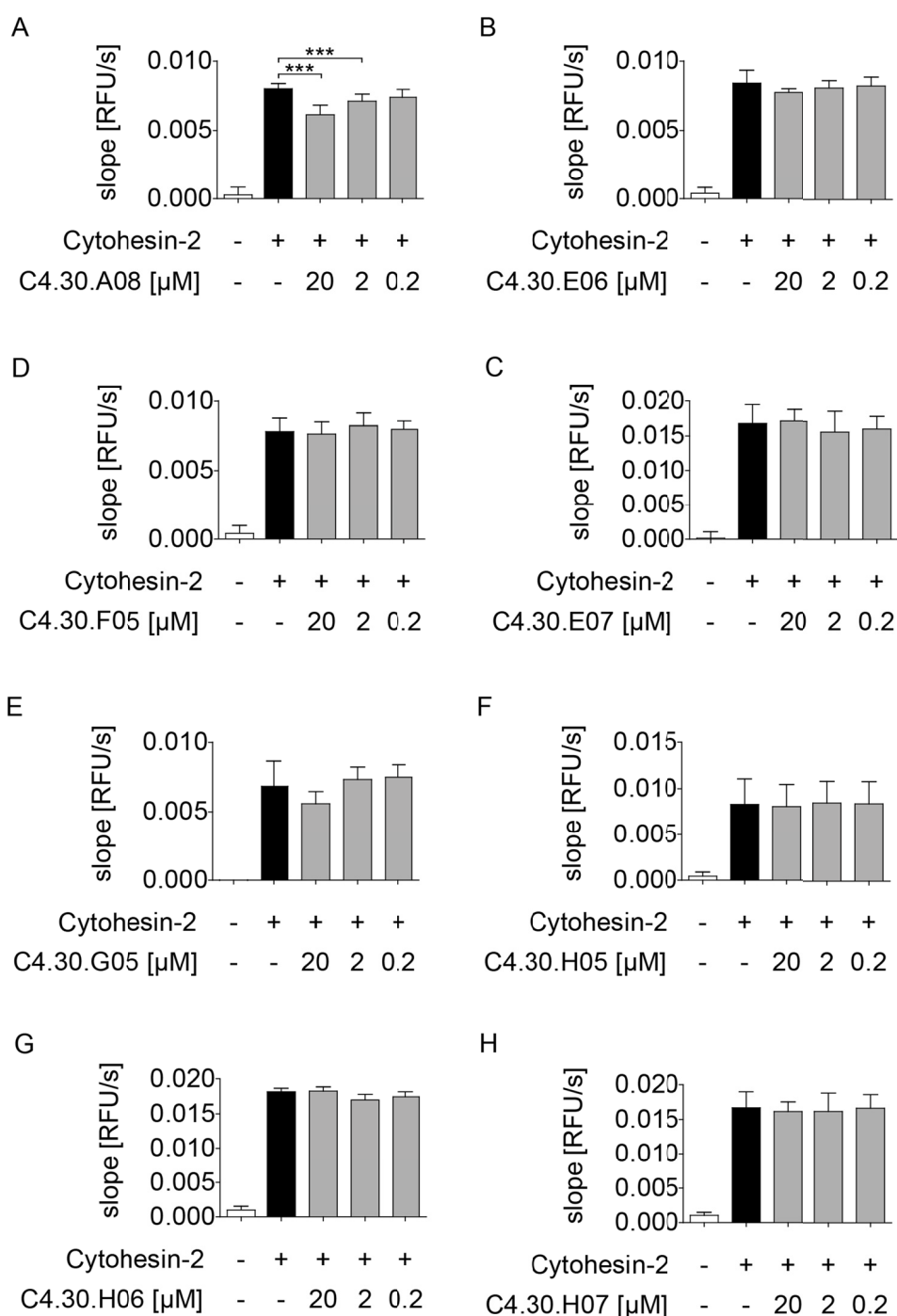
Supporting figure 20 **Effects of secondary hits on the Cytohesin-2-Arf1 nucleotide exchange.**[23]
The secondary hits (compound solutions from library stocks) were observed in the nucleotide exchange assay with GEF Cytohesin-2 (Sec7 domain) and Arf1 with tryptophan fluorescence read-out. The reaction with Arf1 only is shown in white, the reaction with Cytohesin-2 in black and the reaction with compound, Cytohesin-2, and Arf1 in grey. Variations in the enzymatic activity are due to the use of distinct protein batches. **A)** For C4.30.A08 inhibitory effects were observed. No inhibition was observed in **B)** C4.30.E06 **C)** C4.30.E07 **D)** C4.30.F05 **E)** C4.30.G05 **F)** C4.30.H05 **G)** C4.30.H06 **H)** C4.30.H07. Data from at least two independent experiments are plotted as mean ± SD. The significance was calculated by the use of the one-way-ANOVA with the Tukey post-test, p-values: *p < 0.05, **p < 0.01, ***p < 0.001.

---

[23] Experiments C4.30.A08, C4.30.E6, C4.30.F05, C4.30.G05, C4.30.H05, K1.3.F10, K1.13.A07 were performed by Franziska Wolter, and planned as well as analysed by Christine Wosnitza.
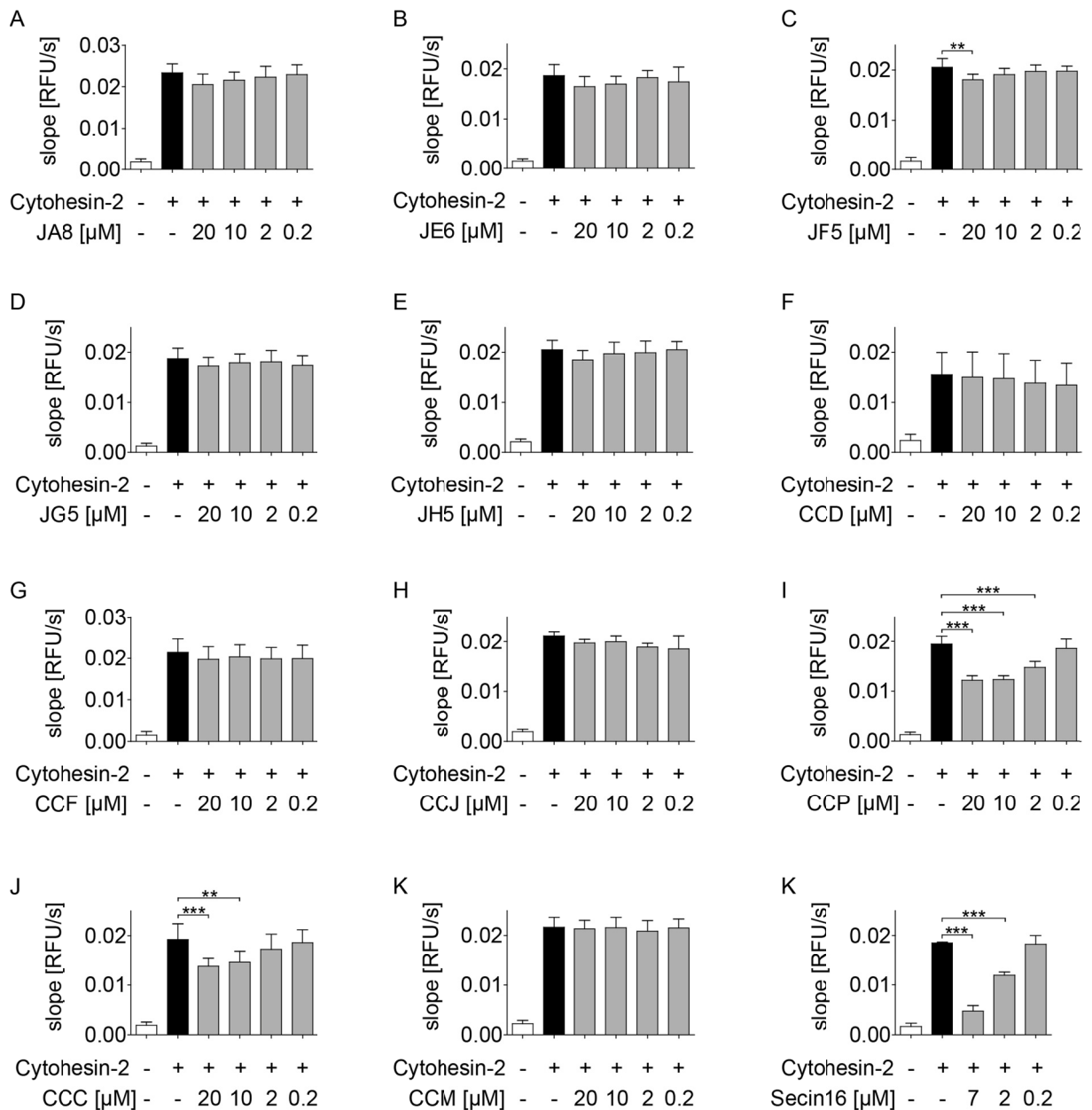
Supporting figure 21   JH5 derivates in the Cytohesin-2-Arf1 nucleotide exchange.[24]
The compounds were monitored in the nucleotide exchange assay with GEF Cytohesin-2 (Sec7 domain) and
Arf1 with tryptophan fluorescence read-out. The reaction with Arf1 only is shown in white, the reaction with
Cytohesin-2 in black and the reaction with compound, Cytohesin-2, and Arf1 in grey. **A)** JA8 **B)** JE6 **C)** JF5 **D)**
JG5 **E)** JH5 **F)** CCD **G)** CCF **H)** CCJ **I)** CCP **J)** CCC **K)** CCM **L)** control compound Secin16 that inhibit the
Cytohesin-2 dependent Arf1 nucleotide exchange as described before.[321] Inhibitory and thus unspecific
characteristics were found in C, I and J. Data from at least two independent experiment is plotted as mean ±
SD. The significance was calculated by the use of the one-way-ANOVA with the Tukey post-test, p-values: *p
< 0.05, **p < 0.01, ***p < 0.001.

---

[24] Experiment was kindly performed by Nicole Krämer and planned / analysed by Christine Wosnitza.
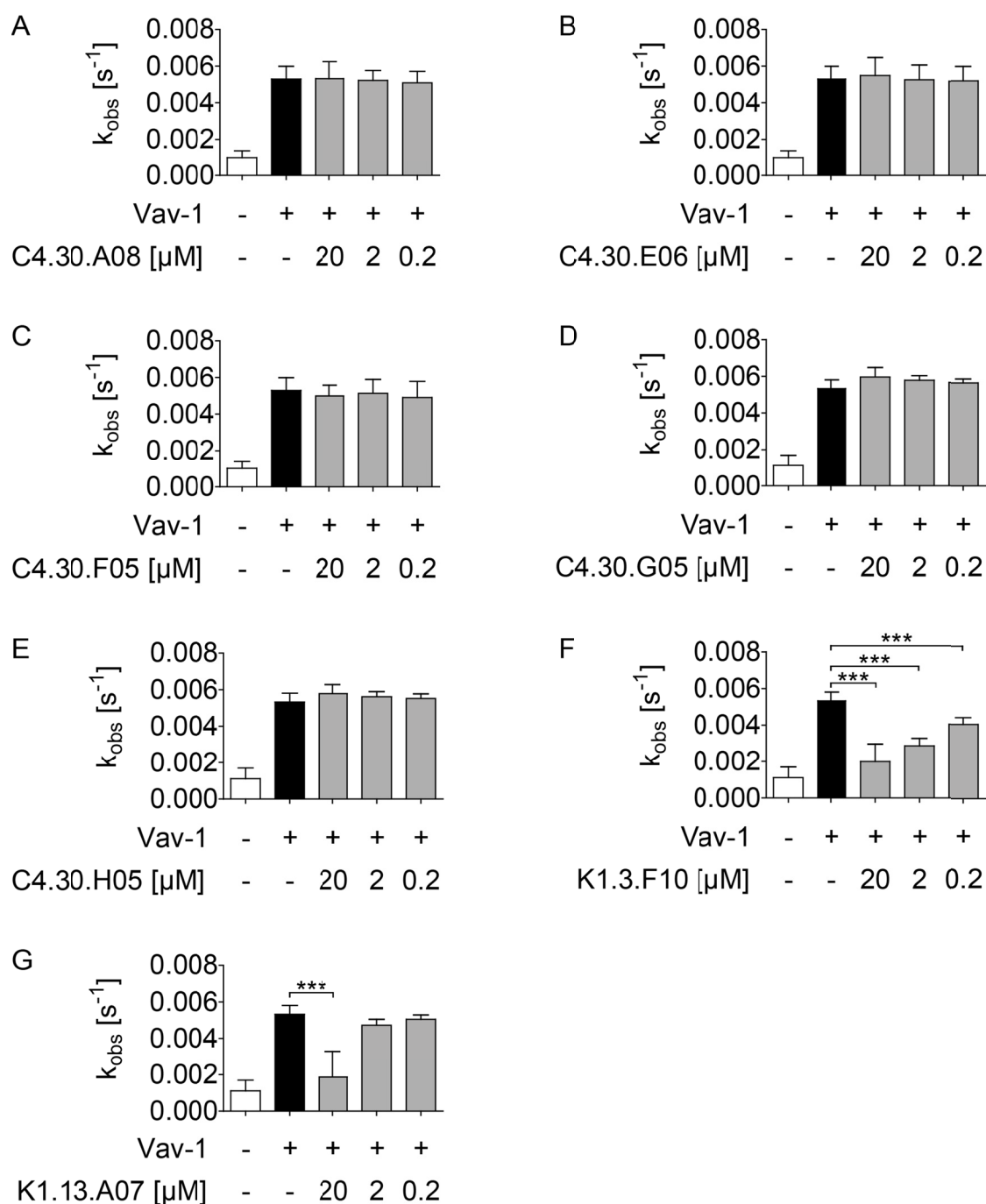
Supporting figure 22   **Effects of secondary hits on the Vav-1-Rac1 nucleotide exchange.[25]**
The secondary hits (compound solutions from library stocks) were analysed in the nucleotide exchange assay with GEF Vav-1 and the GTPase Rac1. The reaction with Rac1 only is shown in white, the reaction with Vav-1 in black and the reaction with compound in grey. **A)** C4.30.A08 **B)** C4.30.E6 **C)** C4.30.F05 **D)** C4.30.G05 **E)** C4.30.H05 **F)** K1.3.F10 **G)** K1.13.A07. Inhibitory and thus unspecific characteristics were observed in F and G. Data from at least two independent experiments are plotted as mean ± SD. The significance was calculated by the use of the one-way-ANOVA with the Tukey post-test, p-values: *$p < 0.05$, **$p < 0.01$, ***$p < 0.001$.

---

[25] Experiments C4.30.A08, C4.30.E6, C4.30.F05, C4.30.G05, C4.30.H05, K1.3.F10, K1.13.A07 were planned and analysed by Christine Wosnitza and performed by Franziska Wolter.
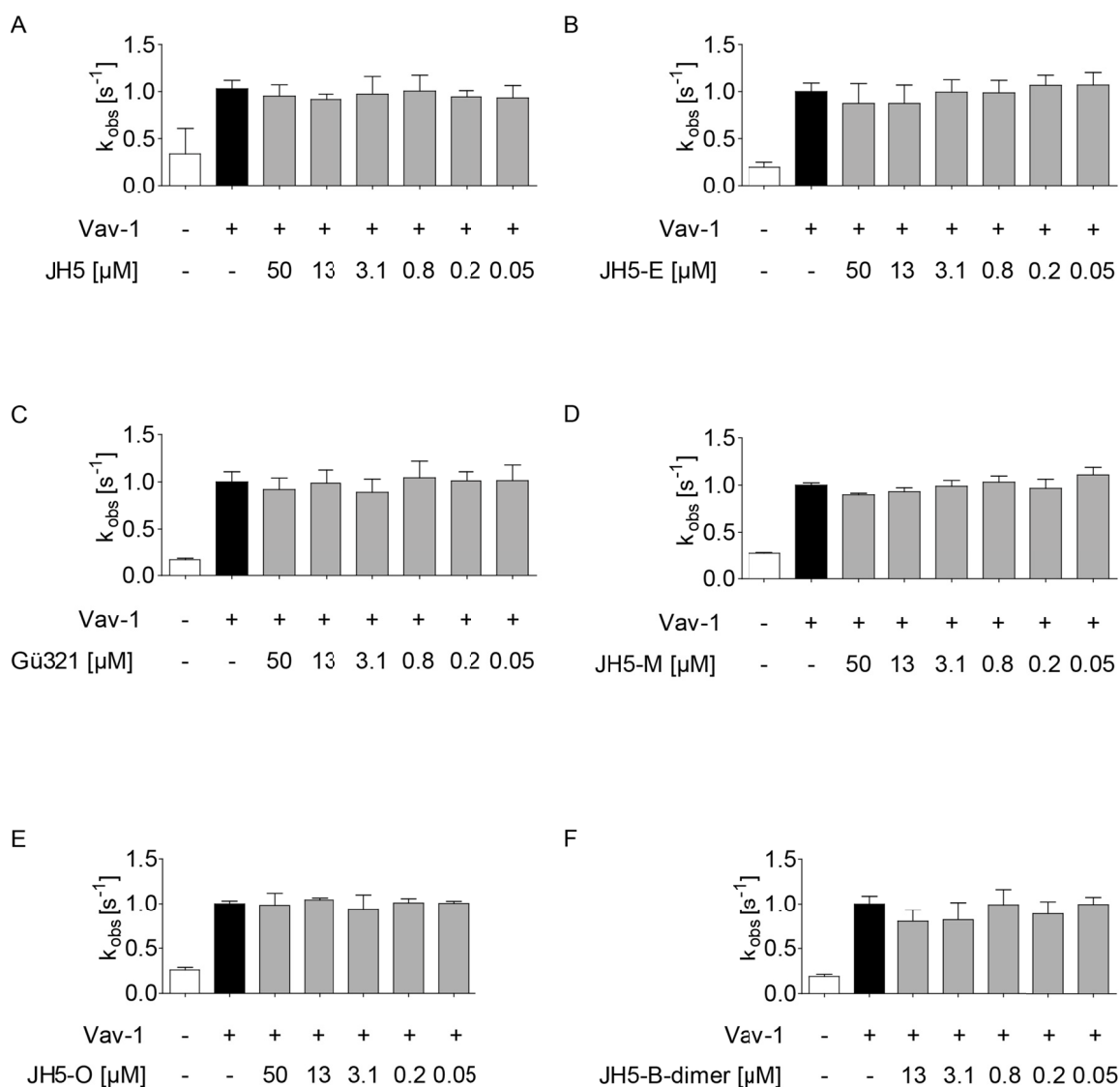
Supporting figure 23   Re-synthesized compounds in the Vav-1-Rac1 nucleotide exchange.[26]
The lead compounds Gü321, JH5 and JH5 derivatives were observed in the nucleotide exchange assay with GEF Vav-1 and Rac1. The reaction with Rac1 only is shown in white, the reaction with Vav-1 in black and the reaction with compound in grey. **A)** JH5 **B)** JH5-E **C)** Gü321 **D)** JH5-M **E)** JH5-O **F)** JH5-B-dimer. None of the compounds affected the Vav-1 mediated nucleotide exchange.

---

[26] Experiment was planned and analysed by Christine Wosnitza and kindly performed by Nicole Krämer.

8.6 Rabex-5GEF nucleotide exchange assay

A

B
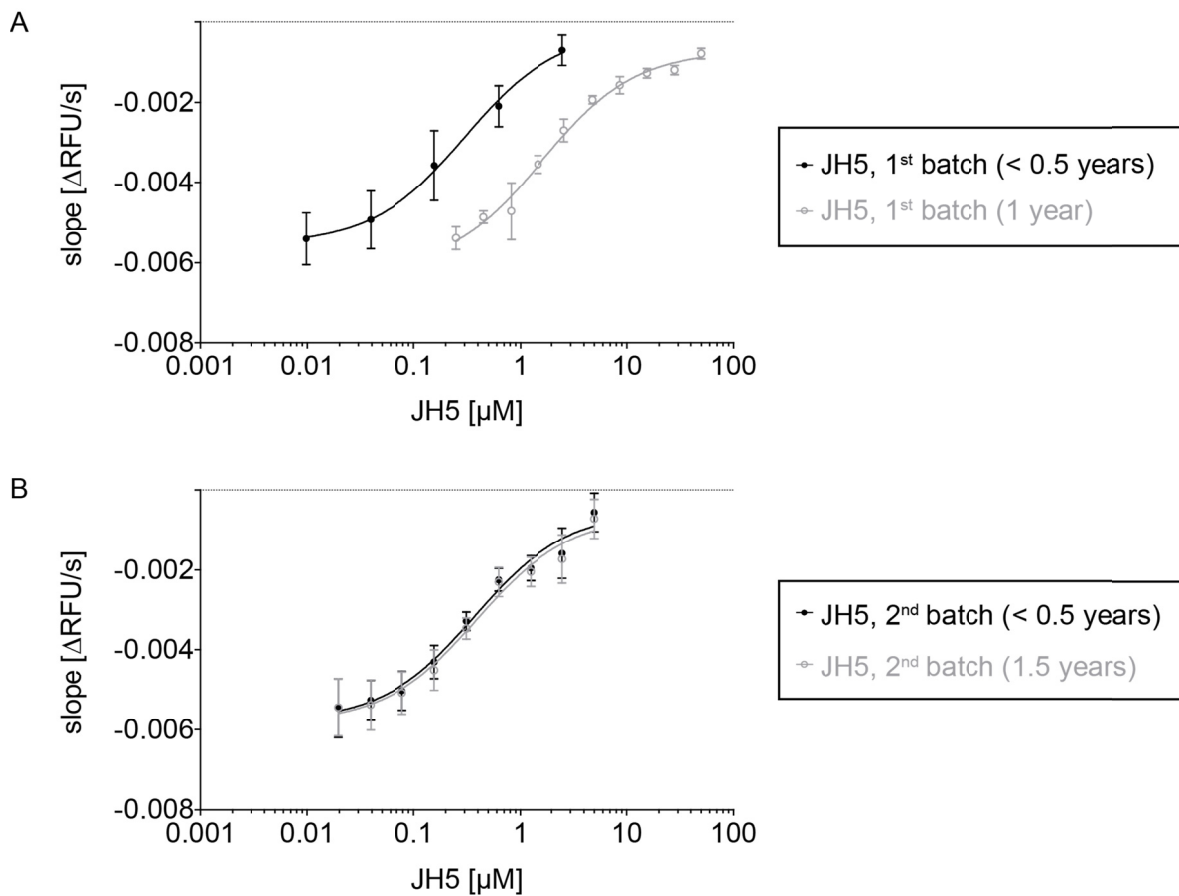
Supporting figure 24   JH5 activity was dependent on its age and storage conditions.
A) The first batch of JH5 was stored as solid at RT in the dark. During the first six months the same activity of the compound was observed and an IC_{50} of 0.3 μM (95 % CI 0.2 - 0.4 μM) was observed. After a year of storage, the IC_{50} of JH5 increased to 1.6 μM (95% CI 1.3 - 2.1 μM). **B)** The second batch of JH5 was stored as solid at -20 °C. The obtained IC_{50} after the synthesis corresponds to the first batch and was calculated to be 0.4 μM (95 % CI 0.3 - 0.5 μM). After 1.5 years, the IC_{50} was still at 0.4 μM (95 % CI 0.3 - 0.5 μM). Thus, storage of solid at -20 °C counteracts the observed loss of activity.

A

B
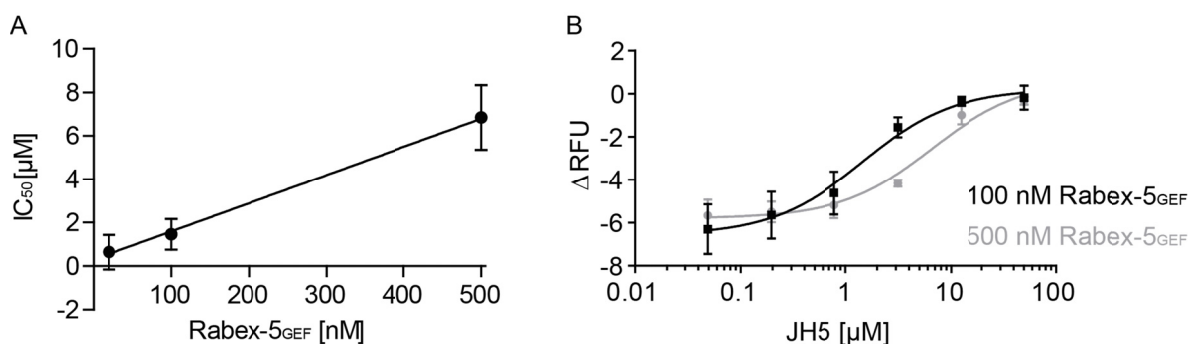
Supporting figure 25   JH5 activity was dependent on the Rabex-5GEF concentration.
A) The IC_{50} of JH5 is depicted on the y-axis, the Rabex-5GEF concentration used in the corresponding experiments on the x-axis. The IC_{50} was determined in a Rab5c-Rabex-5GEF nucleotide exchange assay by plotting the ΔRFU against the logarithmic compound concentration. It was possible to estimate that the dependency of the IC_{50} from the Rabex-5GEF concentration followed a linear correlation. **B)** JH5 in a nucleotide exchange assay with 100 nM Rabex-5GEF and 500 nM Rabex-5GEF resulted in IC_{50} values of 1.4 μM (95 % CI 0.9 – 2.4 μM) and 6.6 μM (95 % CI 4.3 – 10.0 μM), respectively.
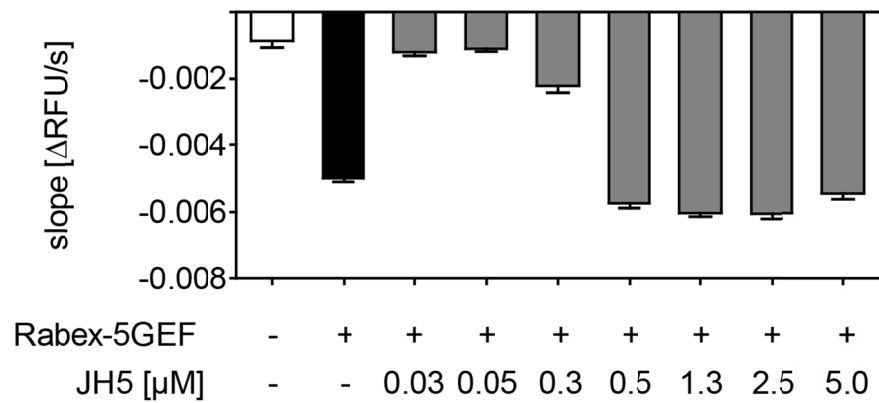
Supporting figure 26   JH5 was active in the Rabex-5GEF-Rab5a nucleotide exchange.
The nucleotide exchange was performed analogue to the Rabex-5GEF-Rab5c nucleotide exchange. An IC50 of 1.8 µM (95 % CI 0.9 - 3.5 µM) was obtained. These results were comparable to the nucleotide exchange inhibition observed for Rab5c. In conclusion, the inhibitory effect of JH5 on Rabex-5GEF was observed for Rab5a and Rab5c in a comparable manner.
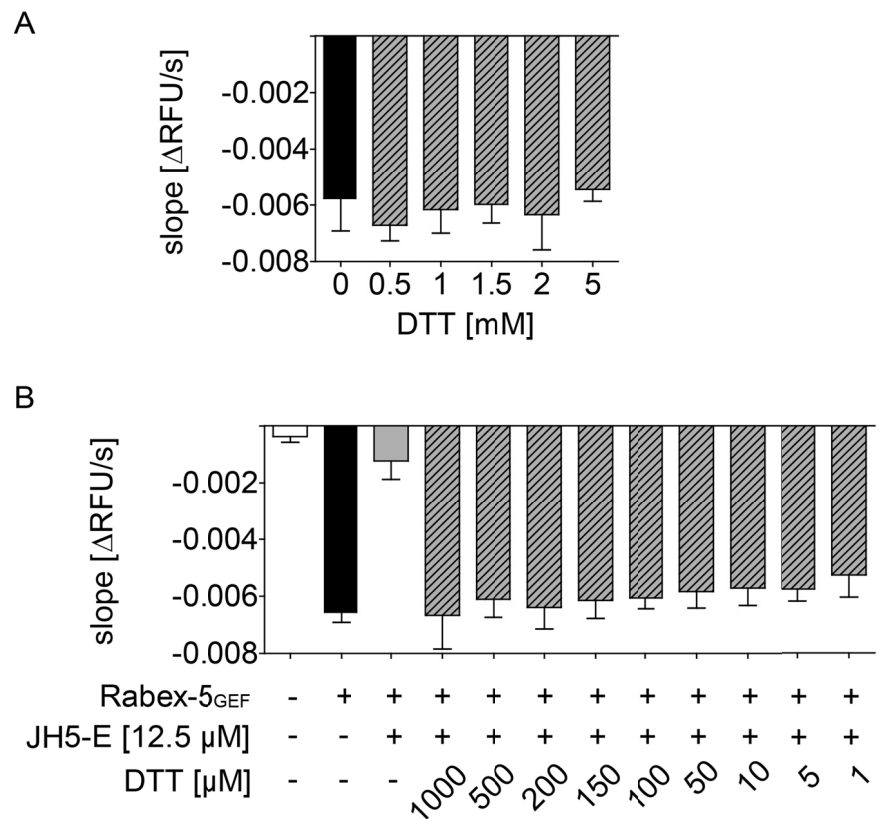
Supporting figure 27   Nucleotide exchange of Rabex-5GEF on Rab5c in the presence of DTT.[27]
A) Rabex-5GEF nucleotide exchange assay in presence of indicated DTT concentrations. The nucleotide exchange rate is unaffected. **B)** Rabex-5GEF mediated nucleotide exchange is inhibited by 12.5 µM JH5-E (grey column). The inhibitory effect of JH5-E is abrogated by addition of DTT in concentrations from 1 mM to 1 nM (striped columns). In summary, the presence of DTT does not affect the Rabex-5GEF-Rab5c nucleotide exchange but blunts the activity of JH5-E.

---

[27] Measurements were planned by C.I. Wosnitza and kindly performed by Nicole Krämer

8.7 Molecular interaction
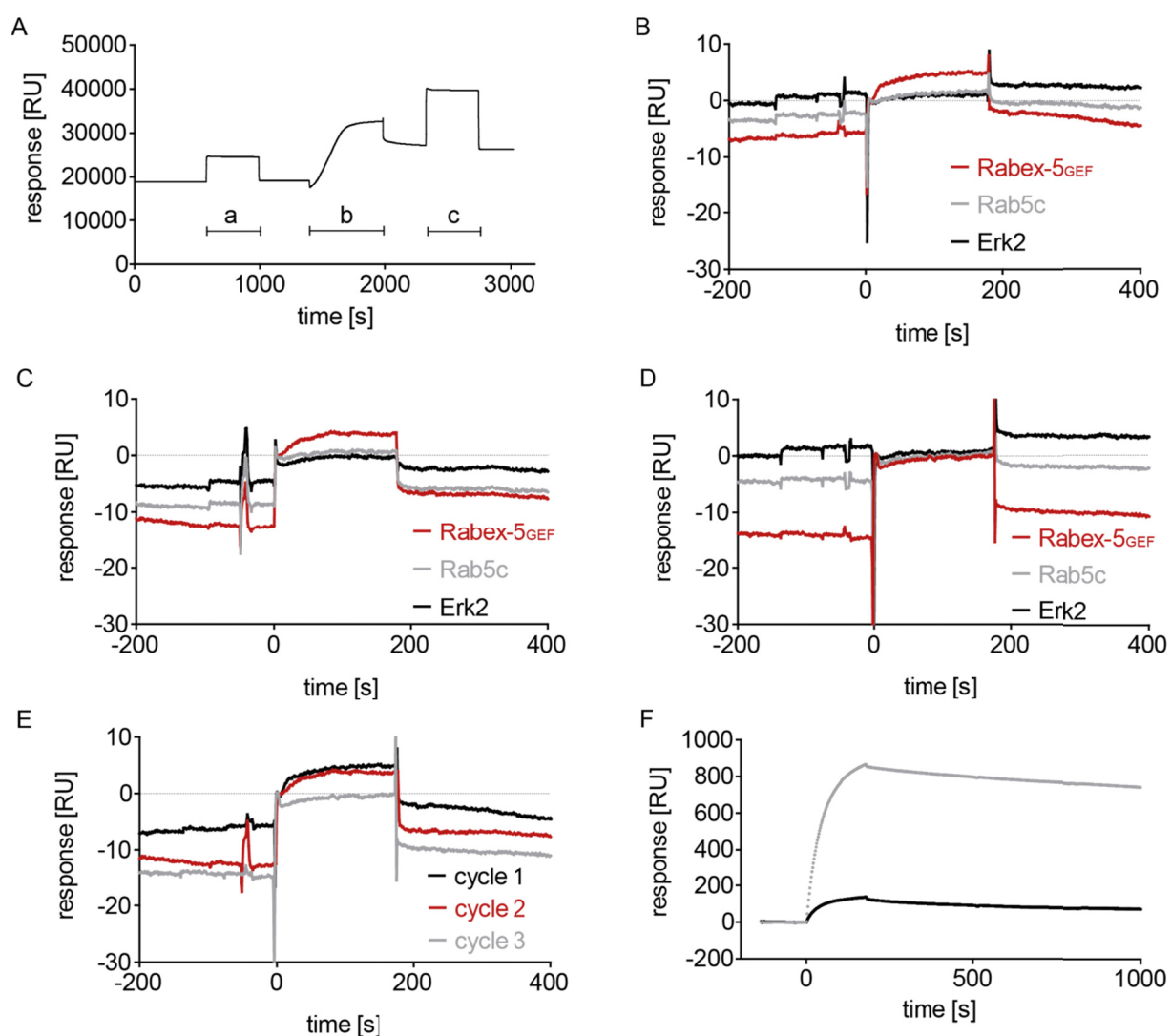
Supporting figure 28   Preliminary surface plasmon resonance experiments.
A) Coupling of protein to the sensorchip, here Rabex-5GEF as example. **a)** 7 minutes EDC + NHS (1:1) **b)** 10 minutes Rabex-5GEF (10 µg/mL) **c)** 7 minutes ethanolamine (1 M; pH 8.5). **B)** Response units [RU] on the y-axis and time [s] on the x-axis. The first injection of 50 µM C4.30.F05 onto sensorchip with Rabex-5GEF, Rab5c and Erk protein coupled. Injection was performed at t=0. Potentially binding to Rabex-5GEF was observed, no reaction with Rab5c and Erk2 protein. However, total response units are very low (less than 10 RU) due to the small size difference the compound can induce. **C)** Same procedure as in B, second injection. **D)** Same procedure as in B, third injection. **E)** Overlay of the Rabex-5GEF curves from B-D marked as cycle 1 (B), cycle 2 (C) and cycle 3 (D). The potential binding behaviour of C4.30.F05 to Rabex-5GEF was not reproducible in cycle 3. **F)** Since the injection of compound did not result in reproducible results over several cycles, a control Rab5c interaction with Rabex-5GEF was analysed on a fresh sensorchip. The first injection of Rab5c onto coupled Rabex-5GEF produced a strong interaction; the second interaction already resulted in decreased signal. This was taken as sign that the protein was not stable on the sensorchip and could not be used over several rounds of analysis as done in general. Together with the observation that the interaction resulted in very low signals when protein was coupled it was decided that this method is not suitable for determination of protein-compound interaction. It was planned to return to this method as soon as a biotinylated JH5 derivative should be available.
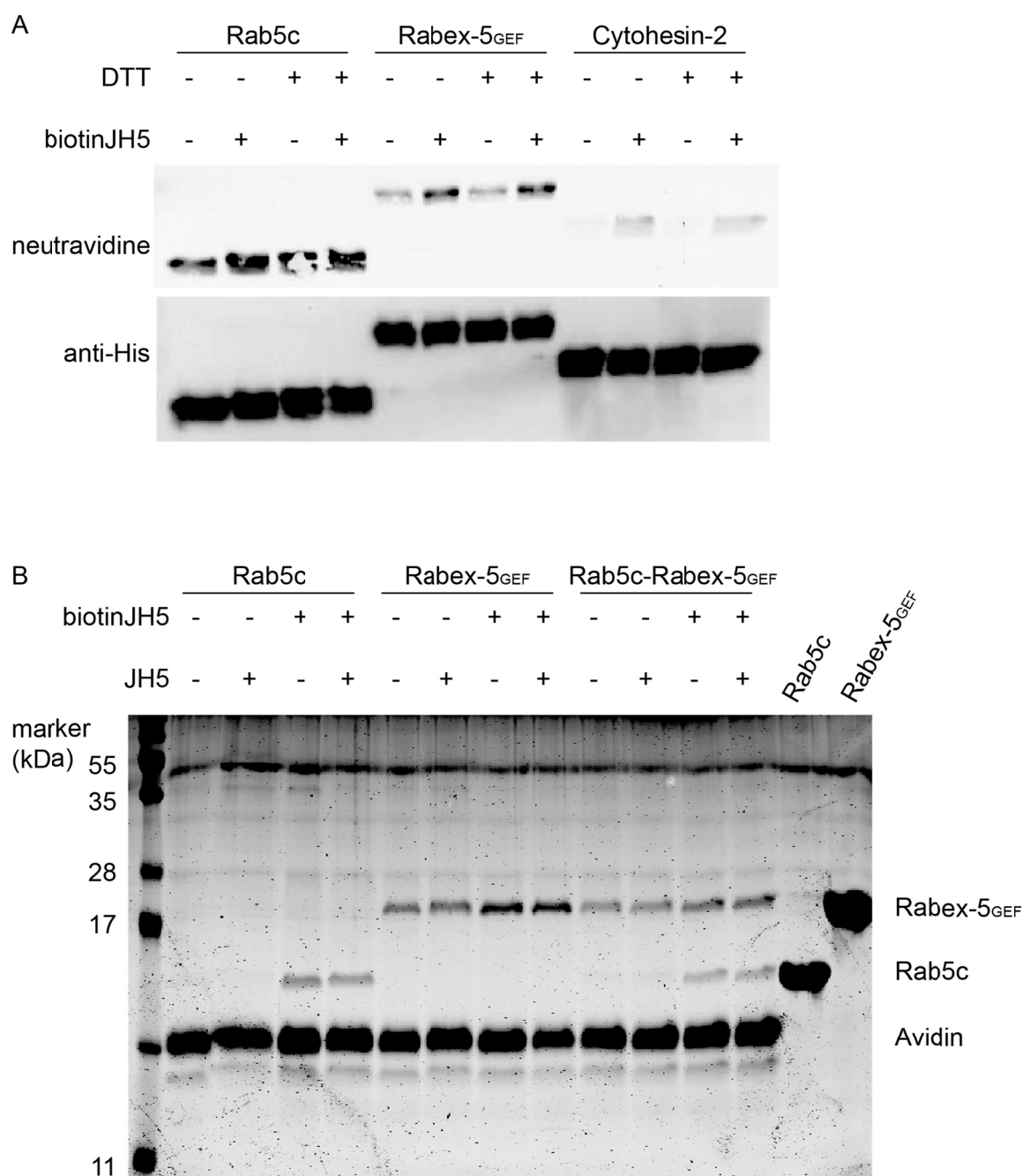
Supporting figure 29   The compound biotinJH5 is not comparable to JH5.
A) The compound biotinJH5 was supposed to be used to investigate whether a covalent binding mechanism between JH5 and Rabex-5GEF was existent. Therefore, the proteins used in this experiment were incubated with biotinJH5 in absence and presence of DTT and subjected to western blotting. Detection with Neutravidine allowed visualization of the biotin-tag. The anti-His antibody detected the proteins and confirmed equal loading in all lanes. The Rab5c samples with and without biotinJH5 revealed a similar staining with Neutravidine indicating non-specific background interaction. The Rabex-5GEF samples were stronger labelled by Neutravidine in presence of biotinJH5 indicating an interaction between the small molecule and Rabex-5GEF. However, the same effect was observed with Cytohesin-2 which is in contrast to interaction and activity observed with JH5. Hence, the biotinJH5 was found to be less specific than JH5. Moreover, in none of the samples biotinJH5 interaction could be abrogated with DTT. This is in contrast to the behaviour of JH5. **B)** A pull-down approach was used to investigate if biotinJH5 bound to Rabex-5GEF or Rab5c or the complex of both proteins. For all three conditions binding of biotinJH5 could not be displaced by the addition of JH5. In summary, these findings indicated that biotinJH5 differs from JH5. The compound biotinJH5 was found to be non-specific, not DTT sensitive and interacted with Cytohesin-2. In summary, it was different than JH5.
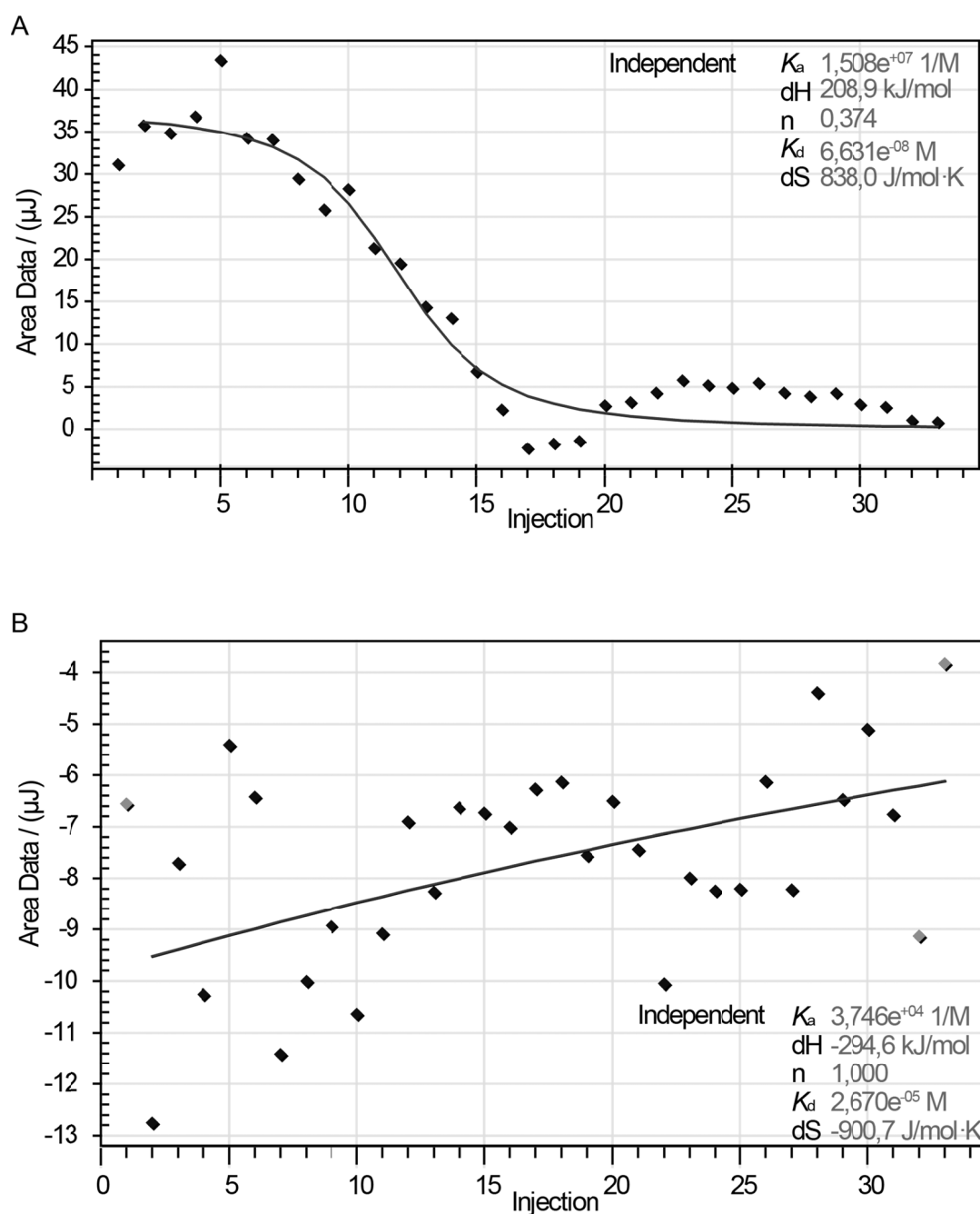
Supporting figure 30   Preliminary ITC data: Rabex-5GEF and JH5
On the y-axis is the area under the ITC curve (µJ) that corresponds to the total heat exchange per injection depicted. The x-axis gives the number of injection that shows the increase of titrant (JH5, 60 µM). In the sample cell Rabex-5GEF was present in 6 µM concentration. The constants obtained from the independent fit (manufacturers' protocol) were binding affinity (K_a), enthalpy (dH), stoichiometry (n), dissociation constant (K_d), and entropy (dS). A) The only one of many measurements resulting in a sigmoidal curve. However, the stoichiometry (n) could only be 0.4 to enable fitting of the curve. This does not support the assumed 1:1 interaction. Moreover, this measurement could not be reproduced. It is likely than this measurement represents an artefact e.g. impurities in one of the ITC cells. B) One representative measurement. In the most measurements the maximal interval between minimum and maximum signal was only about 10 µJ. This indicates that the measurements are very close to the background which makes data interpretation challenging. Moreover, not sigmoidal curve with plateaus was obtained. Since no conclusive data was obtained with ITC the method for identification of the compounds interaction partner and a corresponding K_d were not pursued further.
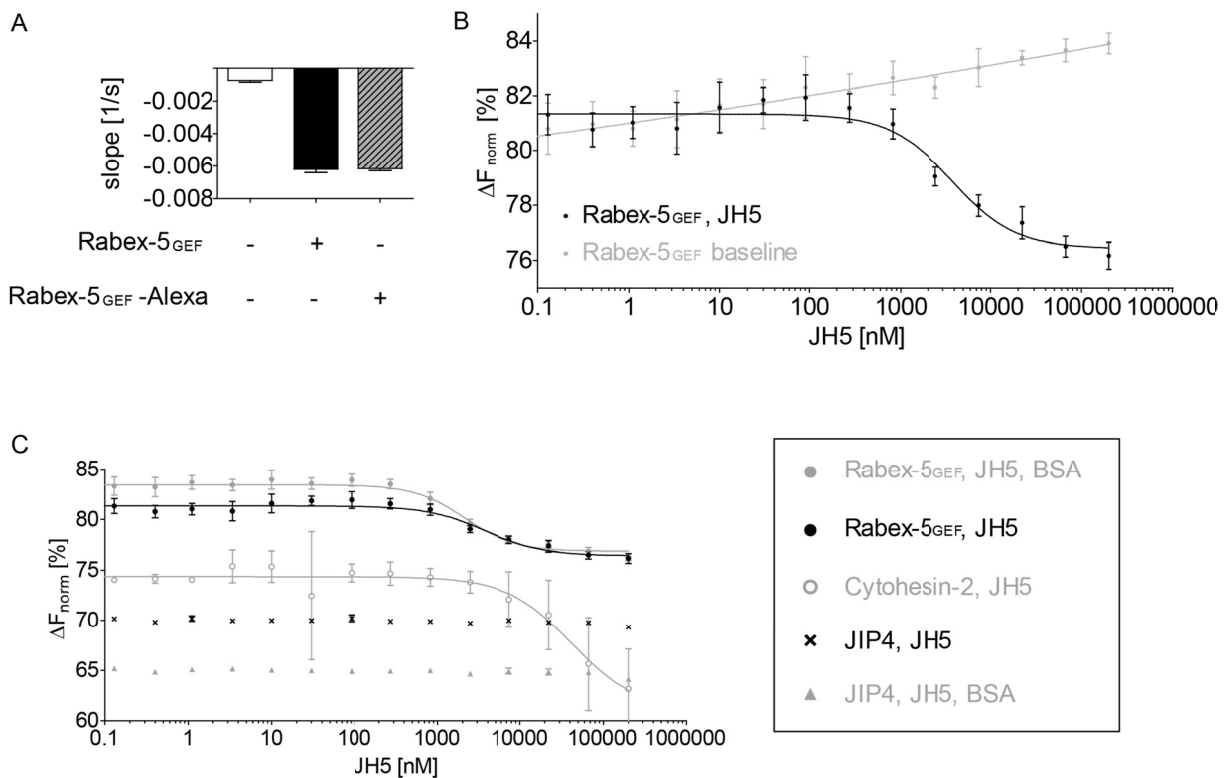
Supporting figure 31 MST with Alexa647-Rabex-5GEF.

MST analytic using Rabex-5GEF with Alexa647 label reveals specific binding of JH5 to Rabex-5GEF. **A)** Nucleotide exchange assay for comparison of Rabex-5GEF and Rabex-5GEF-Alexa activity showed that the label did not disturb the protein activity. Readout was the tryptophan fluorescence of Rab5c which without Rabex-5GEF addition had little intrinsic nucleotide exchange activity (white column). Rabex-5GEF-Alexa (grey, striped column) increased the nucleotide exchange in the same magnitude as unlabelled Rabex-5GEF (black column). **B)** In understand the new method MST, initial tests like background levels and fluctuations were analysed. Therefore, the baseline was recorded by monitoring the labelled protein in the MST buffer without addition of compound. A drift of the baseline was observed (grey curve), however, this drift is unlikely to be problematic since the direction of the drift is opposite to the change in the Rabex-5GEF interaction curve with JH5. **C)** The interaction of JH5 with Rabex-5GEF revealed a K_d of 3.8 μM (95% CI: 2.7-5.3 μM) and did not change significantly in presence of 500 nM BSA. In presence of BSA the determined K_d was 2.1 μM (95% CI: 1.6-2.8 μM). As control for specificity the proteins JIP4[28] and Cytohesin-2-Sec7-domain were analysed. Both, in absence and presence of BSA no interaction between JH5 and JIP4 was detected. With Cytohesin-2-Sec7 a weak interacting was observed, however no saturation was reached even with 200 μM JH5. The calculated K_d of 42.4 μM (95 % CI 9.8 – 183.5 μM) has to be considered inaccurate due to the large 95 % CI. This indicated that JH5 interacts specifically with Rabex-5GEF.

---

[28] Fluorescein labelled JIP4 was a kindly provided by Benjamin Weiche and Cytohesin-2-Alexa647 was a kind gift of Heike Blockus.
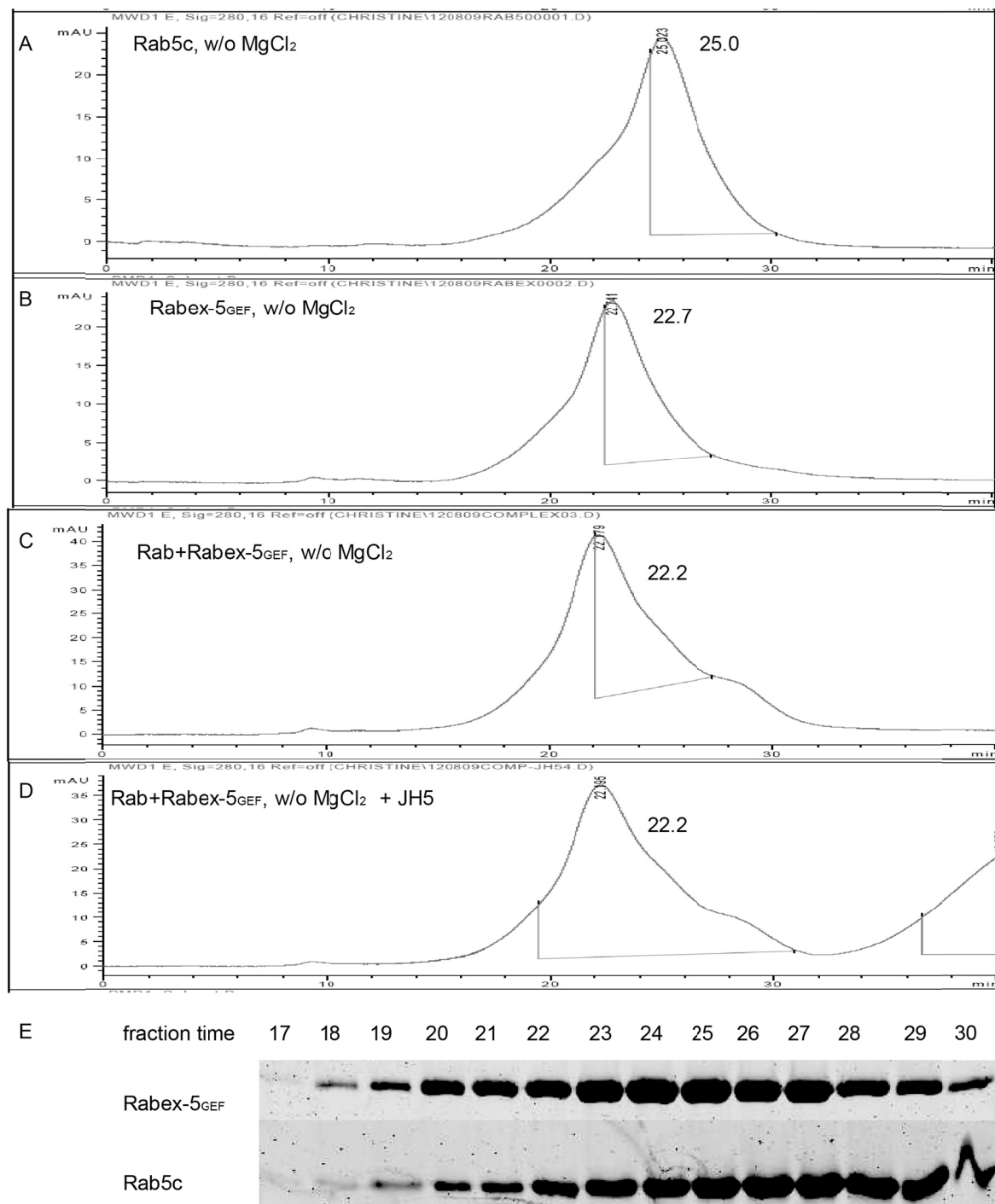
Supporting figure 32   Size exclusion chromatography: Rab5c-Rabex-5GEF complex formation.
The experiment was performed in presence and absence of JH5. **A)** Rab5c was observed with a retention time
of 25.0 minutes. **B)** Rabex-5GEF was observed with a retention time of 22.7 minutes. **C)** The complex of Rab5c
and Rabex-5GEF was detected at a retention time of 22.2 minutes. **D)** The complex in presence of JH5 was
observed at 22.2 minutes, the same retention time as for the untreated complex. **E)** Fractions from the runs
depicted in A and B were monitored via SDS-PAGE. Rabex-5GEF and Rab5c run in overlapping fractions which
makes a clear separation between the peaks of the single proteins and the complex challenging. Therefore, this
approach was not pursued any further.

183

8.8   Compound and protein solubility

About 30 % of all compounds have a solubility of less than 10 µM in aqueous buffers.[271] JH5 and derivatives were found to be well soluble.
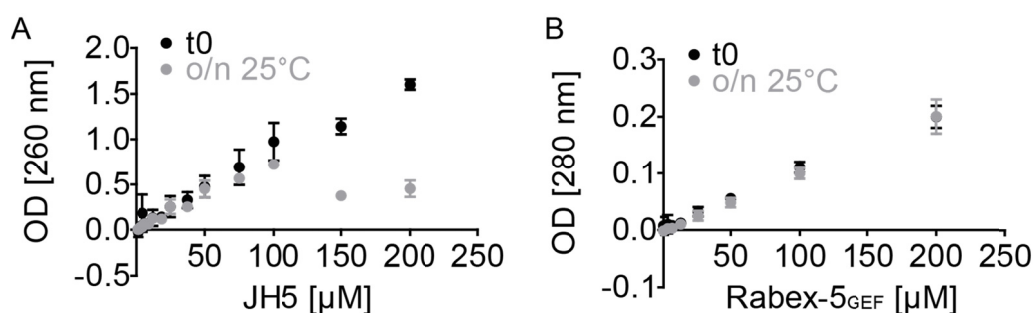
Supporting figure 33   Solubility of JH5 and Rabex-5GEF in ITC buffer
The solubility of compound and proteins was determined by measuring the absorption at an appropriate wavelength. Samples were incubated, centrifuged and the supernatant was transferred to a fresh tube before absorption determination. The ITC buffer consists of 20 mM Tris, pH 8.0 at RT, 100 mM NaCl, 2 mM MgCl$_2$, 2% DMSO. **A)** The solubility of JH5 is undisturbed until 50 µM. **B)** Rabex-5GEF is soluble to at least 200 µM.
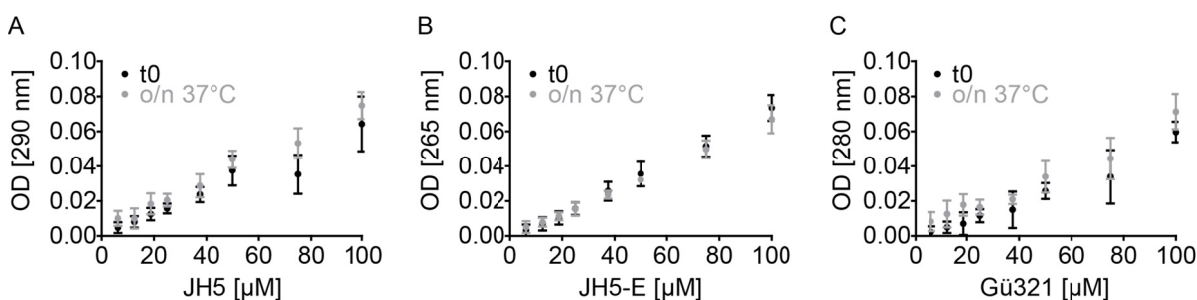
Supporting figure 34   Solubility of JH5, JH5-E and Gü321 in RPMI with 0.5 % DMSO.
The solubility of the compounds was determined by measurement of the absorption at an appropriate wavelength as described in Supporting figure 33. As buffer, RPMI medium without phenolred was used. DMSO concentration was limited to 0.5 % to investigate the potential of the compounds in cellular application where DMSO use is limited. **A)** The solubility of JH5 is undisturbed until 50 µM and acceptable to 100 µM. **B)** JH5-E has similar solubility as JH5 and stays in solution till 100 µM. **C)** Gü321 is also soluble until 100 µM.
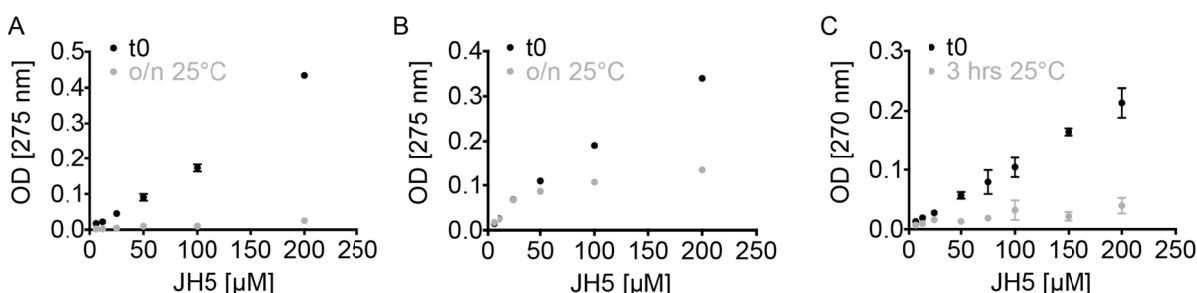
Supporting figure 35   Solubility of CS-dimers 1-3 in nucleotide exchange buffer.
The solubility of the compounds was determined by measurement of the absorption at an appropriate wavelength as described in Supporting figure 33. **A)** Solubility of CS-dimer 1 is undisturbed until 200 µM upon initial dissolving in buffer. However, after o/n incubation at 25 °C the compound had precipitated in all tested concentrations. **B)** CS-dimer 2 was soluble up to 50 µM, even after incubation o/n. **C)** CS-dimer 3 was soluble at the initial dissolving in buffer, however, already after 3 hours at 25 °C the compound precipitated.
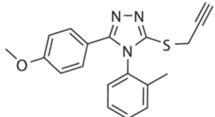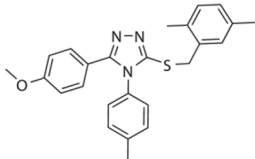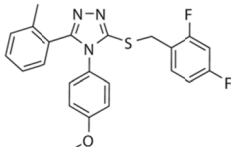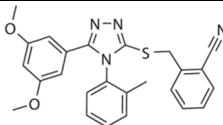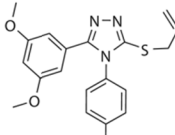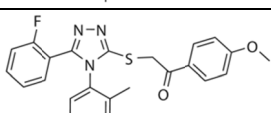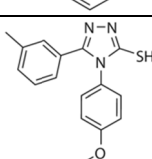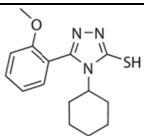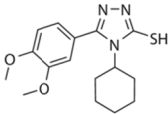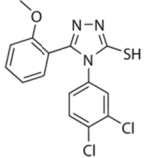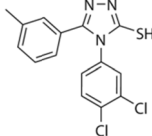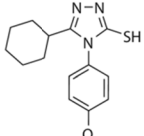
8.9 SAR

Supporting table 17   **Inactive, structurally similar compounds**

Name	Structure	ΔRFU[a]	Active?[b]	Free thiol?[c]
C2.02.A06		3.3054	N	N
C3.01.H08		3.967	N	N
C3.02.H02		3.9639	N	N
C4.02.A06		3.628	N	N
C4.02.C10		3.4306	N	N
C4.02.E10		11.41	N	N
C4.02.F09		3.9661	N	N
C4.05.E11		5.04375	N	N
C4.05.H10		7.0977	N	N
C4.06.A05		3.3139	N	N
C4.06.B02		3.8636	N	N

Name	Structure	ΔRFU[a]	Active?[b]	Free thiol?[c]
C4.06.B06		4.1567	N	N
C4.06.C06		3.6425	N	N
C4.06.D08		4.1928	N	N
C4.06.E06		3.7834	N	N
C4.06.F04		3.4311	N	N
C4.06.H04		3.06927	N	N
C4.30.A06		1.6339	W	Y
C4.30.A08		0.6781	Y	Y
C4.30.B06		-2.1293	Y	Y
C4.30.B08		3.7752	N	Y
C4.30.C06		2.5437	N	Y
C4.30.E06		0.1987	Y	Y

Name	Structure	ΔRFU[a]	Active?[b]	Free thiol?[c]
C4.30.F05		0.2382	Y	Y
C4.30.F06		2.7037	N	Y
C4.30.H07		0.8115	Y	Y

80% similarity search with Chem Finder (ChemOffice 2002) based on the JH5 structure. **[a]** ΔRFU value observed in the screening. **[b]** N = no: the ΔRFU was observed to have a value of at least two. w= weak activity: compounds decreasing the ΔRFU to less than the value 2. Y = yes: compounds that decreased the ΔRFU to the value 1 or less. **[c]** N = no, Y = yes. Grey highlighted compounds were tested for activity and found to be active in the low micromolar range.

8.10 Rabex-5GEF cysteine mutants
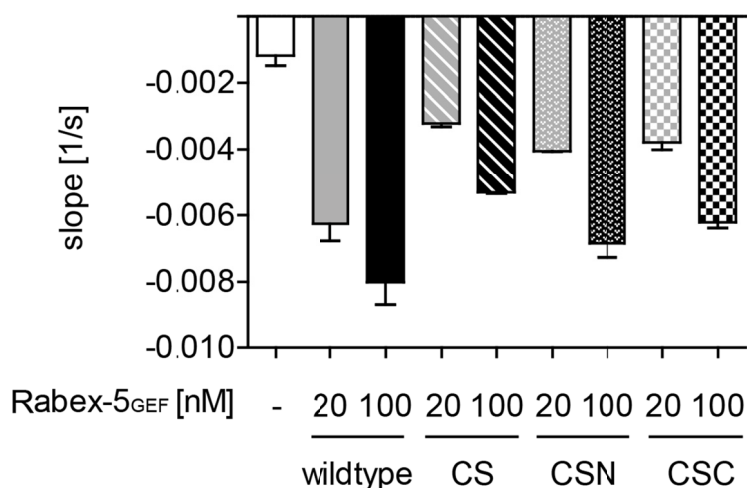
Supporting figure 36 **Activity of Rabex-5GEF cysteine to serine mutants.**
The activity of the proteins was observed in the Rabex-5GEF-Rab5c nucleotide exchange assay. For each Rabex-5GEF protein, a sample with 20 nM and one with 100 nM was performed. Especially in the 20 nM samples the decrease of activity of all cysteine-to-serine mutants was observed. Nevertheless, at least 50 % residual activity was detected. Using 100 nM Rabex-5GEF protein, for all constructs an acceptable measurement window was observed. For the definition of the mutants see Figure 41 in the main text.

8.11 Mass spectrometry

Supporting table 18   **Mass spectrometry of JH5 treated, digested Rabex-5GEF.**

Sequence	# PSMs	Protein Group Accessions	Modifications	MH+ [Da]
DLSIEEQSECAQ	31	Rabex5	C10(Propionamide)	1422,60466
DAQSLNLSQEDF	137	Rabex5		1366,61260
DAQSLNLSQE	207	Rabex5		1104,51653
DRYMSGQTSP	147	Rabex5		1141,49443
DMVVKAIT	228	Rabex5	M2(Oxidation)	892,48027
DMVVKAIT	127	Rabex5		876,48601
GHHHHHHGSIET	2	Rabex5		1385,62029
DRYMSGQTSP	53	Rabex5	M4(Oxidation)	1157,48931
TDRVSKEFIE	21	Rabex5		1223,62663
IYKQTKLFLE	34	Rabex5		1282,74065
CAQDFYHNVAE	1	Rabex5		1296,53093
FLKTFHKTGQE	13	Rabex5		1335,70427
KLDAQSLNLSQE	28	Rabex5		1345,69524
CAQDFYHNVAE	17	Rabex5	C1(Propionamide)	1367,56841
DFDRYMSGQTSP	28	Rabex5		1403,59038
DFDRYMSGQTSP	59	Rabex5	M6(Oxidation)	1419,58440
VSDMVVKAITDIIE	15	Rabex5		1532,82195
VSDMVVKAITDIIE	43	Rabex5	M4(Oxidation)	1548,82720
QSECAQDFYHNVAE	1	Rabex5	Q1(Deamidated); C4(Carbamidomethyl); Q6(Deamidated)	1699,66142
FIEFLKTFHKTGQE	4	Rabex5		1724,90091
DIPEVSDMVVKAITDIIE	16	Rabex5	M8(Oxidation)	2003,02312
KLDAQSLNLSQEDFDRYMSGQTSP	5	Rabex5		2730,27134
KLDAQSLNLSQEDFDRYMSGQTSP	18	Rabex5	M18(Oxidation)	2746,26267
FIEFLKTFHKTGQEIYKQTKLFLE	1	Rabex5		2988,61538
IQYITR	26	Rabex5		793,45683
HIFNAIK	800	Rabex5		842,48790
IMDQIEK	548	Rabex5		876,44945
WVTPQML	44	Rabex5	M6(Oxidation)	890,44505
DKLACITK	56	Rabex5		891,49675
IMDQIEK	252	Rabex5	M2(Oxidation)	892,44438
EFIEFLK	228	Rabex5		925,50298
SNIQYITR	16	Rabex5		994,53057
LSQEDFDR	22	Rabex5		1009,45873
PEVSDMVVK	4	Rabex5	M6(Oxidation)	1019,50707
AITDIIEMD	32	Rabex5	M8(Oxidation)	1036,48540
TDIIEMDSK	24	Rabex5		1051,49785
TDIIEMDSK	48	Rabex5	M6(Oxidation)	1067,49297
LVLLGESAVGK	24	Rab5c		1085,65471
NLSQEDFDR	20	Rabex5		1123,49797
IPEVSDMVVK	28	Rabex5	M7(Oxidation)	1132,59209
LFLEGMHYK	228	Rabex5	M6(Oxidation)	1153,57134
ITDIIEMDSK	18	Rabex5	M7(Oxidation)	1180,57182
HIFNAIKITK	104	Rabex5		1184,71460

Sequence	# PSMs	Protein Group Accessions	Modifications	MH+ [Da]
AITDIIEMDSK	512	Rabex5		1235,61870
LQSNIQYITR	968	Rabex5		1235,67412
VSKEFIEFLK	200	Rabex5		1239,69829
VEKIMDQIEK	144	Rabex5	M5(Oxidation)	1248,65032
AITDIIEMDSK	1476	Rabex5	M8(Oxidation)	1251,60991
LFLEGMHYKR	128	Rabex5	M6(Oxidation)	1309,67436
LMTGEDGYYFT	4	Rabex5	M2(Oxidation)	1312,54070
SLNLSQEDFDR	18	Rabex5		1323,61772
TFHKTGQEIYK	220	Rabex5		1351,69780
AITDIIEMDSKR	164	Rabex5		1391,71794
QASPNIVIALAGNK	12	Rab5c		1395,79485
AITDIIEMDSKR	300	Rabex5	M8(Oxidation)	1407,71416
LMTGEDGYYFTNL	24	Rabex5	M2(Oxidation)	1539,66655
IMDQIEKYIMTR	172	Rabex5	M2(Oxidation); M10(Oxidation)	1572,77593
TAMNVNEIFMAIAK	8	Rab5c	M3(Oxidation); M10(Oxidation)	1584,77617
PPRLQSNIQYITR	4	Rabex5		1585,88028
NEPASADDFLPTLIY	10	Rabex5		1665,80034
LDAQSLNLSQEDFDR	152	Rabex5		1750,82353
GNPPRLQSNIQYITR	216	Rabex5		1756,94529
LSQEDFDRYMSGQTSP	30	Rabex5	M10(Oxidation)	1876,80156
GAQAAIVVYDITNTDTFAR	12	Rab5c		2026,02481
NEPASADDFLPTLIYIVLK	156	Rabex5		2119,13138
ITKNEPASADDFLPTLIYIVLK	8	Rabex5		2461,35770
DLSIEEQSECAQDFYHNVAER	32	Rabex5		2483,07840
DLSIEEQSECAQDFYHNVAER	76	Rabex5	C10(Propionamide)	2554,11509
LDAQSLNLSQEDFDRYMSGQTSP	108	Rabex5		2602,16997
LDAQSLNLSQEDFDRYMSGQTSP	260	Rabex5	M17(Oxidation)	2618,16904
NEPASADDFLPTLIYIVLKGNPPR	4	Rabex5		2640,40042
HIFNAIK	9	Rabex5	N4(Deamidated)	843,47197
GKVPPERVEK	86	Rabex5		1138,65837
TFHKTGQEIYKQTK	16	Rabex5		1708,90097
GNPPRLQSNIQYITR	7	Rabex5	Q7(Deamidated)	1757,93058
AITDIIEMDSKRVPR	22	Rabex5	M8(Oxidation)	1759,93778
DLSIEEQSECAQDFYHNVAER	23	Rabex5	C10(Carbamidomethyl); Q12(Deamidated)	2541,08402
WVTPQMLCVPVNEDIPEVSDMVVK	8	Rabex5	Q5(Deamidated); M6(Oxidation); C8(Carbamidomethyl); M21(Oxidation)	2818,33939
DLSIEEQSECAQ	15	Rabex5		1351,56951
DLSIEEQSECAQ	12	Rabex5	Q7(Deamidated); C10(Carbamidomethyl)	1409,57390
TSAKTAMNVNE	11	Rab5c		1165,55229
AQAYADDNSLLFME	2	Rab5c	M13(Oxidation)	1603,69512
IIEMDSK	4	Rabex5		835,42302
PPERVEK	10	Rabex5		854,47331

Sequence	# PSMs	Protein Group Accessions	Modifications	MH+ [Da]
WVTPQML	12	Rabex5		874,44884
VPPERVEK	12	Rabex5		953,54198
DKLACITK	24	Rabex5	C5(Propionamide)	962,53374
LQSNIQYIT	12	Rabex5		1079,57305
QSNIQYITR	34	Rabex5		1122,59087
LFLEGMHYK	132	Rabex5		1137,57561
SKEFIEFLK	2	Rabex5		1140,62993
TGQEIYKQTK	4	Rabex5		1195,63602
TDIIEMDSKR	6	Rabex5		1207,59990
VEKIMDQIEK	52	Rabex5		1232,65573
FHKTGQEIYK	2	Rabex5		1250,65079
FDRYMSGQTSP	4	Rabex5	M5(Oxidation)	1304,55986
EDIPEVSDMVVK	12	Rabex5	M9(Oxidation)	1376,66045
IMDQIEKYIMTR	4	Rabex5		1540,78800
IMDQIEKYIMTR	76	Rabex5	M2(Oxidation)	1556,78153
LSQEDFDRYMSGQTSP	14	Rabex5		1860,80181
WVTPQMLCVPVNEDIPEVSDMVVK	28	Rabex5	C8(Propionamide); M21(Oxidation)	2815,36577
WVTPQMLCVPVNEDIPEVSDMVVK	44	Rabex5	M6(Oxidation); C8(Propionamide); M21(Oxidation)	2831,36431
TGQEIYK	20	Rabex5		838,43041
AITDIIEMD	8	Rabex5		1020,49010
KIMDQIEK	2	Rabex5	M3(Oxidation)	1020,53996
IMDQIEKY	10	Rabex5	M2(Oxidation)	1055,50786
ITDIIEMDSK	20	Rabex5		1164,58306
TDIIEMDSKR	8	Rabex5	M6(Oxidation)	1223,59294
DIPEVSDMVVK	6	Rabex5	M8(Oxidation)	1247,61418
WVTPQMLCVPVNEDIPEVSDMVVK	16	Rabex5	C8(Propionamide)	2799,37809
DSKRVPR	49	Rabex5		857,49523
DLSIEEQSECAQ	2	Rabex5	C10(Propionamide); Q12(Deamidated)	1423,58843
DMVVKAITDIIEM	1	Rabex5	M2(Oxidation); M13(Oxidation)	1509,75188
TDRVSKE	56	Rabex5		834,43169
EVSDMVVK	2	Rabex5		906,45964
NIQYITR	6	Rabex5		907,50011
FYHNVAER	2	Rabex5		1035,50420
FLEGMHYK	4	Rabex5	M5(Oxidation)	1040,48662
DLSIEEQSE	8	Rabex5		1049,46135
IPEVSDMVVK	8	Rabex5		1116,59599
NEPASADDFLPT	2	Rabex5		1276,56914
FDRYMSGQTSP	6	Rabex5		1288,56267
ITDIIEMDSKR	2	Rabex5	M7(Oxidation)	1336,67888
EDIPEVSDMVVK	4	Rabex5		1360,66619
LQSNIQYITRF	2	Rabex5		1382,74187
LMTGEDGYYFTN	14	Rabex5		1410,58721
LMTGEDGYYFTN	6	Rabex5	M2(Oxidation)	1426,58281
NEDIPEVSDMVVK	6	Rabex5	M10(Oxidation)	1490,70427
AQSLNLSQEDFDR	2	Rabex5		1522,71123
LMTGEDGYYFTNL	4	Rabex5		1523,67302
EDFDRYMSGQTSP	2	Rabex5	M7(Oxidation)	1548,62798

Sequence	# PSMs	Protein Group Accessions	Modifications	MH+ [Da]
VNEDIPEVSDMVVK	4	Rabex5	M11(Oxidation)	1589,77251
LDAQSLNLSQEDFD	6	Rabex5		1594,72600
DAQSLNLSQEDFDR	4	Rabex5		1637,74394
YVFCPETTDDEKK	36	Rabex5	C4(Propionamide)	1645,74040
QEDFDRYMSGQTSP	4	Rabex5		1660,69084
QEDFDRYMSGQTSP	6	Rabex5	M8(Oxidation)	1676,68682
LDAQSLNLSQEDFDRY	4	Rabex5		1913,88921
CVPVNEDIPEVSDMVVK	12	Rabex5	C1(Propionamide)	1943,94292
CVPVNEDIPEVSDMVVK	2	Rabex5	C1(Propionamide); M14(Oxidation)	1959,93839
NLSQEDFDRYMSGQTSP	12	Rabex5		1974,85002
NLSQEDFDRYMSGQTSP	12	Rabex5	M11(Oxidation)	1990,84563
ITKNEPASADDFLPTLIY	2	Rabex5		2008,01921
SLNLSQEDFDRYMSGQTSP	6	Rabex5		2174,96465
SLNLSQEDFDRYMSGQTSP	6	Rabex5	M13(Oxidation)	2190,95952
WVTPQMLCVPVNEDIPEVSDMVVK	4	Rabex5	M6(Oxidation); M21(Oxidation)	2760,32480
LDAQSLNLSQEDFDRYMSGQTSP	1	Rabex5	N7(Deamidated)	2603,17051

Supporting table 19   **Mass spectrometry of DMSO treated, digested Rabex-5GEF.**

Sequence	# PSMs	Protein Group Accessions	Modifications	MH+ [Da]
DAQSLNLSQEDF	48	Rabex5		1366,61260
DAQSLNLSQE	56	Rabex5		1104,51702
DLSIEEQSECAQ	12	Rabex5		1351,56890
DLSIEEQSECAQ	9	Rabex5	C10(Propionamide)	1422,60649
DRYMSGQTSP	40	Rabex5		1141,49419
DMVVKAIT	32	Rabex5	M2(Oxidation)	892,48107
DLSIEEQSECAQ	8	Rabex5	C10(Carbamidomethyl); Q12(Deamidated)	1409,57195
DMVVKAIT	26	Rabex5		876,48607
DLSIEEQSECAQ	14	Rabex5	C10(Propionamide); Q12(Deamidated)	1423,58940
DRYMSGQTSP	42	Rabex5	M4(Oxidation)	1157,48967
DDTTVKFEIW	3			1253,60344
TSAKTAMNVNE	1	Rab5c		1165,55217
IYKQTKLFLE	13	Rabex5		1282,73857
KLDAQSLNLSQE	18	Rabex5		1345,69548
CAQDFYHNVAE	8	Rabex5	C1(Propionamide)	1367,57012
DFDRYMSGQTSP	11	Rabex5		1403,59050
DFDRYMSGQTSP	45	Rabex5	M6(Oxidation)	1419,58440
VSDMVVKAITDIIE	24	Rabex5	M4(Oxidation)	1548,81584
AQAYADDNSLLFME	1	Rab5c	M13(Oxidation)	1603,69219

Sequence	# PSMs	Protein Group Accessions	Modifications	MH+ [Da]
KLDAQSLNLSQEDFD RYMSGQTSP	12	Rabex5	M18(Oxidation)	2746,25992
IQYITR	18	Rabex5		793,45708
HIFNAIK	412	Rabex5		842,48833
IMDQIEK	212	Rabex5		876,44945
WVTPQML	14	Rabex5	M6(Oxidation)	890,44457
DKLACITK	24	Rabex5		891,49681
IMDQIEK	116	Rabex5	M2(Oxidation)	892,44432
IEMDSKR	4	Rabex5	M3(Oxidation)	894,43553
EFIEFLK	184	Rabex5		925,50334
DKLACITK	20	Rabex5	C5(Propionamide)	962,53526
AITDIIEMD	18	Rabex5	M8(Oxidation)	1036,48625
DLSIEEQSE	16	Rabex5		1049,46294
IMDQIEKY	12	Rabex5	M2(Oxidation)	1055,50786
TDIIEMDSK	34	Rabex5	M6(Oxidation)	1067,49224
LFLEGMHYK	188	Rabex5	M6(Oxidation)	1153,57134
ITDIIEMDSK	28	Rabex5	M7(Oxidation)	1180,57744
HIFNAIKITK	88	Rabex5		1184,71488
AITDIIEMDSK	348	Rabex5		1235,61919
LQSNIQYITR	408	Rabex5		1235,67388
VSKEFIEFLK	180	Rabex5		1239,69853
VEKIMDQIEK	124	Rabex5	M5(Oxidation)	1248,64946
AITDIIEMDSK	1016	Rabex5	M8(Oxidation)	1251,61296
LFLEGMHYKR	96	Rabex5	M6(Oxidation)	1309,67156
TFHKTGQEIYK	140	Rabex5		1351,70036
AITDIIEMDSKR	84	Rabex5		1391,71904
QASPNIVIALAGNK	20	Rab5c		1395,79497
AITDIIEMDSKR	412	Rabex5	M8(Oxidation)	1407,71489
LMTGEDGYYFTNL	8	Rabex5	M2(Oxidation)	1539,66191
IMDQIEKYIMTR	36	Rabex5	M10(Oxidation)	1556,77970
IMDQIEKYIMTR	228	Rabex5	M2(Oxidation); M10(Oxidation)	1572,77605
PPRLQSNIQYITR	6	Rabex5		1585,87845
LDAQSLNLSQEDFDR	112	Rabex5		1750,82366
GNPPRLQSNIQYITR	164	Rabex5		1756,94547
LSQEDFDRYMSGQTS P	22	Rabex5	M10(Oxidation)	1876,80193
LDAQSLNLSQEDFDR Y	28	Rabex5		1913,88567
NEPASADDFLPTLIYI VLK	108	Rabex5		2119,13120
ITKNEPASADDFLPTL IYIVLK	32	Rabex5		2461,36136
DLSIEEQSECAQDFY HNVAER	28	Rabex5		2483,08097
DLSIEEQSECAQDFY HNVAER	60	Rabex5	C10(Propionamide)	2554,11563
LDAQSLNLSQEDFDR YMSGQTSP	76	Rabex5		2602,17368
LDAQSLNLSQEDFDR YMSGQTSP	152	Rabex5	M17(Oxidation)	2618,16533
NEPASADDFLPTLIYI VLKGNPPR	16	Rabex5		2640,39988
HIFNAIK	2	Rabex5	N4(Deamidated)	843,47209
GKVPPERVEK	74	Rabex5		1138,65691

Sequence	# PSMs	Protein Group Accessions	Modifications	MH+ [Da]
TFHKTGQEIYKQTK	14	Rabex5		1708,90134
AITDIIEMDSKRVPR	80	Rabex5	M8(Oxidation)	1759,93686
DLSIEEQSECAQDFYHNVAER	16	Rabex5	C10(Carbamidomethyl); Q12(Deamidated)	2541,07798
DLSIEEQSECAQDFYHNVAER	3	Rabex5	Q7(Deamidated); C10(Propionamide); Q12(Deamidated); N17(Deamidated)	2557,08359
SNIQYITR	12	Rabex5		994,53282
LSQEDFDR	4	Rabex5		1009,45897
PEVSDMVVK	2	Rabex5	M6(Oxidation)	1019,50640
LVLLGESAVGK	8	Rab5c		1085,65471
QSNIQYITR	26	Rabex5		1122,58977
NLSQEDFDR	10	Rabex5		1123,50115
IPEVSDMVVK	12	Rabex5	M7(Oxidation)	1132,59233
DIPEVSDMVVK	2	Rabex5	M8(Oxidation)	1247,61626
FDRYMSGQTSP	2	Rabex5	M5(Oxidation)	1304,55791
LMTGEDGYYFT	4	Rabex5	M2(Oxidation)	1312,53935
SLNLSQEDFDR	4	Rabex5		1323,61504
AQDFYHNVAER	2	Rabex5		1349,62424
EDIPEVSDMVVK	2	Rabex5	M9(Oxidation)	1376,66191
NEDIPEVSDMVVK	22	Rabex5	M10(Oxidation)	1490,70453
TAMNVNEIFMAIAK	12	Rab5c	M3(Oxidation); M10(Oxidation)	1584,77703
GAQAAIVVYDITNTDTFAR	8	Rab5c		2026,02097
AVEFQEAQAYADDNSLLFMETSAK	12	Rab5c	M19(Oxidation)	2694,22611
WVTPQMLCVPVNEDIPEVSDMVVK	24	Rabex5	M6(Oxidation); C8(Propionamide); M21(Oxidation)	2831,36357
WVTPQMLCVPVNEDIPEVSDMVVK	4	Rabex5	M6(Oxidation); C8(Carbamidomethyl); N12(Deamidated); M21(Oxidation)	2818,32804
TDRVSKE	24	Rabex5		834,43151
TDRVSKEFIE	4	Rabex5		1223,62554
GHHHHHHGSIE	1	Rabex5		1284,57048
CAQDFYHNVAE	2	Rabex5		1296,53288
FLKTFHKTGQE	12	Rabex5		1335,70317
VSDMVVKAITDIIE	2	Rabex5		1532,82060
QSECAQDFYHNVAE	2	Rabex5	C4(Propionamide)	1711,69805
FIEFLKTFHKTGQE	4	Rabex5		1724,89690
DIPEVSDMVVKAITDIIE	5	Rabex5	M8(Oxidation)	2003,02104
TGQEIYK	4	Rabex5		838,43059
PPERVEK	4	Rabex5		854,47356
LFLEGMH	4	Rabex5	M6(Oxidation)	862,41277
WVTPQML	8	Rabex5		874,44890
NIQYITR	2	Rabex5		907,49993
VPPERVEK	8	Rabex5		953,54180
LQSNIQYI	10	Rabex5		978,52629
TDIIEMDSK	20	Rabex5		1051,49773
PTLIYIVLK	2	Rabex5		1059,67974
TFHKTGQEI	2	Rabex5		1060,54338

Sequence	# PSMs	Protein Group Accessions	Modifications	MH+ [Da]
LFLEGMHYK	36	Rabex5		1137,57524
ITDIIEMDSK	6	Rabex5		1164,58025
NEPASADDFLPT	8	Rabex5		1276,56853
EDIPEVSDMVVK	2	Rabex5		1360,66741
FCPETTDDEKK	2	Rabex5	C2(Propionamide)	1383,61237
QSLNLSQEDFDR	10	Rabex5		1451,67620
NEDIPEVSDMVVK	22	Rabex5		1474,70945
NEPASADDFLPTLI	2	Rabex5		1502,73454
ITKNEPASADDFLPT	8	Rabex5		1618,79692
QEDFDRYMSGQTSP	6	Rabex5	M8(Oxidation)	1676,68852
SQEDFDRYMSGQTSP	6	Rabex5		1747,72234
SQEDFDRYMSGQTSP	10	Rabex5	M9(Oxidation)	1763,71721
NEPASADDFLPTLIYI	4	Rabex5		1778,88579
LSQEDFDRYMSGQTSP	10	Rabex5		1860,80754
CVPVNEDIPEVSDMVVK	6	Rabex5	C1(Propionamide)	1943,95110
CVPVNEDIPEVSDMVVK	10	Rabex5	C1(Propionamide); M14(Oxidation)	1959,94280
NLSQEDFDRYMSGQTSP	10	Rabex5		1974,85002
NLSQEDFDRYMSGQTSP	10	Rabex5	M11(Oxidation)	1990,84331
ITKNEPASADDFLPTLIYI	2	Rabex5		2121,11211
QSLNLSQEDFDRYMSGQTSP	16	Rabex5		2303,02373
QSLNLSQEDFDRYMSGQTSP	8	Rabex5	M14(Oxidation)	2319,01689
WVTPQMLCVPVNEDIPEVSDMVVK	16	Rabex5	C8(Propionamide); M21(Oxidation)	2815,36870

Supporting table 20   Cysteine-Modifications identified in MS (alkylation approach).

# [a]	Modification [b]	Sequence Motif	Highest Peptide Confidence [c]			
			DMSO, urea	DMSO	JH5, urea	JH5
59	Propionamide	IEEQSEcAQDFYH	High	High	High	High
59	Carbamidomethyl	IEEQSEcAQDFYH	High	High	High	High
59	Trioxidation	IEEQSEcAQDFYH	n.d.	High	n.d.	n.d.
103	Carbamidomethyl	LYKYVFcPETTDD	High	High	High	High
103	Propionamide	LYKYVFcPETTDD	High	High	High	High
103	Trioxidation	LYKYVFcPETTDD	n.d.	High	n.d.	High
103	Oxidation	LYKYVFcPETTDD	n.d.	High	n.d	n.d.
103	Dioxidation	LYKYVFcPETTDD	n.d.	High	n.d.	n.d.
132	Carbamidomethyl	VTPQMLcVPVNED	High	High	High	High
132	Propionamide	VTPQMLcVPVNED	High	High	High	High
132	Oxidation	VTPQMLcVPVNED	n.d.	n.d.	n.d.	n.d.
168	Carbamidomethyl	PRDKLAcITKCSK	High	High	High	High
168	Propionamide	PRDKLAcITKCSK	High	High	High	High
168	Dioxidation	PRDKLAcITKCSK	n.d.	High	n.d.	n.d.
168	Trioxidation	PRDKLAcITKCSK	n.d.	High	n.d.	High
172	Propionamide	LACITKcSKHIFN	High	High	High	High
172	Carbamidomethyl	LACITKcSKHIFN	n.d.	High	High	High
172	Trioxidation	LACITKcSKHIFN	n.d.	High	n.d.	n.d.

# [a]	Modification [b]	Sequence Motif	Highest Peptide Confidence [c]			
			DMSO, urea	DMSO	JH5, urea	JH5
220	Propionamide	QYITRFcNPSRLM	High	n.s.c.	n.s.c.	High
220	Carbamidomethyl	QYITRFcNPSRLM	n.d.	n.s.c.	n.s.c.	High
238	Trioxidation	YYFTNLcCAVAFI	High	High	High	High
238	Dioxidation	YYFTNLcCAVAFI	High	High	High	n.d.
238	Oxidation	YYFTNLcCAVAFI	High	High	High	n.d.
238	Carbamidomethyl	YYFTNLcCAVAFI	High	High	High	High
238	Propionamide	YYFTNLcCAVAFI	High	High	High	High
239	Propionamide	YFTNLCcAVAFIE	High	High	High	High
239	Oxidation	YFTNLCcAVAFIE	High	High	High	n.d.
239	Carbamidomethyl	YFTNLCcAVAFIE	High	High	High	n.d.
239	Dioxidation	YFTNLCcAVAFIE	High	High	High	High
239	Trioxidation	YFTNLCcAVAFIE	High	High	High	High

The protein samples (5 µM) were incubated with either DMSO or JH5 (100 µM) for 30 minutes at RT. Urea treated samples were incubated additional 10 minutes in 8 M urea. The samples were purified by gel filtration and SDS-PAGE. **[a]** # indicates the position within the Rabex-5GEF sequence. **[b]** All types of oxidation are introduced accidentally, carbamidomethyl modifications arise from the treatment with iodoacetamide, and propionamide modifications are introduced by treatment with acrylamide. **[c]** n.d. = not detected, n.s.c. = no sequence coverage.
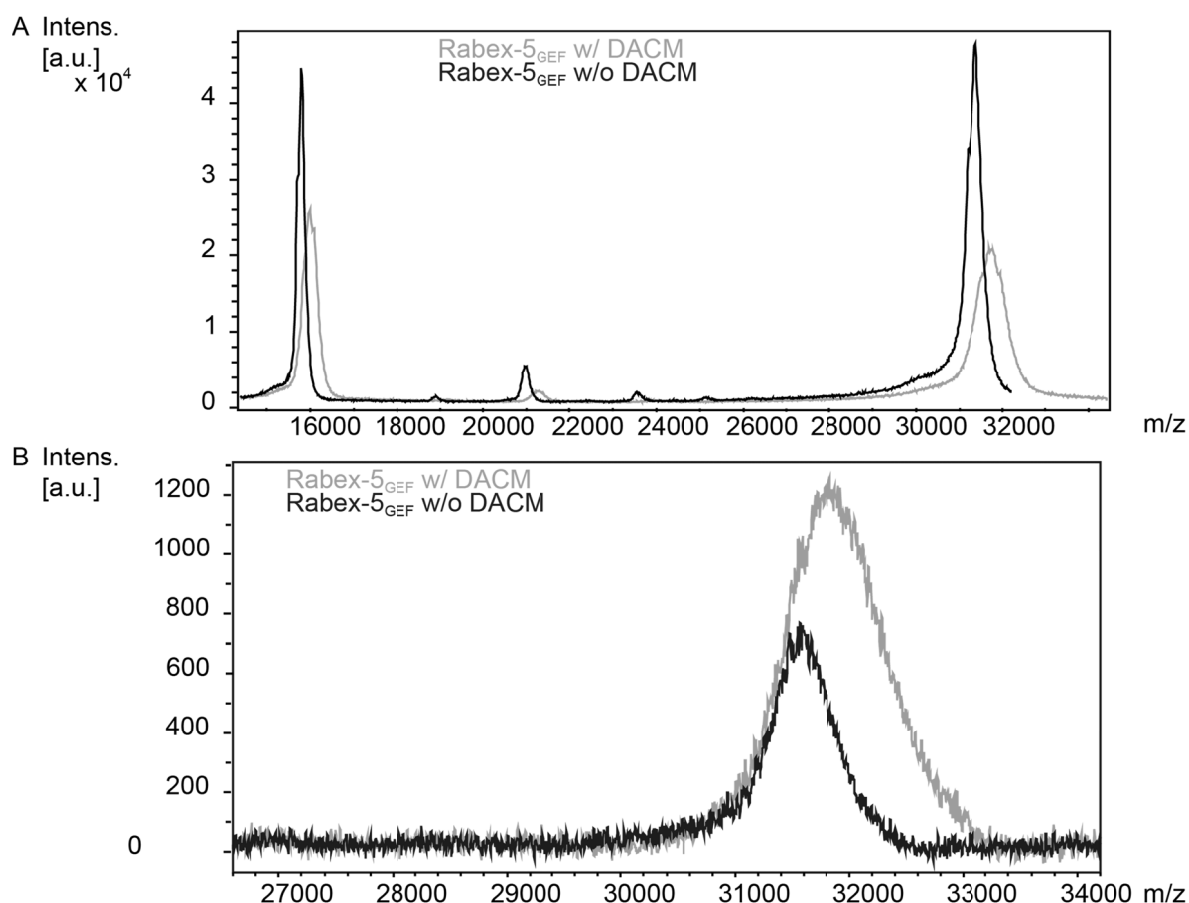
Supporting figure 37   MALDI-TOF analysis of Rabex-5GEF ± DACM as positive control.
Rabex-5GEF was treated with either DMSO or the fluorescent label N-(7-Dimethylamino-4–Methylcoumarin-3-yl))-Maleimide (DACM), a fluorescent label for covalent attachment with the size of 298 Da. The samples were subjected to MALDI-TOF. Mass spectra in the range of 14,000 - 34,000 Da were recorded in the first experiment **(A)** and in the range of 26,000 - 34,000 Da in the second measurement **(B)**. In both cases, a mass shift was observed after treatment with DACM. **A)** The mass shift is visible in all three protein peaks (z = 1, 2, 3).
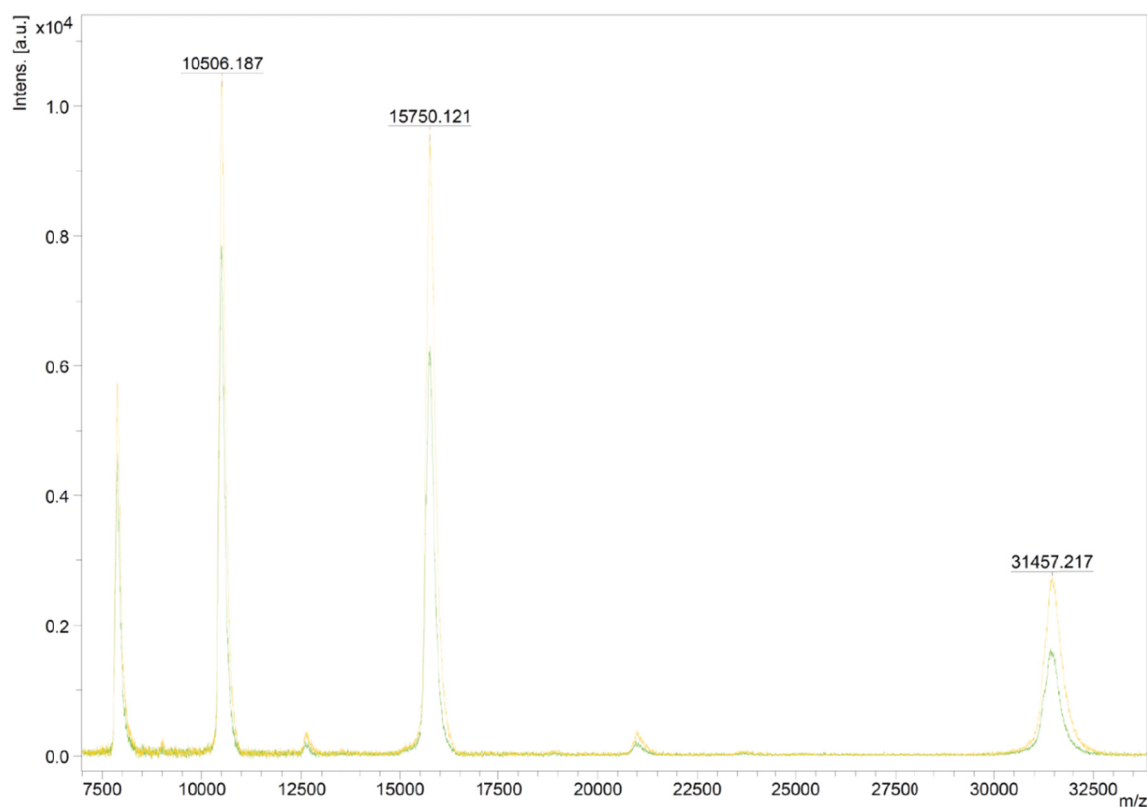
Supporting figure 38   MS analysis of Rabex-5GEF protein in absence and presence of JH5.
Rabex-5GEF was treated with either DMSO or JH5 and the protein mass was analysed by MALDI-TOF. Mass spectra with (yellow) and without (green) JH5 did not show any difference indicating that no covalent modification of the proteins by JH5 was introduced.

8.12 Cellular assays
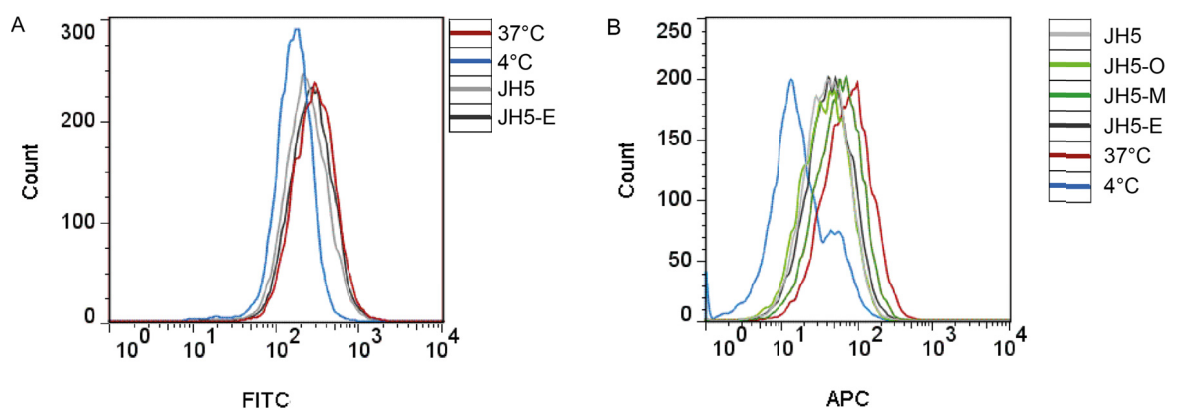
Supporting figure 39   Internalization assay, examples of representative raw data curves.
The data shows one representative curve for each condition chosen from several independent experiments. The corresponding quantification is shown in Figure 44. y-axis: count of cells, x-axis: fluorescence intensity. **A)** Transferrin receptor internalization. The FITC channel was used for detection. The negative control (blue) was the incubation of cells at 4°C. For the positive control the cells were incubated at 37°C (red). The internalization in the presence of the compounds JH5 (grey) and JH5-E (black) was not significantly different from the positive control. **B)** EGFR endocytosis, the APC channel was used for detection. The negative control (blue) and positive control (red) were obtained under the same conditions as in A. The compounds JH5 (grey) and JH5-O (light green) and JH5-E (black) induce a slight shift of the curve towards lower fluorescence intensities. The compound JH5-M (dark green) had fluorescence levels comparable to the positive control.

A

B

C

D
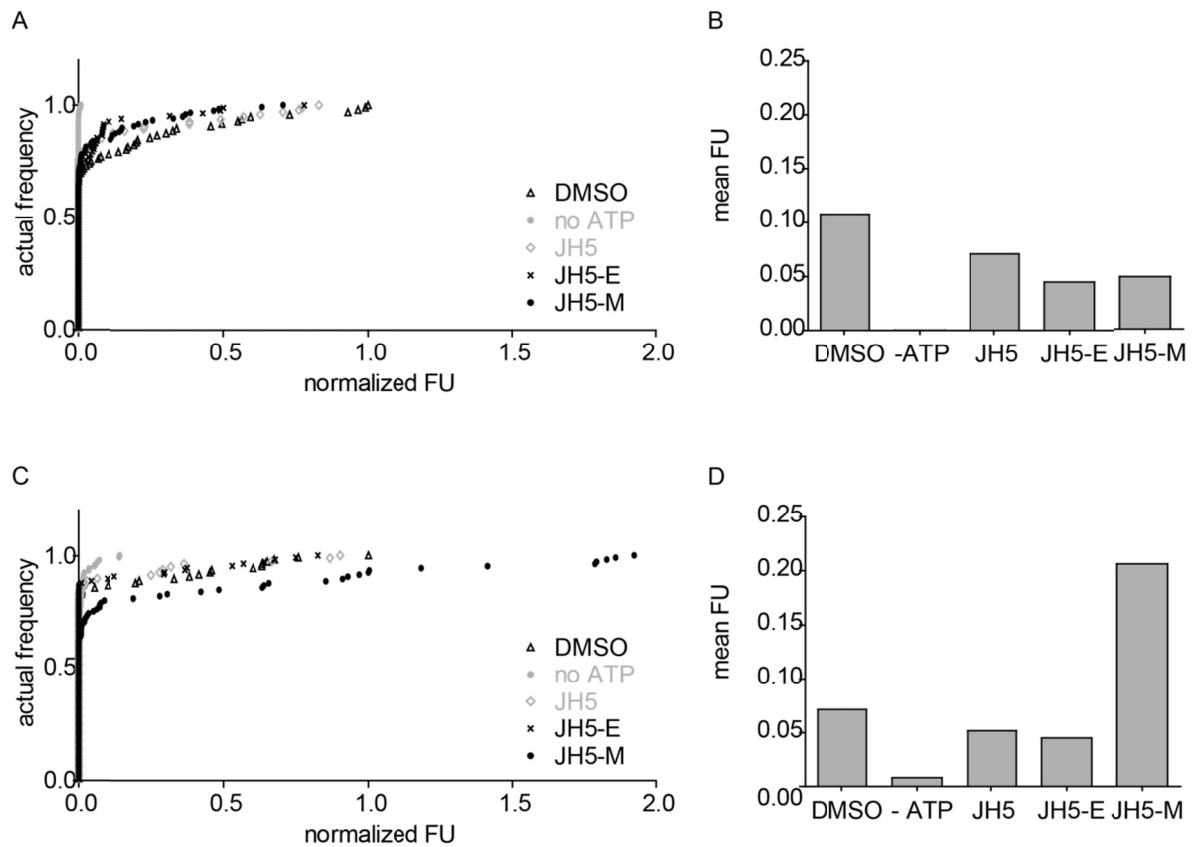
Supporting figure 40   PI3P level on early phagosomes.
A, B) Early phagosomes containing latex-beads were purified from J774E macrophages (murine cells). The phagosomes were incubated with cytosol (supernatant of J774E cell homogenate) and 40 μM compounds for 10 minutes on ice. After addition of an ATP-regenerating system, salts, 4 μM 2 x-FYVE-GST and 1 mM DTT the phagosomes were incubated for 60 minutes at 37 °C. The phagosomes were washed and fixated on cover slips to enable detection of the immune fluorescence. **A)** The normalized fluorescence units (FU) are plotted against the actual frequency. **B)** The graph illustrates the mean fluorescence units (FU) of all samples. As positive control, DMSO treated samples were used. Samples which had been incubated in absence of ATP served as negative controls. The positive control shows that the phagosomes bind to the 2xFYVE-GST under the standard conditions which represented the level of PI3P on the phagosomes. The addition of all compounds lowered the level of PI3P. However, this was also true for the negative compound JH5-M. **C, D)** The same experiment was performed in absence of DTT. JH5-M showed a strong increase in the mean FU. JH5 and JH5-E (= CCT) showed similar PI3P level as the DMSO control. The data is by courtesy of Andreas Jeschke and Professor Dr. A. Haas (University of Bonn).

197
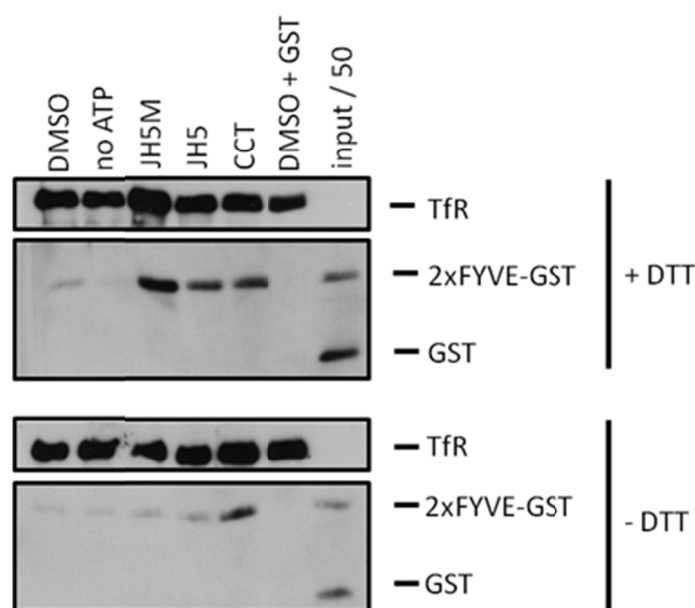
Supporting figure 41   PI3P level on early endosomes.
The experiment was performed as described in Supporting figure 40 with exception of the use of early endosomes instead of phagosomes. The associated PI3P was probed with 2x-FYVE-GST and detected by western blotting. As loading control the transferrin receptor level (TfR) was monitored. As positive control the early endosomes were treated with DMSO. As negative control the addition of ATP was omitted. For comparison, a loading control was added showing 50 % of the input. In the upper panel, the compounds increased the signal compared to the positive control. However, since this experiment was only performed once no conclusions can be drawn from it. The experiment was performed in presence and absence of DTT. The main purpose of this experiment was to investigate if omission of DTT was possible. This was investigated since the compounds were inactive in presence of DTT. Unfortunately, the assay did not work in absence of DTT (lower panel). In conclusion, the assay system was thought to be unsuitable for the investigation of the effect of the Rabex-5GEF inhibitors on the PI3K level. CCT = JH5-E. The data is by courtesy of Andreas Jeschke and Professor Dr. A. Haas (University of Bonn).

8.13 Compound analytics

The library stock compounds used in this study were monitored by HPLC-MS. The storage conditions of the library, though of course carefully controlled, may lead to degradation of the molecules. For every screening performed with the library they have to be thawed and refrozen. This process might have harmed the compounds. Therefore, it was necessary to analyse the integrity of the compounds. Furthermore, the identity of the compounds also had to be investigated to exclude any mistaken identity. In order to do that the compounds were analysed with high performance liquid chromatography (HPLC) and subsequent mass spectrometry (MS) analysis. A single peak in HPLC corroborates that the compound was still pure and not degraded. The correct mass affirms that the identity of the compound was unchanged.

8.13.1   HPLC analysis of library compounds

HPLC was performed as described under (Section 7.2.1). The compounds were detected at a wavelength of 254 nm.[29]
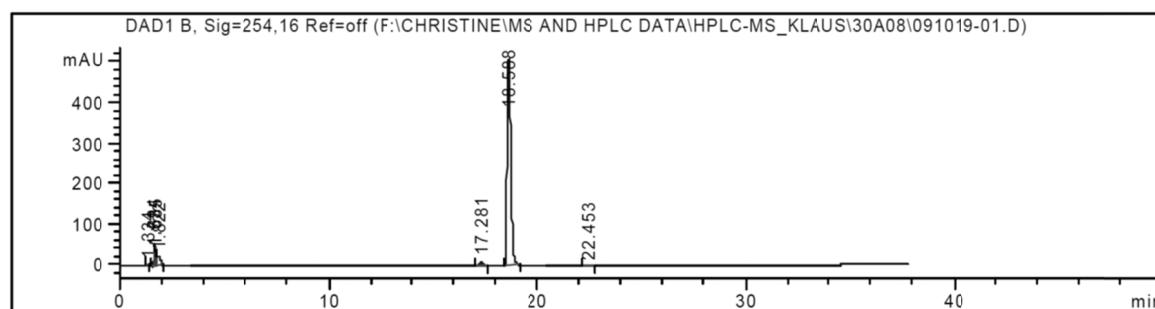
Supporting figure 42   Chromatogram of HPLC of compound C4.30_A08.

Supporting table 21   HPLC parameters of compound C4.30_A08.

Peak #	Retention time [min]	Width [min]	Height [mAU]	Area [%]
1	1.334	0.1514	1.31601	0.2111
2	1.634	0.0551	33.18445	1.5615
3	1.685	0.0902	33.10936	2.7950
4	1.822	0.1308	23.40814	3.0612
5	17.281	0.2034	10.42211	1.8465
6	18.588	0.2029	511.36163	90.2999
7	22.453	0.2185	1.16543	0.2249
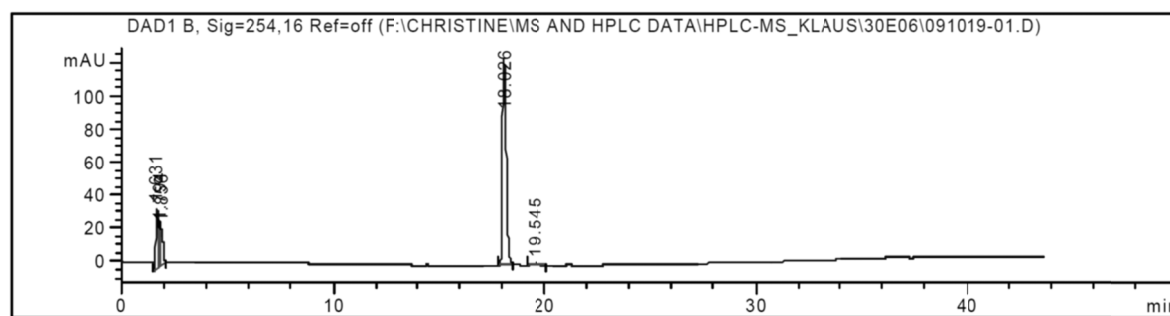
Supporting figure 43   Chromatogram of HPLC of compound C4.30_E06.

Supporting table 22   HPLC parameters of compound C4.30_E06.

Peak #	Retention time [min]	Width [min]	Height [mAU]	Area [%]
1	1.631	0.1340	37.13287	16.7523
2	1.794	0.0476	24.50011	3.7100
3	1.856	0.0948	22.80379	7.2190
4	18.026	0.2091	124.53014	70.9826
5	19.545	0.3107	1.27268	1.336

[29] HPLC measurements of C4.30_A08, C4.30_E06, C4.30_F05, C4.30_G05, C4.30_H05, K1.03_F10 and K1.13_A07 were kindly performed by Klaus Rotscheidt.

Supporting figure 44   **Chromatogram of HPLC of compound C4.30_F05.**

Supporting table 23   **HPLC parameters of compound C4.30_F05.**

Peak #	Retention time [min]	Width [min]	Height [mAU]	Area [%]
1	1.619	0.1238	40.10752	17.7522
2	1.789	0.1470	26.25958	12.4138
3	15.889	0.1841	124.52567	69.8340
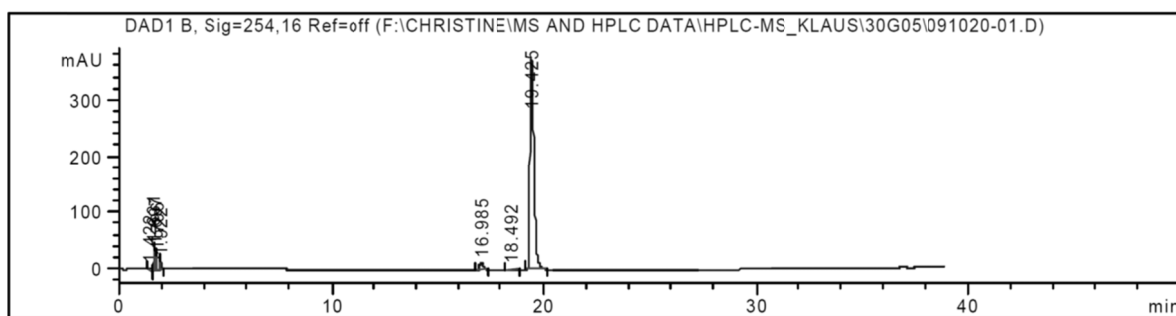
Supporting figure 45   **Chromatogram of HPLC of compound C4.30_G05.**

Supporting table 24   **HPLC parameters of compound C4.30_G05.**

Peak #	Retention time [min]	Width [min]	Height [mAU]	Area [%]
1	1.422	0.1535	4.03415	0.8106
2	1.631	0.0792	39.69354	3.5511
3	1.697	0.0698	35.48033	2.8957
4	1.796	0.0968	25.93780	3.2137
5	1.922	0.0673	16.39911	1.3253
6	16.985	0.2014	12.88431	2.7757
7	18.492	0.2028	1.12117	0.2374
8	19.425	0.2156	374.54614	85.1906
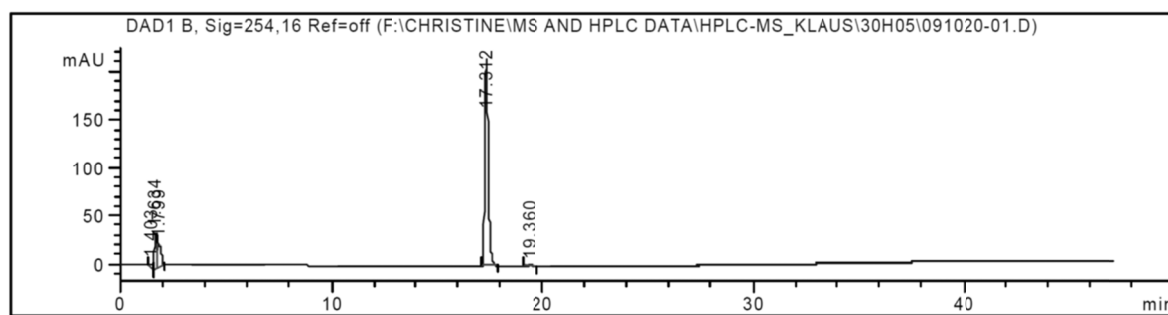
Supporting figure 46   Chromatogram of HPLC of compound C4.30_H05.

Supporting table 25   HPLC parameters of compound C4.30_H05.

Peak #	Retention time [min]	Width [min]	Height [mAU]	Area [%]
1	1.403	0.1791	3.74606	1.6075
2	1.634	0.1357	38.03612	12.0787
3	1.799	0.1222	25.50172	7.5787
4	17.312	0.1822	215.48932	78.0255
5	19.360	0.2704	1.25053	0.7096
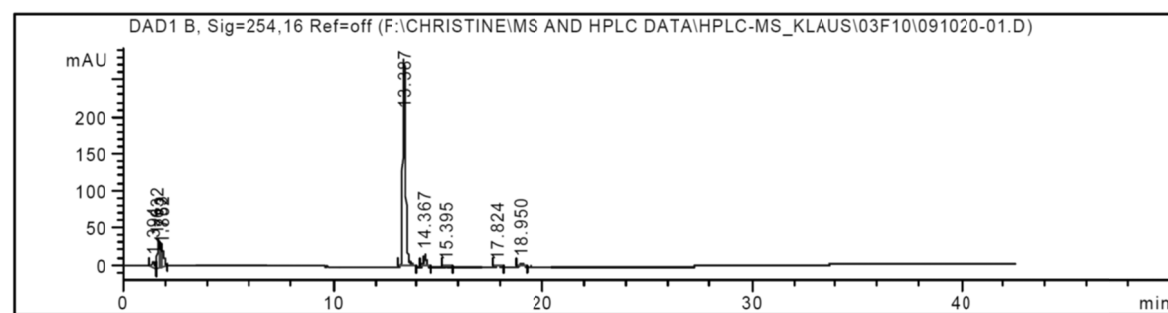
Supporting figure 47   Chromatogram of HPLC of compound K1.03_F10.

Supporting table 26   HPLC parameters of compound K1.03_F10.

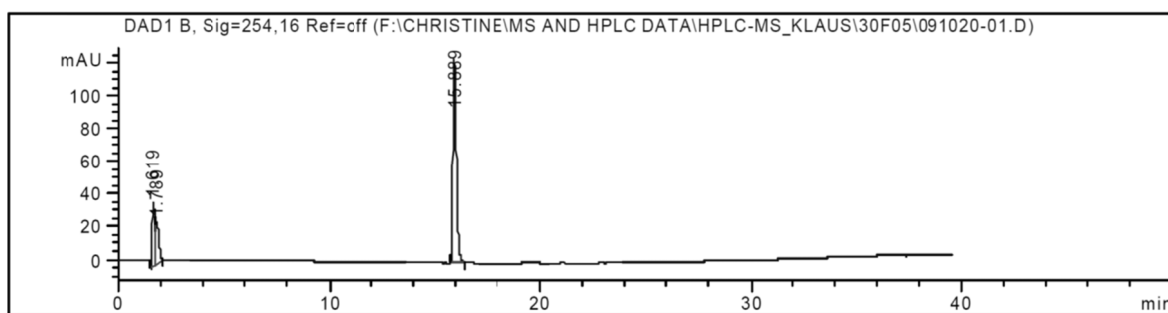| Peak #	Retention time [min]	Width [min]	Height [mAU]	Area [%]
1	1.394	0.1278	8.88411	2.2411
2	1.632	0.1302	38.58643	9.9536
3	1.783	0.0476	24.58773	2.1221
4	1.852	0.0982	22.78351	4.3030
5	13.387	0.1536	280.87637	74.6107
6	14.367	0.1646	15.22457	4.1491
7	15.395	0.1868	1.19213	0.3857
8	17.824	0.1683	2.19600	0.6576
9	18.950	0.1823	58.81245	4.88972
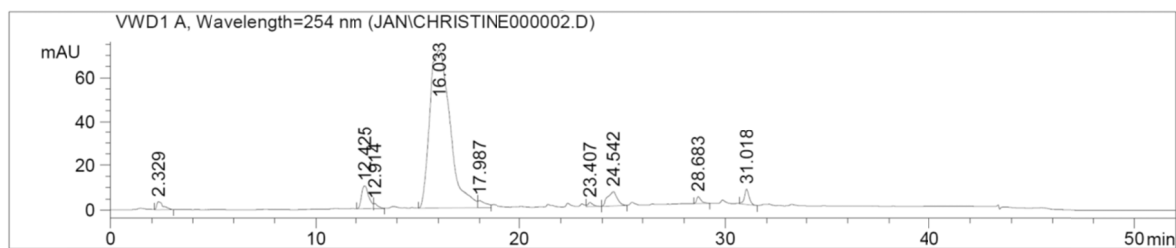
Supporting figure 48   Chromatogram of HPLC of compound K1.05_F02.

Supporting table 27   HPLC parameters of compound K1.05_F02.

Peak #	Retention time [min]	Width [min]	Height [mAU]	Area [%]
1	2.329	0.3133	3.63234	1.4237
2	12.425	0.3684	10.14752	4.3046
3	12.914	0.2072	2.31253	0.6051
4	16.033	0.8949	71.75903	85.3262
5	17.987	0.3535	3.23922	1.5627
6	23.407	0.2288	1.82300	0.5162
7	24.542	0.4484	6.25474	3.5919
8	28.683	0.2263	3.09006	0.8161
9	31.018	0.2368	6.67570	1.8534
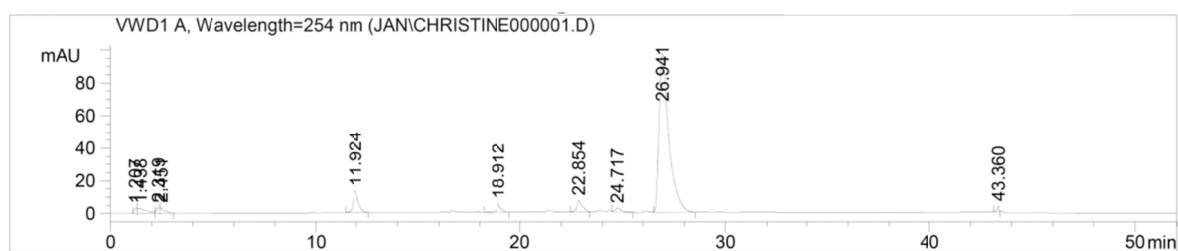
Supporting figure 49   Chromatogram of HPLC of compound Gü61.

Supporting table 28   HPLC parameters of compound Gü61.

Peak #	Retention time [min]	Width [min]	Height [mAU]	Area [%]
1	1.207	0.1171	3.15104	0.6391
2	1.438	0.3705	3.01236	2.2240
3	2.319	0.1850	3.47741	1.0080
4	2.451	0.1678	3.44171	1.1405
5	11.924	0.3052	13.06589	6.8155
6	18.912	0.2109	5.50981	2.1485
7	22.854	0.2721	7.12876	3.5220
8	24.717	0.3273	2.54166	1.4550
9	26.941	0.4778	97.12012	80.4755
10	43.360	0.0857	3.79699	0.5720
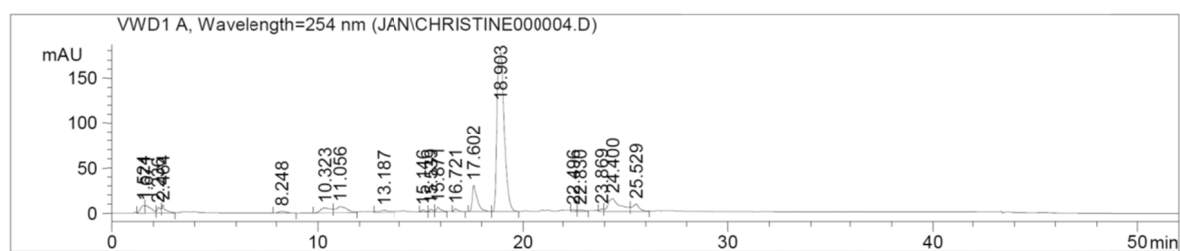
Supporting figure 50   Chromatogram of HPLC of compound K1.08_C11.

Supporting table 29   HPLC parameters of compound K1.08_C11.

Peak #	Retention time [min]	Width [min]	Height [mAU]	Area [%]
1	1.524	0.2274	8.53732	1.8256
2	1.671	0.2620	8.13006	2.3439
3	2.236	0.1622	6.07668	1.0912
4	2.464	0.1550	8.98645	1.5661
5	8.248	0.3969	1.96174	0.7612
6	10.323	0.4921	5.36141	2.6812
7	11.056	0.4876	6.75492	3.7464
8	13.187	0.4997	1.94484	1.0230
9	15.146	0.1694	2.04968	0.3568
10	15.539	0.1650	2.57997	0.4347
11	15.871	0.2050	5.01029	1.0955
12	16.721	0.2119	3.08082	0.6833
13	17.602	0.2305	28.99230	7.1595
14	18.903	0.3704	176.37601	62.5821
15	22.496	0.1813	2.13174	0.4029
16	22.830	0.3088	1.87095	0.5978
17	23.869	0.1646	2.81956	0.4788
18	24.400	0.4966	14.43632	8.3279
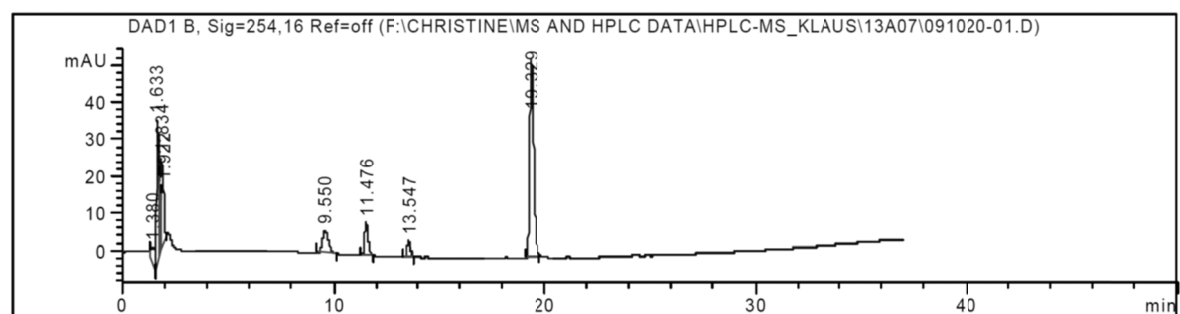
Supporting figure 51   Chromatogram of HPLC of compound K1.13_A07.

Supporting table 30   HPLC parameters of compound K1.13_A07.

Peak #	Retention time [min]	Width [min]	Height [mAU]	Area [%]
1	1.380	0.1848	4.00457	3.4409
2	1.633	0.1284	39.38551	22.1349
3	1.834	0.0858	25.62424	9.1024
4	1.922	0.0665	16.55815	4.5942
5	9.550	0.3271	6.08059	7.5236
6	11.476	0.1890	8.82907	6.2476
7	13.547	0.1753	4.28329	2.8180
8	19.329	0.2168	53.27155	44.1385

8.13.2   MS analysis of library compounds

ESI-MS measurements in the positive mode generate [M+H]+ ions, M being the molecule of interest. The mass corresponding to the peak in the original form is observed mass - 1.[30]

Supporting figure 52   Infusion MS of compound C4.30_A08.
The peak 290.2 belongs to the theoretical exact mass of the compound of 289.1.
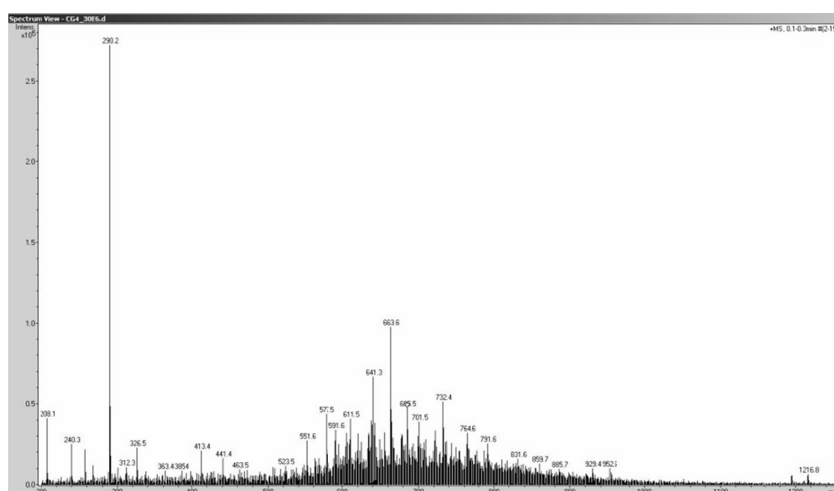
Supporting figure 53   Infusion MS of compound C4.30_E06.
The peak 290.2 belongs to the theoretical exact mass of the compound of 289.1.
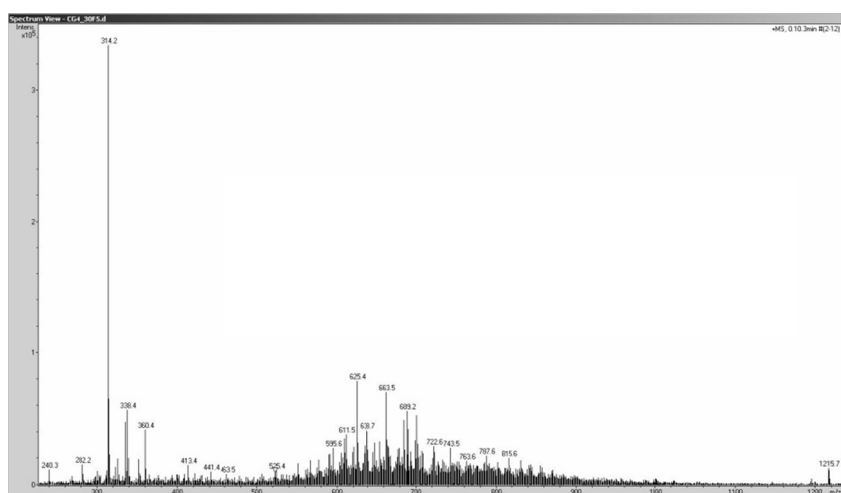
Supporting figure 54   Infusion MS of compound C4.30_F05.
The peak 314.2 belongs to the theoretical exact mass of the compound of 313.1.

Supporting figure 55   Infusion MS of compound C4.30_G05.
The peak 274.2 belongs to the theoretical exact mass of the compound of 273.1.
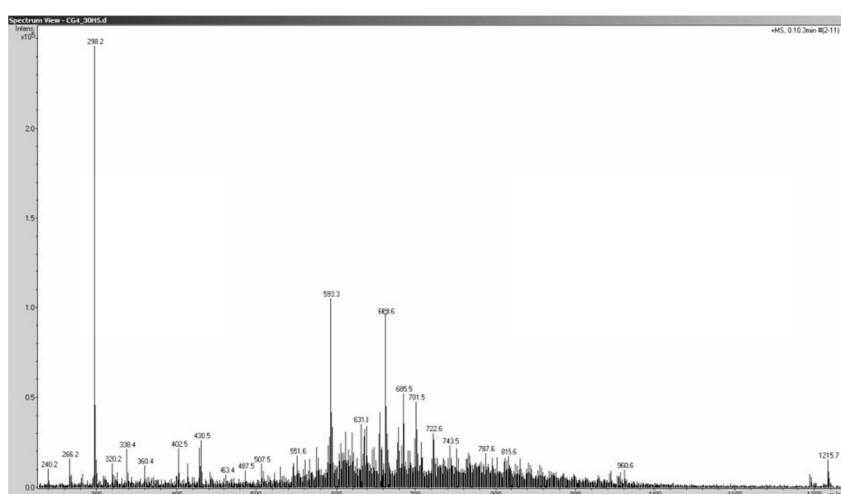
Supporting figure 56   Infusion MS of compound C4.30_H05.
The peak 298.2 belongs to the theoretical exact mass of the compound of 297.1.
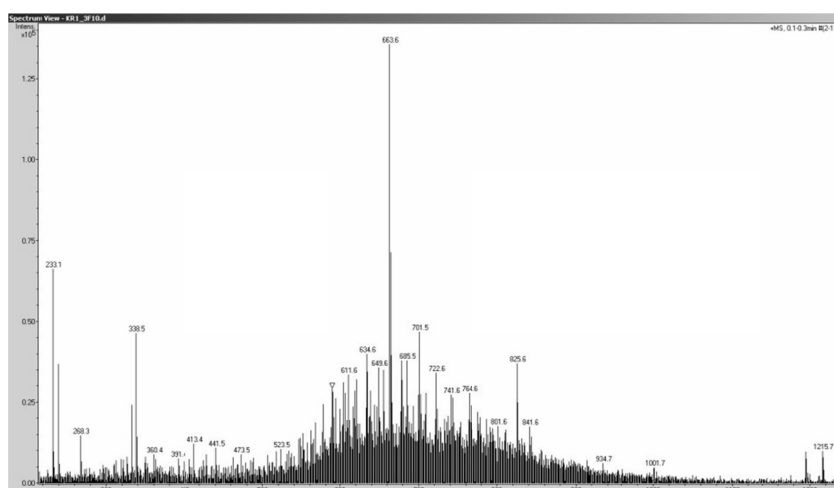
Supporting figure 57   **Infusion MS of compound K1.03_F10.**

None of the detected peaks belongs to the theoretical exact mass of the compound of 310.0.
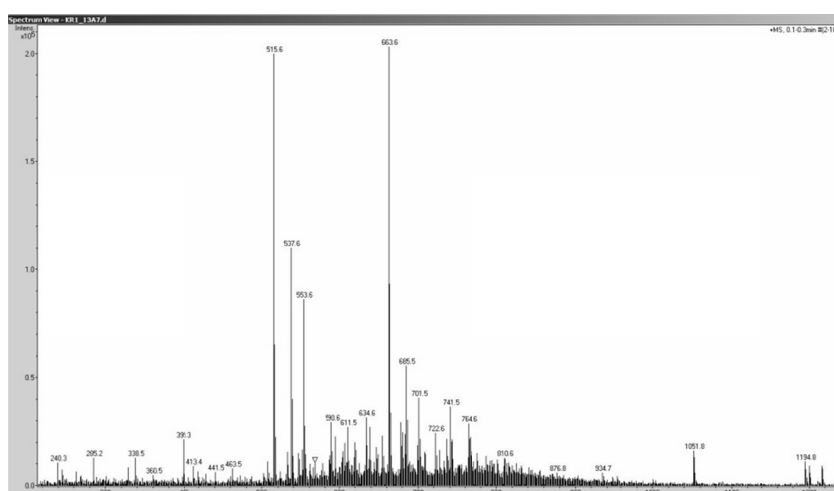
Supporting figure 58   **Infusion MS of compound K1.13_A07.**

None of the detected peaks belongs to the theoretical exact mass of the compound of 324.0.
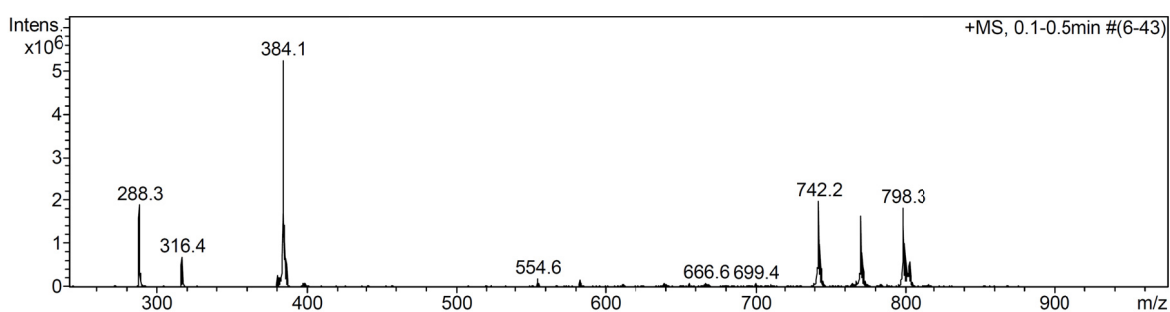
Supporting figure 59   **Infusion MS of compound Gü61.**

The peak 384.1 corresponds well with the theoretical exact mass of the compound of 383.1. The MS spectrum was obtained with the compound from the stock (not stored in DMSO).
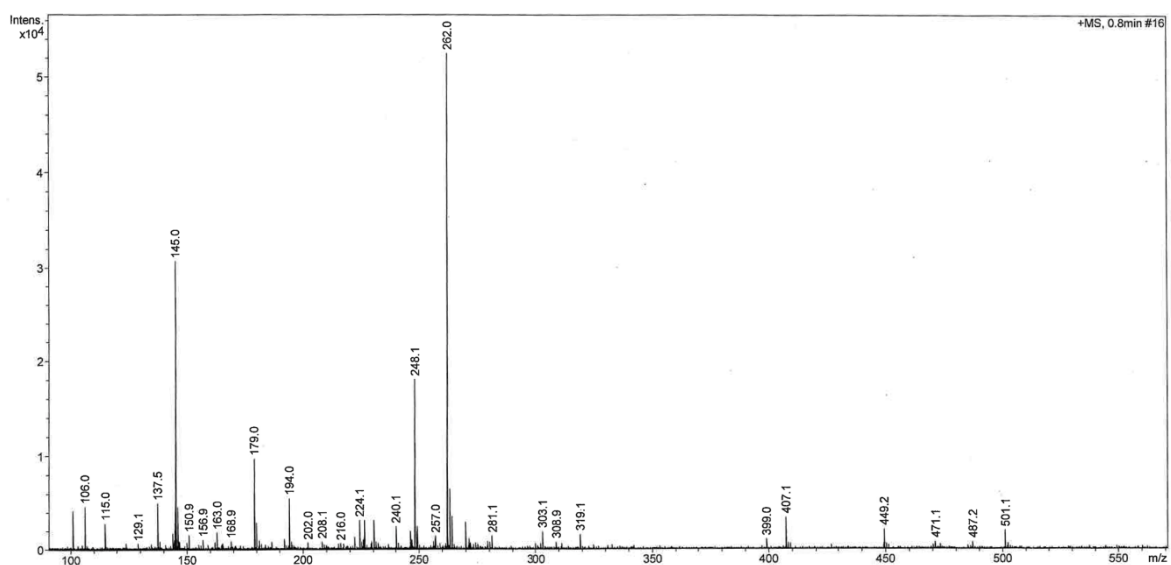
Supporting figure 60   Infusion MS of compound K1.05.F02.
The expected peak of 384.1 was not detected. The MS spectrum was obtained with the compound from the library (stored in DMSO).[31]
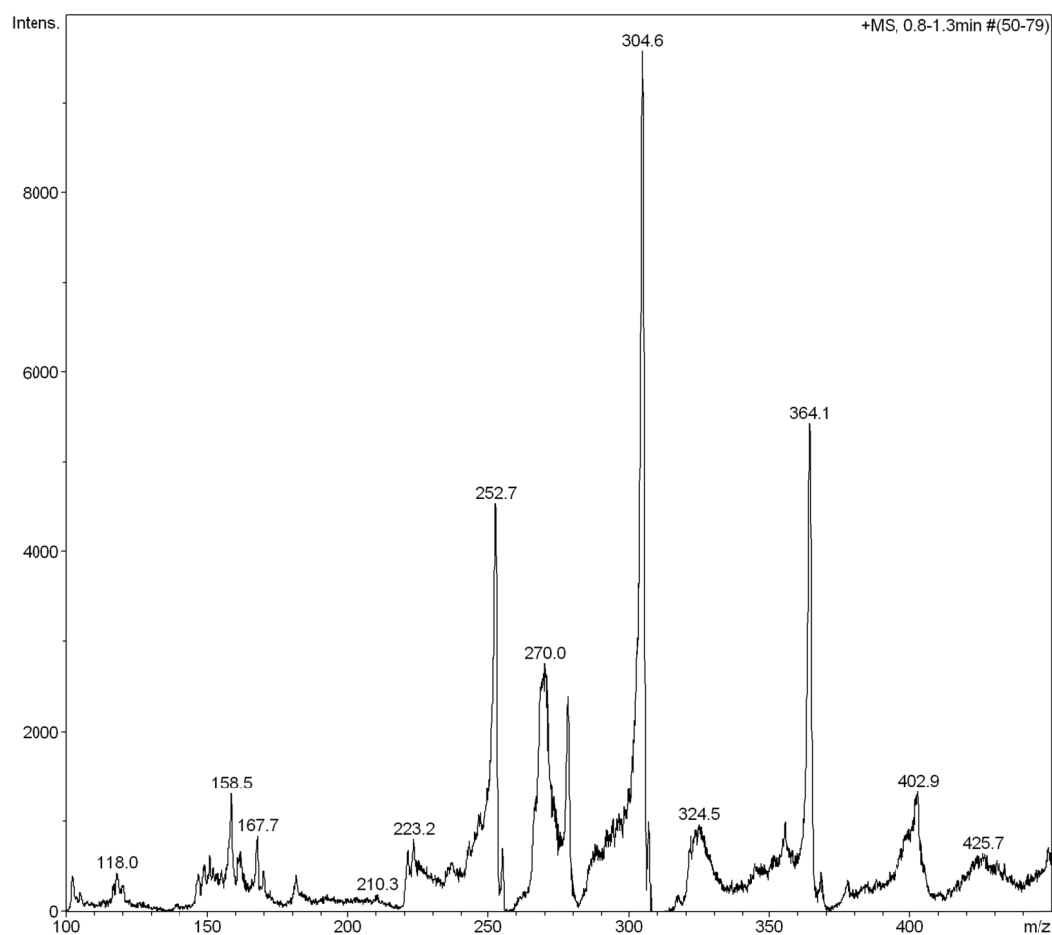
Supporting figure 61   Infusion MS of compound Gü321.
The peak 304.6 corresponds well with sodium signal of the theoretical exact mass of the compound of 281.1 Da.[32]

---

[31] The measurement was kindly performed by Dr. Marianne Engeser (University of Bonn).
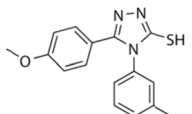
8.13.3 Analytical compound data of synthesised compounds
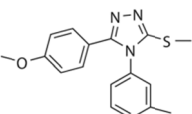
The synthesis of the compounds as well as their analytics was kindly performed by *Dr. Jeffrey S. Hannam*. The compound analytics given in supporting table 31 for completeness is courtesy of *Dr. Jeffrey S. Hannam*. In addition, several compounds were purchased. Their source is given in Supporting table 32.

^{1}H- and ^{13}C-NMR-spectra were measured with a nuclear magnetic resonance spectrometer AM300 ([1]H = 300 MHz; [13]C = 75.5 MHz) or AM400 ([1]H = 400 MHz; [13]C = 100.6 MHz) from *BRUKER*, Karlsruhe. d_6-DMSO and CDCl$_3$ were used as solvents. The chemical shifts were plotted as δ-values in ppm. The [1]H-spectra were calibrated on the d_6-DMSO residual content at δ = 2.52 ppm or on the CDCl$_3$ residual content at δ = 7.27 ppm. The ^{13}C-spectra were calibrated on the d$_6$-DMSO residual content at δ = 39.5 ppm or on the CDCl$_3$ residual content at δ = 77.0 ppm. Coupling constants are given in hertz (Hz) and the following notations indicate the multiplicity of the signals: s (singlet), d (doublet), brs (broad singlet), t (triplet), q (quartet), m (multiplet).
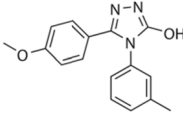
EI-Mass spectra were measured on a MAT-95XL from *Finnigan*, Bremen. ESI-Mass spectra were measured with a micrOTOF-Q flight time spectrometer from *Bruker Daltonik*, Bremen using an *Agilent* 1200 Series HPLC-facility.
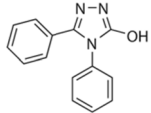
Supporting table 31   Analytical data of synthesised compounds.
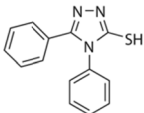
JH5	
Structure	
IUPAC name	5-(4-methoxyphenyl)-4-m-tolyl-4H-1,2,4-triazole-3-thiol
^{1}H NMR (400 MHz, d_6-DMSO, 298 K)	δ 14.02 (1H, s), 7.44-7.36 (1H, m), 7.34-7.31 (2H, m), 7.29-7.22 (2H, m), 7.20 (1H, brs), 7.15-7.09 (1H, m), 6.95-6.87 (2H, m), 3.75 (s, 3H), 2.34 (s, 3H)
^{13}C NMR (100 MHz, d_6-DMSO, 298 K)	δ 168.4 (s), 160.6 (s), 150.3 (s), 138.9 (s), 134.6 (s), 130.1 (d), 129.6 (d), 129.1 (s), 129.0 (d), 125.7 (d), 117.9 (s), 114.0 (d), 55.2 (q), 20.7 (q)
Mass	HRMS (EI) Calcd for C$_{16}$H$_{14}$N$_3$OS: 296.0858 [M$^+$]. Found: 296.0858
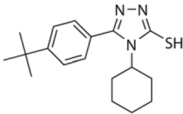
JH5-M	
Structure	
IUPAC name	3-(4-methoxyphenyl)-5-(methylthio)-4-m-tolyl-4H-1,2,4-triazole
^{1}H NMR (400 MHz, d_6-DMSO, 298 K)	δ 7.48-7.35 (2H, m), 7.34-7.28 (2H, m), 7.25 (1H, brs), 7.21-7.16 (1H, m), 6.95-6.88 (2H, m), 3.75 (3H, s), 2.61 (3H, s), 2.35 (3H, s)
^{13}C NMR (100 MHz, d_6-DMSO, 298 K)	δ 160.2 (s), 154.1 (s), 152.3 (s), 139.8 (s), 134.0 (d), 130.7 (d), 129.8 (d), 127.9 (d), 124.8 (d), 119.0 (d), 114.0 (d), 55.2 (q), 20.7 (q), 14.4 (q)
Mass	HRMS (EI) Calcd for C$_{17}$H$_{17}$N$_3$OS: 311.1092 [M$^+$]. Found: 311.1091

---
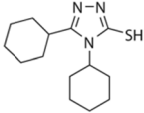
[32] The MS was performed with kind help of Dr. Damian Ackermann.
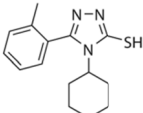
JH5-O

Structure	
IUPAC name	5-(4-methoxyphenyl)-4-m-tolyl-4H-1,2,4-triazole-3-ol
^{1}H NMR (400 MHz, d_6-DMSO, 298 K)	δ 12.04 (1H, s), 7.34 (1H, t, *J* = 7.8 Hz), 7.27-7.18 (3H, m), 7.16 (1H, brs), 7.04-6.98 (1H, m), 6.93-6.88 (2H, m), 3.75 (3H, s), 2.33 (3H, s)
^{13}C NMR (100 MHz, d_6-DMSO, 298 K)	δ 160.2 (s), 154.6 (s), 145.2 (s), 138.9 (s), 133.8 (d), 129.2 (d), 129.0 (d), 128.2 (d), 124.9 (d), 119.3 (d), 55.2 (q), 20.7 (q)
Mass	HRMS (EI) Calcd for $C_{15}H_{14}NOS$: 280.1092 [M$^+$]. Found: 280. 1088
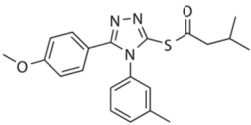
CCO

Structure	
IUPAC name	4,5-diphenyl-4H-1,2,4-triazol-3-ol
^{1}H NMR (400 MHz, d_6-DMSO, 298 K)	δ 12.18 (1H, s), 7.50-7.27 (10H, m)
^{13}C NMR (75 MHz, d_6-DMSO, 298 K)	δ 154.5 (s), 145.3 (s), 133.7 (s), 129.8 (d), 129.3 (d), 128.5 (d), 127.7 (d), 127.5 (d), 127.0 (s)
Mass	HRMS (EI) Calcd for $C_{14}H_{10}N_3S$: 236.0829 [M$^+$]. Found: 236.0822
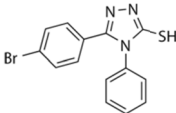
CCD

Structure	
IUPAC name	4,5-diphenyl-4H-1,2,4-triazole-3-thiol
^{1}H NMR (400 MHz, d_6-DMSO, 298 K)	δ 14.15 (1H, s), 7.54-7.30 (10H, m)
^{13}C NMR (100 MHz, d_6-DMSO, 298 K)	δ 168.6 (s), 150.4 (s), 134.5 (s), 130.3 (d), 129.4 (d), 129.3 (d), 128.7 (d), 128.7 (d), 128.5 (d), 128.2 (d), 125.8 (s)
Mass	HRMS (EI) Calcd for $C14H10N3S$: 252.0600 [M+]. Found: 252.0603

CCJ

Structure	
IUPAC name	5-(4-methoxyphenyl)-4-m-tolyl-4H-1,2,4-triazole-3-thiol
^{1}H NMR (400 MHz, d_6-DMSO, 298 K)	δ 14.02 (1H, s), 7.59 (2H, d, *J* = 8.4 Hz), 7.48 (2H, d, *J* = 8.4 Hz), 4.26 (1H, brs), 2.30 (2H, brs), 1.75-1.71 (4H, m), 1.59-1.50 (1H, m), 1.23-1.10 (2H, m), 1.02-0.90 (1H, m)
^{13}C NMR (100 MHz, d_6-DMSO, 298 K)	δ 166.0 (s), 153.3 (s), 151.6 (s), 129.3 (d), 125.5 (d), 123.9 (s), 56.9 (d), 34.6 (s), 30.9 (q), 29.1 (t), 25.4 (t), 24.6 (t)
Mass	HRMS (EI) Calcd for $C_{18}H_{24}N_3S$: 315.1769 [M$^+$]. Found: 315.1770
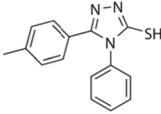
CCF	
Structure	
IUPAC name	4,5-dicyclohexyl-4H-1,2,4-triazole-3-thiol
^{1}H NMR (400 MHz, d_6-DMSO, 298 K)	δ 13.45 (1H, s), 4.38 (1H, brs), 2.90-2.81 (1H, m), 1.85-1.55 (11H, m), 1.50-1.15 (11H, m)
^{13}C NMR (100 MHz, d_6-DMSO, 298 K)	δ 165.3 (s), 156.0 (s), 55.4 (d), 34.2 (t), 31.8 (t), 25.5 (t), 25.3 (t), 25.2 (t), 24.5 (t)
Mass	HRMS (ESI+) Calcd for $C_{14}H_{24}N_3S$ [M+H]* 266.1685 [M+]. Found: 266.1685
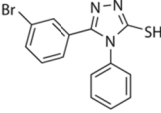
CCV	
Structure	
IUPAC name	4-cyclohexyl-5-o-tolyl-4H-1,2,4-triazole-3-thiol
^{1}H NMR (400 MHz, d_6-DMSO, 298 K)	δ 13.91 (1H, s), 7.56-7.49 (m, 1H), 7.46-7.34 (3H, m), 4.25 (1H, brs), 2.16 (3H, s), 1.84-1.64 (6H, m), 1.56-1.46 (1H, m), 1.25-1.05 (2H, m), 0.90-0.72 (1H, m)
^{13}C NMR (75 MHz, d_6-DMSO, 298 K)	δ 168.3 (s), 136.6 (s), 134.2 (s), 130.6 (d), 130.0 (d), 127.8 (d), 125.4 (d), 52.8 (d), 31.9 (t), 25.2 (t), 24.8 (t), 19.6 (q)
Mass	HRMS (EI+) Calcd for $C_{15}H_{21}N_3S$: 273.1299 [M+]. Found:
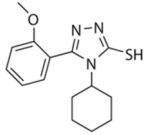
JH5-E	
Structure	
IUPAC name	S-5-(4-methoxyphenyl)-4-m-tolyl-4H-1,2,4-triazole-3-yl 3-methylbutanethioate
^{1}H NMR (400 MHz, d_6-DMSO, 298 K)	δ 7.42 (1H, t, J = 7.6 – Hz), 7.38-7.30 (3H, m), 7.24 (1H, s), 7.20-7.15 (1H, m), 6.98-6.92 (2H, m), 3.76 (s, 3H), 3.08 (2H, d, J = 6.85 Hz), 2.34 (3H, s), 2.29-2.19 (m, 1H), 1.03 (6H, d, J = 6.9 Hz)
^{13}C NMR (100 MHz, d_6-DMSO, 298 K)	δ 169.8 (s), 169.2 (s), 161.8 (s), 149.7 (s), 139.1 (s), 134.3 (s), 130.4 (d), 129.29 (d), 129.25 (d), 126.0 (d), 121.5 (d), 114.0 (d), 55.3 (q), 44.5 (d), 24.4 (t), 22.2 (q), 20.7 (q)
Mass	HRMS (EI) Calcd for $C_{16}H_{15}N_3O_2S$: 381.1511 [M+]. Found: 381.1517
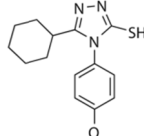
JH5-B[33]	
Structure	
IUPAC name	5-(4-bromophenyl)-4-phenyl-4H-1,2,4-triazole-3-thiol
^{1}H NMR (400 MHz, d_6-DMSO, 298 K)	δ 14.20 (1H, s), 7.61-7.56 (2H, m), 7.54-7.49 (3H, m), 7.41-7.36 (2H, m), 7.27-7.23 (2H, m)
^{13}C NMR (100 MHz, d_6-DMSO, 298 K)	δ 168.7 (s), 149.7 (s), 139.2 (s), 134.3 (s), 131.6 (d), 130.2 (d), 129.5 (s), 129.3 (d), 128.7 (d), 125.0 (d), 124.0 (s)
Mass	HRMS (EI) Calcd for $C_{14}H_9BrN_3S$: 329.9706 [M+]. Found: 329.9703

---

[33] In the labbooks this compound is named 4Br-monomer.

JH5-A[34]	
Structure	
IUPAC name	4-phenyl-5-m-tolyl-4H-1,2,4-triazole-3-thiol
^{1}H NMR (400 MHz, d_6-DMSO, 298 K)	δ 14.10 (1H, s), 7.55-7.46 (m, 3H), 7.36-7.33 (2H, m), 7.23-7.13 (4H, m), 2.28 (3H, s)
^{13}C NMR (100 MHz, d_6-DMSO, 298 K)	δ 168.5 (s), 150.6 (s), 140.2 (s), 134.6 (s), 129.31 (d), 129.26 (d), 129.1 (d), 128.7 (d), 128.1 (d), 122.9 (s), 20.8 (q)
Mass	HRMS (EI) Calcd for $C_{15}H_{12}N_3S$: 266.0757 [M$^+$]. Found: 266.0757

JH5-C[35]	
Structure	
IUPAC name	5-(3-bromophenyl)-4-phenyl-4H-1,2,4-triazole-3-thiol
^{1}H NMR (400 MHz, d_6-DMSO, 298 K)	δ 14.23 (1H, s), 7.65-7.60 (1H, m), 7.55-7.50 (3H, m), 7.48-7.46 (1H, m), 7.42-7.38 (2H, m), 7.32-7.29 (2H, m)
^{13}C NMR (100 MHz, d_6-DMSO, 298 K)	δ 168.7 (s), 149.4 (s), 134.4 (s), 133.1 (s), 130.8 (d), 130.7 (d), 129.6 (d), 129.4 (d), 128.7 (d), 127.9 (s), 127.2 (d), 121.5
Mass	HRMS (EI) Calcd for $C_{14}H_9BrN_3S$: 329.9706 [M$^+$]. Found: 329.9703

JA8	
Structure	
IUPAC name	4-cyclohexyl-5-(2-methoxyphenyl)-4H-1,2,4-triazole-3-thiol
^{1}H NMR (400 MHz, d_6-DMSO, 298 K)	δ 13.81 (1H, s), 7.62 (1H, ddd, J = 8.4, 7.4, 1.8 Hz), 7.40 (1H, dd, , J = 7.4, 1.8 Hz), 7.22 (1H, dd, , J = 8.5, 1.0 Hz), 7.11(1H, td, , J = 7.4, 1.0 Hz), 4.03 (1H, brs), 3.82 (3H, s), 2.13 (2H, brs), 1.75-1.60 (4H, m), 1.56-1.50 (1H, m), 1.20-1.05 (2H, m), 0.97-0.87 (1H, m)
^{13}C NMR (100 MHz, d_6-DMSO, 298 K)	δ 165.8 (s), 157.6 (s), 148.9 (s), 132.8 (d), 131.9 (d), 120.5 (d), 115.4 (s), 111.5 (d), 57.2 (d), 55.4 (q), 25.4 (t), 24.7 (t)
Mass	HRMS (EI) Calcd for $C_{15}H_{18}rN_3S$: 288.1176 [M$^+$]. Found: 288.1171

JE6	
Structure	
IUPAC name	5-cyclohexyl-4-(4-methoxyphenyl)-4H-1,2,4-triazole-3-thiol
^{1}H NMR (400 MHz, d_6-DMSO, 298 K)	δ 13.65 (1H, s), 7.39-7.27 (2H, m), 7.17-7.05 (2H, m), 3.85 (3H, s), 2.37 (1H, tt, J = 11.4, 3.4 Hz), 1.81-1.51 (5H, m), 1.50-1.24 (2H, m), 1.21-1.00 (3H, m)
^{13}C NMR (75 MHz, d_6-DMSO, 298 K)	δ 167.8 (s), 159.6 (s), 155.9 (s), 129.6 (d), 126.8 (s), 114.5 (d), 55.4 (q), 40.3 (d), 34.3 (t), 29.9 (t), 25.14 (t), 25.05 (t)
Mass	HRMS (EI) Calcd for $C_{15}H_{18}N_3OS$: 288.1176 [M$^+$]. Found: 288.1164

---

[34] In the labbooks this compound is named C3.30.

[35] In the labbook, this compound is named 3Br-monomer.

JF5	
Structure	
IUPAC name	5-(2-methoxyphenyl)-4-(4-methoxyphenyl)-4H-1,2,4-triazole–3-thiol
^{1}H NMR (400 MHz, d_6-DMSO, 298 K)	δ 14.02 (1H, s), 7.51-7.39 (2H, m), 7.18-7.09 (2H, m), 7.01 (1H, td, J = 7.5, 0.9 Hz), 6.98-6.87 (3H, m), 3.74 (3H, s), 3.50 (3H, s)
^{13}C NMR (100 MHz, d_6-DMSO, 298 K)	δ 167.9 (s), 159.1 (s), 156.9 (s), 149.8 (s), 132.5 (d), 131.6 (d), 129.0 (d), 126.9 (s), 120.4 (d), 115.0 (s), 113.6 (d), 111.4 (d), 55.3 (q), 55.1 (q)
Mass	HRMS (ESI+) Calcd for C$_{17}$H$_{15}$N$_3$O$_2$S: 314.0958 [M+H]*. Found: 314.0951

JH5-N-dimer	
Structure	
IUPAC name	3-((4-amino-5-p-tolyl-4H-1,2,4-triazol-3-ylthio)methylthio)-5-p-tolyl-4H-1,2,4-triazol-4-amine
^{1}H NMR (300 MHz, d_6-DMSO, 298 K)	δ 7.92 (2H, d, J = 8.0 Hz), 7.36 (2H, d, J = 8.0 Hz), 6.21 (4H, s), 5.00 (2H, s), 2.40 (6H, s)
^{13}C NMR (75 MHz, d_6-DMSO, 298 K)	δ 154.4 (s), 152.2 (s), 139.4 (s), 129.0 (d), 127.7 (s), 123.9 (s), 34.1(t), 20.9 (q)
Mass	HRMS (ESI+) Calcd for C$_{19}$H$_{20}$N$_8$S$_2$Na: 447.1145 [M+Na]*. Found: 447.1127

CS-dimer 1[36]	
Structure	
IUPAC name	3-(4-bromophenyl)-5-((5-(4-methoxyphenyl)-1,3,4-oxadiazol-2-yl)methylthio)-4-phenyl-4H-1,2,4-triazole
^{1}H NMR (300 MHz, d_6-DMSO, 298 K)	δ 7.95-7.90 (2H, m), 7.51-7.45 (3H, m), 7.44-7.39 (2H, m), 7.32-7.26 (2H, m), 7.24-7.19 (2H, m), 7.00-6.95 (2H, m), 4.72 (2H, s), 3.87 (3H, s)
^{13}C NMR (75 MHz, d_6-DMSO, 298 K)	δ 165.5 (s), 162.5 (s), 161.9 (s), 154.5 (s), 150.9 (s), 133.4 (s), 131.9 (d), 130.3 (s), 130.4 (d), 130.2 (d), 129.6 (d), 128.7 (d), 127.1 (s), 124.8 (s), 115.9 (s), 114.4 (d), 55.4 (q), 34.1(t), 20.9 (q)
Mass	HRMS (ESI+) Calcd for C$_{24}$H$_{19}$BrN$_5$O$_2$S: 520.0437 [M+H]*. Found: 520.0445

CS-dimer 2	
Structure	
IUPAC name	3-(4-methoxyphenyl)-5-((5-(4-methoxyphenyl)-1,3,4-oxadiazol-2-yl)methylthio)-4-m-tolyl-4H-1,2,4-triazole
^{1}H NMR (300 MHz, d_6-DMSO, 298 K)	δ 7.95-7.91 (2H, m), 7.42-7.35 (2H, m), 7.34-7.25 (2H, m), 7.01-6.95 (4H, m), 6.83-6.78 (2H, m), 4.68 (2H, s), 3.86 (3H, s), 3.78 (3H, s), 2.34 (3H, s)
^{13}C NMR (75 MHz, d_6-DMSO, 298 K)	δ 165.4 (s), 162.4 (s), 162.0 (s), 161.0 (s), 155.0 (s), 150.2 (s), 140.5 (s), 133.5 (s), 131.0 (d), 129.8 (d), 129.7 (d), 128.7 (d), 127.6 (d), 124.3 (d), 117.9 (s), 115.9 (s), 114.3 (d), 114.0 (d), 55.4 (q), 55.2 (q), 26.5 (t), 21.2 (t)
Mass	HRMS (ESI+) Calcd for C$_{26}$H$_{23}$N$_5$O$_2$SNa: 508.1414 [M+Na]*. Found: 508.1417

---

[36] In the labbook, all CS-dimers (1-3) are named CH$_2$-S-dimers.

CS-dimer 3	
Structure	
IUPAC name	3-(4-methoxyphenyl)-5-((5-(4-methoxyphenyl)-4-m-tolyl-4H-1,2,4-triazol-3-yl)methylthio)-4-m-tolyl-4H-1,2,4-triazole
^{1}H NMR (300 MHz, d_6-DMSO, 298 K)	δ 7.55-7.45 (3H, m), 7.43-7.32 (6H, m), 7.29-7.19 (4H, m), 7.09-7.04 (2H, m), 6.83-6.76 (2H, m), 4.40 (2H, s), 3.78 (3H, s), 2.40 (3H, s)
^{13}C NMR (75 MHz, d_6-DMSO, 298 K)	δ 161.2 (s), 154.4 (s), 153.4 (s), 151.2 (s), 151.0 (s), 140.7 (s), 133.7 (s), 133.5 (s), 131.8 (d), 131.2 (d), 130.13 (d), 130.08 (d), 129.99 (d), 129.95 (d), 129.6 (d), 127.9 (d), 127.4 (d), 125.3 (s), 124.6 (d), 124.5 (s), 114.1 (d), 55.3 (q), 27.0 (t), 21.3 (q), 21.2 (t)
Mass	HRMS (ESI+) Calcd for $C_{31}H_{25}BrN_6OSNa$: 631.0886 [M+Na]*. Found: 631.0880

Supporting table 32   **Source of commercially obtained compounds.**

Name	IUPAC name	Structure	Supplier
JH5-N	4-Amino-5-(4-methylphenyl)-4H-1,2,4-triazole-3-thiol		Fluorochem Ltd, Hadfield, UK
JH5-B-dimer	5-(4-Bromophenyl)-3-((5-(4-bromophenyl)-4-phenyl-1,2,4-triazolidin-3-yl)methyl)-4-phenyl-1,2,4-triazolidine		AKos GmbH, Steinen, Germany
JH5-C-dimer	5-(3-Bromophenyl)-3-((5-(3-bromophenyl)-4-phenyl-1,2,4-triazolidin-3-yl)methyl)-4-phenyl-1,2,4-triazolidine		AKos GmbH, Steinen, Germany
JH5-A-dimer	4-Phenyl-3-((4-phenyl-5-(4-tolyl)-1,2,4-triazolidin-3-yl]methyl)-5-(4-tolyl)-1,2,4-triazolidine		AKos GmbH, Steinen, Germany
CCC	1H-1,2,4-Triazole-3-thiol		Alfa Aesar, Ward Hill, MA, USA
CCM	4-Methyl--4H-1,2,4-triazole-3-thiol		Acros Organics, Thermo Fisher Scientific, Geel, Belgium
CCP	5-Phenyl--1H-1,2,4-triazole-3-thiol		Sigma-Aldrich (Aldich), St. Louis, MO, USA

213

REFERENCES

1. Di Fiore, P.P. and P. De Camilli, *Endocytosis and signaling. an inseparable partnership.* Cell, 2001. **106**(1): p. 1-4.

2. Miaczynska, M., L. Pelkmans, and M. Zerial, *Not just a sink: endosomes in control of signal transduction.* Current opinion in cell biology, 2004. **16**(4): p. 400-6.

3. Vetter, I.R. and A. Wittinghofer, *The guanine nucleotide-binding switch in three dimensions.* Science, 2001. **294**(5545): p. 1299-304.

4. Bourne, H.R., D.A. Sanders, and F. McCormick, *The GTPase superfamily: a conserved switch for diverse cell functions.* Nature, 1990. **348**(6297): p. 125-32.

5. Grosshans, B.L., D. Ortiz, and P. Novick, *Rabs and their effectors: achieving specificity in membrane traffic.* Proceedings of the National Academy of Sciences of the United States of America, 2006. **103**(32): p. 11821-7.

6. Barr, F. and D.G. Lambright, *Rab GEFs and GAPs.* Current opinion in cell biology, 2010. **22**(4): p. 461-70.

7. Cherfils, J. and P. Chardin, *GEFs: structural basis for their activation of small GTP-binding proteins.* Trends in biochemical sciences, 1999. **24**(8): p. 306-11.

8. Trahey, M. and F. McCormick, *A cytoplasmic protein stimulates normal N-ras p21 GTPase, but does not affect oncogenic mutants.* Science, 1987. **238**(4826): p. 542-5.

9. Scolnick, E.M., A.G. Papageorge, and T.Y. Shih, *Guanine nucleotide-binding activity as an assay for src protein of rat-derived murine sarcoma viruses.* Proceedings of the National Academy of Sciences of the United States of America, 1979. **76**(10): p. 5355-9.

10. Bos, J.L., *ras oncogenes in human cancer: a review.* Cancer research, 1989. **49**(17): p. 4682-9.

11. Baines, A.T., D. Xu, and C.J. Der, *Inhibition of Ras for cancer treatment: the search continues.* Future medicinal chemistry, 2011. **3**(14): p. 1787-808.

12. Wennerberg, K., K.L. Rossman, and C.J. Der, *The Ras superfamily at a glance.* Journal of cell science, 2005. **118**(Pt 5): p. 843-6.

13. Etienne-Manneville, S. and A. Hall, *Rho GTPases in cell biology.* Nature, 2002. **420**(6916): p. 629-35.

14. Zerial, M. and H. McBride, *Rab proteins as membrane organizers.* Nature reviews. Molecular cell biology, 2001. **2**(2): p. 107-17.

15. Mizuno-Yamasaki, E., F. Rivera-Molina, and P. Novick, *GTPase networks in membrane traffic.* Annual review of biochemistry, 2012. **81**: p. 637-59.

16. Yudin, D. and M. Fainzilber, *Ran on tracks--cytoplasmic roles for a nuclear regulator.* Journal of cell science, 2009. **122**(Pt 5): p. 587-93.

17. Seabra, M.C., *Membrane association and targeting of prenylated Ras-like GTPases.* Cellular signalling, 1998. **10**(3): p. 167-72.

18. Seabra, M.C. and C. Wasmeier, *Controlling the location and activation of Rab GTPases.* Current opinion in cell biology, 2004. **16**(4): p. 451-7.

19. Ullrich, O., et al., *Membrane association of Rab5 mediated by GDP-dissociation inhibitor and accompanied by GDP/GTP exchange.* Nature, 1994. **368**(6467): p. 157-60.

20. Soldati, T., et al., *Membrane targeting of the small GTPase Rab9 is accompanied by nucleotide exchange.* Nature, 1994. **369**(6475): p. 76-8.

21. Goody, R.S. and W. Hofmann-Goody, *Exchange factors, effectors, GAPs and motor proteins: common thermodynamic and kinetic principles for different functions.* European biophysics journal : EBJ, 2002. **31**(4): p. 268-74.

22. Bos, J.L., H. Rehmann, and A. Wittinghofer, *GEFs and GAPs: critical elements in the control of small G proteins.* Cell, 2007. **129**(5): p. 865-77.

23. Itzen, A. and R.S. Goody, *GTPases involved in vesicular trafficking: structures and mechanisms.* Seminars in cell & developmental biology, 2011. **22**(1): p. 48-56.

24. Pereira-Leal, J.B. and M.C. Seabra, *Evolution of the Rab family of small GTP-binding proteins.* Journal of molecular biology, 2001. **313**(4): p. 889-901.

25. Marshall, C.J., *Ras effectors.* Current opinion in cell biology, 1996. **8**(2): p. 197-204.

26. Pfeffer, S.R., *Rab GTPases: specifying and deciphering organelle identity and function.* Trends in cell biology, 2001. **11**(12): p. 487-91.

27. Bruce Alberts, A.J., Julian Lewis, Martin Raff, Keith Roberts, Peter Walter, *Molecular Biology of the Cell*. 5th ed2007: Garland Science.

28. Mayr, L.M. and D. Bojanic, *Novel trends in high-throughput screening.* Current opinion in pharmacology, 2009. **9**(5): p. 580-8.

29.   Gruenberg, J. and F.R. Maxfield, *Membrane transport in the endocytic pathway.* Current opinion in cell biology, 1995. **7**(4): p. 552-63.

30.   Mellman, I., *Endocytosis and molecular sorting.* Annual review of cell and developmental biology, 1996. **12**: p. 575-625.

31.   Gu, F. and J. Gruenberg, *Biogenesis of transport intermediates in the endocytic pathway.* FEBS letters, 1999. **452**(1-2): p. 61-6.

32.   Steinman, R.M., et al., *Endocytosis and the recycling of plasma membrane.* The Journal of cell biology, 1983. **96**(1): p. 1-27.

33.   Haucke, V., *Phosphoinositide regulation of clathrin-mediated endocytosis.* Biochemical Society transactions, 2005. **33**(Pt 6): p. 1285-9.

34.   Huotari, J. and A. Helenius, *Endosome maturation.* The EMBO journal, 2011. **30**(17): p. 3481-500.

35.   Doherty, G.J. and H.T. McMahon, *Mechanisms of endocytosis.* Annual review of biochemistry, 2009. **78**: p. 857-902.

36.   Schmid, S.L., *Clathrin-coated vesicle formation and protein sorting: An integrated process.* Annual review of biochemistry, 1997. **66**: p. 511-548.

37.   Jovic, M., et al., *The early endosome: a busy sorting station for proteins at the crossroads.* Histology and histopathology, 2010. **25**(1): p. 99-112.

38.   Woodman, P.G., *Biogenesis of the sorting endosome: the role of Rab5.* Traffic, 2000. **1**(9): p. 695-701.

39.   Bonifacino, J.S. and R. Rojas, *Retrograde transport from endosomes to the trans-Golgi network.* Nature reviews. Molecular cell biology, 2006. **7**(8): p. 568-79.

40.   Miaczynska, M. and M. Zerial, *Mosaic organization of the endocytic pathway.* Experimental cell research, 2002. **272**(1): p. 8-14.

41.   Stenmark, H., *Rab GTPases as coordinators of vesicle traffic.* Nature reviews. Molecular cell biology, 2009. **10**(8): p. 513-25.

42.   Sorensen, J.B., *Conflicting views on the membrane fusion machinery and the fusion pore.* Annual review of cell and developmental biology, 2009. **25**: p. 513-37.

43.   Jahn, R. and R.H. Scheller, *SNAREs--engines for membrane fusion.* Nature reviews. Molecular cell biology, 2006. **7**(9): p. 631-43.

44.   Chavrier, P., et al., *Localization of low molecular weight GTP binding proteins to exocytic and endocytic compartments.* Cell, 1990. **62**(2): p. 317-29.

45.   Sonnichsen, B., et al., *Distinct membrane domains on endosomes in the recycling pathway visualized by multicolor imaging of Rab4, Rab5, and Rab11.* The Journal of cell biology, 2000. **149**(4): p. 901-14.

46.   de Renzis, S., B. Sonnichsen, and M. Zerial, *Divalent Rab effectors regulate the sub-compartmental organization and sorting of early endosomes.* Nature cell biology, 2002. **4**(2): p. 124-33.

47.   Vitale, G., et al., *Distinct Rab-binding domains mediate the interaction of Rabaptin-5 with GTP-bound Rab4 and Rab5.* The EMBO journal, 1998. **17**(7): p. 1941-51.

48.   Deneka, M., et al., *Rabaptin-5alpha/rabaptin-4 serves as a linker between rab4 and gamma(1)-adaptin in membrane recycling from endosomes.* The EMBO journal, 2003. **22**(11): p. 2645-57.

49.   Wright, L.P. and M.R. Philips, *Thematic review series: lipid posttranslational modifications. CAAX modification and membrane targeting of Ras.* Journal of lipid research, 2006. **47**(5): p. 883-91.

50.   Seabra, M.C., et al., *Rab geranylgeranyl transferase. A multisubunit enzyme that prenylates GTP-binding proteins terminating in Cys-X-Cys or Cys-Cys.* The Journal of biological chemistry, 1992. **267**(20): p. 14497-503.

51.   Alexandrov, K., et al., *Rab escort protein-1 is a multifunctional protein that accompanies newly prenylated rab proteins to their target membranes.* The EMBO journal, 1994. **13**(22): p. 5262-73.

52.   Sanford, J.C., Y. Pan, and M. Wessling-Resnick, *Prenylation of Rab5 is dependent on guanine nucleotide binding.* The Journal of biological chemistry, 1993. **268**(32): p. 23773-6.

53.   Chavrier, P., et al., *Hypervariable C-terminal domain of rab proteins acts as a targeting signal.* Nature, 1991. **353**(6346): p. 769-72.

54.   Gorvel, J.P., et al., *rab5 controls early endosome fusion in vitro.* Cell, 1991. **64**(5): p. 915-25.

55.   Stenmark, H., et al., *Distinct structural elements of rab5 define its functional specificity.* The EMBO journal, 1994. **13**(3): p. 575-83.

56.   Ali, B.R., et al., *Multiple regions contribute to membrane targeting of Rab GTPases.* Journal of cell science, 2004. **117**(Pt 26): p. 6401-12.

57.   Ridley, A.J., *Rho GTPases and cell migration.* Journal of cell science, 2001. **114**(Pt 15): p. 2713-22.

58.   Dirac-Svejstrup, A.B., T. Sumizawa, and S.R. Pfeffer, *Identification of a GDI displacement factor that releases endosomal Rab GTPases from Rab-GDI.* The EMBO journal, 1997. **16**(3): p. 465-72.

59.   Pfeffer, S.R., A.B. Dirac-Svejstrup, and T. Soldati, *Rab GDP dissociation inhibitor: putting rab GTPases in the right place.* The Journal of biological chemistry, 1995. **270**(29): p. 17057-9.

60.   Yang, C., V.I. Slepnev, and B. Goud, *Rab proteins form in vivo complexes with two isoforms of the GDP-dissociation inhibitor protein (GDI).* The Journal of biological chemistry, 1994. **269**(50): p. 31891-9.

61.   Sivars, U., D. Aivazian, and S.R. Pfeffer, *Yip3 catalyses the dissociation of endosomal Rab-GDI complexes.* Nature, 2003. **425**(6960): p. 856-9.

62.   Blumer, J., et al., *Specific localization of Rabs at intracellular membranes.* Biochemical Society transactions, 2012. **40**(6): p. 1421-5.

63.   Blumer, J., et al., *RabGEFs are a major determinant for specific Rab membrane targeting.* The Journal of cell biology, 2013. **200**(3): p. 287-300.

64.   Ali, B.R. and M.C. Seabra, *Targeting of Rab GTPases to cellular membranes.* Biochemical Society transactions, 2005. **33**(Pt 4): p. 652-6.

65.   Pfeffer, S.R., *Rab GTPases: master regulators of membrane trafficking.* Current opinion in cell biology, 1994. **6**(4): p. 522-6.

66.   Rybin, V., et al., *GTPase activity of Rab5 acts as a timer for endocytic membrane fusion.* Nature, 1996. **383**(6597): p. 266-9.

67.   Spang, A., *On the fate of early endosomes.* Biol Chem, 2009. **390**(8): p. 753-9.

68.   Cabrera, M. and C. Ungermann, *Guiding endosomal maturation.* Cell, 2010. **141**(3): p. 404-6.

69.   Stenmark, H., et al., *Inhibition of rab5 GTPase activity stimulates membrane fusion in endocytosis.* The EMBO journal, 1994. **13**(6): p. 1287-96.

70.   Bucci, C., et al., *The small GTPase rab5 functions as a regulatory factor in the early endocytic pathway.* Cell, 1992. **70**(5): p. 715-28.

71.   Bucci, C., et al., *Co-operative regulation of endocytosis by three Rab5 isoforms.* FEBS letters, 1995. **366**(1): p. 65-71.

72.   Simpson, J.C. and A.T. Jones, *Early endocytic Rabs: functional prediction to functional characterization.* Biochemical Society symposium, 2005(72): p. 99-108.

73.   Kauppi, M., et al., *The small GTPase Rab22 interacts with EEA1 and controls endosomal membrane trafficking.* Journal of cell science, 2002. **115**(Pt 5): p. 899-911.

74.   Simpson, J.C., et al., *A role for the small GTPase Rab21 in the early endocytic pathway.* Journal of cell science, 2004. **117**(Pt 26): p. 6297-311.

75.   Rodriguez-Gabin, A.G., et al., *Role of rRAB22b, an oligodendrocyte protein, in regulation of transport of vesicles from trans Golgi to endocytic compartments.* Journal of neuroscience research, 2001. **66**(6): p. 1149-60.

76.   Tijsterman, M., et al., *Genes required for systemic RNA interference in Caenorhabditis elegans.* Current biology : CB, 2004. **14**(2): p. 111-6.

77.   Zhu, H., et al., *Rabaptin-5-independent membrane targeting and Rab5 activation by Rabex-5 in the cell.* Mol Biol Cell, 2007. **18**(10): p. 4119-28.

78.   Letunic, I., et al., *SMART 4.0: towards genomic data integration.* Nucleic acids research, 2004. **32**(Database issue): p. D142-4.

79.   Carney, D.S., B.A. Davies, and B.F. Horazdovsky, *Vps9 domain-containing proteins: activators of Rab5 GTPases from yeast to neurons.* Trends in cell biology, 2006. **16**(1): p. 27-35.

80.   Horiuchi, H., et al., *A novel Rab5 GDP/GTP exchange factor complexed to Rabaptin-5 links nucleotide exchange to effector recruitment and function.* Cell, 1997. **90**(6): p. 1149-59.

81.   Tall, G.G., et al., *Ras-activated endocytosis is mediated by the Rab5 guanine nucleotide exchange activity of RIN1.* Developmental cell, 2001. **1**(1): p. 73-82.

82.   Saito, K., et al., *A novel binding protein composed of homophilic tetramer exhibits unique properties for the small GTPase Rab5.* The Journal of biological chemistry, 2002. **277**(5): p. 3412-8.

83.   Kajiho, H., et al., *RIN3: a novel Rab5 GEF interacting with amphiphysin II involved in the early endocytic pathway.* Journal of cell science, 2003. **116**(Pt 20): p. 4159-68.

84.   Woller, B., et al., *Rin-like, a novel regulator of endocytosis, acts as guanine nucleotide exchange factor for Rab5a and Rab22.* Biochimica et biophysica acta, 2011. **1813**(6): p. 1198-210.

85.   Otomo, A., et al., *ALS2, a novel guanine nucleotide exchange factor for the small GTPase Rab5, is implicated in endosomal dynamics.* Human molecular genetics, 2003. **12**(14): p. 1671-87.

86.   Hadano, S., et al., *ALS2CL, the novel protein highly homologous to the carboxy-terminal half of ALS2, binds to Rab5 and modulates endosome dynamics.* FEBS letters, 2004. **575**(1-3): p. 64-70.

87.   Sato, M., et al., *Caenorhabditis elegans RME-6 is a novel regulator of RAB-5 at the clathrin-coated pit.* Nature cell biology, 2005. **7**(6): p. 559-69.

88.   Lodhi, I.J., et al., *Gapex-5, a Rab31 guanine nucleotide exchange factor that regulates Glut4 trafficking in adipocytes.* Cell metabolism, 2007. **5**(1): p. 59-72.

89.   Zhang, X., et al., *Varp is a Rab21 guanine nucleotide exchange factor and regulates endosome dynamics.* Journal of cell science, 2006. **119**(Pt 6): p. 1053-62.

90. Hunker, C.M., et al., *Rab5-activating protein 6, a novel endosomal protein with a role in endocytosis.* Biochemical and biophysical research communications, 2006. **340**(3): p. 967-75.

91. Christoforidis, S., et al., *The Rab5 effector EEA1 is a core component of endosome docking.* Nature, 1999. **397**(6720): p. 621-5.

92. Simonsen, A., et al., *EEA1 links PI(3)K function to Rab5 regulation of endosome fusion.* Nature, 1998. **394**(6692): p. 494-8.

93. Nielsen, E., et al., *Rabenosyn-5, a novel Rab5 effector, is complexed with hVPS45 and recruited to endosomes through a FYVE finger domain.* The Journal of cell biology, 2000. **151**(3): p. 601-12.

94. Mu, F.T., et al., *EEA1, an early endosome-associated protein. EEA1 is a conserved alpha-helical peripheral membrane protein flanked by cysteine "fingers" and contains a calmodulin-binding IQ motif.* The Journal of biological chemistry, 1995. **270**(22): p. 13503-11.

95. Lippe, R., et al., *Functional synergy between Rab5 effector Rabaptin-5 and exchange factor Rabex-5 when physically associated in a complex.* Mol Biol Cell, 2001. **12**(7): p. 2219-28.

96. Christoforidis, S., et al., *Phosphatidylinositol-3-OH kinases are Rab5 effectors.* Nature cell biology, 1999. **1**(4): p. 249-52.

97. Schu, P.V., et al., *Phosphatidylinositol 3-kinase encoded by yeast VPS34 gene essential for protein sorting.* Science, 1993. **260**(5104): p. 88-91.

98. Rubino, M., et al., *Selective membrane recruitment of EEA1 suggests a role in directional transport of clathrin-coated vesicles to early endosomes.* J Biol Chem, 2000. **275**(6): p. 3745-8.

99. McBride, H.M., et al., *Oligomeric complexes link Rab5 effectors with NSF and drive membrane fusion via interactions between EEA1 and syntaxin 13.* Cell, 1999. **98**(3): p. 377-86.

100. Gillooly, D.J., et al., *Localization of phosphatidylinositol 3-phosphate in yeast and mammalian cells.* The EMBO journal, 2000. **19**(17): p. 4577-88.

101. Wilson, J.M., et al., *EEA1, a tethering protein of the early sorting endosome, shows a polarized distribution in hippocampal neurons, epithelial cells, and fibroblasts.* Molecular biology of the cell, 2000. **11**(8): p. 2657-71.

102. Pfeffer, S., *A model for Rab GTPase localization.* Biochemical Society transactions, 2005. **33**(Pt 4): p. 627-30.

103. Miaczynska, M., et al., *APPL proteins link Rab5 to nuclear signal transduction via an endosomal compartment.* Cell, 2004. **116**(3): p. 445-56.

104. Schenck, A., et al., *The endosomal protein Appl1 mediates Akt substrate specificity and cell survival in vertebrate development.* Cell, 2008. **133**(3): p. 486-97.

105. Zoncu, R., et al., *A phosphoinositide switch controls the maturation and signaling properties of APPL endosomes.* Cell, 2009. **136**(6): p. 1110-21.

106. Barbieri, M.A., et al., *Evidence for a symmetrical requirement for Rab5-GTP in in vitro endosome-endosome fusion.* The Journal of biological chemistry, 1998. **273**(40): p. 25850-5.

107. Schnatwinkel, C., et al., *The Rab5 effector Rabankyrin-5 regulates and coordinates different endocytic mechanisms.* PLoS biology, 2004. **2**(9): p. E261.

108. Ohya, T., et al., *Reconstitution of Rab- and SNARE-dependent membrane fusion by synthetic endosomes.* Nature, 2009. **459**(7250): p. 1091-7.

109. Patki, V., et al., *A functional PtdIns(3)P-binding motif.* Nature, 1998. **394**(6692): p. 433-4.

110. Lawe, D.C., et al., *The FYVE domain of early endosome antigen 1 is required for both phosphatidylinositol 3-phosphate and Rab5 binding - Critical role of this dual interaction for endosomal localization.* Journal of Biological Chemistry, 2000. **275**(5): p. 3699-3705.

111. Platta, H.W. and H. Stenmark, *Endocytosis and signaling.* Current opinion in cell biology, 2011. **23**(4): p. 393-403.

112. Magadan, J.G., et al., *Rab22a regulates the sorting of transferrin to recycling endosomes.* Molecular and cellular biology, 2006. **26**(7): p. 2595-614.

113. Mesa, R., et al., *Overexpression of Rab22a hampers the transport between endosomes and the Golgi apparatus.* Experimental cell research, 2005. **304**(2): p. 339-53.

114. Jordens, I., et al., *Rab proteins, connecting transport and vesicle fusion.* Traffic, 2005. **6**(12): p. 1070-7.

115. Echard, A., et al., *Interaction of a Golgi-associated kinesin-like protein with Rab6.* Science, 1998. **279**(5350): p. 580-5.

116. McLauchlan, H., et al., *A novel role for Rab5-GDI in ligand sequestration into clathrin-coated pits.* Current biology : CB, 1998. **8**(1): p. 34-45.

117. Shiba, Y., et al., *gamma-adaptin interacts directly with rabaptin-5 through its ear domain.* Journal of biochemistry, 2002. **131**(3): p. 327-336.

118. Conner, S.D. and S.L. Schmid, *Identification of an adaptor-associated kinase, AAK1, as a regulator of clathrin-mediated endocytosis.* The Journal of cell biology, 2002. **156**(5): p. 921-9.

119. Semerdjieva, S., et al., *Coordinated regulation of AP2 uncoating from clathrin-coated vesicles by rab5 and hRME-6.* J Cell Biol, 2008. **183**(3): p. 499-511.

120. Shin, H.W., et al., *An enzymatic cascade of Rab5 effectors regulates phosphoinositide turnover in the endocytic pathway.* The Journal of cell biology, 2005. **170**(4): p. 607-18.

121. Nielsen, E., et al., *Rab5 regulates motility of early endosomes on microtubules.* Nature cell biology, 1999. **1**(6): p. 376-82.

122. Hoepfner, S., et al., *Modulation of receptor recycling and degradation by the endosomal kinesin KIF16B.* Cell, 2005. **121**(3): p. 437-50.

123. Stenmark, H., et al., *Rabaptin-5 is a direct effector of the small GTPase Rab5 in endocytic membrane fusion.* Cell, 1995. **83**(3): p. 423-32.

124. Morrison, H.A., et al., *Regulation of early endosomal entry by the Drosophila tumor suppressors Rabenosyn and Vps45.* Molecular biology of the cell, 2008. **19**(10): p. 4167-76.

125. Lanzetti, L., et al., *Rab5 is a signalling GTPase involved in actin remodelling by receptor tyrosine kinases.* Nature, 2004. **429**(6989): p. 309-14.

126. Spaargaren, M. and J.L. Bos, *Rab5 induces Rac-independent lamellipodia formation and cell migration.* Molecular biology of the cell, 1999. **10**(10): p. 3239-50.

127. Buccione, R., J.D. Orth, and M.A. McNiven, *Foot and mouth: podosomes, invadopodia and circular dorsal ruffles.* Nature reviews. Molecular cell biology, 2004. **5**(8): p. 647-57.

128. Swanson, J.A. and C. Watts, *Macropinocytosis.* Trends in cell biology, 1995. **5**(11): p. 424-8.

129. Araki, N., et al., *Actinin-4 is preferentially involved in circular ruffling and macropinocytosis in mouse macrophages: analysis by fluorescence ratio imaging.* Journal of cell science, 2000. **113 (Pt 18)**: p. 3329-40.

130. Feliciano, W.D., et al., *Coordination of the Rab5 cycle on macropinosomes.* Traffic, 2011. **12**(12): p. 1911-22.

131. Palamidessi, A., et al., *Endocytic trafficking of Rac is required for the spatial restriction of signaling in cell migration.* Cell, 2008. **134**(1): p. 135-47.

132. Lanzetti, L., *A novel function of Rab5 in mitosis.* Small GTPases, 2012. **3**(3).

133. Audhya, A., A. Desai, and K. Oegema, *A role for Rab5 in structuring the endoplasmic reticulum.* The Journal of cell biology, 2007. **178**(1): p. 43-56.

134. Capalbo, L., et al., *Rab5 GTPase controls chromosome alignment through Lamin disassembly and relocation of the NuMA-like protein Mud to the poles during mitosis.* Proceedings of the National Academy of Sciences of the United States of America, 2011. **108**(42): p. 17343-8.

135. Vieira, A.V., C. Lamaze, and S.L. Schmid, *Control of EGF receptor signaling by clathrin-mediated endocytosis.* Science, 1996. **274**(5295): p. 2086-9.

136. Delprato, A., E. Merithew, and D.G. Lambright, *Structure, exchange determinants, and family-wide rab specificity of the tandem helical bundle and Vps9 domains of Rabex-5.* Cell, 2004. **118**(5): p. 607-17.

137. Yoshimura, S., et al., *Family-wide characterization of the DENN domain Rab GDP-GTP exchange factors.* The Journal of cell biology, 2010. **191**(2): p. 367-81.

138. Mori, Y., T. Matsui, and M. Fukuda, *Rabex-5 regulates dendritic localization of Rab17 and neurite morphogenesis in hippocampal neurons.* The Journal of biological chemistry, 2013.

139. Yan, H., et al., *Rabex-5 ubiquitin ligase activity restricts Ras signaling to establish pathway homeostasis in Drosophila.* Current biology : CB, 2010. **20**(15): p. 1378-82.

140. Tam, S.Y., et al., *RabGEF1 is a negative regulator of mast cell activation and skin inflammation.* Nat Immunol, 2004. **5**(8): p. 844-52.

141. Penengo, L., et al., *Crystal structure of the ubiquitin binding domains of rabex-5 reveals two modes of interaction with ubiquitin.* Cell, 2006. **124**(6): p. 1183-95.

142. Mattera, R., et al., *The Rab5 guanine nucleotide exchange factor Rabex-5 binds ubiquitin (Ub) and functions as a Ub ligase through an atypical Ub-interacting motif and a zinc finger domain.* J Biol Chem, 2006. **281**(10): p. 6874-83.

143. Zhu, H., Z. Liang, and G. Li, *Rabex-5 is a Rab22 effector and mediates a Rab22-Rab5 signaling cascade in endocytosis.* Mol Biol Cell, 2009. **20**(22): p. 4720-9.

144. Lee, S., et al., *Structural basis for ubiquitin recognition and autoubiquitination by Rabex-5.* Nat Struct Mol Biol, 2006. **13**(3): p. 264-71.

145. Opipari, A.W., Jr., M.S. Boguski, and V.M. Dixit, *The A20 cDNA induced by tumor necrosis factor alpha encodes a novel type of zinc finger protein.* The Journal of biological chemistry, 1990. **265**(25): p. 14705-8.

146. Delprato, A. and D.G. Lambright, *Structural basis for Rab GTPase activation by VPS9 domain exchange factors.* Nat Struct Mol Biol, 2007. **14**(5): p. 406-12.

147. Esters, H., et al., *Vps9, Rabex-5 and DSS4: proteins with weak but distinct nucleotide-exchange activities for Rab proteins.* J Mol Biol, 2001. **310**(1): p. 141-56.

148. Mattera, R. and J.S. Bonifacino, *Ubiquitin binding and conjugation regulate the recruitment of Rabex-5 to early endosomes.* Embo J, 2008. **27**(19): p. 2484-94.

149. Aikawa, Y., *Rabex-5 protein regulates the endocytic trafficking pathway of ubiquitinated neural cell adhesion molecule L1.* The Journal of biological chemistry, 2012. **287**(39): p. 32312-23.

150. Gournier, H., et al., *Two distinct effectors of the small GTPase Rab5 cooperate in endocytic membrane fusion.* The EMBO journal, 1998. **17**(7): p. 1930-40.

151. Griffiths, G. and J. Gruenberg, *The arguments for pre-existing early and late endosomes.* Trends in cell biology, 1991. **1**(1): p. 5-9.

152. Vonderheit, A. and A. Helenius, *Rab7 associates with early endosomes to mediate sorting and transport of Semliki forest virus to late endosomes.* PLoS biology, 2005. **3**(7): p. e233.

153. Rink, J., et al., *Rab conversion as a mechanism of progression from early to late endosomes.* Cell, 2005. **122**(5): p. 735-49.

154. Poteryaev, D., et al., *Identification of the switch in early-to-late endosome transition.* Cell, 2010. **141**(3): p. 497-508.

155. Nordmann, M., et al., *The Mon1-Ccz1 complex is the GEF of the late endosomal Rab7 homolog Ypt7.* Current biology : CB, 2010. **20**(18): p. 1654-9.

156. Nottingham, R.M. and S.R. Pfeffer, *Defining the boundaries: Rab GEFs and GAPs.* Proceedings of the National Academy of Sciences of the United States of America, 2009. **106**(34): p. 14185-6.

157. Rivera-Molina, F.E. and P.J. Novick, *A Rab GAP cascade defines the boundary between two Rab GTPases on the secretory pathway.* Proceedings of the National Academy of Sciences of the United States of America, 2009. **106**(34): p. 14408-13.

158. Barbieri, M.A., et al., *Epidermal growth factor and membrane trafficking. EGF receptor activation of endocytosis requires Rab5a.* The Journal of cell biology, 2000. **151**(3): p. 539-50.

159. Sigismund, S., et al., *Clathrin-mediated internalization is essential for sustained EGFR signaling but dispensable for degradation.* Developmental cell, 2008. **15**(2): p. 209-19.

160. Lanzetti, L., et al., *The Eps8 protein coordinates EGF receptor signalling through Rac and trafficking through Rab5.* Nature, 2000. **408**(6810): p. 374-7.

161. Raiborg, C., T. Slagsvold, and H. Stenmark, *A new side to ubiquitin.* Trends Biochem Sci, 2006. **31**(10): p. 541-4.

162. Sigismund, S., et al., *Clathrin-independent endocytosis of ubiquitinated cargos.* Proceedings of the National Academy of Sciences of the United States of America, 2005. **102**(8): p. 2760-5.

163. Balaji, K., et al., *RIN1 Orchestrates the Activation of RAB5 GTPases and ABL Tyrosine Kinases to Determine EGFR Fate.* Journal of cell science, 2012.

164. Barbieri, M.A., et al., *Protein kinase B/akt and rab5 mediate Ras activation of endocytosis.* The Journal of biological chemistry, 1998. **273**(31): p. 19367-70.

165. Schlessinger, J., *Cell signaling by receptor tyrosine kinases.* Cell, 2000. **103**(2): p. 211-25.

166. Colicelli, J., *Signal transduction: RABGEF1 fingers RAS for ubiquitination.* Current biology : CB, 2010. **20**(15): p. R630-2.

167. Xu, L., et al., *Feedback regulation of Ras signaling by Rabex-5-mediated ubiquitination.* Current biology : CB, 2010. **20**(15): p. 1372-7.

168. Arozarena, I., F. Calvo, and P. Crespo, *Ras, an actor on many stages: posttranslational modifications, localization, and site-specified events.* Genes & cancer, 2011. **2**(3): p. 182-94.

169. Jura, N., et al., *Differential modification of Ras proteins by ubiquitination.* Molecular cell, 2006. **21**(5): p. 679-87.

170. Kalesnikoff, J., et al., *Roles of RabGEF1/Rabex-5 domains in regulating Fc epsilon RI surface expression and Fc epsilon RI-dependent responses in mast cells.* Blood, 2007. **109**(12): p. 5308-17.

171. Kalesnikoff, J., et al., *RabGEF1 regulates stem cell factor/c-Kit-mediated signaling events and biological responses in mast cells.* Proc Natl Acad Sci U S A, 2006. **103**(8): p. 2659-64.

172. Rios, E.J., et al., *Rabaptin-5 regulates receptor expression and functional activation in mast cells.* Blood, 2008. **112**(10): p. 4148-57.

173. Abbas, A.K., Lichtman, A.H., *Cellular and Molecular Immunology.* 5th Edithion ed2005, Philadelphia, PA, USA: Elsevier Saunders.

174. Drews, J., *Drug discovery: a historical perspective.* Science, 2000. **287**(5460): p. 1960-4.

175. Stockwell, B.R., *Chemical genetics: ligand-based discovery of gene function.* Nature reviews. Genetics, 2000. **1**(2): p. 116-25.

176. Patel, D.V. and E.M. Gordon, *Applications of small-molecule combinatorial chemistry to drug discovery.* Drug discovery today, 1996. **1**(4): p. 134-144.

177. Overington, J.P., B. Al-Lazikani, and A.L. Hopkins, *How many drug targets are there?* Nature reviews. Drug discovery, 2006. **5**(12): p. 993-6.

178. Hung, D.T., T.F. Jamison, and S.L. Schreiber, *Understanding and controlling the cell cycle with natural products.* Chemistry & biology, 1996. **3**(8): p. 623-39.

179. Alaimo, P.J., M.A. Shogren-Knaak, and K.M. Shokat, *Chemical genetic approaches for the elucidation of signaling pathways.* Current opinion in chemical biology, 2001. **5**(4): p. 360-7.

180. Weiss, W.A., S.S. Taylor, and K.M. Shokat, *Recognizing and exploiting differences between RNAi and small-molecule inhibitors.* Nature chemical biology, 2007. **3**(12): p. 739-44.

181. Stockwell, B.R., *Exploring biology with small organic molecules.* Nature, 2004. **432**(7019): p. 846-54.

182. Ohlmeyer, M. and M.M. Zhou, *Integration of small-molecule discovery in academic biomedical research.* The Mount Sinai journal of medicine, New York, 2010. **77**(4): p. 350-7.

183. Sarbassov, D.D., et al., *Rictor, a novel binding partner of mTOR, defines a rapamycin-insensitive and raptor-independent pathway that regulates the cytoskeleton.* Current biology : CB, 2004. **14**(14): p. 1296-302.

184. Schreiber, S.L., *Small molecules: the missing link in the central dogma.* Nature chemical biology, 2005. **1**(2): p. 64-6.

185. Spring, D.R., *Chemical genetics to chemical genomics: small molecules offer big insights.* Chemical Society reviews, 2005. **34**(6): p. 472-82.

186. Verkman, A.S., *Drug discovery in academia.* American journal of physiology. Cell physiology, 2004. **286**(3): p. C465-74.

187. Ditchfield, C., et al., *Aurora B couples chromosome alignment with anaphase by targeting BubR1, Mad2, and Cenp-E to kinetochores.* The Journal of cell biology, 2003. **161**(2): p. 267-80.

188. Hauf, S., et al., *The small molecule Hesperadin reveals a role for Aurora B in correcting kinetochore-microtubule attachment and in maintaining the spindle assembly checkpoint.* The Journal of cell biology, 2003. **161**(2): p. 281-94.

189. Hafner, M., et al., *Inhibition of cytohesins by SecinH3 leads to hepatic insulin resistance.* Nature, 2006. **444**(7121): p. 941-4.

190. Vigil, D., et al., *Ras superfamily GEFs and GAPs: validated and tractable targets for cancer therapy?* Nature reviews. Cancer, 2010. **10**(12): p. 842-57.

191. Shima, F., et al., *In silico discovery of small-molecule Ras inhibitors that display antitumor activity by blocking the Ras-effector interaction.* Proceedings of the National Academy of Sciences of the United States of America, 2013. **110**(20): p. 8182-7.

192. Maurer, T., et al., *Small-molecule ligands bind to a distinct pocket in Ras and inhibit SOS-mediated nucleotide exchange activity.* Proceedings of the National Academy of Sciences of the United States of America, 2012. **109**(14): p. 5299-304.

193. Sun, Q., et al., *Discovery of small molecules that bind to K-Ras and inhibit Sos-mediated activation.* Angewandte Chemie, 2012. **51**(25): p. 6140-3.

194. Palmioli, A., et al., *First experimental identification of Ras-inhibitor binding interface using a water-soluble Ras ligand.* Bioorganic & medicinal chemistry letters, 2009. **19**(15): p. 4217-22.

195. Airoldi, C., et al., *Glucose-derived Ras pathway inhibitors: evidence of Ras-ligand binding and Ras-GEF (Cdc25) interaction inhibition.* Chembiochem : a European journal of chemical biology, 2007. **8**(12): p. 1376-9.

196. Taveras, A.G., et al., *Ras oncoprotein inhibitors: the discovery of potent, ras nucleotide exchange inhibitors and the structural determination of a drug-protein complex.* Bioorganic & medicinal chemistry, 1997. **5**(1): p. 125-33.

197. Peri, F., et al., *Design, synthesis and biological evaluation of sugar-derived Ras inhibitors.* Chembiochem : a European journal of chemical biology, 2005. **6**(10): p. 1839-48.

198. Spoerner, M., et al., *A novel mechanism for the modulation of the Ras-effector interaction by small molecules.* Biochemical and biophysical research communications, 2005. **334**(2): p. 709-13.

199. Rosnizeck, I.C., et al., *Stabilizing a weak binding state for effectors in the human ras protein by cyclen complexes.* Angewandte Chemie, 2010. **49**(22): p. 3830-3.

200. Kato-Stankiewicz, J., et al., *Inhibitors of Ras/Raf-1 interaction identified by two-hybrid screening revert Ras-dependent transformation phenotypes in human cancer cells.* Proceedings of the National Academy of Sciences of the United States of America, 2002. **99**(22): p. 14398-403.

201. Lu, Y., et al., *Solution phase parallel synthesis and evaluation of MAPK inhibitory activities of close structural analogues of a Ras pathway modulator.* Bioorganic & medicinal chemistry letters, 2004. **14**(15): p. 3957-62.

202. Waldmann, H., et al., *Sulindac-derived Ras pathway inhibitors target the Ras-Raf interaction and downstream effectors in the Ras pathway.* Angewandte Chemie, 2004. **43**(4): p. 454-8.

203. Muller, O., et al., *Identification of potent Ras signaling inhibitors by pathway-selective phenotype-based screening.* Angewandte Chemie, 2004. **43**(4): p. 450-4.

204. Khazak, V., et al., *Selective Raf inhibition in cancer therapy.* Expert opinion on therapeutic targets, 2007. **11**(12): p. 1587-609.

205. Gao, Y., et al., *Rational design and characterization of a Rac GTPase-specific small molecule inhibitor.* Proceedings of the National Academy of Sciences of the United States of America, 2004. **101**(20): p. 7618-23.

206. Shutes, A., et al., *Specificity and mechanism of action of EHT 1864, a novel small molecule inhibitor of Rac family small GTPases.* The Journal of biological chemistry, 2007. **282**(49): p. 35666-78.

207. Agola, J.O., et al., *A competitive nucleotide binding inhibitor: in vitro characterization of Rab7 GTPase inhibition.* ACS chemical biology, 2012. **7**(6): p. 1095-108.

208. Walker, K. and M.F. Olson, *Targeting Ras and Rho GTPases as opportunities for cancer therapeutics.* Current opinion in genetics & development, 2005. **15**(1): p. 62-8.

209. Mossessova, E., R.A. Corpina, and J. Goldberg, *Crystal structure of ARF1*Sec7 complexed with Brefeldin A and its implications for the guanine nucleotide exchange mechanism.* Molecular cell, 2003. **12**(6): p. 1403-11.

210. Renault, L., B. Guibert, and J. Cherfils, *Structural snapshots of the mechanism and inhibition of a guanine nucleotide exchange factor.* Nature, 2003. **426**(6966): p. 525-30.

211. Klausner, R.D., J.G. Donaldson, and J. Lippincott-Schwartz, *Brefeldin A: insights into the control of membrane traffic and organelle structure.* The Journal of cell biology, 1992. **116**(5): p. 1071-80.

212. Meacci, E., et al., *Cytohesin-1, a cytosolic guanine nucleotide-exchange protein for ADP-ribosylation factor.* Proceedings of the National Academy of Sciences of the United States of America, 1997. **94**(5): p. 1745-8.

213. Mayer, G., et al., *Controlling small guanine-nucleotide-exchange factor function through cytoplasmic RNA intramers.* Proceedings of the National Academy of Sciences of the United States of America, 2001. **98**(9): p. 4961-5.

214. Viaud, J., et al., *Structure-based discovery of an inhibitor of Arf activation by Sec7 domains through targeting of protein-protein complexes.* Proceedings of the National Academy of Sciences of the United States of America, 2007. **104**(25): p. 10370-5.

215. Saenz, J.B., et al., *Golgicide A reveals essential roles for GBF1 in Golgi assembly and function.* Nature chemical biology, 2009. **5**(3): p. 157-65.

216. Robineau, S., M. Chabre, and B. Antonny, *Binding site of brefeldin A at the interface between the small G protein ADP-ribosylation factor 1 (ARF1) and the nucleotide-exchange factor Sec7 domain.* Proceedings of the National Academy of Sciences of the United States of America, 2000. **97**(18): p. 9913-8.

217. Saenz, J.B., T.A. Doggett, and D.B. Haslam, *Identification and characterization of small molecules that inhibit intracellular toxin transport.* Infection and immunity, 2007. **75**(9): p. 4552-61.

218. Bouquier, N., et al., *A cell active chemical GEF inhibitor selectively targets the Trio/RhoG/Rac1 signaling pathway.* Chemistry & biology, 2009. **16**(6): p. 657-66.

219. Blangy, A., et al., *Identification of TRIO-GEFD1 chemical inhibitors using the yeast exchange assay.* Biology of the cell / under the auspices of the European Cell Biology Organization, 2006. **98**(9): p. 511-22.

220. Schmidt, S., et al., *Identification of the first Rho-GEF inhibitor, TRIPalpha, which targets the RhoA-specific GEF domain of Trio.* FEBS letters, 2002. **523**(1-3): p. 35-42.

221. Bouquier, N., et al., *Aptamer-derived peptides as potent inhibitors of the oncogenic RhoGEF Tgat.* Chemistry & biology, 2009. **16**(4): p. 391-400.

222. Coxon, F.P., et al., *Phosphonocarboxylate inhibitors of Rab geranylgeranyl transferase disrupt the prenylation and membrane localization of Rab proteins in osteoclasts in vitro and in vivo.* Bone, 2005. **37**(3): p. 349-58.

223. Leung, K.F., R. Baron, and M.C. Seabra, *Thematic review series: lipid posttranslational modifications. geranylgeranylation of Rab GTPases.* Journal of lipid research, 2006. **47**(3): p. 467-75.

224. Steele-Mortimer, O., et al., *The N-terminal domain of a rab protein is involved in membrane-membrane recognition and/or fusion.* The EMBO journal, 1994. **13**(1): p. 34-41.

225. Sanford, J.C., Y. Pan, and M. Wessling-Resnick, *Properties of Rab5 N-terminal domain dictate prenylation of C-terminal cysteines.* Molecular biology of the cell, 1995. **6**(1): p. 71-85.

226. Merithew, E., et al., *Determinants of Rab5 interaction with the N terminus of early endosome antigen 1.* The Journal of biological chemistry, 2003. **278**(10): p. 8494-500.

227. Merithew, E., et al., *Structural plasticity of an invariant hydrophobic triad in the switch regions of Rab GTPases is a determinant of effector recognition.* The Journal of biological chemistry, 2001. **276**(17): p. 13982-8.

228. Inglese, J., et al., *High-throughput screening assays for the identification of chemical probes.* Nature chemical biology, 2007. **3**(8): p. 466-79.

229. Pan, J.Y., J.C. Sanford, and M. Wessling-Resnick, *Effect of guanine nucleotide binding on the intrinsic tryptophan fluorescence properties of Rab5.* The Journal of biological chemistry, 1995. **270**(41): p. 24204-8.

230. Nelson, S.L., *Academic HTS: diverse portraits.* Drug Discovery Today: Technologies, 2009. **5**(1): p. 29-33.

231. Zhang, J.H., T.D. Chung, and K.R. Oldenburg, *A Simple Statistical Parameter for Use in Evaluation and Validation of High Throughput Screening Assays.* Journal of biomolecular screening, 1999. **4**(2): p. 67-73.

232. Feng, B.Y., et al., *High-throughput assays for promiscuous inhibitors.* Nature chemical biology, 2005. **1**(3): p. 146-8.

233. Linke, D., *Detergents: an overview.* Methods in enzymology, 2009. **463**: p. 603-17.

234. Lipinski, C.A., et al., *Experimental and computational approaches to estimate solubility and permeability in drug discovery and development settings.* Advanced drug delivery reviews, 2001. **46**(1-3): p. 3-26.

235. Lombardino, J.G. and J.A. Lowe, 3rd, *The role of the medicinal chemist in drug discovery--then and now.* Nature reviews. Drug discovery, 2004. **3**(10): p. 853-62.

236. Leon, R., et al., *Identification and characterization of binding sites on S100A7, a participant in cancer and inflammation pathways.* Biochemistry, 2009. **48**(44): p. 10591-600.

237. Liu, L., et al., *Use of stabilizing mutations to engineer a charged group within a ligand-binding hydrophobic cavity in T4 lysozyme.* Biochemistry, 2009. **48**(37): p. 8842-51.

238. Wienken, C.J., et al., *Protein-binding assays in biological liquids using microscale thermophoresis.* Nature communications, 2010. **1**: p. 100.

239. Jerabek-Willemsen, M., et al., *Molecular interaction studies using microscale thermophoresis.* Assay and drug development technologies, 2011. **9**(4): p. 342-53.

240. Shinkai, H., et al., *bis(2-(Acylamino)phenyl) disulfides, 2-(acylamino)benzenethiols, and S-(2-(acylamino)phenyl) alkanethioates as novel inhibitors of cholesteryl ester transfer protein.* Journal of medicinal chemistry, 2000. **43**(19): p. 3566-72.

241. Okamoto, H., et al., *A cholesteryl ester transfer protein inhibitor attenuates atherosclerosis in rabbits.* Nature, 2000. **406**(6792): p. 203-7.

242. Schwartz, G.G., et al., *Effects of dalcetrapib in patients with a recent acute coronary syndrome.* The New England journal of medicine, 2012. **367**(22): p. 2089-99.

243. Furuhata, A., et al., *Thiolation of protein-bound carcinogenic aldehyde. An electrophilic acrolein-lysine adduct that covalently binds to thiols.* The Journal of biological chemistry, 2002. **277**(31): p. 27919-26.

244. Budzikiewicz, H., Schäfer, M., *Massenspektrometrie*2005, Weinheim: Wiley-VCH GmbH & Co KGaA.

245. Gross, J.H., *Massenspektrometrie*2013: Springer Spektrum.

246. Torres, V.A., et al., *Caspase 8 promotes peripheral localization and activation of Rab5.* The Journal of biological chemistry, 2008. **283**(52): p. 36280-9.

247. Liu, J., et al., *Nerve growth factor-mediated neurite outgrowth via regulation of Rab5.* Mol Biol Cell, 2007. **18**(4): p. 1375-84.

248. Ku, B., et al., *VipD of Legionella pneumophila targets activated Rab5 and Rab22 to interfere with endosomal trafficking in macrophages.* PLoS pathogens, 2012. **8**(12): p. e1003082.

249. Vanlandingham, P.A. and B.P. Ceresa, *Rab7 regulates late endocytic trafficking downstream of multivesicular body biogenesis and cargo sequestration.* The Journal of biological chemistry, 2009. **284**(18): p. 12110-24.

250. Miller, K., et al., *Localization of the epidermal growth factor (EGF) receptor within the endosome of EGF-stimulated epidermoid carcinoma (A431) cells.* The Journal of cell biology, 1986. **102**(2): p. 500-9.

251. Mayle, K.M., A.M. Le, and D.T. Kamei, *The intracellular trafficking pathway of transferrin.* Biochimica et biophysica acta, 2012. **1820**(3): p. 264-81.

252. Arcaro, A. and M.P. Wymann, *Wortmannin is a potent phosphatidylinositol 3-kinase inhibitor: the role of phosphatidylinositol 3,4,5-trisphosphate in neutrophil responses.* The Biochemical journal, 1993. **296 (Pt 2)**: p. 297-301.

253. Bisswanger, H., *Practical Enzymology.* 2nd edition ed2011: Wiley-VCH Verlag GmbH & Co. KGaA.

254. Lazo, J.S., et al., *Identification of a potent and selective pharmacophore for Cdc25 dual specificity phosphatase inhibitors.* Molecular pharmacology, 2002. **61**(4): p. 720-8.

255. Beier, J.I., et al., *Activation of ErbB2 by 2-methyl-1,4-naphthoquinone (menadione) in human keratinocytes: role of EGFR and protein tyrosine phosphatases.* FEBS letters, 2006. **580**(7): p. 1859-64.

256. Theis, J., *Identifizierung und Charakterisierung eines neuen Inhibitors der PH-Domäne der Cytohesin-Familie.* 2011.

257. Hama, H., G.G. Tall, and B.F. Horazdovsky, *Vps9p is a guanine nucleotide exchange factor involved in vesicle-mediated vacuolar protein transport.* The Journal of biological chemistry, 1999. **274**(21): p. 15284-91.

258. Eisenthal, R., M.J. Danson, and D.W. Hough, *Catalytic efficiency and kcat/KM: a useful comparator?* Trends in biotechnology, 2007. **25**(6): p. 247-9.

259. Mayr, L.M. and P. Fuerst, *The future of high-throughput screening.* Journal of biomolecular screening, 2008. **13**(6): p. 443-8.

260. Niebel, B., *Modulierung der Guaninnukleotid Austauschfaktoren Tiam1 und Vav1 durch RNA-Aptamere.* 2011.

261. Niebel, B., et al., *ADLOC: an aptamer-displacement assay based on luminescent oxygen channeling.* Chemistry, 2010. **16**(36): p. 11100-7.

262. Gribbon, P. and A. Sewing, *Fluorescence readouts in HTS: no gain without pain?* Drug discovery today, 2003. **8**(22): p. 1035-43.

263. Hertzberg, R.P. and A.J. Pope, *High-throughput screening: new technology for the 21st century.* Current opinion in chemical biology, 2000. **4**(4): p. 445-51.

264. Gardas, A. and A. Lewartowska, *Coating of proteins to polystyrene ELISA plates in the presence of detergents.* Journal of immunological methods, 1988. **106**(2): p. 251-5.

265. Ryan, A.J., et al., *Effect of detergent on "promiscuous" inhibitors.* Journal of medicinal chemistry, 2003. **46**(16): p. 3448-51.

266. Tjernberg, A., et al., *DMSO-related effects in protein characterization.* Journal of biomolecular screening, 2006. **11**(2): p. 131-7.

267. Allen, M., J. Reeves, and G. Mellor, *High throughput fluorescence polarization: a homogeneous alternative to radioligand binding for cell surface receptors.* Journal of biomolecular screening, 2000. **5**(2): p. 63-9.

268. Turek-Etienne, T.C., et al., *Evaluation of fluorescent compound interference in 4 fluorescence polarization assays: 2 kinases, 1 protease, and 1 phosphatase.* Journal of biomolecular screening, 2003. **8**(2): p. 176-84.

269. Schwedt, G., Vogt, C., *Analytische Trennmethoden*2010, Weinheim: WILEY-VCH Verlag GmbH & Co.KGaA.

270. Posner, B.A., H. Xi, and J.E. Mills, *Enhanced HTS hit selection via a local hit rate analysis.* Journal of chemical information and modeling, 2009. **49**(10): p. 2202-10.

271. Di, L. and E.H. Kerns, *Biological assay challenges from compound solubility: strategies for bioassay optimization.* Drug discovery today, 2006. **11**(9-10): p. 446-51.

272. Kalliokoski, T., et al., *Comparability of Mixed IC50 Data - A Statistical Analysis.* PLoS One, 2013. **8**(4): p. e61007.

273. Rix, U. and G. Superti-Furga, *Target profiling of small molecules by chemical proteomics.* Nature chemical biology, 2009. **5**(9): p. 616-24.

274. Arsenis, C. and D.B. McCormick, *Purification of Liver Flavokinase by Column Chromatography on Flavin-Cellulose Compounds.* The Journal of biological chemistry, 1964. **239**: p. 3093-7.

275. Lerman, L.S., *A Biochemically Specific Method for Enzyme Isolation.* Proceedings of the National Academy of Sciences of the United States of America, 1953. **39**(4): p. 232-6.

276. Lomenick, B., R.W. Olsen, and J. Huang, *Identification of direct protein targets of small molecules.* ACS chemical biology, 2011. **6**(1): p. 34-46.

277. Eckert, H. and J. Bajorath, *Molecular similarity analysis in virtual screening: foundations, limitations and novel approaches.* Drug discovery today, 2007. **12**(5-6): p. 225-33.

278. Estrach, S., et al., *The Human Rho-GEF trio and its target GTPase RhoG are involved in the NGF pathway, leading to neurite outgrowth.* Current biology : CB, 2002. **12**(4): p. 307-12.

279. Miller, D.S., et al., *Xenobiotic transport across isolated brain microvessels studied by confocal microscopy.* Molecular pharmacology, 2000. **58**(6): p. 1357-67.

280. Osaki, T., et al., *Intracellular localization and concentration as well as photodynamic effects of benzoporphyrin derivative monoacid ring A in four types of rodent tumor cells.* Cancer letters, 2006. **243**(2): p. 281-92.

281. Beyer, U., et al., *Differences in the intracellular distribution of acid-sensitive doxorubicin-protein conjugates in comparison to free and liposomal formulated doxorubicin as shown by confocal microscopy.* Pharmaceutical research, 2001. **18**(1): p. 29-38.

282. Kansy, M., F. Senner, and K. Gubernator, *Physicochemical high throughput screening: parallel artificial membrane permeation assay in the description of passive absorption processes.* Journal of medicinal chemistry, 1998. **41**(7): p. 1007-10.

283. Avdeef, A. and O. Tsinman, *PAMPA--a drug absorption in vitro model 13. Chemical selectivity due to membrane hydrogen bonding: in combo comparisons of HDM-, DOPC-, and DS-PAMPA models.* European journal of pharmaceutical sciences : official journal of the European Federation for Pharmaceutical Sciences, 2006. **28**(1-2): p. 43-50.

284. van Breemen, R.B. and Y. Li, *Caco-2 cell permeability assays to measure drug absorption.* Expert opinion on drug metabolism & toxicology, 2005. **1**(2): p. 175-85.

285. Tengholm, A., B. Hellman, and E. Gylfe, *Mobilization of Ca2+ stores in individual pancreatic beta-cells permeabilized or not with digitonin or alpha-toxin.* Cell calcium, 2000. **27**(1): p. 43-51.

286. Chen, Z.G., *Small-molecule delivery by nanoparticles for anticancer therapy.* Trends in molecular medicine, 2010. **16**(12): p. 594-602.

287.   Liu, C., et al., *Eradication of large colon tumor xenografts by targeted delivery of maytansinoids.* Proceedings of the National Academy of Sciences of the United States of America, 1996. **93**(16): p. 8618-23.

288.   Saito, G., J.A. Swanson, and K.D. Lee, *Drug delivery strategy utilizing conjugation via reversible disulfide linkages: role and site of cellular reducing activities.* Advanced drug delivery reviews, 2003. **55**(2): p. 199-215.

289.   Cai, S.X., et al., *Dipeptidyl aspartyl fluoromethylketones as potent caspase inhibitors: SAR of the N-protecting group.* Bioorganic & medicinal chemistry letters, 2004. **14**(21): p. 5295-300.

290.   Brown, R.D. and Y.C. Martin, *An evaluation of structural descriptors and clustering methods for use in diversity selection.* SAR and QSAR in environmental research, 1998. **8**(1-2): p. 23-39.

291.   Martin, Y.C., J.L. Kofron, and L.M. Traphagen, *Do structurally similar molecules have similar biological activity?* Journal of medicinal chemistry, 2002. **45**(19): p. 4350-8.

292.   Williams L.E., K.B.A., Burt T., Kuzmak B., Morand K.L. *High throughput screening degradation study: determination of storage options and retention limits.* in *7th annual conference of the Society for Biomolecular Screening.* 2001. Baltimore.

293.   Nie, D., *Compound Library Management*, in *A practical guide to assay development and high-troughput screening in drug discovery*, T. Chen, Editor 2010, CRC Press. p. 193 - 211.

294.   Morand, K.L., Cheng, X., *Organic compound stability in large, diverse pharmaceutical screening collections*, in *Analysis and purification methods in combinatorial chemistry*, B. Yan, Editor 2004, John Wiley and Sons, Inc.: Hoboken, New Jersey, USA. p. 323-350.

295.   Ilouga, P.E., et al., *Investigation of 3 industry-wide applied storage conditions for compound libraries.* Journal of biomolecular screening, 2007. **12**(1): p. 21-32.

296.   Albertoni, B., *Synthesis and analysis of inhibitors of the binding of siRNA to the PAZ domain*, 2007, LIMES, University of Bonn; Laboratory of Organic Chemistry, ETH Zürich.

297.   Shoichet, B.K., *Screening in a spirit haunted world.* Drug discovery today, 2006. **11**(13-14): p. 607-615.

298.   McGovern, S.L., et al., *A specific mechanism of nonspecific inhibition.* Journal of medicinal chemistry, 2003. **46**(20): p. 4265-72.

299.   McGovern, S.L., et al., *A common mechanism underlying promiscuous inhibitors from virtual and high-throughput screening.* Journal of medicinal chemistry, 2002. **45**(8): p. 1712-22.

300.   Frenkel, Y.V., et al., *Concentration and pH dependent aggregation of hydrophobic drug molecules and relevance to oral bioavailability.* Journal of medicinal chemistry, 2005. **48**(6): p. 1974-83.

301.   Coan, K.E., et al., *Promiscuous aggregate-based inhibitors promote enzyme unfolding.* Journal of medicinal chemistry, 2009. **52**(7): p. 2067-75.

302.   McNamara, C.R. and A. Degterev, *Small-molecule inhibitors of the PI3K signaling network.* Future medicinal chemistry, 2011. **3**(5): p. 549-65.

303.   Norman, R.A., D. Toader, and A.D. Ferguson, *Structural approaches to obtain kinase selectivity.* Trends in pharmacological sciences, 2012. **33**(5): p. 273-8.

304.   Pagano, A., et al., *In vitro formation of recycling vesicles from endosomes requires adaptor protein-1/clathrin and is regulated by rab4 and the connector rabaptin-5.* Mol Biol Cell, 2004. **15**(11): p. 4990-5000.

305.   Fecik, R.A., et al., *The search for orally active medications through combinatorial chemistry.* Medicinal research reviews, 1998. **18**(3): p. 149-85.

306.   Porter, D.J., et al., *Mechanism-based inactivation of dihydropyrimidine dehydrogenase by 5-ethynyluracil.* The Journal of biological chemistry, 1992. **267**(8): p. 5236-42.

307.   Van Kuilenburg, A.B., et al., *Subcellular localization of dihydropyrimidine dehydrogenase.* Biological chemistry, 1997. **378**(9): p. 1047-53.

308.   Carmi, C., et al., *Irreversible inhibition of epidermal growth factor receptor activity by 3-aminopropanamides.* Journal of medicinal chemistry, 2012. **55**(5): p. 2251-64.

309.   Leproult, E., et al., *Cysteine mapping in conformationally distinct kinase nucleotide binding sites: application to the design of selective covalent inhibitors.* Journal of medicinal chemistry, 2011. **54**(5): p. 1347-55.

310.   Hagenstein, M.C. and N. Sewald, *Chemical tools for activity-based proteomics.* Journal of biotechnology, 2006. **124**(1): p. 56-73.

311.   Albertoni, B., *Biophysical analysis of protein-protein and protein-small molecule interactions*, 2011.

312.   Lenz, T., J.J. Fischer, and M. Dreger, *Probing small molecule-protein interactions: A new perspective for functional proteomics.* Journal of proteomics, 2011. **75**(1): p. 100-15.

313.   Barglow, K.T. and B.F. Cravatt, *Activity-based protein profiling for the functional annotation of enzymes.* Nature methods, 2007. **4**(10): p. 822-7.

314.   Adam, G.C., et al., *Mapping enzyme active sites in complex proteomes.* Journal of the American Chemical Society, 2004. **126**(5): p. 1363-8.

315.   Okerberg, E.S., et al., *High-resolution functional proteomics by active-site peptide profiling.* Proceedings of the National Academy of Sciences of the United States of America, 2005. **102**(14): p. 4996-5001.

316. Sadaghiani, A.M., S.H. Verhelst, and M. Bogyo, *Tagging and detection strategies for activity-based proteomics.* Current opinion in chemical biology, 2007. **11**(1): p. 20-8.

317. Arkin, M.R. and J.A. Wells, *Small-molecule inhibitors of protein-protein interactions: progressing towards the dream.* Nature reviews. Drug discovery, 2004. **3**(4): p. 301-17.

318. Whitty, A. and G. Kumaravel, *Between a rock and a hard place?* Nature chemical biology, 2006. **2**(3): p. 112-8.

319. Shoichet, B.K., *Virtual screening of chemical libraries.* Nature, 2004. **432**(7019): p. 862-5.

320. Naylor, E., et al., *Identification of a chemical probe for NAADP by virtual screening.* Nature chemical biology, 2009. **5**(4): p. 220-6.

321. Stumpfe, D., et al., *Targeting multifunctional proteins by virtual screening: structurally diverse cytohesin inhibitors with differentiated biological functions.* ACS chemical biology, 2010. **5**(9): p. 839-49.

322. Landry, J., J.T. Slama, and R. Sternglanz, *Role of NAD(+) in the deacetylase activity of the SIR2-like proteins.* Biochemical and biophysical research communications, 2000. **278**(3): p. 685-90.

323. Grozinger, C.M., et al., *Identification of a class of small molecule inhibitors of the sirtuin family of NAD-dependent deacetylases by phenotypic screening.* The Journal of biological chemistry, 2001. **276**(42): p. 38837-43.

324. Lau, O.D., et al., *HATs off: selective synthetic inhibitors of the histone acetyltransferases p300 and PCAF.* Molecular cell, 2000. **5**(3): p. 589-95.

325. Barr, A.J., *Protein tyrosine phosphatases as drug targets: strategies and challenges of inhibitor development.* Future medicinal chemistry, 2010. **2**(10): p. 1563-76.

326. MacKintosh, C. and R.W. MacKintosh, *Inhibitors of protein kinases and phosphatases.* Trends in biochemical sciences, 1994. **19**(11): p. 444-8.

327. Davies, S.P., et al., *Specificity and mechanism of action of some commonly used protein kinase inhibitors.* The Biochemical journal, 2000. **351**(Pt 1): p. 95-105.

328. Butcher, E.C., *Can cell systems biology rescue drug discovery?* Nature reviews. Drug discovery, 2005. **4**(6): p. 461-7.

329. Delaney, J.S., *Predicting aqueous solubility from structure.* Drug discovery today, 2005. **10**(4): p. 289-95.

330. Popa-Burke, I.G., et al., *Streamlined system for purifying and quantifying a diverse library of compounds and the effect of compound concentration measurements on the accurate interpretation of biological assay results.* Analytical chemistry, 2004. **76**(24): p. 7278-87.

331. Kozikowski, B.A., et al., *The effect of freeze/thaw cycles on the stability of compounds in DMSO.* Journal of biomolecular screening, 2003. **8**(2): p. 210-5.

332. Waybright, T.J., J.R. Britt, and T.G. McCloud, *Overcoming problems of compound storage in DMSO: solvent and process alternatives.* Journal of biomolecular screening, 2009. **14**(6): p. 708-15.

333. Welsch, M.E., S.A. Snyder, and B.R. Stockwell, *Privileged scaffolds for library design and drug discovery.* Current opinion in chemical biology, 2010. **14**(3): p. 347-61.

334. Wells, J.A. and C.L. McClendon, *Reaching for high-hanging fruit in drug discovery at protein-protein interfaces.* Nature, 2007. **450**(7172): p. 1001-9.

335. Sun, Q., et al., *Rubicon controls endosome maturation as a Rab7 effector.* Proceedings of the National Academy of Sciences of the United States of America, 2010. **107**(45): p. 19338-43.

336. Alsenz, J. and M. Kansy, *High throughput solubility measurement in drug discovery and development.* Advanced drug delivery reviews, 2007. **59**(7): p. 546-67.

337. KRamer, M.F.C., D.M., *Enzymatic Amplification of DNA by PCR: Standard Procedures and Optimization.* Current protocols in molecular biology. Vol. Supplement 46. 2000: John Wiley and Sons, Inc.

338. Voytas, D., *Resolution and recovery of large DNA fragments, Section II, Unit 2.5A.* Current Protocols in Molecular Biology. Vol. Core Publication, Supplement 51. 1987, 2000: John Wiley and Sons, Inc.

339. *Section 1 Escherichia coli.* Current Protocols in Molecular Biology. Vol. Core Publication, supplement 27. 1987: John Wiley and Sons, Inc.

340. Hochuli, E., et al., *Genetic Approach to Facilitate Purification of Recombinant Proteins with a Novel Metal Chelate Adsorbent.* Nat Biotech, 1988. **6**(11): p. 1321-1325.

341. Smith, D.B. and K.S. Johnson, *Single-step purification of polypeptides expressed in Escherichia coli as fusions with glutathione S-transferase.* Gene, 1988. **67**(1): p. 31-40.

342. Bradford, M.M., *A rapid and sensitive method for the quantitation of microgram quantities of protein utilizing the principle of protein-dye binding.* Analytical biochemistry, 1976. **72**: p. 248-54.

343. Laemmli, U.K., *Cleavage of Structural Proteins during the Assembly of the Head of Bacteriophage T4.* Nature, 1970. **227**(5259): p. 680-685.

344. Gallagher, S.R., *One-Dimensional SDS Gel Electrophoresis of Proteins*, in *Current Protocols in Molecular Biology*1999, John Wiley and Sons, Inc.

345. Sasse, J.G., S.R., *Detection of Proteins, Section III, Unit 10.6*, in *Current Protocols in Molecular Biology*2000, John Wiley and Sons, Inc.

346. Bill, A., et al., *A homogeneous fluorescence resonance energy transfer system for monitoring the activation of a protein switch in real time.* Journal of the American Chemical Society, 2011. **133**(21): p. 8372-9.

347. Gallagher, S.R., *One-Dimensional Electrophoresis Using Nondenaturing Conditions*, in *Current Protocols in Molecular Biology*1999, John Wiley and Sons, Inc.

348. Duhr, S. and D. Braun, *Why molecules move along a temperature gradient.* Proceedings of the National Academy of Sciences of the United States of America, 2006. **103**(52): p. 19678-82.

349. Hagel, L., *Gel-Filtration Chromatography*, in *Current Protocols in Molecular Biology*2001, John Wiley & Sons, Inc.

350. *Modification of Cysteine, Unit 15.1*, in *Current Protocols Protein Science*1996, John Wiley and Sons, Inc.

351. Shevchenko, A., et al., *In-gel digestion for mass spectrometric characterization of proteins and proteomes.* Nature protocols, 2006. **1**(6): p. 2856-60.

352. Rosenfeld, J., et al., *In-gel digestion of proteins for internal sequence analysis after one- or two-dimensional gel electrophoresis.* Analytical biochemistry, 1992. **203**(1): p. 173-9.

353. Phelan, M.C., *Basic Techniques for Mammalian Cell Tissue Culture*, in *Current Protocols Cell Biology*1998, John Wiley and Sons, Inc.

354. Zabner, J., et al., *Cellular and molecular barriers to gene transfer by a cationic lipid.* The Journal of biological chemistry, 1995. **270**(32): p. 18997-9007.

355. Bill, A., et al., *Cytohesins are cytoplasmic ErbB receptor activators.* Cell, 2010. **143**(2): p. 201-11.

356. Kyhse-Andersen, J., *Electroblotting of multiple gels: a simple apparatus without buffer tank for rapid transfer of proteins from polyacrylamide to nitrocellulose.* Journal of biochemical and biophysical methods, 1984. **10**(3-4): p. 203-9.

357. Towbin, H., T. Staehelin, and J. Gordon, *Electrophoretic transfer of proteins from polyacrylamide gels to nitrocellulose sheets: procedure and some applications.* Proceedings of the National Academy of Sciences of the United States of America, 1979. **76**(9): p. 4350-4.

358. Lua, B.L. and B.C. Low, *Activation of EGF receptor endocytosis and ERK1/2 signaling by BPGAP1 requires direct interaction with EEN/endophilin II and a functional RhoGAP domain.* Journal of cell science, 2005. **118**(Pt 12): p. 2707-21.

359. Schmees, C., et al., *Macropinocytosis of the PDGF beta-receptor promotes fibroblast transformation by H-RasG12V.* Molecular biology of the cell, 2012. **23**(13): p. 2571-82.

ACKNOWLEDGEMENTS

There are many people who contributed in one way or another to this thesis and it is a pleasure to thank those who made this possible.

First, I would like to express my special thankfulness to my supervisor Michael Famulok for the opportunity to perform this thesis and his constant support from my early steps in research until now, the encouragement to work independently, his expert guidance, the possibility to participate in three international conferences, and the fantastic infrastructure of this lab.

I sincerely thank Günter Mayer for his supervision in the beginning of this thesis, his constant interest in my work until today, his enthusiastic encouragement and constructive criticism, as well as inspiring discussions and his sincere support of my career ambitions. I also appreciate that he kindly accepted to be the second referee.

I would like to express my sincere appreciation to Anton Schmitz for taking over the supervision of my project, the fruitful scientific debates, for guidance and support in interpreting scientific data, for enthusiastically taking care of the cysteine-mutants, and his honest, clear and refreshing way of discussion.

I am very grateful to Michael Hoch and Sebastian Franken for accepting with alacrity and pleasure to be referees of this thesis.

There are many collaborators whose contributions have enabled and expanded this thesis. These include Marc Sylvester and Sebastian Franken (Institute for Biochemistry and Molecular Biology, University of Bonn) who performed all mass spectrometry measurements presented in Section 3.4 and who supported the project with great enthusiasm. Andreas Jeschke and Albert Haas (Institute for Cell Biology, University of Bonn) greatly promoted the cellular studies by their contribution of the PI3P level determinations (Section 3.5.5) and invaluable discussions. Marianne Engesser (Kekulé-Institute for Organic Chemistry and Biochemistry, University of Bonn) gave precious advice on mass spectrometry measurements. Michael Gütschow (Pharmaceutical Institute, University of Bonn) kindly provided the compounds Gü61 and Gü321, the Rac1 plasmid was a gift of Roger S. Goody (Max Planck Institute of Molecular Physiology, Dortmund), and the Rab5a plasmid was shared by Qing Zhong (University of California, Berkeley, USA). I would like to thank Aymelt Itzen (TU München) for kindly providing the DrrA plasmid, the Rab1 protein, and some further plasmids (not used in this work), as well as an inspiring discussion. I sincerely appreciate that Anna Delprato (BioScience Project, Wakefield, MA, USA) kindly supplied the plasmids for Rabex-5GEF and Rab5c proteins and that she was always available for questions and discussions.

I especially thank Jeffrey Hannam for his constant supply with new compounds, his patience with all my chemical questions and his invaluable support in assembling the analytical data. I acknowledge the general technical assistance of Yvonne Aschenbach and Volkmar Fieberg, the help of Klaus Rotscheidt with the library and the pipetting robot,

the assistance of Katia Schöler with the flow cytometry measurements, and the support of Barbara Albertoni, Damian Ackermann, and Jan Vinkenborg with mass spectrometry measurements. Moreover, I thank all my interns for their contributions, in particular Franziska Wolter. Finally, I sincerely appreciate the invaluable support of Nicole Krämer with protein production, exchange assay performance, ITC, pull-down assay optimization. Her conscientious way of work was a tremendous professional help and her friendship was a delightful company through the ups and downs of this thesis.

It is a great pleasure to thank all the members of the Famulok and Mayer labs for their help and support. This includes in particular Anna Hall, Anna Schüller, Anton Schmitz, Barbara Albertoni, Benjamin Weiche, Björn Niebel, Christina Lünse, Falk Rohrbach, Finn Lohmann, Jan Vinkenborg, Jeffrey Hannam, Julian Valero, Justina Stark, Katia Schöler, Maren Hamann, Marie-Sophie Ahmed, Martina Bettio, Mohamed Hussein, Monika Pofahl, Nicole Krämer, Sabine Lennarz, Sandra Ulrich, Stephanie Kath-Schorr, Sven Freudenthal and Yvonne Aschenbach.

I highly appreciate the help my proofreading team, who commented on longer or shorter parts of this work, especially Anton Schmitz and Stephanie Kath-Schorr, but also, Barbara Albteroni, Jan Vinkenborg, Benjamin Weiche, Lukas Wosnitza, Christina Lünse, Björn Niebel, Falk Rohrbach and Jeffrey Hannam.

I am grateful to the NRW International Graduate Research School LIMES - Chemical Biology for funding this thesis. I would like to thank the GradStudents, especially of "round one", for the great times spent that we together at scientific and social activities.

I wish to express my heartfelt gratitude to my family for their love, support, encouragement, and their faith in me, for adapting their plans to my lab time management and for doing their best to understand what I am doing in the lab. This includes especially my husband Lukas, my parents Maria and Anton, my brother Martin and my aunt Irene but also all the other Wölffe, Wosnitzas, Wollmanns and Walchas.

I wholeheartedly thank my mentor Eva-Maria Streier for her cordial encouragement and precious support, her ingenious problem solving ideas, for fostering and reviewing my professional ideas, and for sympathetically accompanying me during the last two years.

I sincerely thank my friends André Liesegang, Anita Tiefensee & Hans Verbeek, Anna Hall, Anna-Lena Steckelberg & Benjamin Weiche, Anne Voigt, Annette Ottinger, Barbara Albertoni, Christina Lünse, Christine Hopp, Corina Brückner, Dominik Klapdor, Falk Rohrbach, Florian Hahnfeldt & his family, Jan Vinkenborg, Klaudia & Simon Marcus, Martina Bettio, Nicole Krämer, Sherman Antao, Silke Krumbein, and Steffi Krahe & her family for their friendship and encouragement. I am so lucky to have all of you in my life and could not have done it without you. I am looking forward to see and hear much more of you soon.

Finally, I want to express my deepest gratitude to my husband Lukas for his love, encouragement, support, and understanding, for sharing the good times and the bad ones, and for believing in me whenever I did not. Truly, I would not have finished this project without you – so as back in old times, this title will be yours, too.